Dissertation zur Erlangung des Doktorgrades
der Fakultät für Chemie und Pharmazie
der Ludwig-Maximilians-Universität München

Präbiotische Entstehung von RNA-Nukleosiden unter stark und schwach reduzierender Atmosphäre

Jonas Feldmann

aus

Wesel, Deutschland

2022

Erklärung

Diese Dissertation wurde im Sinne von §7 der Promotionsordnung vom 28. November 2011 von Herrn Prof. Dr. Thomas Carell betreut.

Eidesstattliche Erklärung

Diese Dissertation wurde eigenständig und ohne unerlaubte Hilfe erarbeitet.

München, den 07.12.2022

_____

(Jonas Feldmann)

Dissertation eingereicht am	13.12.2022
Erstgutachter	Prof. Dr. Thomas Carell
Zweitgutachter	Dr. Pavel Kielkowski
Mündliche Prüfung am	20.01.2023

Meiner Familie gewidmet

Danksagung

Zunächst möchte ich mich bei meinem Doktorvater *Prof. Dr. Thomas Carell* bedanken. In den letzten Jahren durfte ich an spannenden und herausfordernden Projekten mitwirken. Die gebotene Freiheit, eigene Ideen umsetzen zu dürfen sowie das entgegengebrachte Vertrauen habe ich stets geschätzt. Vor allem werde ich mich gerne an die offenen Diskussionen zurückerinnern, welche gelegentlich kontrovers, jedoch immer konstruktiv und eine positive Bereicherung waren. Auch für seine geradlinige Unterstützung meiner persönlichen Zukunftspläne kann ich mich mehr als glücklich schätzen.

Dr. Pavel Kielkowski danke ich vielmals für die Übernahme des Zweitgutachtens. Den Mitgliedern der Prüfungskommission sei für das Beisitzen der mündlichen Prüfung gedankt.

Dr. Markus Müller möchte ich für anregende Diskussionen aller Art danken. Ohne seine wissenschaftliche Unterstützung sowie sein zuverlässiges Labormanagement würde die tägliche Arbeit nicht so reibungslos ablaufen, wie wir es dankenswerterweise gewohnt sind.

Ein großer Dank geht ebenfalls an *Kerstin Kurz* für die zuverlässige, oft spontane Versorgung mit Chemikalien. Ihre Liebe zu Pflanzen hat unsere ursprünglich trostlosen Räumlichkeiten in ein lebenswertes Stückchen Grün verwandelt. *Claudia Scherübl* danke ich für die Instandhaltung des NMR.

Frau *Slava Gärtner* und *Dr. Nada Raddaoui* danke ich für die gewissenhafte Durchführung sämtlicher bürokratischer Aufgaben.

Für das gewissenhafte Korrekturlesen meiner Arbeit bedanke ich mich bei *Yasmin Gärtner* und *Dr. Stefan Wiedemann*.

Die erfolgreiche Forschung konnte nur durch ein perfekt eingespieltes Team gelingen, zu welchem seit Beginn meiner Promotion *Dr. Sidney Becker* und *Dr. Stefan Wiedemann* angehören. Auch ist die Unterstützung durch unsere internationalen Freunde *Dr. Joan Guillem Mayans*

Peñarrubia und *Mads Koch Skaanning* zu nennen. Vielen Dank und Erfolg an *Erik Boinowitz*, welcher mit viel Engagement unser Erbe angetreten ist.

Meinen Masterstudenten *Felix Xu* und *Tobias Kernmayr* danke ich für die Geduld mit mir sowie die Motivation, welche nicht selbstverständlich ist und euch hoffentlich beibehalten bleibt. Meinen Forschungspraktikanten *Marcus Lommel*, *Konstantin Kublik*, *Tony Mansour* und *Clara Testard* danke ich für ihre große Hilfe im Labor.

Zudem möchte ich mich bei allen Laborkollegen bedanken, welche die Arbeit auch in stressigen Zeiten erträglich gemacht haben. Dies gilt vor allen meinen direkten Kollegen aus dem alten sowie dem neuen *12er* Labor: *Dr. Michael Stadlmeier*, *Dr. Clemens Dialer*, *Dr. Simon Veth*, *Dr. Florian Schelter*, *Dr. Stefan Wiedemann*, *Johann de Graaff*, *Felix Müller*, *Ewa Węgrzyn* und *Julie Brossier*. Meinen Kollegen *Dr. Matthias Heiß*, *Dr. Anna Holovan* und *Jahongir Nabiev* danke ich für die angenehme Arbeitsatmosphäre während meiner letzten Monate im Büro.

Besonderer Dank gilt *Dr. Mirko Wagner*. Danke für deine uneigennützige und aufmunternde Art sowie sämtliche Notfallpizzen während meiner Nachtschichten.

Meinen *kraotischen* Freunden *Yasmin Gärtner* und *Dr. Matthias Heiß* danke ich für die gelegentliche Ablenkung in Form von Kaffee, Negroni und bestem Humor. Ohne euch hätte die Zeit nur halb so viel Spaß gemacht.

Zuletzt möchte ich mich bei meiner Familie und meinen Freunden bedanken, welche mich das letzte Jahrzehnt über begleitet haben. Ohne die finanzielle Unterstützung meiner Eltern wäre es mir nicht möglich gewesen, mein Studium auf eine solch unbeschwerte Art zu absolvieren. Ohne ihre Motivation hätte ich es wohl gar nicht erst begonnen. Danke auch an meinen Bruder *Simon* und meine Großeltern, dass ich mich nach all den Jahren abseits der Heimat immer noch in Hamminkeln zu Hause fühle.

„Wir sagen Dankeschön!“

Die Flippers, 40 Jahre

Publikationsliste

Im Rahmen meiner Promotion erstellte Publikationen:

- J. Feldmann, T. Carell, A chemical pathway to the origin of biomolecules and the emergence of an RNA-peptide world. *Bunsen-Magazin* **2022**, *24*, 147–150.
- S. Becker†, J. Feldmann†, S. Wiedemann†, H. Okamura, C. Schneider, K. Iwan, A. Crisp, M. Rossa, T. Amatov, T. Carell, Unified prebiotically plausible synthesis of pyrimidine and purine RNA ribonucleotides. *Science* **2019**, *366*, 76–82.
- H. Okamura, S. Becker, N. Tiede, S. Wiedemann, J. Feldmann, T. Carell, A one-pot, water compatible synthesis of pyrimidine nucleobases under plausible prebiotic conditions, *Chem. Commun.* **2019**, *55*, 1939–1942.

Unveröffentlichte Manuskripte:

- J. Feldmann†, M. K. Skaanning†, M. Lommel, P. Mayer, and T. Carell, A unifying concept for the prebiotic formation of RNA pyrimidine nucleosides.
- J. Feldmann†, S. Wiedemann†, S. Becker, T. Carell, The emergence of biomolecules under early Earth conditions.

Weitere Publikationen:

- J. Feldmann, Y. Li, Y. Tor, Emissive Synthetic Cofactors: A Highly Responsive NAD^+ Analogue Reveals Biomolecular Recognition Features, *Chem. Eur. J.* **2019**, *25*, 4379–4389.

† Die Autoren haben zu gleichen Teilen zum Manuskript beigetragen

Konferenzbeiträge

11/2022 J. Feldmann, S. Wiedemann, E. Boinowitz, S. Becker, T. Carell, The Origin of Biomolecules Under Plausible Early Earth Conditions, Posterpräsentation, Scientific School and Conference on Bioinspired Complex Systems from Basic Science to Practical Applications, The Minerva Center for Bio-hybrid Complex Systems, Jerusalem, Israel.

08/2022 J. Feldmann, S. Wiedemann, S. Becker, T. Carell, The Origin of Biomolecules Under Plausible Early Earth Conditions, Vortrag, Tohoku University 13th Chemistry Summer School, Tohoku Universität, Japan.

06/2022 J. Feldmann, S. Wiedemann, S. Becker, T. Carell, The Emergence of Biomolecules Under a Redox-Neutral, HCN-free Atmosphere, Posterpräsentation, Molecular Origins of Life 2022 – CAS Conference, München.

08/2021 J. Feldmann, S. Wiedemann, S. Becker, T. Carell, A Redox-Neutral Atmosphere Allows Prebiotic Formation of Biomolecules, Posterpräsentation, Molecular Origins of Life 2021 – CAS Conference, München.

08/2019 J. Feldmann, S. Becker, S. Wiedemann, T. Carell, Unified Prebiotic Syntheses of all Canonical RNA Building Blocks, Posterpräsentation, 136th International BASF Summer Course, BASF, Ludwigshafen.

03/2019 J. Feldmann, New Prebiotic Approaches to RNA, Vortrag, SFB 749 Symposium, Venice International University, Italien.

10/2018 S. Becker, S. Wiedemann, J. Feldmann, T. Carell, Prebiotic Origin of all Four RNA Building Blocks, Posterpräsentation, Molecular Origins of Life 2018 – CAS Conference, München.

10/2015 J. Feldmann, C. Ebert, T. Carell, Synthesis of N^2-Acetylaminofluorenyl-2'-deoxyguanosine for the Investigation of the Nucleotide Excision Repair Mechanism, Undergraduate Research Conference on Molecular Sciences, Wildbad-Kreuth.

Inhaltsverzeichnis

Zusammenfassung

Die Entstehung des Lebens ist ein bislang ungelöstes Rätsel, welches die Menschheit seit Jahrtausenden fasziniert. Die Frage nach dem Übergang von lebloser zu lebender Materie führte zur Entwicklung verschiedenster Hypothesen, von welchen die *RNA-Welt-Hypothese* eine der prominentesten ist. Diese besagt, dass Ribonukleinsäure (RNA) als universeller Baustein die Entstehung erster Lebensformen ermöglichte, da RNA sowohl genetische Informationen speichern als auch (bio)chemische Reaktionen katalysieren kann. Die sogenannte *RNA-Peptid-Welt-Hypothese* geht einen Schritt weiter und postuliert die synergistische Koevolution von RNA und Peptiden. So könnte RNA die Bildung von Peptiden begünstigt haben, welche ihrerseits die Vervielfältigung der RNA katalysiert haben könnten. Diese Szenarien erfordern die präbiotische Synthese und Verfügbarkeit von Aminosäuren sowie komplementärer Pyrimidin- und Purinnukleoside, welche durch Basenpaarung die RNA-Replikation ermöglichen. Zur Entstehung dieser Bausteine auf der frühen Erde werden in der Literatur verschiedene Reaktionswege postuliert, welche sich in ihren Reaktionsbedingungen, Startmaterialien und Nukleosidierungsstrategien teils erheblich unterscheiden. Aufgrund chemischer Inkompatibilitäten zwischen den postulierten Pyrimidin- und Purinsynthesewegen ist die gleichzeitige Bildung aller kanonischer RNA-Bausteine am selben Ort bislang allerdings nicht erklärbar.

In dieser Arbeit wurde ein neuer Reaktionsweg zu Pyrimidinnukleosiden unter präbiotisch plausiblen Bedingungen entwickelt. Dieser basiert auf 3-Aminoisoxazolylharnstoff (Abbildung 1), welcher als Pyrimidinvorstufe regioselektiv ribosyliert und anschließend zu den kanonischen Pyrimidinen umgewandelt werden kann. Die Verwendung mineralischer Borophosphate erlaubt zudem die bevorzugte Bildung von Furanosid-5‘-monophosphaten und -diphosphaten. Zudem konnte die Kompatibilität zu einem bereits publizierten Purinsyntheseweg demonstriert werden, was die gemeinsame Bildung aller kanonischen RNA-Nukleoside erstmals ermöglicht.

Die direkte Ribosylierung der Pyrimidinvorstufe erfordert die Anwesenheit freier Ribose, welche durch die Formosereaktion aus Formaldehyd entstanden sein könnte. Ihre selektive Bildung ist jedoch umstritten, weswegen indirekte Nukleosidierungsstrategien publiziert wurden, welche den schrittweisen Aufbau des Furanoserings *in situ* ermöglichen. Diese Strategie wurde angewandt, um die neu entdeckten Pyrimidinvorstufe auch in der Abwesenheit freier

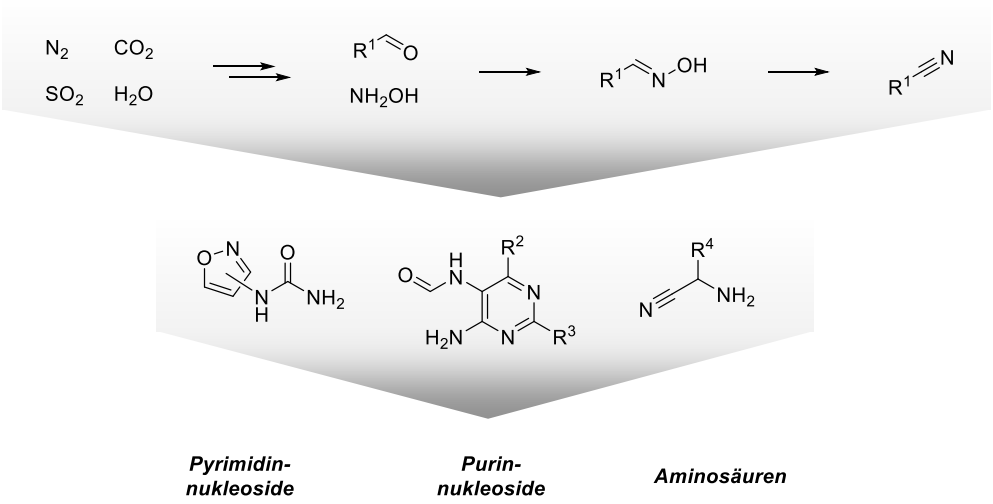

Abbildung 1. Reaktionswege und Intermediate, welche im Rahmen dieser Arbeit zur Bildung von Nukleosiden und Aminosäuren unter präbiotisch plausiblen Bedingungen entwickelt wurden.

Ribose zu Nukleosiden umsetzen zu können. Durch die Verknüpfung der verschiedenen Pyrimidin-Synthesestrategien konnte ihre Kompatibilität demonstriert und ihre Vorteile in einem gemeinsamen Reaktionsweg vereint werden. Dieser neue Reaktionsweg basiert maßgeblich auf Cu(I/II), welches neben seiner Funktion als Redoxkatalysator auch die präbiotische Anreicherung der Pyrimidinvorstufe ermöglicht.

Ein weiteres Problem ist die präbiotische Verfügbarkeit reaktiver Nitrile wie Blausäure, Cyanamid und Cyanoacetylen. Diese gelten als Ausgangsverbindungen für Nukleoside und Aminosäuren und bilden sich unter stark reduzierende Bedingungen in ausreichenden Mengen. Aktuelle Studien lassen jedoch vermuten, dass die frühe Erdatmosphäre nicht stark, sondern nur schwach reduzierend war. Unter diesen Bedingungen ist die effiziente Bildung solcher Nitrile jedoch problematisch, was die präbiotische Plausibilität vieler postulierter Bildungswege in Frage stellt. Zur Lösung dieses Problems wurde im Rahmen dieser Arbeit ein Reaktionsweg entwickelt, welcher die Bildung von Biomolekülen unter einer schwach reduzierenden Atmosphäre ermöglicht. Ausgehend von Wasser, Stickstoff, Kohlendioxid und Schwefeldioxid wird zunächst die Bildung von Aldehyden und Hydroxylamin angenommen (Abbildung 1). Diese kondensieren zu einer Vielzahl an Aldoximen, deren Dehydratation Zugang zu reaktiven Nitrilen bietet. Von diesen ausgehend wurden neue Syntheserouten zu bekannten Aminosäure- sowie Purinvorstufen entwickelt und ein neuer Reaktionsweg zu Uridin etabliert. Hieraus

ergibt sich ein Reaktionsnetzwerk, welches die systematische Bildung reaktiver Ausgangsverbindungen zur Entstehung des Lebens unter geologisch plausiblen Bedingungen ermöglicht.

Abstract

The origin of life is an unsolved mystery that has fascinated mankind since ever. The question about the transition from lifeless to living matter led to the development of various hypotheses, of which the *RNA world hypothesis* is one of the most prominent. This hypothesis states that ribonucleic acid (RNA), as a universal building block, was the basis for the emergence of the first forms of life, since RNA can both store genetic information and catalyze (bio)chemical reactions. The so-called *RNA-peptide world hypothesis* goes one step further and postulates the synergistic co-evolution of RNA and peptides. Thus, RNA could have favored the formation of peptides, which in turn could have catalyzed the amplification of RNA. These scenarios require the prebiotic synthesis and availability of amino acids as well as complementary pyrimidine and purine nucleosides, which enable RNA replication through base pairing. For the formation of these building blocks on the early Earth, various reaction pathways are postulated in the literature, some of which differ considerably in their reaction conditions, starting materials and nucleosidation strategies. However, due to chemical incompatibilities between the postulated pyrimidine and purine synthesis pathways, the simultaneous formation of all canonical RNA building blocks at the same site cannot be explained so far.

In this work, a new reaction pathway to pyrimidine nucleosides was developed under prebiotically plausible conditions. This is based on 3-aminoisoxazolylurea (Figure 1), which can be regioselectively ribosylated to give a pyrimidine precursor, which subsequently converts to the canonical pyrimidines. The use of borophosphate minerals allows the preferential formation of furanoside-5'-monophosphates and -diphosphates. In addition, compatibility with a previously published purine synthesis pathway was demonstrated, allowing the joint formation of all canonical RNA nucleosides for the first time.

Direct ribosylation of the pyrimidine precursor requires the presence of free ribose, which could have been formed from formaldehyde by the formose reaction. However, its selective formation is controversial, which is why indirect nucleosidation strategies have been published that allow the stepwise assembly of the furanose ring *in situ*. This strategy was applied to convert the newly discovered pyrimidine precursor to nucleosides even in the absence of free ribose. By linking the different pyrimidine synthesis strategies, their compatibility was demonstrated, and their advantages were combined in a common reaction pathway. This new

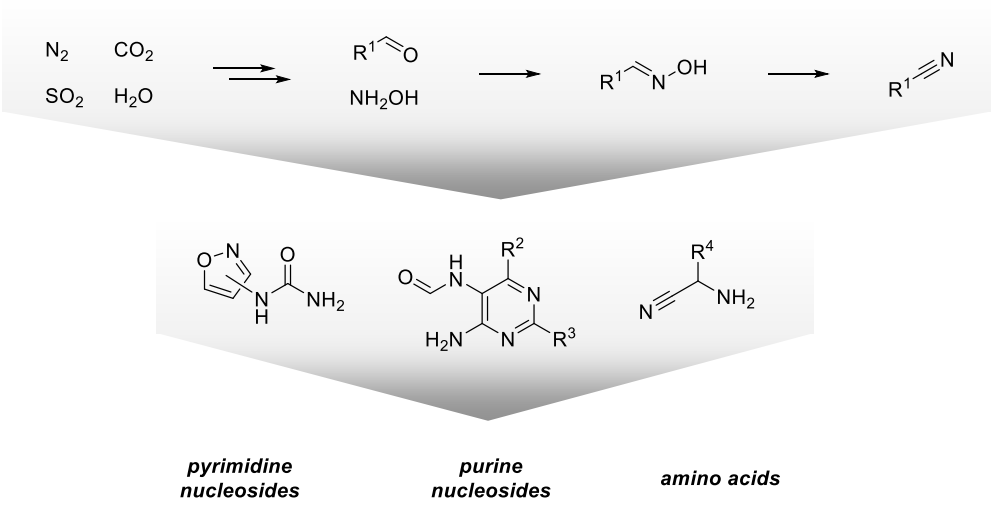

Figure 1. Reaction pathways and intermediates developed in this work that allow the formation of nucleosides and amino acids under prebiotically plausible conditions.

reaction pathway is largely based on Cu(I/II), which, in addition to its function as a redox catalyst, also enables the prebiotic enrichment of the pyrimidine precursor.

Another problem is the prebiotic availability of reactive nitriles such as hydrocyanic acid, cyanamide and cyanoacetylene. These are considered starting compounds for nucleosides and amino acids and form in sufficient quantities under highly reducing conditions. However, recent studies suggest that the early Earth's atmosphere was weakly reducing rather than strongly reducing. Under these conditions, however, the efficient formation of such nitriles is problematic, calling into question the prebiotic plausibility of many postulated pathways. To solve this problem, a reaction pathway was developed in this work that allows the formation of biomolecules under a weakly reducing atmosphere. Starting with water, nitrogen, carbon dioxide and sulfur dioxide, the formation of aldehydes and hydroxylamine is first assumed (Figure 1). These condense to form a variety of aldoximes, whose dehydration provides access to reactive nitriles. From these, new synthetic routes to known amino acid as well as purine precursors were developed and a new reaction pathway to uridine was established. The result is a new reaction network that enables the systematic formation of reactive starting compounds for the origin of life under geologically plausible conditions.

1. Einleitung

1.1 Präbiotische Chemie

Von der Theologie über die Philosophie bis hin zu den Naturwissenschaften ist die Frage nach der Entstehung des Lebens Gegenstand vieler Diskussionen und Theorien. Nachdem der Philosoph *Thales* bereits 2500 v.Chr. den Ursprung des Lebens auf Wasser als materielle Substanz zurückführte,[1] wurde vor kurzem (ca. 4500 Jahre später) das *James-Webb*-Teleskop von NASA und ESA ins Weltall ausgesandt, um im Universum nach Wasser und Spuren von Leben zu suchen.[2] In den letzten Jahrzehnten ermöglichten neue Erkenntnisse in Astrophysik und Geologie präzisiere Einblicke in die Entstehung der Erde und ihre ursprüngliche Beschaffenheit (Kapitel 1.2).[3-4] Die Biologie hat auf Grundlage fossiler Indizien stringente Theorien entwickelt, welche die Evolution komplexer Lebewesen erklären.[5-7] Dabei lässt sich die Abstammung dieser Lebewesen auf einen gemeinsamen Vorläufer zurückführen, welcher gemeinhin als LUCA (*last universal common ancestor*; dt.: letzter allgemeiner gemeinsamer Vorfahr) bezeichnet wird.[8-10] Als einzelliger, thermophiler Organismus lebte LUCA wahrscheinlich vor mehr als 3,5 Mrd. Jahren unter den hohen Temperaturen von Tiefseeschloten.[9] Während dieser Organismus zunächst als vergleichsweise einfach und rudimentär beschrieben wurde,[9] geben phylogenetische Studien heutzutage Hinweise auf dessen molekulare Komplexität. So wird vermutet, dass LUCA unter Verwendung verschiedener Enzyme, Kofaktoren und (modifizierter) Nukleoside bereits Kohlenstoffdioxid, Stickstoff und Wasserstoff autotroph verstoffwechseln konnte und dabei auf Eisen-Schwefel-Cluster sowie Übergangsmetalle angewiesen war.[11] Dementsprechend handelt es sich bei LUCA keineswegs um die erste lebende Zelle, sondern um eine weiterentwickelte Spezies, welche sich bereits durch evolutionäre Selektionsprozesse anpassen und spezialisieren konnte. Die erste lebende Zelle, oder vorsichtiger ausgedrückt, das erste lebende System, ist hingegen weitgehend unerforscht und ihre Eigenschaften eher spekulativer Natur.[12-14]

Es ist nun die Aufgabe der präbiotischen Chemie zu zeigen, wie aus zunächst lebloser Materie die ersten Moleküle entstehen konnten, deren Selektion und Interaktion später die Bildung lebender Systeme ermöglichten. Diese Frage zu lösen ist nicht trivial. Zwar gibt es Hinweise über die Bedingungen auf der frühen Erde und eine ungefähre Vorstellung darüber, aus welchen Biomolekülen LUCA möglicherweise bestand. Der Übergang von der abiotischer zur biotischen Welt bleibt jedoch weitgehend eine *„Blackbox“*. Weder können astronomische

Beobachtungen die Bildung komplexer Biomoleküle auf der frühen Erde erklären, noch lassen uns phylogenetische Studien in die Zeit vor LUCA blicken. Auch gibt es aus jener Zeit keine Fossile, welche die präbiotischen Ereignisse als Momentaufnahmen festhalten.[15]

Daher ist interdisziplinäres Wissen und ein wenig Kreativität gefragt, um Reaktionswege zu finden, welche die Bildung komplexer Biomoleküle aus einfachsten Verbindungen wie Wasser, Stickstoff und Kohlenstoffdioxid erklären können. Doch welche Reaktionswege gelten als präbiotisch plausibel, wo sie sich weder beweisen noch widerlegen lassen? Diese Frage veranlasste *Orgel* dazu, drei allgemeine Bedingungen zu formulieren, welche seiner Meinung nach das Prädikat „präbiotisch plausibel“ rechtfertigen:[16]

i. Startmaterialien müssen in ausreichenden Mengen am Reaktionsort vorhanden sein
ii. Reaktionen müssen in Wasser oder der Abwesenheit eines Lösungsmittels ablaufen
iii. Reaktionsprodukte müssen sich in signifikanten Mengen bilden

Ob und wie weit die gelisteten Punkte im Einzelfall zutreffen, ist jedoch nicht immer eindeutig und ist einer stetigen Revision unterworfen. Dies liegt vor allem daran, dass neue Forschungsergebnisse aus Astrophysik und Geologie oft auch neues Licht auf die präbiotischen Bedingungen sowie die Verfügbarkeit chemischer Verbindungen auf der frühen Erde werfen. Vor dem Hintergrund aktueller Erkenntnisse können diese Kriterien jedoch eine vorläufige Beurteilung zur präbiotischen Plausibilität chemischer Reaktionen ermöglichen.[16]

Für die Präbiotik wegweisende Experimente gehen bereits bis ins 19. Jahrhundert zurück. So entdeckte *Butlerow*[17] bereits im Jahre 1861 die Formosereaktion, welche die Bildung von Zuckern aus Formaldehyd und katalytischen Mengen Glycolaldehyd ermöglicht. Die dazu erforderlichen Ausgangsverbindungen konnten später von *Löb*[18] in einer CO_2/H_2O-Atmosphäre hergestellt werden. *Urey* und *Miller*[19] demonstrierten im Jahre 1953 mit ihrem weltbekannten Gasentladungsexperiment die Synthese von Aminosäuren, deren Mechanismus zum Teil zuvor von *Strecker*[20] beschrieben wurde. Die Polymerisation von HCN zur Nukleobase Adenin geht auf *Oró*[21] im Jahre 1960 zurück. An diese Meilensteine schließen sich viele weitere Entdeckungen und Hypothesen verschiedenster Fachrichtungen an, welche die präbiotische Forschung mittlerweile als interdisziplinäres Großprojekt aufblühen lassen.[22] Die stetig zunehmenden Erkenntnisse und das wachsende Interesse zeigen sich auch in der Vielzahl kürzlich erschienener Übersichtsartikel – von der Entstehung interstellarer Moleküle[23] und chiraler Asymmetrien[24] über Phosphate[25], Peptide[26], kanonische[27] und nicht-kanonische[28] Nukleoside bis hin zu biologischer Homochiralität,[29] Ribozymen[30-31] und Ribosomen[32].

1.2 Die Frühe Erde

1.2.1 Historischer Kontext

Eine der ersten Theorien zur Entstehung des Lebens unter vermeintlich plausiblen Bedingungen geht auf den russischen Biochemiker *Oparin* im Jahre 1924 zurück.[33] Ähnliche Überlegungen wurden kurze Zeit später vom Evolutionsbiologen *Haldane* veröffentlicht[34] und untermauerten die ursprüngliche Theorie, welche später als *Oparin–Haldane*-Hypothese bekannt wurde.[35] Diese besagt, dass sich die ersten organischen Moleküle durch thermische oder photochemische Prozesse in einer reduzierenden Erdatmosphäre bildeten, welche hauptsächlich aus Ammoniak, Methan und anderen wasserstoffreichen Verbindungen bestand.[33-38]

Zu dieser Zeit wurden reduzierende Gase bereits in der Jupiteratmosphäre nachgewiesen, weswegen auch *Urey* mutmaßte, dass die frühe Erdatmosphäre ebenfalls reduzierend gewesen sein muss und trotz der Flüchtigkeit des Wasserstoffs und der geringen Erdgravitation längere Zeit bestehen konnte.[39-40] Diese und *Oparins* Schlussfolgerungen veranlassten *Miller* schließlich, seine Gasentladungsexperimente in einem Gasgemisch aus Wasserstoff, Ammoniak, Methan und Wasser durchzuführen.[19, 41] Die erfolgreichen Ergebnisse wurden daraufhin genutzt, um die präbiotische Plausibilität einer stark reduzierenden Atmosphäre *ad hoc* zu rechtfertigen.[42]

1.2.2 Redox-Bedingungen

Ca. 100 Jahre nach Formulierung der *Oparin–Haldane*-Hypothese besitzen wir heute genauere Kenntnisse über die astrogeologischen Gegebenheiten auf der hadäischen[3] Erde.[42] So wissen wir, dass die frühe Erde nach ihrer Entstehung vor 4,57 Mrd. Jahren tatsächlich eine reduzierende primäre Erdatmosphäre besaß, welche aus eingefangenem Sonnennebel (vorwiegend Wasserstoff) bestand. Allerdings war diese viel kurzlebiger als von Ureys angenommen und konnte der Erde möglicherweise schon nach Tagen entweichen.[42-43] Dies bietet eine Erklärung dafür, weswegen heutzutage alle flüchtigen Elemente auf der Erde im Verhältnis zu ihrem solaren Vorkommen verarmt sind.[44-45] Jedoch ist das Vorkommen an Edelgasen auf der

[3]Das Hadaikum ist das erste geologische Erdzeitalter von der Entstehung unserer Erde bis 4 Mrd. Jahre vor unserer Zeit.

Erde viel stärker erschöpft als das der reaktiven Gase Wasserstoff, Stickstoff, Kohlenstoff und Sauerstoff.[46] Diese Beobachtung veranlasste *Brown* zu der Hypothese, dass diese durch chemische Reaktionen von der sich anreichernden Erdmasse aufgenommen wurden, während die Edelgase ins Weltall entweichen konnten.[46] Zurück blieben vermutlich große Mengen an CO_2, etwas N_2 und H_2O sowie Spuren von CO und H_2.[46-50] Diese sekundäre Atmosphäre wird folglich als schwach reduzierend bis oxidierend beschrieben,[47-50] während die von Miller und Urey aufgestellte Hypothese einer stark reduzierenden Atmosphäre als nicht mehr zeitgemäß gilt.[42]

Die Entstehung der sekundären Atmosphäre ging mit dem stetigen Einschlag chondritischer Meteoriten einher, welche als undifferenzierte Bestandteile des Sonnennebels aus Silikaten, Metallen und Sulfiden bestehen.[51] Der Protoplanet *Theia* (4,51 Ga) verursachte schließlich die Bildung unseres Mondes, welcher seit jeher die Erde umkreist und ihre Umlaufbahn stabilisiert.[52-55] Während dieser Zeit trennten sich allmählich Silikate und Metalle unter Ausdifferenzierung von Erdkern und Erdmantel, in welchem das Vorkommen an siderophilen Elementen immer mehr erschöpfte.[56-57] Gleichzeitig disproportionierte Eisen(II) zu Eisen(0), welches vom Erdkern aufgenommen wurde, sowie zu Eisen(III), welches als oxidierte Spezies im Mantel zurückblieb.[58] Entsprechend lassen physikalische Studien vermuten, dass die Sauerstofffugazität[4] des Mantels während der Erdentstehung zunahm[59] und nach vollständiger Ausdifferenzierung Werte erzielte, die den Bedingungen auf der heuten Erde entsprechen.[58, 60] Dies konnte auch experimentell anhand von Zirkonen bestätigt werden, deren radiometrische Datierung ein Alter von 4,36 Mrd. Jahren offenbarte.[61] Eine Bestimmung des Cer(III)/Cer(IV)-Verhältnisses erlaubte Rückschlüsse auf eine durchschnittliche Sauerstofffugazität von ΔFMQ -0,5 ± 2,3.[61] Diese Ergebnisse werden durch weitere experimentelle Studien[62-63] gestützt, welche gleichbleibende Redoxbedingungen über die letzten 3,8 Ga vermuten lassen. Kenntnisse über den Redoxzustand des Erdmantels sind von entscheidender Bedeutung, da diese sowohl Aufschluss über die Zusammensetzung des Mantels selbst als auch über die der

[4]Die Sauerstofffugazität (f_{O2}) entspricht dem effektiven Partialdruck von Sauerstoff in bestimmten Mineralien bzw. Gesteinen. Sie wird meist relativ zu Referenzwerten aus Fayalit-Magnetit-Quarz- (FMQ) oder Eisen-Wüstit- (IW) Puffersystemen angegeben. Die Sauerstofffugazität des heutigen Erdmantels beträgt f_{O2} ≈ ΔFMQ ± 2 log-Einheiten.[60]

sekundären Atmosphäre gibt. Betrachtet man die mineralische Zusammensetzung des Mantels, so lag Silizium als Silikat, Phosphor als Phosphat, Schwefel als Sulfit oder Sulfat, und Bor als Borat vor.[64] Weiterhin kann angenommen werden, dass ein Mantel nahe des FMQ-Puffers hauptsächlich die Gase CO_2, H_2O, SO_2 und N_2 in die sekundäre Atmosphäre ausgestoßen haben muss.[42, 60, 64-65] Während die exakte Zusammensetzung unbestimmt bleibt, gehen einige Studien von einem CO_2-Anteil von >70 % aus, andere sogar von >95 %. Eine solche Atmosphäre wird aufgrund ihres Redoxpotentials häufig als *oxidativ neutral*[66] bezeichnet bzw. als *schwach reduzierend*[67-68], sollten Spuren von H_2, CH_4 oder CO vorhanden gewesen sein.[64]

1.2.3 Verfügbarkeit Chemischer Verbindungen

In einer solchen Atmosphäre erzeugen Blitzentladungen und UV-Strahlung große Mengen an Nitrit und Nitrat,[66, 69] weshalb die NO_X^--Konzentration in den frühen Ozeanen zuweilen sogar auf 20 mM geschätzt wird.[70] Ebenfalls ist die Reduktion von Nitrit zu Ammoniak ein plausibles Szenario,[71-72] sofern Eisen(II) nicht vollständig disproportioniert vorliegt.[58] Auch die Reaktion zwischen Schwefeldioxid und Wasser unter Bildung von Hydrogensulfit,[73] dessen Konzentration im millimolaren Bereich gelegen haben könnte, gilt als unausweichlich.[74] Zusätzlich kann die Verfügbarkeit von Formaldehyd angenommen werden, dessen Synthese aus Kohlenstoffdioxid und Wasser redoxunabhängig ist.[18, 75] Die Bildung von Glycolaldehyd erfolgt unter schwach reduzierenden Bedingungen zwar nur in Spuren,[67] soll zur Katalyse der Formosereaktion und Bildung komplexer Zucker jedoch ausgereicht haben.[64, 76]

Trotz der Verfügbarkeit wichtiger Verbindungen stellte die Annahme einer schwach reduzierenden Atmosphäre ein Problem für die präbiotische Chemie dar, nicht zuletzt, da sie die Plausibilität der populären *Urey–Miller*-Experimente grundlegend in Frage stellt. Es zeigte sich sowohl experimentell[66, 77] als auch theoretisch,[78] dass unter den angenommenen Bedingungen (C/O <1) häufig postulierte Ausgangsverbindungen wie Blausäure, Cyanamid oder Cyanoacetylen nicht effizient gebildet werden. Somit gilt eine schwach reduzierende Atmosphäre als chemisch *unproduktiv*, wohingegen eine stark reduzierende Atmosphäre als *produktiv* bezeichnet wird.[64]

1.2.4 Geochemische Hypothesen und Szenarien

Die ineffiziente Bildung reaktiver Nitrile (Abbildung 2) unter schwach reduzierenden Bedingungen[66, 77-78] stellt ein Dilemma dar, da diese Verbindungen Zugang zu wichtigen Biomolekülen bieten (*vide infra*). Zur Lösung dieses Problems wurden verschiedene geochemische Szenarien entwickelt, welche die Entstehung dieser Verbindungen unter den vermeintlich *unproduktiven* Bedingungen erklären sollen.

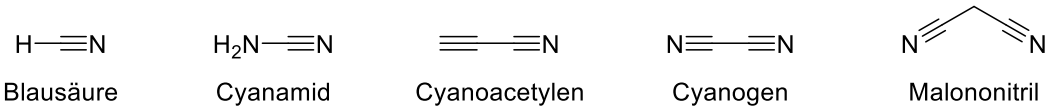

Abbildung 2. Nitrilische Verbindungen. Postulierte Vorläufermoleküle, welche die Entstehung des Lebens eingeleitet haben könnten, deren Bildung unter schwach reduzierenden Bedingungen jedoch problematisch ist.

Stark reduzierende Bedingungen

Eine verbreitete Hypothese zur Entstehung solcher Nitrile postuliert die Bildung einer temporär stark reduzierten Erdatmosphäre. So wird angenommen, dass beispielsweise der *Moneta*-Einschlag[79] vor 4,48 Mrd. Jahren genug Eisen auf die Erde gebracht haben könnte, um große Wassermengen zu reduzieren und eine Wasserstoff-Atmosphäre zu bilden.[80] Ihre Halbwertszeit wurde aufgrund der Flüchtigkeit des Wasserstoffs[80-82] auf 40 Mio. Jahre[64] geschätzt, was vor dem Hintergrund chemisch evolutionärer Prozesse eine lediglich geringe Zeitspanne darstellt. Zudem müssen Meteoriten für dieses Szenario eine bestimmte Größe gehabt haben. Ein zu kleiner Meteorit wäre nicht in der Lage gewesen eine ausreichende Reduktionskraft über längere Zeit zu generieren.[73, 80] Hingegen hätte ein zu großer Meteorit die Erdkruste entweder lokal[83] oder global[84] zum Schmelzen gebracht und somit bereits entstandenes organisches Material zerstört.[73] Ein Meteorit idealer Größe könnte jedoch die reduktive Bildung von Nitrilen wie Blausäure, Cyanoacetylen oder Cyanamid ermöglicht haben.[64] In diesem Zusammenhang wird gelegentlich vom Großen Bombardement (engl.: *Late Heavy Bombardment*, LHB) gesprochen.[85] Dieses hypothetische Ereignis postuliert den vermehrten Einschlag von Meteoriten auf die frühe Erde und ihren Mond und soll vor ca. 4,1 bis 3,8 Mrd. Jahren stattgefunden haben.[86-87] Ob dadurch genug Reduktionskraft generiert werden konnte,

bleibt jedoch fraglich, vor allem da die LHB-Theorie zunehmend angezweifelt wird, da sie möglicherweise auf Fehlinterpretationen beruht.[88-90]

Geochemische Akkumulation von Blausäure

Weitere Modelle postulieren die allmähliche Anreicherung von HCN, welches sich in Spuren durch aerodynamische Meteoritenablation[91] unter schwach reduzierenden Bedingungen gebildet haben könnte. Als flüchtige Verbindung (Sdp. = 25,6 °C) kann HCN jedoch nicht durch einfaches Eindampfen einer wässrigen Lösung aufkonzentriert werden.[92] Hierfür bedarf es eines eutektischen Gemischs, welches bei -23,4 °C eine maximale HCN-Konzentration von 74,5 mol% aufweist.[92] Alternativ könnte HCN in der Gegenwart von gelöstem Eisen(II) zunächst als Ferrocyanid $[Fe(CN)_6]^{4-}$ gebunden und angereichert worden sein, um nach anschließender Freisetzung präbiotische Reaktionen einzuleiten.[93-94] Studien lassen jedoch vermuten, dass dieses dynamische Gleichgewicht vernachlässigbar ist, da Ferrocyanide lediglich bei niedrigen Temperaturen und hohen HCN-Bildungsraten als stabiles Depot fungieren können.[93]

Interstellarer Ursprung

Während das Vorkommen chemischer Verbindungen auf der frühen Erde noch nicht vollständig geklärt werden konnte, konnte ihre Existenz im interstellaren Medium schon vor längerer Zeit nachgewiesen werden. So gibt es heute umfangreiche Datenbanken,[95-97] welche neben Blausäure, Cyanamid und Cyanoacetylen mehr als 270 interstellar und circumstellar detektierte Moleküle listen. Dies führte zu der Hypothese, dass organische Moleküle möglicherweise nicht *in situ* auf der frühen Erde entstanden sind, sondern durch Kometen, Asteroiden und interplanetare Staubpartikel auf diese gelangen konnten.[98-100] Es ist jedoch anzunehmen, dass in einem solchen Szenario der Großteil des organischen Materials durch das Eintreten in die Erdatmosphäre sowie den anschließenden Einschlag thermisch zerstört wurde.[98-103] Die Bedeutung interstellarer Moleküle zur Entstehung terrestrischen Lebens gilt daher oft als *übertrieben*[43].

1.3 Die RNA- und RNA-Peptid-Welt

Die Gemeinsamkeiten heutiger Lebewesen lassen sich auf zwei fundamentale Merkmale reduzieren. Das erste Merkmal ist die Speicherung genetischer Informationen mittels DNA oder RNA, welche durch Replikation die Weitergabe von Erbinformation ermöglicht. Zusätzlich besitzen lebende Organismen die Fähigkeit, biochemische Prozesse mit Hilfe von Proteinen (Enzymen) zu katalysieren. Da Proteine im Speziellen auch die DNA-Replikation katalysieren und die DNA wiederum für die Protein-Codierung verantwortlich ist, besteht eine gegenseitige Abhängigkeit beider Spezies.[104]

Evolutionär ist es schwierig, diese intrinsische Abhängigkeit durch das spontane Auftreten beider Biomoleküle zu erklären, welche sich zunächst unabhängig voneinander gebildet haben müssten. Ausgehend von dieser Problematik formulierte Gilbert im Jahre 1986 die sogenannte RNA-Welt-Hypothese. Diese besagt, dass weder DNA noch Proteine die ersten lebenden Prozesse eingeleitet haben, sondern RNA, da diese sowohl genetische Informationen speichern als auch chemische Reaktionen katalysieren kann. Folglich könnte RNA als eigenständiges Biomolekül sowohl die Aufgaben der DNA als auch die der Proteine übernommen und ein selbstreplizierendes System generiert haben. Dieses könnte durch evolutionäre Prozesse die zentralen Aufgaben anschließend auf die stabilere DNA sowie die katalytisch flexibleren Proteine übertragen haben.[105]

Eine weitere Hypothese geht auf *Eigen*[106] im Jahre 1981 zurück und beschreibt die Co-Evolution von RNA und Peptiden in einer sogenannten RNA-Peptid-Welt.[106-108] Aktuelle Studien demonstrieren, dass RNA-Peptid-Chimäre tatsächlich eine RNA-assoziierte Peptidsynthese ermöglichen.[108] Diese könnten die Entwicklung der ribosomalen Peptidsynthese eingeleitet haben und das Auftreten nicht-kanonischer Nukleoside in der heutigen rRNA bzw. tRNA erklären.[108]

Eine RNA-(Peptid)-Welt ist jedoch nur dann plausibel, wenn auch die Entstehung von RNA- bzw. Peptidbausteinen auf der frühen Erde möglich war. Daher versuchen Wissenschaftler Reaktionswege zu finden, wie aus einfachen Vorläufermolekülen (*vide supra*) Bausteine wie Zucker (Kapitel 1.3.1), Nukleobasen (Kapitel 1.3.2), Nukleoside (Kapitel 1.3.3) oder Aminosäuren (Kapitel 1.3.4) entstehen konnten.[26-28]

1.3.1 Zucker

Zucker sind essenzielle Bausteine biologischen Lebens und tragen neben metabolischen und immunologischen Funktionen auch zur Speicherung unserer Erbinformation bei. Ein wichtiger Vertreter ist die Ribose, welche als Baustein sowohl in RNA als auch DNA (als 2'-Desoxyribose) anzutreffen ist. Entsprechend sind Zucker auch von präbiotischer Bedeutung – sowohl aus protometabolischer Sicht als auch aus Sicht der RNA-Welt-Hypothese. Die präbiotisch wichtigsten Zuckervorstufen, Formaldehyd und Glycolaldehyd, bilden sich unter elektrischer Entladung in einer CO_2/H_2O-Atmosphäre.[18, 75] Mechanistische Studien von *Schreiner et al.* zeigen, dass die Dimerisierung von Formaldehyd zu Glycolaldehyd in Gasphase über Hydroxymethylen verläuft (Abbildung 3a),[109] welches durch UV-Strahlung gebildet und in einer konzertierten Carbonyl-En-Reaktion mit Formaldehyd unter Bildung des C2-Zuckers reagiert.[109] Die wichtigste Synthese komplexerer Zucker unter präbiotischen Bedingungen geht auf *Butlerow* zurück und wird landläufig als Formosereaktion bezeichnet.[17, 110] In dieser autokatalytischen Reaktion polymerisiert Formaldehyd in Gegenwart von Calciumhydroxid zu einer Vielzahl unterschiedlichster Zucker. Es folgten weitere Studien,[111-112] bis schließlich *Breslow* im Jahre 1959 einen Mechanismus zur Formosereaktion postulierte (Abbildung 3b).[113] Hierbei reagieren zunächst Formaldehyd und Glycolaldehyd in einer Aldolreaktion zu Glycerinaldehyd. Eine anschließende *Lobry-de-Bruyn–Alberda-van-Ekenstein*-Umlagerung ergibt Dihydroxyaceton, welches mit einem weiteren Äquivalent Formaldehyd in einer Aldolreaktion Ketotetrose bildet. Nach erneuter Isomerisierung kann die entstandene Aldotetrose eine retro-Aldolreaktion eingehen, wodurch zwei Äquivalente Glycolaldehyd entstehen und der Formosezyklus geschlossen wird. Reagieren dessen Intermediate in abgeänderter Reihenfolge, entsteht eine Vielzahl komplexer Zucker, von welchen der RNA-Baustein Ribose ebenfalls in Spuren (<1 %) entsteht.[114-115] Diese niedrige Ausbeute ist unter anderem auf die Isomerisierung von Glycolaldehyd zu Dihydroxyaceton zurückzuführen, welches nicht nur zu Ribose, sondern auch anderen, komplexeren Zuckern reagiert. Um eine Keto-Enol-Tautomerisierung zu vermeiden verwendeten *Eschenmoser et al.* Glycolaldehyd-2-phosphat (Abbildung 4a),[116] welches durch Phosphorylierung von Glycolaldehyd mit Diamidophosphat bzw. Amidotriphosphat zugänglich ist.[117-118] Eine Aldolreaktion mit Formaldehyd gibt Glycerinaldehyd-2-phosphat, welches diastereoselektiv mit Glycolaldehyd-2-phosphat zu Ribose-2,4-diphosphat reagiert.[116] Dieses

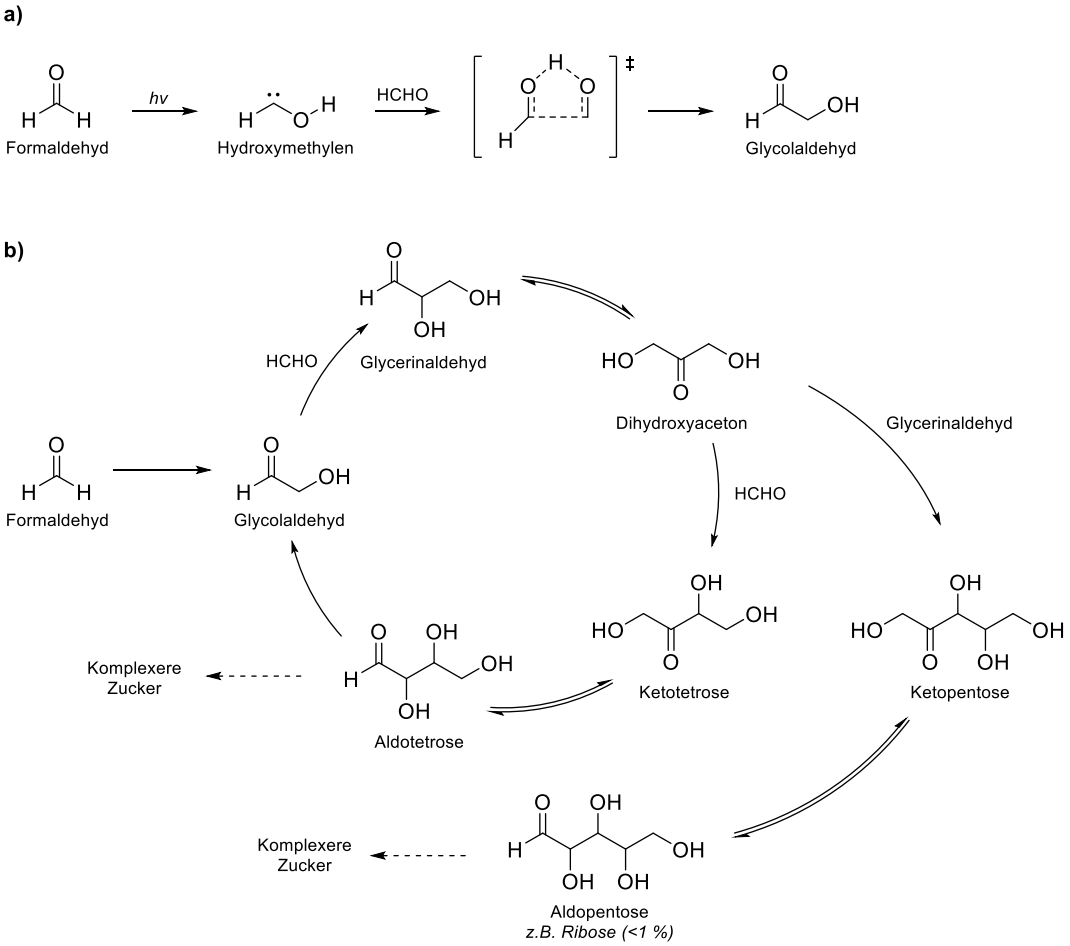

Abbildung 3. Zuckersynthese. (a) Dimerisierung von Formaldehyd über Hydroxymethylen zu Glycolaldehyd nach *Schreiner et al.*[109] (b) Formosezyklus zur autokatalysierten Synthese komplexer Kohlenhydrate aus Formaldehyd. [17, 113]

bildet sich unter kinetischer Kontrolle als Hauptprodukt neben weiteren Pentose-2,4-diphosphat-Isomeren.[116] Als weiterer Vorteil ist die pH-Stabilität der phosphorylierten Zuckerspezies zu nennen, welche ungeschützt zu unkontrollierter Polymerisation (Teer-Bildung) neigen.[76, 116]

Dass die Stabilität und Tautomerisierungseigenschaften von Zuckern nicht nur durch Phosphorylierung, sondern auch durch Borat-Komplexierung beeinflusst werden kann, konnte durch *Benner et al.* erfolgreich demonstriert werden (Abbildung 4b).[76, 119-120] Er stellte fest, dass eine Lösung aus Glycolaldehyd, Glycerinaldehyd und Calciumhydroxid durch Zugabe von Boratmineralien kein braunes Polymergemisch bildet wie sonst üblich, sondere kürzere Zucker wie beispielsweise Aldopentosen entstehen.[119] Mechanistisch scheint eine Borat-induzierte Enolisierung des Glycolaldehyds die Aldolreaktion mit Glycerinaldehyd zu begünstigen.[119] Gleichzeitig stabilisiert das Borat sowohl Glycerinaldehyd als auch die entstehenden

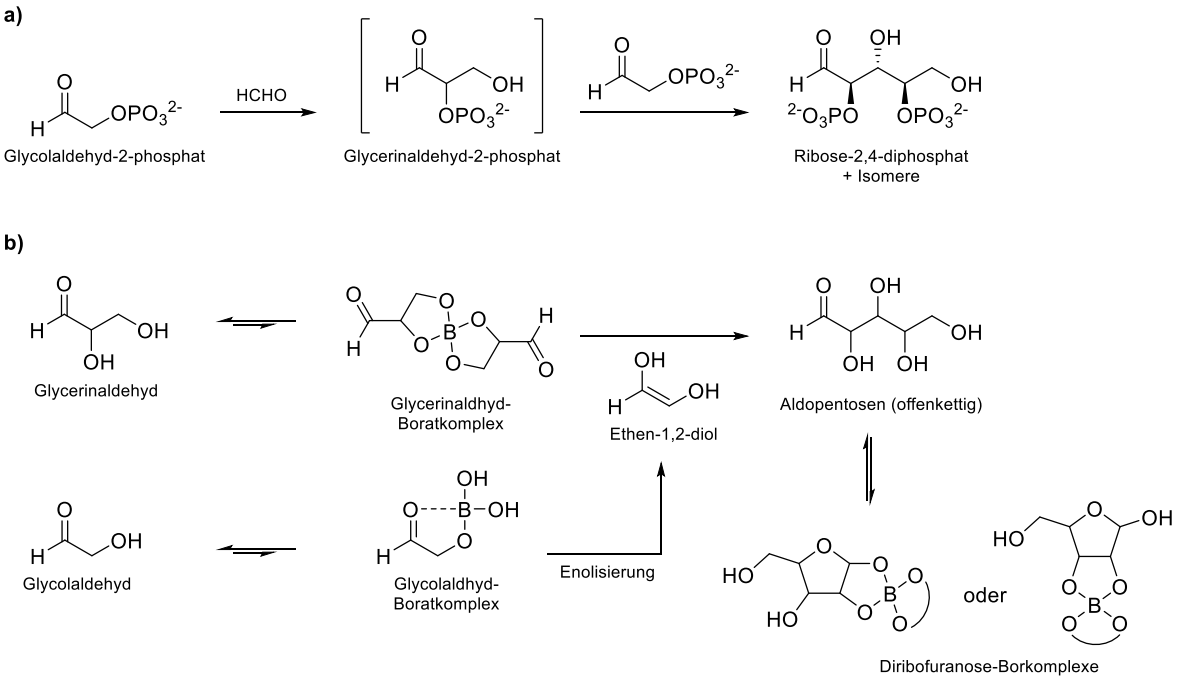

Abbildung 4. Bildung von Ribose. (a) Aldolkondensation zwischen Glycolaldehyd-2-phosphat und Formaldehyd nach *Eschenmoser et al.*[116] (b) Synthese und Stabilisierung von Ribofuranose in Gegenwart von Borat nach *Benner et al.*[119]

Ribofuranosen durch Komplexierung der 1,2- oder 2,3-*cis*-Diole.[119] Als Boratquelle wurden die natürlich vorkommenden Minerale Kernit ($Na_2B_4O_7$), Ulexit ($NaCaB_5O_9 \cdot 8H_2O$) und Colemanit ($Ca_2B_6O_{11} \cdot 5H_2O$) verwendet und als präbiotisch plausibel postuliert,[119] auch wenn das geologische Borat-Vorkommen auf der frühen Erde nicht unumstritten ist.[121] Die Boratkatalysierte Aldolreaktion begünstigt zwar die Entstehung von Aldopentosen, jedoch werden neben Ribose auch Arabinose, Xylose und Lyxose in ähnlichen Ausbeuten gebildet.[119]

Eine größere Selektivität gegenüber Ribose erlauben Aldolreaktionen, welche in der Gegenwart von Zink-Prolin-Komplexen durchgeführt werden (Abbildung 5).[122] Auf diese Weise bilden sich ausgehend von Glycerinaldehyd und Glycolaldehyd die Aldopentosen Ribose (19 %), Arabinose (14 %), Xylose (9 %) und Lyxose (21 %).[122] Die Selektivität gegenüber Ribose und Lyxose wird auf ihre *erythro*-Konfiguration zurückgeführt, wohingegen die Bildung von Arabinose und Xylose (*threo*-Konfiguration) kinetisch ungünstiger ist.[122]

Während sich die Isomerisierung durch Phosphate bzw. Borate beeinflussen lässt, stellt die hohe Reaktivität der Aldehydgruppen meist ein gesondertes Problem dar. Da Aldehyde für die reversible Bildung stabiler Bisulfit-Addukte bekannt sind,[123-125] entwickelten *Benner et al.* ein

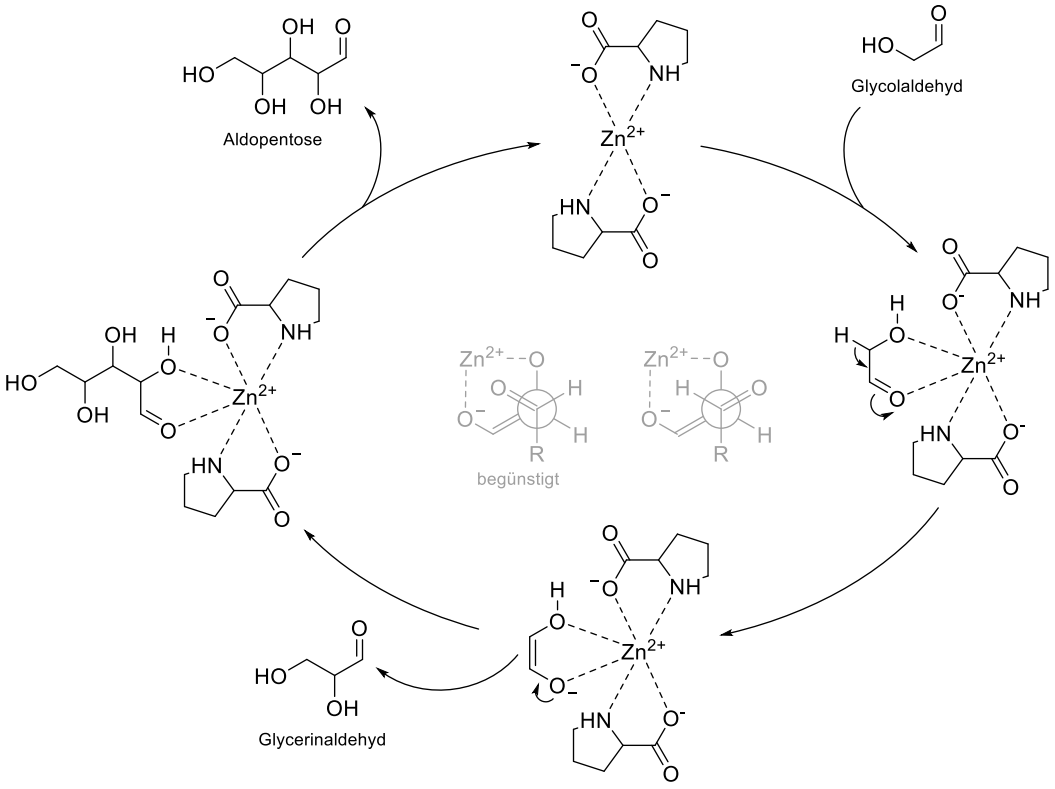

Abbildung 5. Zn^{2+}-Pro-katalysierte Synthese von Aldopentosen. Zink-Prolin-Komplexe katalysieren die Aldolreaktion zwischen Glycolaldehyd und Glycerinaldehyd. Die *erythro*-konfigurierten Aldopentosen Ribose und Lyxose entstehen bevorzugt, während Arabinose und Xylose (*threo*-Konfiguration) in geringeren Ausbeuten gebildet werden.[122]

präbiotisches Szenario, welches die Stabilisierung und Anreicherung von Zuckern in Gegenwart von SO_2 ermöglicht. Hierbei reagiert vulkanisches SO_2 unter wässrigen Bedingungen zu Hydrogensulfit, welches im Sauren mit Aldosen zu den entsprechenden Bisulfit-Addukten (α-Hydroxysulfonaten) reagiert. Sobald sich der pH-Wert erhöht, erfolgt die Umkehrreaktion unter Freisetzung der Aldosen, welche nun für präbiotische Reaktionen zur Verfügung stehen.[73, 126]

Da die Zuckerhomologisierung über die Formosereaktion schlecht kontrollierbar ist und oft zu ungewollten Polymerisationsprodukten führt, entwickelten *Sutherland et al.* eine *Kiliani–Fischer*-ähnliche Homologisierungsstrategie unter Verwendung von Blausäure als C1-Baustein.[127-129] Dieser regiert mit Aldehyden zu α-Hydroxynitrilen, welche zu α-Hydroxyiminen unter wässrigen Bedingungen reduziert werden und nach anschließender Hydrolyse die

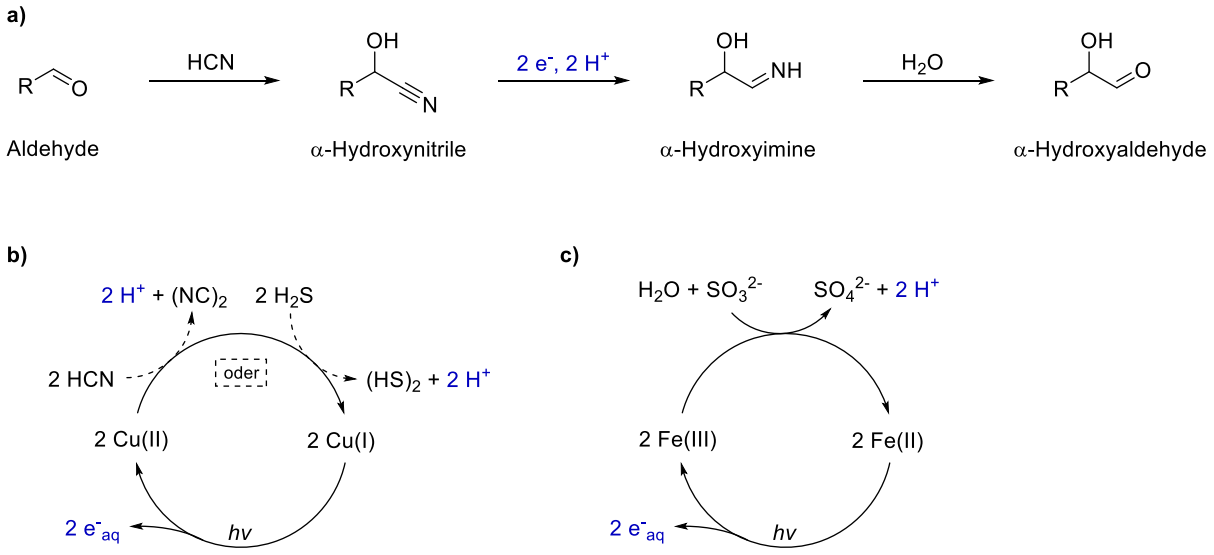

Abbildung 6. Zuckerhomologisierung. (a) Reduktive Homologisierung nach *Sutherland et al*.,[127-129] basierend auf (b) einem Cu(I)/Cu(II)-Photoredoxzyklus mit HCN[127] oder H_2S[128] als Reduktionsmittel bzw. (c) einem Fe(II)/Fe(III)-Photoredoxzyklus mit SO_3^{2-}[129] als Reduktionsmittel.

entsprechenden α-Hydroxyaldehyde bilden (Abbildung 6a).[127] Im Gegensatz zur traditionellen *Kiliani–Fischer*-Synthese, welche üblicherweise auf Wasserstoff und einem Palladium/Bariumsulfat-Katalysator beruht,[130-131] postulieren die Autoren die Bildung solvatisierter Elektronen und Protonen durch Photoredoxkatalyse.[127-129] Diese basiert entweder auf einem Cu(I)/Cu(II)-Katalysezyklus mit Blausäure[127] oder Schwefelwasserstoff[128] als Reduktionsmittel (Abbildung 6b) oder auf einem Fe(II)/Fe(III)-Katalysezyklus mit Hydrogensulfit[129] als reduzierende Spezies (Abbildung 6c). Obwohl die Photoredoxchemie eine mögliche Verknüpfung zwischen Zucker-, Nukleobasen- und Aminosäuresynthese (*vide infra*) darstellt,[132-134] ist die präbiotische Plausibilität der Reaktionsbedingungen vor dem Hintergrund neuester geologischer Kenntnisse (Kapitel 1.2.2) kritisch zu beurteilen.

1.3.2 Nukleobasen

Die erste präbiotische Synthese von Purinbasen gelang *Orò* im Jahre 1960, als er durch Erhitzen einer wässrigen Ammoniumcyanid-Lösungen (>1,0 M) Adenin in ca. 0,5 % Ausbeute erhielt.[21] Diese Beobachtung wurde auf die sequenzielle Polymerisation von HCN zurückgeführt und legte den Grundstein für die präbiotische Nukleosidchemie.[21] Es folgten mehrere mechanistische Studien, welche unter anderem Formamidin, 4-Aminoimidazol-5-carbonitril (AICN) und 2-Aminoimidazol-5-carboxamid (AICA) als Intermediate postulieren (Abbildung 7).[135-136] In ergänzenden Studien beschrieben *Ferris* und *Orgel* die Bedeutung weiterer Zwischenstufen, wie unter anderem Aminomalononitril (AMN) und Diaminomaleonitril (DAMN).[15, 137] Zusätzlich wurden Synthesewege zu weiteren Purinbasen postuliert, von welchen u.a. Guanin, Xanthin und Inosin experimentell nachgewiesen werden konnten.[138-139] Auf der Suche nach Pyrimidinbasen identifizierten Lowe und Ferris vor allem 5-Hydroxyuracil, 4,5-Dihydroxypyrimidin sowie Orotsäure.[140-141] Während Uracil als kanonische Nukleobase zumindest in Spuren nachgewiesen werden konnte, blieb die Suche nach Cytosin jedoch erfolglos.[139]

Trotz der genannten Erfolge wurde die Plausibilität der verwendeten HCN-Konzentrationen (1.0-11.0 M) später in Frage gestellt.[142] Neben der ineffizienten Bildung und Anreicherung von HCN unter schwach reduzierenden Bedingungen (*vide supra*) ist auch die geringe Stabilität ein problematischer Faktor. HCN ist nicht nur thermisch instabil, sondern zersetzt sich vor allem auch in Gegenwart von UV-Strahlung zu Urea, Cyanamid und Guanidin.[143] Zudem hydrolysiert HCN sowohl unter sauren als auch unter basischen Bedingungen zu Formamid und Ameisensäure.[144] Da Formamid im Gegensatz zu HCN wesentlich hydrolysestabiler ist, einen höheren Siedepunkt (Sdp. = 210 °C) besitzt und sich folglich leichter anreichern lässt, wird Formamid häufig als präbiotisch plausiblere Nukleobasen-Vorstufe betrachtet. Diese wurde zum ersten Mal von *Yamada* 1972 für die Synthese von Purin verwendet,[145] worauf viele Wissenschaftler dieser neuen Idee folgten.[146] So konnte durch das Erhitzen von Formamid in der Gegenwart von Metalloxiden die Bildung von Purin, Adenin, Cytosin und verschiedener Pyrimidinone beobachtet werden,[147] während die Verwendung verschiedener Phosphatminerale die zusätzliche Bildung von Hypoxanthin, Uracil und 5,6-Dihydrouracil erzielte.[148]

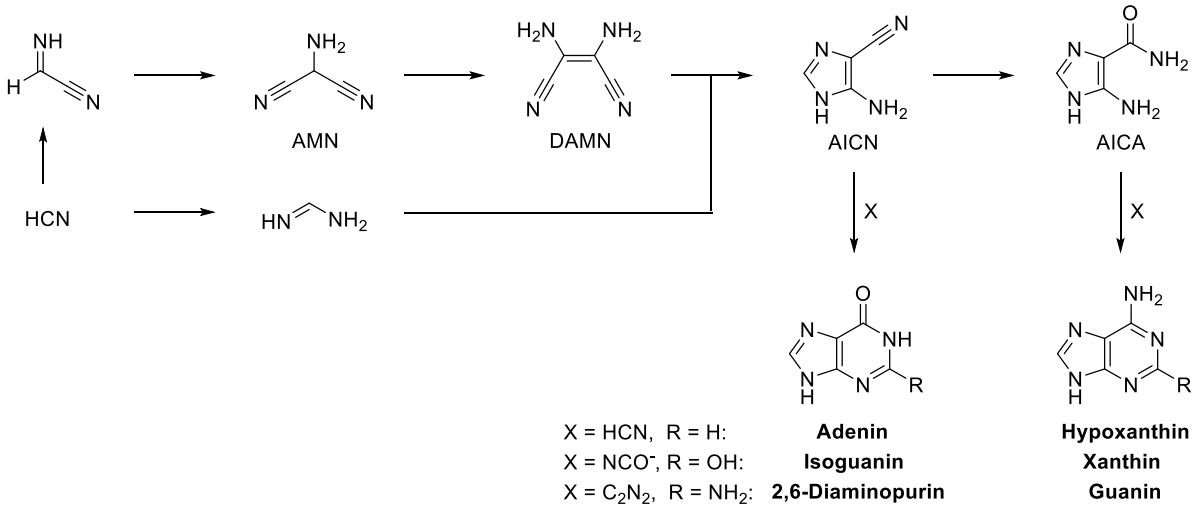

Abbildung 7. Purinsynthese. Synthesewege zu kanonischen und nicht-kanonischen Purinbasen ausgehen von HCN nach *Orò et al.*, *Ferris* und *Orgel*.[135-141]

Zur präbiotischen Synthese der Pyrimidinbasen wurde neben HCN und Formamid vor allem Cyanoacetylen als vielversprechende Ausgangsverbindung verwendet. Dessen Bildung erfolgt typischerweise durch Blitzentladung in einem Methan-Stickstoff-Gasgemisch[149] oder durch Kupfer(II)-katalysierte Kreuzkupplung von HCN und Acetylen.[132] Im Jahre 1966 demonstrierte die Gruppe um *Orgel* erstmals die Bildung von Cytosin aus Cyanoacetylen und Urea mit 5 % Ausbeute.[149] Die Reaktion von Cyanoacetylen mit Kaliumcyanat erzielte bei 100 °C ähnliche Ergebnisse[149] und konnte später von *Ferris et al.* auf 30 °C mit anschließender Hydrolyse optimiert werden (Abbildung 8).[141] Wird diese Reaktion mit zwei Äquivalenten Cyanat in DMF durchgeführt, entsteht *trans*-Cyanovinylurea, welches in 1 M Natronlauge quantitativ zu Cytosin bzw. Uracil reagiert.[150]

Ausgehend von Cyanoacetylen entwickelten *Carell et al.* einen alternativen Syntheseweg, welcher den Zugang zu kanonischen sowie nicht-kanonischen Pyrimidinen bietet. Dieser beginnt mit der Umwandlung von Cyanoacetylen zu einem α,β-ungesättigten Thioamid, indem Cyanoacetylen zunächst mit Dimethylamin und anschließend mit Diammoniumsulfid umgesetzt wird. Die mehrstufige Reaktion des α,β-ungesättigten Thioamids mit *N*-Methyl-*N*-nitrosourea (MNU) ergibt 4-Methylthiouracil (ms^4U), welches als universelle Pyrimidinvorstufe fungiert. Die Hydrolyse von ms^4U ergibt Uracil, während die Umsetzung mit unterschiedlichen

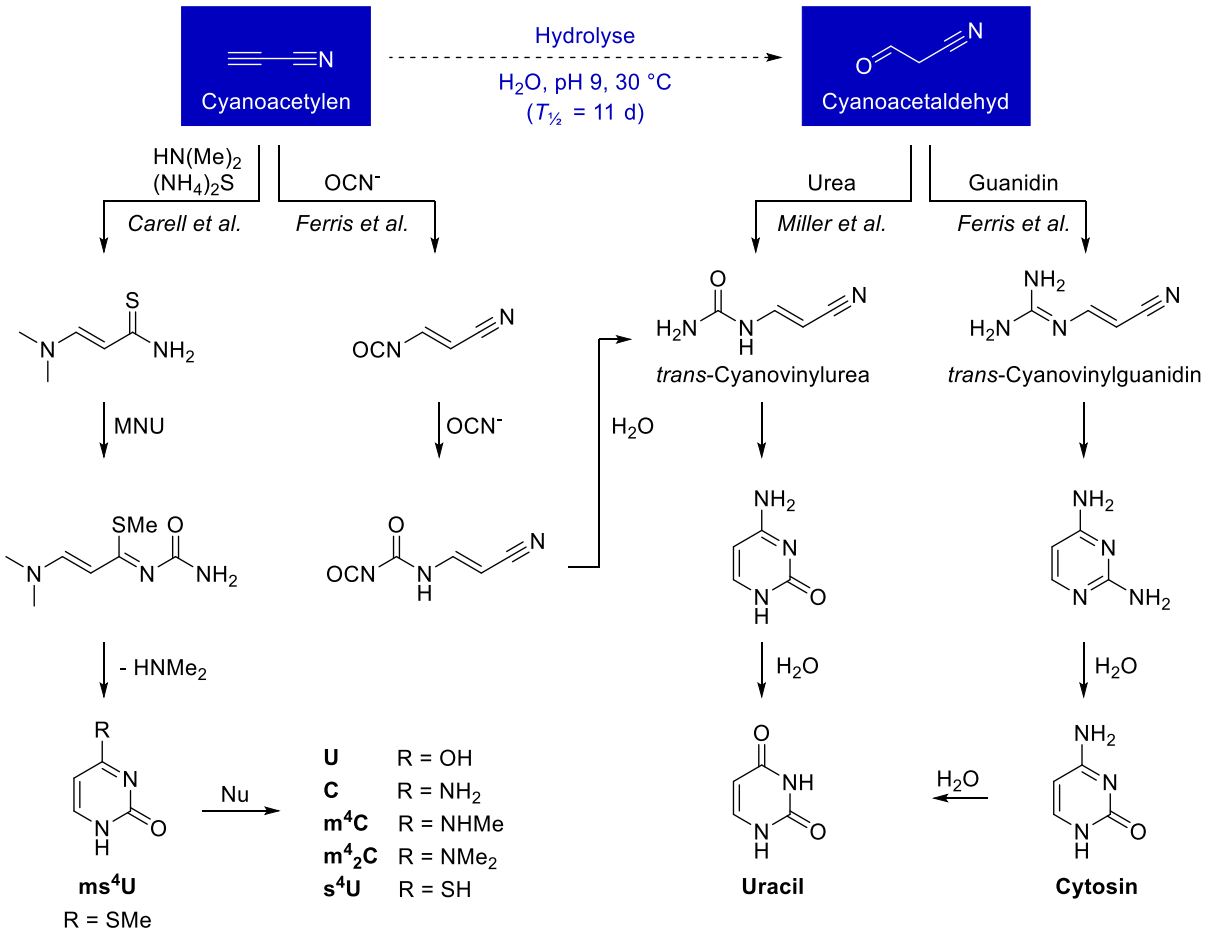

Abbildung 8. Pyrimidinsynthese. Bildung kanonischer und nicht-kanonischer Pyrimidinbasen nach *Miller et al.*[152, 153], *Ferris et al.*[141, 150] und *Carell et al.*[151] ausgehend von Cyanoacetylen bzw. Cyanoacetaldehyd.

Nukleophilen den Zugang zu weiteren Nukleobasen ermöglicht. Auf diese Weise führt die Reaktion mit Aminen wie Ammoniak, Mono- oder Dimethylamin zur Bildung von Cytosin (C), N^4-Methylcytosin (m^4C) bzw. N^4,N^4-Dimethylcytosin ($m^4{}_2C$). Ebenfalls konnte 4-Thiouracil (s^4U) durch Thiolyse von ms^4U erhalten werden.[151]

Während die hohe Reaktivität des Cyanoacetylens die Pyrimidinsynthese allgemein begünstigt, ist dessen rasche Hydrolyse zu Cyanoacetaldehyd ein Dorn im Auge vieler Wissenschaftler. Eine Halbwertszeit von ca. 11 Tagen in wässrigem Puffer (pH 9, 30 °C)[141, 150] macht die langfristige Anreicherung von Cyanoacetylen aus präbiotischer Sicht problematisch. Aus diesem Grund entwickelten *Ferris et al.* eine Pyrimidinsynthese (Abbildung 8), welche nicht von Cyanoacetylen, sondern von dessen Hydrolyseprodukt Cyanoacetaldehyd ausgeht.[150] Wird Cyanoacetaldehyd mit Guanidin umgesetzt, bildet sich 2,4-Diaminopyrimidin, welches anschließend zu Cytosin und Uracil hydrolysiert.[150] Einen ähnlichen Ansatz verfolgten

Miller et al. (Abbildung 8), indem sie konzentrierte Urea-Lösungen (bis 20 M) mit Cyanoacetaldehyd auf 100 °C erhitzten.[152] Hierbei erhielten sie Cytosin in 30-50 % Ausbeute, dessen Bildung über *trans*-Cyanovinylguanidin verläuft.[152] Um präbiotisch plausiblere Bedingungen zu simulieren, wurde die Reaktion mit niedrigeren Harnstoff-Konzentrationen (2 M) unter Nass-Trocken-Zyklen demonstriert, was eine Cytosin-Ausbeute von 12,8 % erzielte.[153] Obwohl verschiedene Szenarien entwickelt wurden um die präbiotische Entstehung von Cyanoacetylen bzw. Cyanoacetaldehyd zu erklären,[132, 149] ist dessen präbiotische Plausibilität nach wie vor stark umstritten.[64, 154]

1.3.3 Nukleoside

Nachdem die Entstehung von Zuckern und Nukleobasen unter präbiotischen Bedingungen demonstriert wurde, folgte die Nukleosidsynthese als logische Konsequenz. Während die präbiotische Forschung zu Zuckern und Nukleobasen vielversprechende Ergebnisse erzielte, erwies sich deren Verknüpfung zu Nukleosiden zunächst als wenig erfolgreich. Dieses Nukleosidierungsproblem – ein Begriff der später von *Leslie Orgel* etabliert wurde – schien lange Zeit unlösbar.[16]

Erst in den letzten Jahren haben neue Nukleosidierungsstrategien die präbiotische Chemie entscheidend vorangebracht. Die unterschiedlichen Ansätze werden zuweilen in zwei Kategorien unterteilt: Die *direkte Nukleosidierung* (Abbildung 9, links) beschreibt die Glykosylierung einer Nukleobase oder einer Vorläuferbase in Gegenwart eines Zuckers. Im Falle der Vorläuferbase entsteht zunächst ein Vorläufernukleosid, welches anschließend in das gewünschte Nukleosid umgewandelt wird. Weiterhin wird von einer *indirekten Nukleosidierung* (Abbildung 9, rechts) gesprochen, wenn sowohl der Zucker als auch die Nukleobase nicht separat gebildet werden, sondern einem gemeinsamen, typischerweise trizyklischen Vorläufermolekül entspringen. Dessen Synthese vereint meist die Schlüsselschritte und Ausgangsverbindungen der Nukleobasen- und Zuckerchemie. Jede dieser Nukleosidierungsstrategien bringt seine eigenen Vor- und Nachteile mit sich, welche im Folgenden an einigen Beispielen erläutert werden.[27]

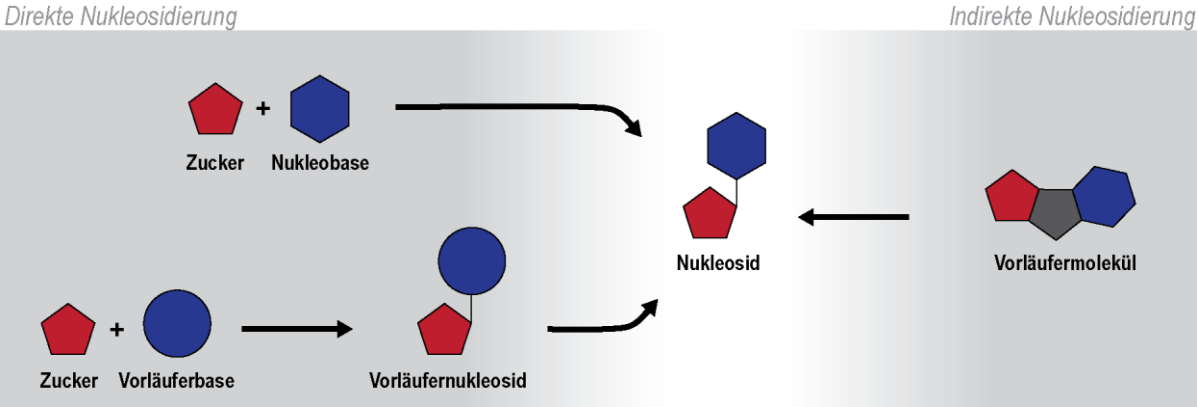

Abbildung 9. Nukleosidierungsstrategien. Während der direkten Nukleosidierung erfolgt die Glykosylierung einer Nukleobase oder Vorläuferbase in Gegenwart eines freien Zuckers. Während der indirekten Nukleosidierung erfolgt der verknüpfte Aufbau von Zucker und Nukleobase unter Bildung eines gemeinsamen Vorläufermoleküls.[27]

1.3.3.1 Direkte Nukleosidierung

Die erste Nukleosidsynthese unter präbiotisch plausiblen Bedingungen geht auf *Orgel* in den 1970er Jahren zurück und basiert auf der direkten Umsetzung von Purinbasen mit D-Ribose und Magnesiumchlorid (Abbildung 10). Tatsächlich konnte die Bildung verschiedener β-D-Ribofuranoside wie Adenosin, Guanosin und Inosin beobachtet werden. Allerdings erwies sich diese Strategie aufgrund geringer Ausbeuten (4-9 %) als ineffizient. Der Grund hierfür ist die Vielzahl nukleophiler Stickstoffatome, welche neben dem *N*(9)-Stickstoff ebenfalls eine glykosidische Bindung ausbilden können. So begünstigt die exozyklische Aminogruppe des Adenins die Bildung von *N*-6-Adenosin, während das kanonische *N*-9-Adenosin lediglich in Spuren von bis zu 4 % Ausbeute entsteht.[155]

Während Purinnukleoside zumindest in Spuren nachgewiesen werden konnten, verlief die Glykosylierung der Pyrimidinbasen Cytosin, Uracil und Thymin unter den oben genannten Bedingungen erfolglos.[156] Diese Beobachtung ist auf eine kinetische Barriere zurückzuführen, welche durch die Delokalisierung des *N*(1)-Elektronenpaars hervorgerufen wird.[157] Das eingangs erwähnte Nukleosidierungsproblem ist also intrinsischer Natur; erklärbar durch die schlechte bzw. ambidente Nukleophilie der kanonischen Nukleobasen.

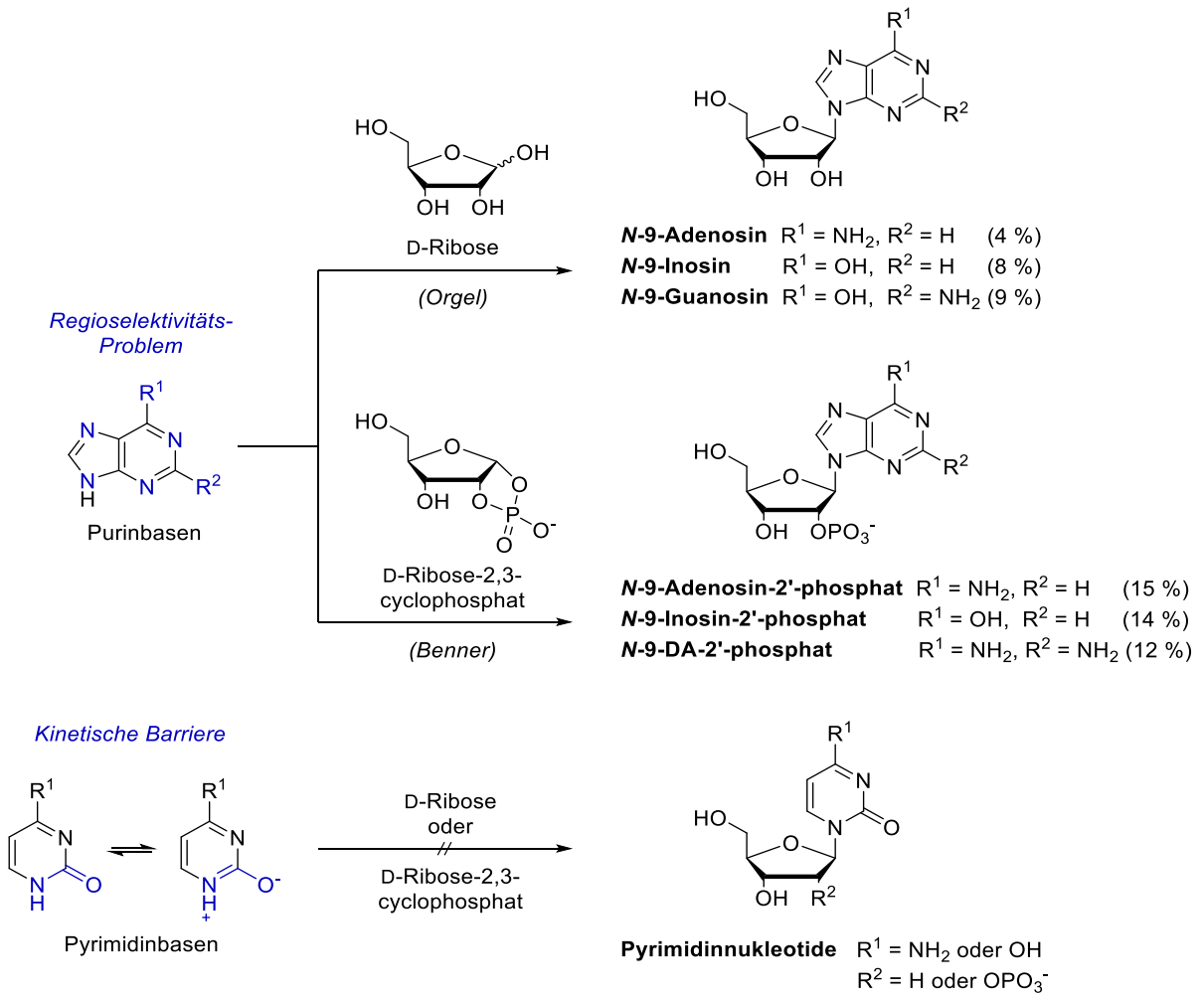

Abbildung 10. Direkte Ribosylierung von Purin- und Pyrimidinbasen. Nach *Orgel* verläuft die Reaktion der Purinbasen mit D-Ribose unselektiv unter der Bildung verschiedener Regio- und Stereoisomere.[155, 159] Nach *Benner* erzielt das entsprechende 2,3-Cyclophosphat als aktivierte Spezies höhere Ausbeuten, ermöglicht jedoch nicht die Bildung von Guanosin-2'-phosphat. Die Glykosylierung der Pyrimidinbasen verläuft in beiden Fällen erfolglos.[156, 159]

Um die direkte Nukleosidierung zu begünstigen, wurde in einigen Studien aktivierte Ribose verwendet. So nutze *Orgel* in ersten Versuchen Ribose-1-phosphat zur Aktivierung des anomeren Zentrums, was sich jedoch als Fehlschlag herausstellte.[16] Auch die Verwendung von Ribose-5-phosphat-1-pyrophosphat wurde als potentielle Lösung postuliert, jedoch nicht weiter verfolgt.[158] Später rückte Ribose-1,2-cyclophosphat in den Fokus, dessen präbiotische Synthese aus Ribose und Amidophosphaten durch *Eschenmoser* etabliert wurde.[118] Mit dieser aktivierten Spezies gelang es *Benner*, Adenosin-, Inosin- und Diaminopurinphosphate in vergleichsweise hohen Ausbeuten (15 %, 14 % bzw. 12 %) zu synthetisieren

(Abbildung 10).[159] Der Zugang zu Guanosin sowie zu den Pyrimidinnukleotiden blieb unter diesen Bedingungen jedoch verwehrt.[159] Erst in späteren Studien konnte unter wasserfreien Bedingungen und hohen Temperaturen alle vier kanonischen Nukleotide nachgewiesen werden – wenn auch nur in geringen Ausbeuten (G und U jeweils < 1 %).[160]

Neben der chemischen Aktivierung von Ribose wurde auch der Einfluss physikalischer Effekte untersucht. So konnte gezeigt werden, dass Tonmineralien wie beispielsweise Kaolinit unter Nass-Trocken-Zyklen die Bildung von β-Adenosin begünstigen.[161] Es wird postuliert, dass dieses Mineral sowohl die Konzentrierung auf dessen Oberfläche ermöglicht als auch katalytisch aktiv ist.[161] Die Verwendung von pyrogenem Siliciumdioxid ermöglicht wiederum die Bildung von Adenosinmonophosphat (AMP) aus KH_2PO_4, D-Ribose und Adenin.[162] Diese Oberflächenreaktion verläuft nachweislich über Phosphoribosylpyrophosphat (PRPP) als reaktives Intermediat.[162] Neben dem Einsatz katalytisch aktiver Minerale bieten auch sogenannte Mikrotropfen einen thermodynamischen Vorteil,[163-164] deren geringer Durchmesser (<1.3 µm) eine signifikante Entropieerniedrigung bewirkt und die Phosphorylierungs-[163] und Glykosylierungsreaktionen[164] exergonisch ablaufen lässt. Ausgehend von D-Ribose, Nukleobasen, Phosphorsäure und bivalenten Magnesiumionen (Mg^{2+}) konnten auf diese Weise Uridin (2,5 %), Adenosin (2,5 %), Cytidin (0,7 %) und Inosin (1,7 %) synthetisiert werden.[164] Die Umsetzung des schlecht löslichen Guanins blieb erfolglos.[164] Trotz der beschriebenen Strategien liefert die Kondensation zwischen Nukleobasen und Ribose keine zufriedenstellenden Ergebnisse, was insgesamt auf eine schlechte Regioselektivität bzw. Ausbeute zurückzuführen ist. [165]

Um das Selektionsproblem zu lösen, glykosylierten *Carell et al.* Formamidopyrimidine (FaPys, Abbildung 11), welche unter thermischen oder basischen Bedingungen zu Purinen reagieren.[165] Im Gegensatz zu kanonischen Nukleobasen bieten FaPys den Vorteil, dass die exozyklischen Aminogruppen (in C4- und C6-Position) aufgrund ihrer Nukleophilie sowie Spiegelsymmetrie eine regioselektive Kondensation mit Aldosen ermöglichen. Auf diese Weise sind Vorstufen zu *N*9-Purinnukleosiden erstmals in hohen Ausbeuten unter präbiotisch plausiblen Bedingungen zugänglich. Die Synthese der FaPys erfolgt durch die Veresterung von Aminopyrimidinen (AminoPys) mit Ameisensäure und erfolgt regioselektiv in *N*5-Position. Diese AminoPys können ihrerseits durch die Reaktion von α-Aminocyaniden mit Guanidin oder Thioharnstoff hergestellt werden (Abbildung 11, blau). Während die α-Aminocyanide als (hydrolysierte) HCN-Trimere angesehen werden können, entstehen die erforderlichen Amidine durch das Einwirken von Ammoniak bzw. Schwefelwasserstoff auf Cyanamid.[166]

Ein später durch *Carell et al.* entwickelter Syntheseweg ermöglicht zusätzlich die präbiotische Bildung weiterer FaPys (Abbildung 11, rot). Dieser Weg beginnt mit der Nitrosierung von Malononitril zu Hydroxyiminomalononitril (HIMN)-Salzen in Gegenwart verschiedener Amidiniumderivate. Die auskristallisierten HIMN-Salze zersetzen sich anschließend unter Zyklisierung zu Nitrosopyrimidinen (NitrosoPys), welche als schlecht lösliche Aromaten aus wässriger Lösung ausfallen und sich somit präbiotisch anreichern lassen. In Gegenwart von Eisen oder Nickel erfolgt eine anschließende Reduktion zu den entsprechenden AminoPys. Wird die Reduktion in verdünnter Ameisensäure durchgeführt, ist eine direkte Umwandlung der NitrosoPys zu FaPys zu beobachten.[167]

Die Kondensationsreaktion zwischen FaPys und D-Ribose erfolgt in der Gegenwart von Borsäure. Eine anschließende intramolekulare Kondensationsreaktion führt zur finalen Zyklisierung und Bildung der kanonischen bzw. nicht-kanonischen *N*9-Purinnukleoside. Während die Ribosylierung regioselektiv verläuft, kann die Isomerie des Zuckers nur eingeschränkt

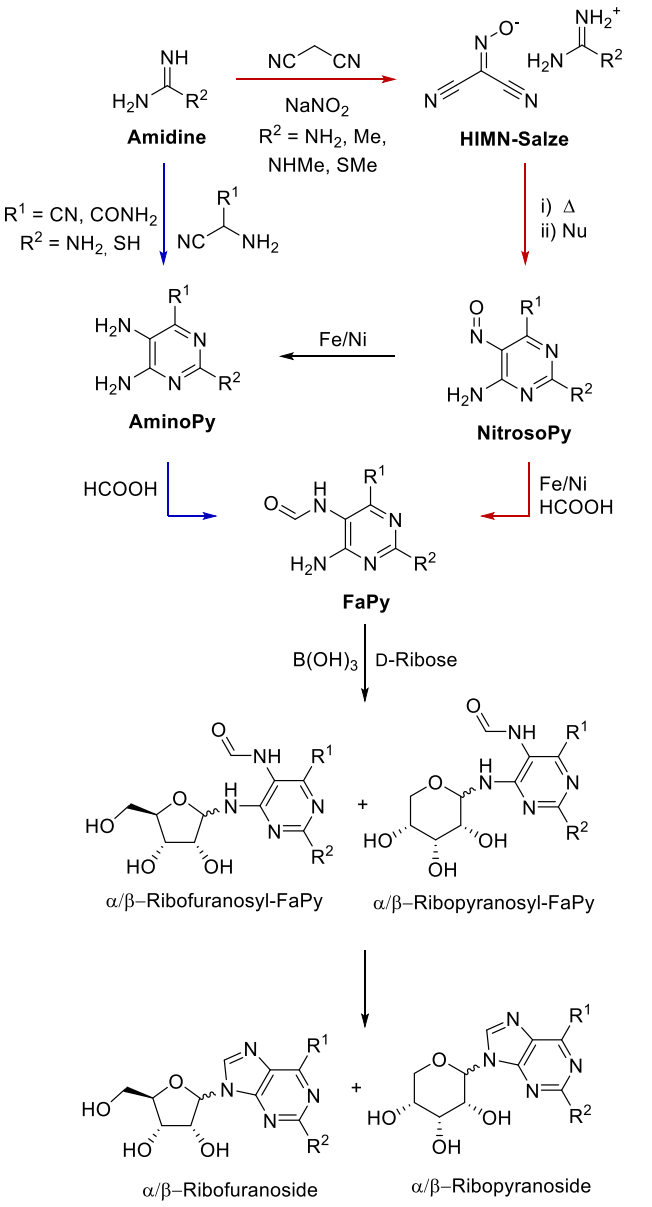

A	$R^1 = NH_2$, $R^2 = H$	**G**	$R^1 = OH$, $R^2 = NH_2$
DA	$R^1 = NH_2$, $R^2 = NH_2$	**m²G**	$R^1 = OH$, $R^2 = NHMe$
m²A	$R^1 = NH_2$, $R^2 = Me$	**m²₂G**	$R^1 = OH$, $R^2 = NMe_2$
ms²A	$R^1 = NH_2$, $R^2 = SMe$		

Abbildung 11. Direkte Ribosylierung von Purin-Vorläuferbasen. Die Synthese erfolgt ausgehend von Malononitrilderivaten und verschiedenen Amidinen, welche durch Nass-Trocken-Zyklen zunächst zu NitrosoPys und anschließend zu FaPys reagieren. Letztere werden selektiv unter Bildung der entsprechenden Furano- und Pyranosiden ribosyliert. Im letzten Schritt erfolgt die Umwandlung der FaPy-Nukleoside zu kanonischen bzw. nicht-kanonischen Nukleosiden.[166, 167]

beeinflusst werden. Zwar stabilisiert Borat furanosidische Isomere, jedoch kann die Bildung von Pyranosiden nicht gänzlich vermieden werden.[166-167]

Eine simple Abfolge von Nass- und Trockenzyklen sowie milde Temperatur- und pH-Änderungen ermöglichen auf diese Weise die präbiotische Synthese verschiedenster Nukleosidvorstufen. Diese bieten nicht nur Zugang zu kanonischen, sondern auch zu nicht-kanonischen Purinnukleosiden, welche, wie heute bekannt, wichtige regulatorische Funktionen in biologischen Systemen ausüben.[167-168]

1.3.3.2 Indirekte Nukleosidierung

Während die Entstehung von Purinnukleosiden mittels direkter Nukleosidierung erklärt werden konnte, stellte die Bildung der Pyrimidinnukleoside eine Herausforderung dar. In Folge dessen entwickelte *Orgel* eine Pyrimidinnukleosid-Synthese (Abbildung 12),[169] welche strategisch dem *de novo* Biosyntheseweg[170] ähnelt. Diese indirekte Nukleosidierung verfolgt den schrittweisen Aufbau der Pyrimidinbase am Furanosering unter Ausbildung eines trizyklischen Systems. Dessen Spaltung generiert anschließend das entsprechende Nukleosid bzw. Nukleotid. Für diese Strategie nutzen *Orgel et al.* wahlweise D-Ribose bzw. D-Ribose-5-phosphat, welche sich mit Cyanamid zu den entsprechenden Aminooxazolinen umsetzen lassen. Diese reagieren anschließen als ambidente Nukleophile mit Cyanoacetylen unter Bildung eines anellierten Pyrimidinrings. Die auf diese Weise entstandenen α-Anhydronukleoside/-tide hydrolysieren in Phosphatpuffer zu den jeweiligen α-Ribonukleoside/-tiden. Unter Einwirkung von UV-Strahlung ist schließlich eine Photoisomerisierung zu den natürlich vorkommenden Anomeren β-Cytidin (4 %) bzw. β-Cytidin-5‘-phosphat (6 %) zu beobachten.[169]

Seit der Veröffentlichung im Jahre 1970 wurde der von *Orgel* postulierte Syntheseweg in vielen Studien aufgegriffen, optimiert und auf verschiedene Nukleoside ausgeweitet (*vide infra*).[171-173] Die schlechten Ausbeuten konnten später auf Nebenreaktionen zurückgeführt werden, wie beispielsweise der C2‘-Epimerisierung oder dem intramolekularen Angriff der C2‘-Hydroxygruppe an den Pyrimidinring unter Bildung von Oxazolidinonen.[174] Wird α-Cytidin-5‘-phosphat vor der Photoisomerisierung acetyliert, kann die Ausbeute an β-Anomeren auf 22 % gesteigert werden.[175]

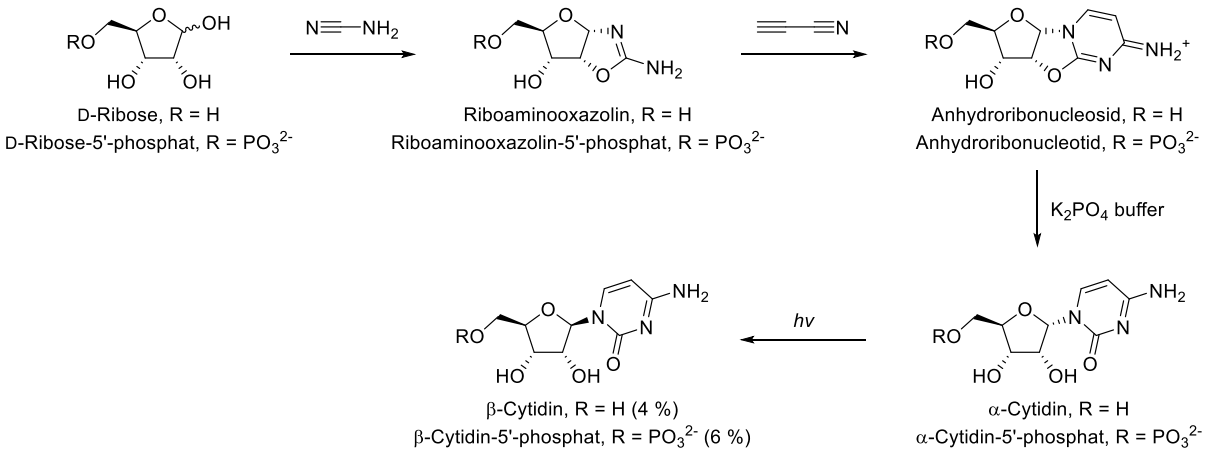

Abbildung 12. Indirekte Ribosylierung von Pyrimidinen. Synthese von β-Cytidin bzw. β-Cytidin-5‘-phosphat nach *Orgel et al.* ausgehen von D-Ribose, Cyanamid und Cyanoacetylen mit anschließender Photoanomerisierung.[169]

Eine Anpassung der oben beschriebenen Syntheseroute erfolgte durch *Sutherland et al.* (Abbildung 13). Diese nutzten im Gegensatz zu *Orgel* keine freie Ribose, sondern etablierten einen schrittweisen Aufbau des Furanoserings aus weniger komplexen Zuckereinheiten. Laut den Autoren beruht die Plausibilität dieser Strategie auf der Instabilität freier Ribose sowie ihrer umstrittenen selektiven Entstehung. Der postulierte Syntheseweg beginnt mit Cyanamid und Glycolaldehyd, welche in einem 1 M Phosphatpuffer zu 2-Aminooxazol reagieren. Nach der Zugabe von Glycerinaldehyd erfolgt die Umsetzung zu Aminooxazolin, welches in allen vier Konfiguration als Arabino- (15 %), Ribo- (25 %), Lyxo- (4 %) und Xyloaminooxazolin (6 %) vorliegt. Die Autoren stellten zunächst die Hypothese auf, dass lediglich Arabinoaminooxazolin für die präbiotische Synthese der Pyrimidinnukleoside von Bedeutung ist (Abbildung 13, blau). Dieses reagiert, analog zur Strategie von *Orgel et al.*, mit Cyanoacetylen zum Arabinoanhydrocytidin. Anstelle einer Hydrolyse erfolgt eine Phosphorylierung im Phosphatpuffer unter Bildung von Cytidin-2‘,3‘-cyclophosphat. Diese erfolgt hierbei zunächst regioselektiv in C3‘-Position, was entsprechend der Kristallstruktur auf eine sterische Abschirmung der 5‘-Hydroxygruppe zurückgeführt werden kann (Abbildung 14). Ein intramolekularer Angriff der Phosphatgruppe an den C2‘-Kohlenstoff führt anschließend zur Spaltung des Oxazolidinrings und Bildung des Pyrimidinnukleotids. Diese C2‘-Inversion erfolgt stereospezifisch unter Ausbildung des Ribo-Epimers.[176]

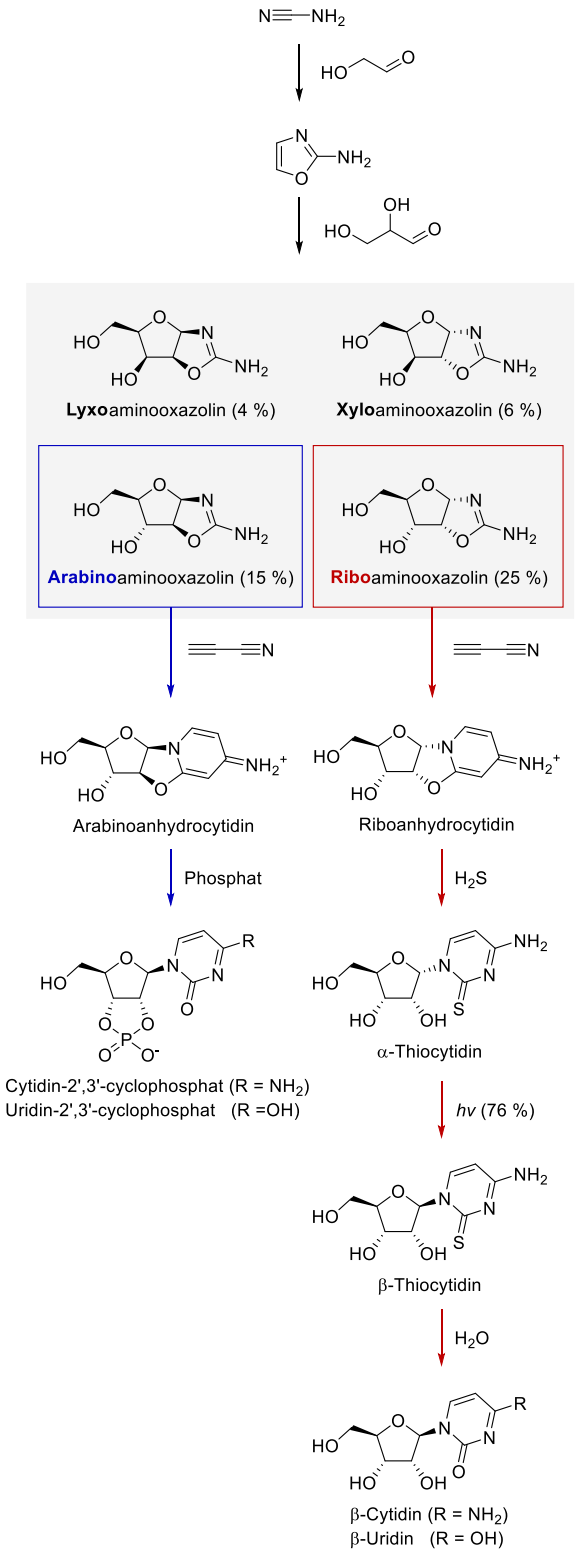

Obwohl dieser Syntheseweg erstmals die Bildung von Pyrimidinnukleosiden in guten Ausbeuten erklären könnte, gibt es Kritikpunkte, die die präbiotische Plausibilität zumindest teilweise in Frage stellen. Hier ist zunächst die sehr hohe Phosphatkonzentration von 1 M zu nennen, welche zur Synthese des 2-Aminooxazols verwendet wurde, die aufgrund der schlechten Löslichkeit von Phosphatmineralien jedoch nur schwer zu erreichen ist.[177] Derart hohe Phosphatkonzentrationen sind ebenfalls erforderlich, um die Hydrolyse des Anhydronukleosids zu vermeiden, welche im ungepufferten System als Konkurrenzreaktion zur Phosphorylierung auftritt.[176] Auch wird die Problematik der selektiven Ribosesynthese nur bedingt gelöst, da die Formosereaktion zwar umgangen wird, jedoch eine Vielzahl unerwünschter Epimere entsteht.[176] Wie die Autoren später selbst bemängeln, lässt sich das benötigte Arabino-Epimer im Gegensatz zum Ribo-Epimer nicht selektiv auskristallisieren und anreichern.[178] Zudem sind Glycolaldehyd und Glycerinaldehyd vergleichsweise instabil und erfordern eine zeitversetzte Zugabe.[179] Um diesen Punkt zu entkräften, demonstrierten *Powner et al.* in

Abbildung 13. Optimierte indirekte Ribosylierung von Pyrimidinen. Synthese von (blau) β-Cytidin- und β-Uridin-2‘,3‘-cyclophosphat[176] bzw. (rot) β-Cytidin und β-Uridin[178] nach *Sutherland et al.* ausgehen von Glycolaldehyd, Glycerinaldehyd, Cyanamid und Cyanoacetylen.

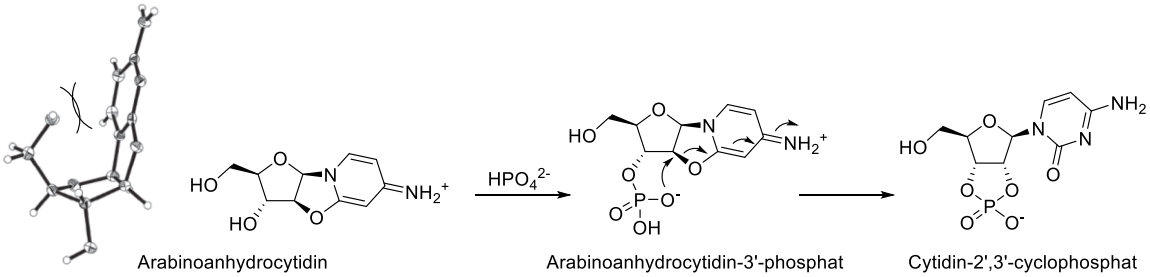

Abbildung 14. Schlüsselschritt der Phosphat-induzierten Ringöffnung. Die Kristallstruktur Arabinoanhydrocytidin offenbart die sterische Abschirmung der 5‘-Hydroxygruppe. Nach selektiver Phosphorylierung in C3‘-Position erfolgt ein intramolekularer Angriff der Phosphatgruppe mit C2‘-Stereoinversion und Spaltung des Oxazolidinrings.[176]

späteren Studien die Stabilisierung, Anreicherung und sequenzielle Freisetzung der aldehydischen Vorstufen durch Aminalbildung.[179] Weiterhin ist anzumerken, dass Cyanoacetylen (7 Äq) erst im dritten Schritt der Syntheseroute reagieren darf. Als reaktive und vergleichsweise hydrolyseempfindliche Spezies ist dessen präbiotische Anreicherung jedoch problematisch.[150] Zuletzt erlaubt die beschriebene Nukleosidierungsstrategie lediglich die Bildung von 2‘,3‘-Cyclophosphaten, jedoch nicht die Bildung kanonischer 5‘-Phosphate oder freier Nukleoside.[176]

Um die Problematik der Arabino-Spezies sowie die Bildung cyclischer Phosphate zu umgehen, entwickelte die Gruppe um *Powner* einen alternativen Syntheseweg (Abbildung 13, rot). Entsprechend der ursprünglichen *Orgel*-Strategie verwendeten *Powner et al.* nun wieder Riboaminooxazolin, welches sich selektiv anreichern lässt und mit Cyanoacetylen zu Riboanhydrocytidin reagiert. Anstatt den Oxazolidinring in Gegenwart von Phosphaten oder mittels Hydrolyse zu spalten, erfolgt eine Thiolyse zu α-Thiocytidin. Die Einführung der Thiongruppe begünstigt die anschließende Photoanomerisierung mit Ausbeuten von bis zu 76 % β-Thiocytidin, welches anschließend zu β-Cytidin und β-Uridin hydrolysieren kann.[178]

Während die 2-Aminooxazolin-basierten Synthesewege die Bildung von Pyrimidinnukleotiden ermöglichen, blieb ein analoger Zugang zu den Purinnukleotiden jedoch verwehrt. Auf der Suche nach einer gemeinsamen Purin- und Pyrimidinvorstufe entwickelten *Powner et al.* einen Syntheseweg basierend auf 2-Thiooxazol (Abbildung 15). Diese Route ähnelt der klassischen 2-Aminooxazolin-Synthese, wobei lediglich Cyanamid durch Thiocyanat ersetzt wird. Dieses reagiert im ersten Schritt mit Glycolaldehyd zu 2-Thiooxazol, welches in Gegenwart von

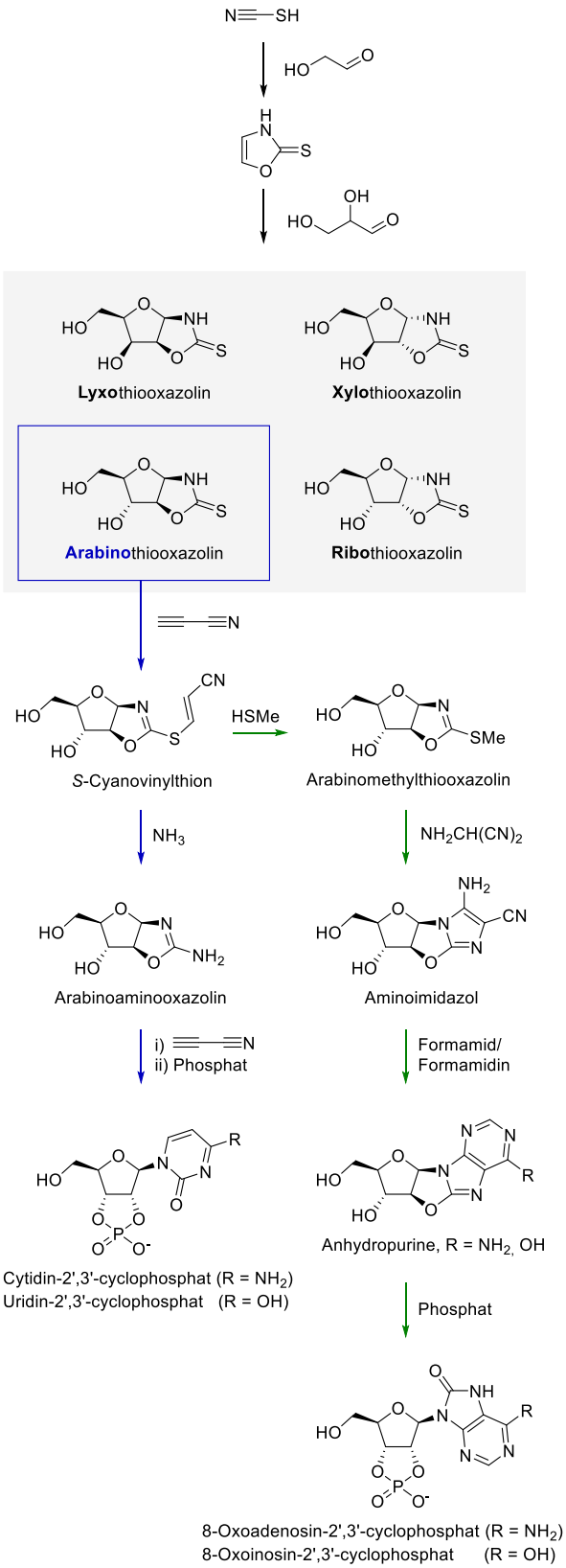

Glycerinaldehyd einen anellierten Furanosering bildet. Diese Reaktion verläuft stereounspezifisch unter der Bildung von Arabino-, Ribo-, Lyxo- und Xylothiooxazolin. Von den vier Epimeren ist für die weitere Reaktion lediglich die Arabinospezies von Bedeutung. Ihre exozyklische Thiolgruppe wird durch Reaktion mit Cyanoacetylen aktiviert (Abbildung 15, blau). Das cyanovinylierte Thiol kann nun als gutes Nukleofug verschiedene Substitutionsreaktionen eingehen. Im Falle einer Ammonolyse bildet sich Arabinoaminooxazolin, welches entsprechend der oben beschriebenen Syntheseroute (*Sutherland et al.*) zu Cytidin- bzw. Uridin-2‘,3‘-cyclophosphat weiterreagiert.

Alternativ kann eine Substitution durch Methanthiol zur Bildung von Methylthiooxazolin führen (Abbildung 15, grün). Wird diese Spezies mit Aminomalononitril umgesetzt, bildet sich ein imidazolisches Ringsystem, welches mit Formamid bzw. Formamidin zu Anhydropurinen reagiert. Im letzten Schritt erfolgt eine Phosphat-induzierte Spaltung des Oxazolidinrings unter der Freisetzung von 8-Oxoadenosin- und 8-Oxoinosin-2‘,3‘-cyclophosphat. Das von den Autoren aufgestellte Szenario bietet somit eine potenzielle Erklärung für

Abbildung 15. Indirekte Ribosylierung von Pyrimidinen und 8-Oxopurinen. Synthese von (blau) Cytidin- und Uridin-2‘,3‘-cyclophosphat sowie (grün) 8-Oxoadenosin- und 8-Oxoinosin-2‘,3‘-cyclophosphat nach *Powner et al.* ausgehend von Glycolaldehyd, Glycerinaldehyd, Thiocyanat und Cyanoacetylen.[180]

die präbiotische Entstehung von 8-Oxopurinnukleotiden, ermöglicht jedoch nicht die Synthese der kanonischen Spezies.[180]

1.3.4 Aminosäuren

Aminosäuren stellen neben Zuckern und Nukleobasen eine weitere essenzielle Substanzklasse dar und sind als Peptidbausteine vor allem für biologische Katalysereaktionen unerlässlich. Die ersten erfolgreichen Versuche zur Entstehung von Aminosäuren erfolgten durch *Miller* und *Urey* in den 1950er Jahren.[19, 41] Diese setzten eine Woche lang einem vermeintlich plausiblen Gasgemisch aus H_2, H_2O, CH_4 und NH_3 elektrische Blitzendladungen aus, worauf im tiefroten Rückstand fünf Aminosäuren papierchromatographisch nachgewiesen werden konnten: Glycin, α-Alanin, β-Alanin und vermutlich Asparaginsäure sowie α-Aminobuttersäure.[19] Experimente in abgeänderten Glasapparaturen[41] und H_2S-haltigen Gasgemischen[181] folgten. Aufbewahrte Proben, welche erst Jahrzehnte später mit neuesten Analysemethoden untersucht wurden, enthielten weitere bis dato unentdeckte Aminosäuren und andere organische Verbindungen.[182-183] Nachdem 1955 sichergestellt wurde, dass keine Mikroorganismen (Kontaminationen) für die Aminosäurebildung verantwortlich waren,[41] wurde ein *Strecker*-ähnlicher Reaktionsmechanismus postuliert.[184] Dieser Mechanismus (Abbildung 16) umfasst die Reaktion zwischen Aldehyden und Ammoniak unter der Bildung von Iminen, welche anschließend mit Blausäure zu α-Aminonitrilen reagieren.[20] Diese hydrolysieren schließlich zu den entsprechenden α-Aminosäuren.[20]

Da die präbiotische Plausibilität des reduzierenden Gasgemisches zunehmend in Frage gestellt wurde,[185-186] führten *Cleaves et al.* Gasentladungsexperimente in einer redox-neutralen $CO_2/N_2/H_2O$-Atmosphäre durch. Unter $CaCO_3$-gepufferten Bedingungen (pH 7) konnten Aminosäuren in bis zu 2,5 % Gesamtausbeute erhalten werden. Identifiziert wurden Serin, Glutaminsäure, Glycin und Alanin, sowie Spuren von Asparaginsäure, α-Aminoisobuttersäure, γ-Aminobutteräure und β-Alanin. Die Entstehung dieser Aminosäuren erklären sich die Autoren mit einem *Strecker*- oder *Bucherer–Bergs*-ähnlichen Reaktionsmechanismus.[66]

Interessante Ergebnisse erzielten *Oró et al.*, als sie eine Lösung von Formaldehyd und Hydroxylamin erhitzten und die Entstehung von Glycin, Alanin, β-Alanin, Asparaginsäure, Serin und Threonin beobachteten. Diese Beobachtungen erklärten sie u.a. durch die Bildung von Blausäure sowie Strecker-Reaktionen mit Formaldehyd bzw. dessen Kondensationsprodukten.[187] Ähnliche Ergebnisse publizierten *Egami et al.*, welche Formaldehyd und Hydroxylamin in

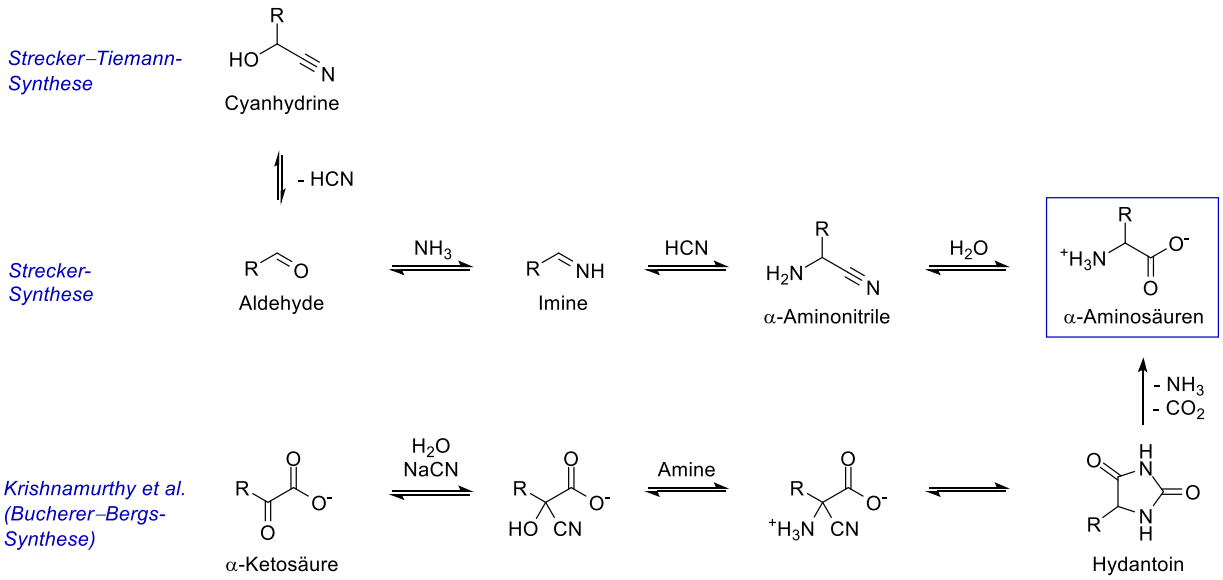

Abbildung 16. Aminosäuresynthesen. Reaktionsmechanismen nach *Strecker*,[20] *Strecker–Tiemann*[188] und *Bucherer–Bergs*[193]. *Krishnamurthy et al.* beschrieben die präbiotische Bedeutung der *Bucherer–Bergs*-Synthese ausgehend von α-Ketosäuren und Aminen wie z.B. Ammoniumhydroxid, Urea, oder Diamidophosphat (DAP).[191]

Gegenwart verschiedener Übergangsmetallsalze und Minerale umsetzten. Auch in diesem Fall wurde die Entstehung von Aminosäuren beobachtet und auf die Bildung von Blausäure und *Strecker*-ähnliche[20, 188] Reaktionen zurückgeführt.[189-190] Die präbiotische Plausibilität von Hydroxylamin war zu diesem Zeitpunkt jedoch unbekannt und die Forschungsergebnisse von *Egami* und *Oró* verloren an Beachtung.

Neuere Studien von *Krishnamurthy et al.* beschreiben die Bildung von Aminosäuren ausgehend von α-Ketosäuren (Abbildung 16).[191] Der kürzlich postulierte Reaktionsweg beginnt mit der Umsetzung von α-Ketosäuren zu α-Aminonitrilen in Gegenwart von Cyanid und verschiedenen Aminen.[191] Während vorangegangene Studien noch von einem decarboxylativen *Strecker*-Mechanismus[192] ausgingen, konnte nun erstmals die Bildung von Hydantoin-Intermediaten nachgewiesen werden. Entsprechend einer *Bucherer–Bergs*-Reaktion[193] konnte so die Umwandlung zu α-Aminosäuren unter Freisetzung von NH_3 und CO_2 beobachtet werden.[191]

Eine weitere Herausforderung stellen Aminosäuren mit komplexen Seitenketten dar, wie beispielsweise Valin und Leucin, deren verzweigte alkylische Seitenketten nicht ohne Weiteres aus der Formosereaktion o.ä. hervorgehen. Zur Lösung dieses Problems postulierten *Sutherland et al.* die Homologisierung alkylischer Carbonyle, basierend auf einer cyanosulfidischen

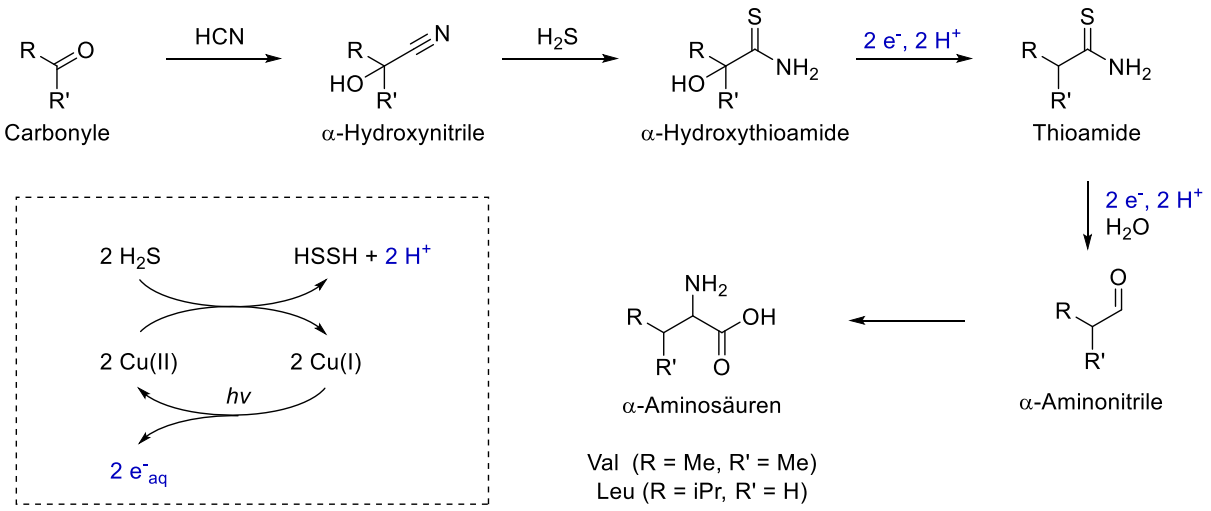

Abbildung 17. Cyanosulfidische Homologisierung. Die von *Sutherland et al.* entwickelte Homologisierung basiert auf einem Cu(I)/Cu(II)-Photoredoxzyklus (Box) mit Hydrogensulfid als Reduktionsmittel.[128, 132]

Photoredoxkatalyse (Abbildung 17). Hierfür werden die Carbonyle durch Blausäure und Schwefelwasserstoff zunächst in α-Hydroxythioamide umgewandelt. In zwei aufeinanderfolgenden Reduktionsschritten wird nun die Hydroxygruppe gespalten und anschließend das Thioamid reduziert. Unter wässrigen Bedingungen entstehen α-Aminonitrile, welche sich zu Valin bzw. Leucin hydrolysieren lassen. Dieser *cyanosulfidische Protometabolismus* nutzt als Reduktionsmittel Schwefelwasserstoff, welcher unter Cu(I)/Cu(II)-Photoredoxkatalyse Protonen und solvatisierte Elektronen freisetzt.[128, 132]

2. Motivation

Die RNA-(Peptid)-Welt-Hypothese besagt, dass Ribonukleotide als universelle Bausteine die Entstehung erster Lebensformen ermöglicht haben. Phylogenetische Studien legen nahe, dass bereits unser letzter allgemeiner gemeinsamer Vorfahr (LUCA) auf die kanonischen Purinnukleoside Adenosin und Guanosin sowie auf die Pyrimidinnukleoside Cytidin und Uridin angewiesen war. Um die Frage nach ihrer präbiotischen Entstehung zu beantworten, wurden verschiedene Szenarien und Reaktionswege postuliert, welche zur Bildung der RNA-Nukleoside beigetragen haben könnten. Ihre gemeinsame Bildung kann bislang jedoch nicht erklärt werden, da die Reaktionswege zu Purin- und Pyrimidinnukleosiden chemisch inkompatibel sind. Zudem lassen sich einige Startmaterialien nur unter Bedingungen herstellen, welche nach heutigem Wissen auf der frühen Erde nicht vorherrschend waren. Dies stellt die präbiotische Plausibilität einiger Hypothesen grundlegend in Frage.

Das Ziel dieser Arbeit war die Synthese von RNA-Nukleosiden unter chemisch kompatiblen und präbiotisch plausiblen Bedingungen. Zunächst galt es, eine alternative Pyrimidinsynthese zu etablieren, welcher mit der der Purine kompatibel ist. Darauf basierend sollte ein geochemisches Szenario entwickelt und die gemeinsame, präbiotisch Bildung aller kanonischen Nukleoside auf der frühen Erde demonstrieren werden. Weiterhin sollten verschiedenen literaturbekannte Pyrimidinsynthesewege auf ihre Kompatibilität hin untersucht und ihre jeweiligen Vorteile in einem gemeinsamen Syntheseweg vereint werden. Vorrangiges Ziel war hier die Umgehung freier Ribose sowie eine frühe Abreaktion reaktiver Verbindungen wie Cyanoacetylen. Zudem sollten Reaktionswege etabliert werden, welche die Bildung typischer Ausgangsverbindungen zu Nukleosiden und Aminosäuren unter plausiblen (schwach reduzierenden) Bedingungen erlaubt. Gegebenenfalls sollten alternative Ausgangsverbindungen erforscht und neue, plausiblere Syntheserouten entwickelt werden.

3. Veröffentlichte Arbeiten

3.1 Vereinte präbiotische Synthese von Pyrimidin- und Purin-RNA-Ribonukleotiden

S. Becker†, J. Feldmann†, S. Wiedemann†, H. Okamura, C. Schneider, K. Iwan, A. Crisp, M. Rossa, T. Amatov, T. Carell, Unified prebiotically plausible synthesis of pyrimidine and purine RNA ribonucleotides. *Science* **2019**, *366*, 76–82.‡

Prolog

Als erster Baustein des Lebens werden der RNA sowohl informationsspeichernde als auch katalytische Funktionen zugeschrieben. Um diese ausüben zu können, bedarf es komplementärer Purin- bzw. Pyrimidinbasen, welche sich zusammen auf der frühen Erde gebildet haben müssen. Mehrere Syntheserouten wurden entwickelt, welche entweder die Entstehung von Purin- oder von Pyrimidinnukleosiden ermöglichen. Allerdings sind diese Reaktionswege chemisch weitgehend inkompatibel und können die gemeinsame Bildung aller RNA-Bausteine am selben Ort nicht ausreichend erklären. Die folgende Studie beschreibt einen neuen Reaktionsweg zur Bildung von Pyrimidinnukleosiden und -Nukleoiden aus primitiven Ausgangsverbindungen unter präbiotisch plausiblen Bedingungen. Hierbei erlaubt 3-Aminoisoxazolylharnstoff als Vorläuferbase eine regioselektive Ribosylierung mit guten Ausbeuten und die Verwendung von Borophosphaten die bevorzugte Entstehung furanosidischer Pyrimidinnukleotide. Dieser Reaktionsweg ist zudem kompatibel mit der Synthese von Purinnukleosiden, was die gemeinsame Bildung aller kanonischen Nukleobasen am selben Ort erstmals erlaubt.

---

† Die Autoren haben zu gleichen Teilen zum Manuskript beigetragen

‡ Für ergänzende Informationen siehe Anhang I

Autorenbeitrag

Siehe Manuskript.

Lizenz

RESEARCH

PREBIOTIC CHEMISTRY

Unified prebiotically plausible synthesis of pyrimidine and purine RNA ribonucleotides

Sidney Becker[1,2*], Jonas Feldmann[1*], Stefan Wiedemann[1*], Hidenori Okamura[1,3], Christina Schneider[1], Katharina Iwan[1,4], Antony Crisp[1], Martin Rossa[1], Tynchtyk Amatov[1,5], Thomas Carell[1]†

Theories about the origin of life require chemical pathways that allow formation of life's key building blocks under prebiotically plausible conditions. Complex molecules like RNA must have originated from small molecules whose reactivity was guided by physico-chemical processes. RNA is constructed from purine and pyrimidine nucleosides, both of which are required for accurate information transfer, and thus Darwinian evolution. Separate pathways to purines and pyrimidines have been reported, but their concurrent syntheses remain a challenge. We report the synthesis of the pyrimidine nucleosides from small molecules and ribose, driven solely by wet-dry cycles. In the presence of phosphate-containing minerals, 5′-mono- and diphosphates also form selectively in one-pot reactions. The pathway is compatible with purine synthesis, allowing the concurrent formation of all Watson-Crick bases.

The discovery of catalytic RNA (*1*) and the development of replicating RNA systems (*2*, *3*) have lent strong support to the concept of an RNA world (*4*). The RNA world hypothesis predicts that life started with RNAs that were able to (self-)recognize and replicate. Through a process of chemical evolution, a complex RNA and later RNA–peptide and protein world supposedly evolved, from which life ultimately emerged (*4*). A prerequisite for the RNA world is the ability to create RNA under prebiotic conditions. This requires as the first elementary step the concurrent formation of pyrimidine and purine nucleosides in the same environment. They must have condensed to form information-carrying polymers able to undergo Darwinian evolution. The question of how the pyrimidine and purine nucleosides could have formed together is an unsolved chemical problem that is under intensive chemical investigation (*5*–*9*). Starting from an early atmosphere mainly composed of N_2 and CO_2 (*10*), the abiotic synthesis of life's building blocks must have occurred on the early Earth in aqueous environments, whose characteristics were determined by the minerals and chemical elements from which the early Earth's crust was made (*11*, *12*). Atmospheric chemistry, impact events, and volcanic activities must have provided the first reactive small molecules. These reacted in surface or deep-sea hydrothermal vents (*13*–*15*), on mineral surfaces (*16*), or in shallow ponds (*17*). Within these environments, volcanic activity, and seasonal or day-night cycles caused fluctuations of pH and temperature. Such fluctuations provided wet-dry conditions allowing precipitation or crystallization of chemicals (*18*). Mixing of microenvironments may have opened up new reaction pathways that led to increasing chemical complexity.

Along these geophysical boundaries, two main reaction pathways have been proposed for the formation of purine and pyrimidine nucleosides. The synthesis of the purines is possible along a continuous pathway based on the reaction of formamidopyrimidine (FaPy) precursors with ribose (*6*, *18*). For the pyrimidines, a reaction sequence involving aminooxazoles has been discovered (*5*). These pathways provide the corresponding nucleosides under very different and partially incompatible conditions, leaving unanswered the question of how purines and pyrimidines could have formed in the same environment. Here, we report a prebiotically plausible pathway to pyrimidine nucleosides that selectively provides the 5′-mono- and 5′-diphosphorylated nucleosides needed for RNA strand formation. By connecting the pathway with the reported purine route (*6*, *18*), we establish a unifying reaction network that allows for the simultaneous formation of both types of nucleosides in the same environment and that is driven by wet-dry cycles.

Results

Prebiotically plausible synthesis of pyrimidine nucleosides

The chemistry leading to pyrimidines starts from cyanoacetylene **1** as the key building block (Fig. 1A). Compound **1** is observed in interstellar clouds and in the atmosphere of Titan (*19*). It has been shown to form in large quantities by electric discharge through a CH_4-N_2 atmosphere (*20*) and is also a product of the Cu(II)-mediated reaction of HCN and acetylene in water (Fig. 1B) (*21*). A recent report suggested that molecules such as **1** are plausible prebiotic starting materials which could have formed in surface hydrothermal vents in significant concentrations (*13*). We found that **1** reacts quickly and cleanly with hydroxylamine **2** or hydroxylurea **3** to give 3-aminoisoxazole **4**. The reaction of **1** with **3** proceeds under slightly basic conditions (pH ~10) with 80 to 90% yield within 2 hours. **3** is formed in almost quantitative yields from the reaction of **2** with cyanate (*22*). Compound **4** formed robustly even if we varied the temperature (10° to 95°C), the reactant concentrations (10 to 100 mM), or added additional compounds, such as urea **5** and/or different metal ions (see below). Reaction of cyanoacetylene **1** with hydroxylamine **2** produced **4** with 17% yield after 2 hours at pH 10.

While hydroxylamine **2** is an accepted building block for prebiotic amino acid syntheses (*23*), its potential formation on the early Earth is unclear. We therefore aimed to demonstrate its prebiotic availability. **2** is ultimately produced by reduction from NO, which is formed in large quantities when lightning passes through moist atmospheres containing N_2 and CO_2 (Fig. 1B) (*10*). NO forms as the main product under these conditions and spontaneously reacts in the presence of water to form nitrite (NO_2^-) and nitrate (NO_3^-), and this leads to the assumption that both anions were quite abundant on the early Earth (*24*–*26*). With Fe(II) as a plausible prebiotic reductant, NO_2^- is converted to NH_3 but not to NH_2OH **2** (*26*). Formation of the latter requires a partial reduction. We found that this can be achieved with HSO_3^-, which forms from volcanic SO_2 and water (*27*). NO_2^- and HSO_3^- react to **2** with up to 85% yield (Fig. 1B and fig. S1) (*28*). We confirmed that this reaction gives first hydroxylamine disulfonate **6** (Fig. 1B), which hydrolyzes to hydroxylamine **2** and HSO_4^-. We found that intermediate **6** reacts with cyanoacetylene **1** as well (88% yield) (Fig. 1B and fig. S2) to give the stable olefin **7**, which upon hydrolysis provides again the key intermediate **4**. The overall yield of **4** via compound **7** is 63% over these two steps. The suggested pyrimidine intermediate **4** is therefore readily available from cyanoacetylene **1** upon reaction with either **2**, **3**, or **6** under prebiotic conditions (Fig. 1B).

When we added urea **5** to a solution of **4**, warming (70° to 95°C) and dry-down resulted in formation of *N*-isoxazolyl-urea **8** (Figs. 1A and 2A) in a spot-to-spot reaction that is catalyzed by Zn^{2+} or Co^{2+}. These metal ions were likely present on the early Earth (*11*, *12*). In the presence of Zn^{2+}, compound **8** is formed in 88% yield after 2 days at 95°C (at 70°C, the same yield is obtained after ~2 to 3 weeks). With Co^{2+}, 68% yield is achieved after 2 days

[1]Center for Integrated Protein Science, Department of Chemistry, LMU München, Butenandtstrasse 5-13, 81377 München, Germany. [2]Department of Chemistry, University of Cambridge, Lensfield Road, Cambridge CB2 1EW, UK. [3]Institute for Multidisciplinary Research for Advanced Materials, Tohoku University, 2-1-1 Katahira, Aoba-ku, Sendai, Miyagi 980-8577, Japan. [4]Centre for Translational Omics, University College London, Great Ormond Street Institute of Child Health, 30 Guilford Street, London WC1N 1EH, UK. [5]Max-Planck-Institut für Kohlenforschung, Kaiser-Wilhelm-Platz 1, 45470 Mülheim an der Ruhr, Germany.
*These authors contributed equally to this work.
†Corresponding author. Email: thomas.carell@lmu.de

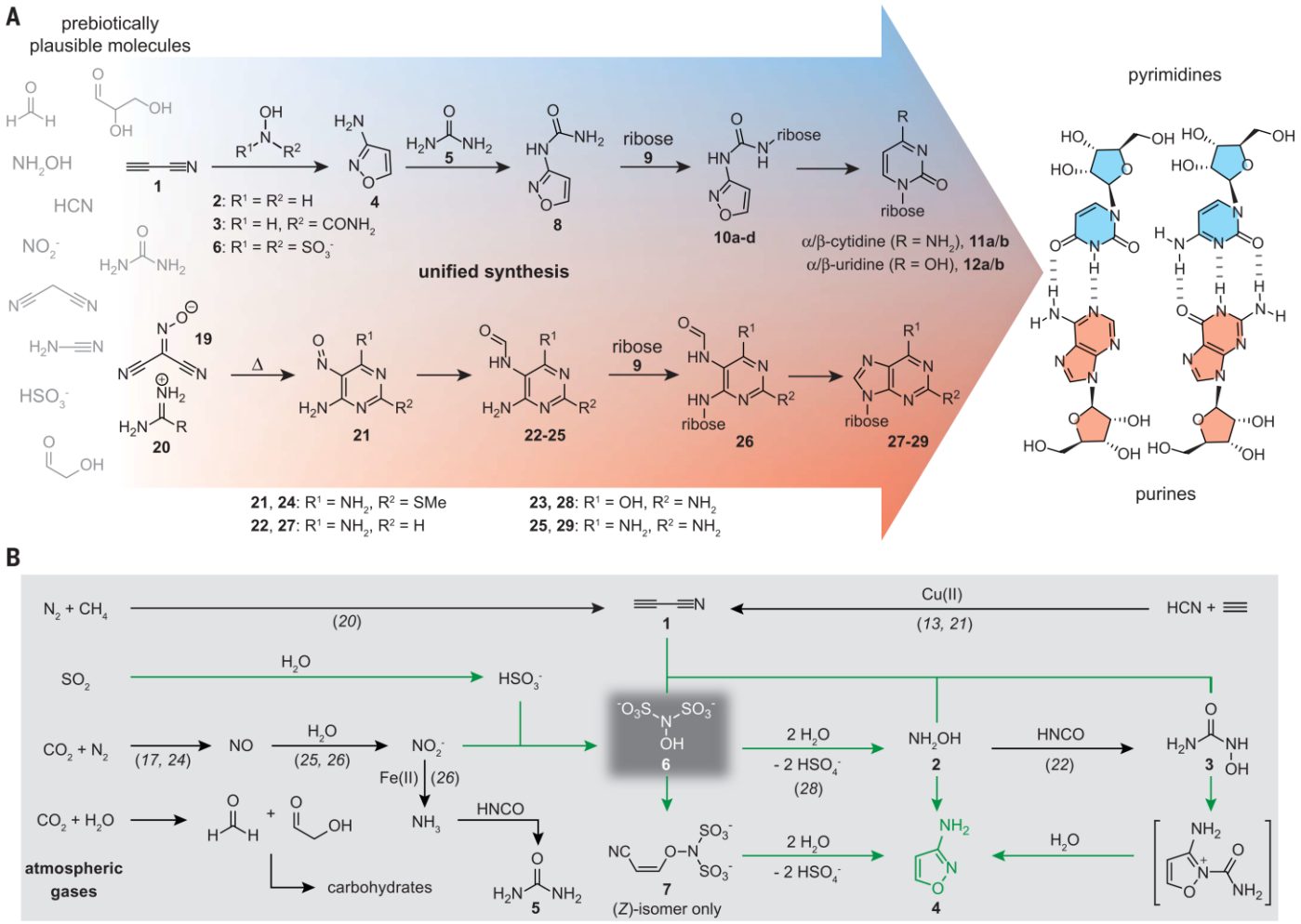

Fig. 1. Unified synthesis of pyrimidine and purine RNA building blocks. (**A**) Starting from plausible prebiotic molecules, the reaction scheme depicts the route toward the pyrimdines via isoxazolylurea **8** (blue background) and the purines via formamidopyrimidines **22** to **25** (red background) (*18*). (**B**) Fundamental chemistry that produces the molecules needed for the pyrimidine pathway. Reactions performed in this work are shown with green arrows, while black arrows represent well-known reactions. Formation of **4** requires reaction of **1** with hydroxylamine **2**, hydroxylurea **3**, or the disulfonate **6** (dark-gray box). **6** is formed from NO_2^- and SO_2/HSO_3^-.

at 95°C. The reaction of **4** to **8** is in all cases a clean process, with the only impurity being unreacted **4** (Fig. 2A). The product **8** can be subsequently physically enriched. Addition of carbonated water to the dried reaction mixture solubilizes **4**, **5**, and **8**, leaving behind the metal ions as hydroxides or carbonates. Subsequent concentration of the supernatant leads to spontaneous crystallization of **8** (55%). This allowed us to obtain a crystal structure of **8** (fig. S3). In order to simulate early Earth chemistry, we performed a one-pot experiment. We mixed **1** with **3**, **5**, and Zn^{2+} or Co^{2+} in a carbonate solution (pH ~10) and obtained compound **4** at 95°C (80 to 90%). Neutralizing the solution to pH ~6 to 7, which may have occurred on the early Earth as a result of acidic rain, followed by dry-down at the same temperature, provided compound **8** with yields between 56% (Zn^{2+}) and 40% (Co^{2+}). The continuous synthesis of the key building block **8** was consequently achieved in a plausible prebiotic setting that could have existed in hydrothermal vents or near volcanic activity, both of which would be able to provide elevated temperatures (fig. S3). The synthesis is also possible at lower temperatures, but with extended reaction times.

For the final step toward nucleosides, we need to assume that, due to flooding or a mixing of environments, **8** came into contact with ribose **9** (Figs. 1A and 2B) or any other sugar unit, such as threose (for TNA) or glyceraldehyde (for GNA), that was able to form a backbone for a pairing system (*29*, *30*). When we mixed **8** with ribose **9** and warmed the mixture to 95°C in the presence of boric acid, we observed a fast and high-yielding reaction that provided the ribosylated products **10a** to **10d** with 95% yield (fig. S4a). Other borate minerals, such as synthetic lüneburgite $\{Mg_3[(PO_4)_2|B_2(OH)_6]\cdot 6H_2O\}$ (*31*) or borax $\{Na_2[B_4O_5(OH)_4]\cdot 10H_2O\}$ (*32*), were also able to catalyze this reaction with high yields (>70%) (fig. S5). The major products were initially the α- and β-pyranosides (**10c** and **10d**), which dominate over the α- and β-furanosides (**10a** and **10b**) (fig. S4a). After heating the mixture under slightly basic conditions at 95°C in the presence of borates, the furanosides (54%; **10a** and **10b**) (Fig. 2B) gradually became the dominant products (fig. S4b). Under these conditions, we also observed hydrolysis of **10a** to **10d** to **8** and **9**. The accumulation of the furanosides **10a** and **10b** is best explained by complexation of their *cis*-diols with borate (*32*).

The final step toward pyrimidine nucleosides requires reductive opening of the isoxazole N-O bond, followed by tautomerization, intramolecular cyclization, and water elimination in a cascade-like fashion (Fig. 2, C and D). We found that this reaction occurred rapidly with Fe^{2+} in the presence of thiols (Fig. 2D) (*33*). Liquid chromatography–mass spectrometry (LC-MS) analysis indicated that cytidine nucleosides **11a** to **11d** formed efficiently under

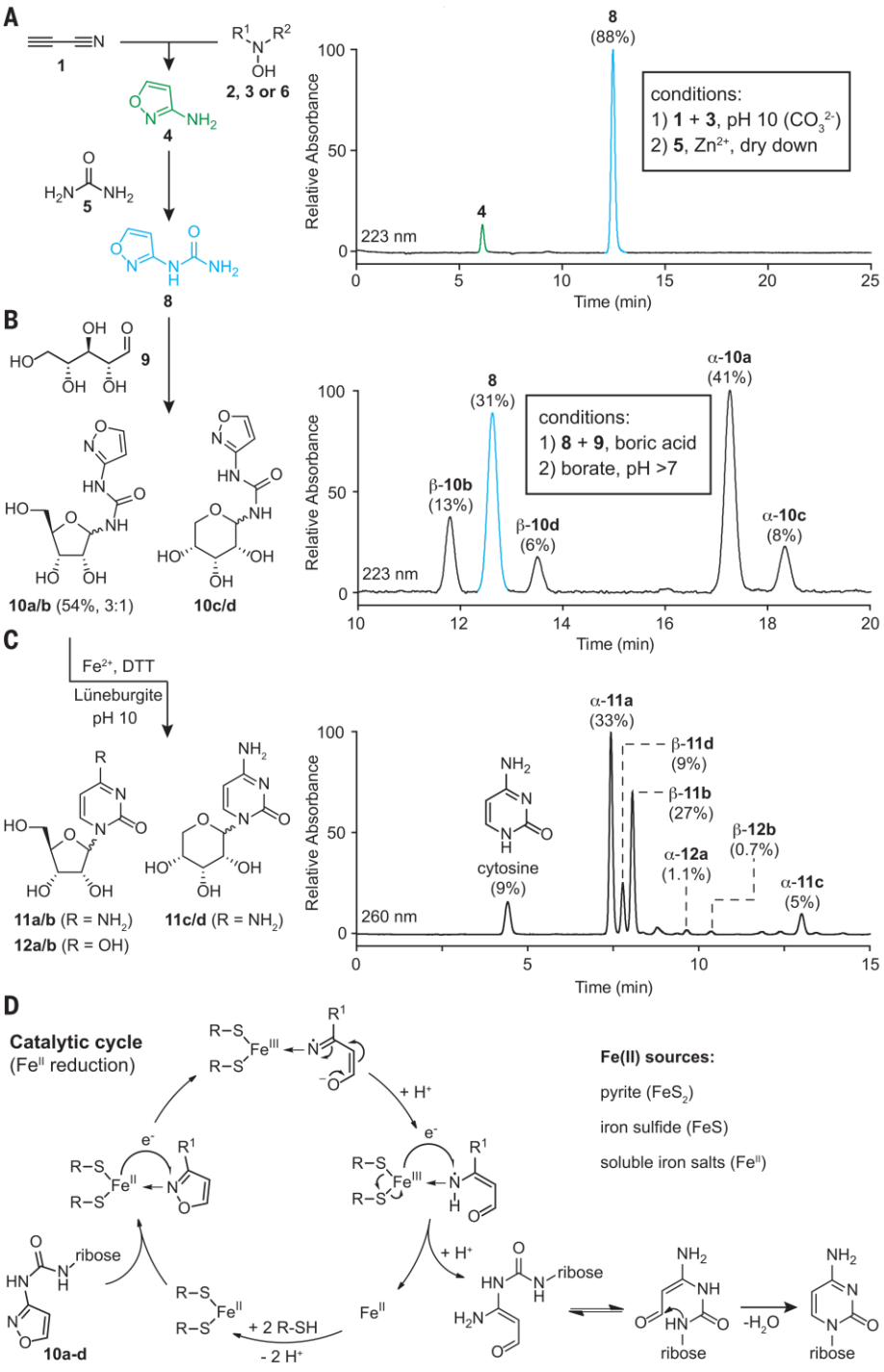

Fig. 2. Formation of pyrimidine nucleosides (11 and 12) from N-isoxazolylurea ribosides 10a and 10b. The different isomers are labeled as follows: **a** = α-furanosyl; **b** = β-furanosyl; **c** = α-pyranosyl; **d** = β-pyranosyl. (**A**) Formation of **4** and its conversion with urea **5** to *N*-isoxazolylurea **8**. (**B**) Ribosylation of **8** with ribose **9** and equilibration of the reaction mixture in the presence of borates gives the furanosidic isomers **10a** and **10b** (54%). (**C**) Pyrimidine nucleoside formation by reductive N-O cleavage from the compound mixture of **10a** and **10b** in the presence of ammonium iron(II) sulfate hexahydrate (0.0005 equiv.). The HPLC results with detection at 260 nm show formation of cytidine (C; **11a** to **11d**) and uridine (U; **12a** and **12b**). (**D**) Proposed catalytic cycle for the Fe^{2+} catalyzed reduction of the N-O bond of the isoxazole moiety.

these conditions, with the furanosidic uridine nucleosides **12a** and **12b** as the corresponding deamination products formed by hydrolysis (Fig. 2C). Reductive pyrimidine formation can be performed with FeS or the mineral pyrite (FeS_2), and both have been discussed in the context of early metabolic pathways (*15*, *34*). Just 0.0001 equiv. of soluble Fe^{2+} in water is sufficient for the reaction. In the absence of Fe^{2+}, pyrimidine formation was not observed. The reduction also appears to be independent of the thiol source, as the products **11a** to **11d** and **12a** and **12b** were obtained regardless of whether we used dithiothreitol (DTT), propanedithiol, mercaptoethanol, or cysteine (fig. S6).

Selective one-pot formation of 5′-nucleoside mono- and diphosphates

The addition of naturally occurring minerals such as hydroxyapatite, colemanite, or (synthetic) lüneburgite to the reductive pyrimidine-forming reaction mixture had a strong influence on the distribution of the four cytidine isomers. Synthetic lüneburgite gave a combined high yield of 85% (Fig. 2C). The natural furanosidic β-cytidine (**11b**) and its α-anomer (**11a**) are formed under these conditions with about the same yields, together with small amounts of α- and β-uridine (**12a** and **12b**). We found only small amounts of the α- and β-cytidine pyranosides (**11c** and **11d**), together with the cytosine base. Because synthetic lüneburgite is known to enable nucleotide formation in the presence of urea (Fig. 3A) (*31*), we simply added urea to the one-pot reaction mixture after pyrimidine formation and allowed the mixture to evaporate to dryness at 85°C over a period of about 20 hours. LC-MS analysis of the reaction mixture showed formation of phosphorylated nucleosides (Fig. 3A) in a substantial 19% yield relative to that for cytidine (Fig. 3B and fig. S7). We assumed that the reaction generated the α- and β-cytidine 5′-monophosphates **13a** and **13b** and the 5′-diphosphorylated cytidines **14a** and **14b**. Owing to hydrolysis, we also expected some α- and β-uridine 5′-monophosphates and 5′-diphosphates **15a** and **15b** and **16a** and **16b**. We isolated the corresponding high-performance LC (HPLC) peaks and removed the phosphate groups enzymatically (Fig. 3, B and C). LC-MS analysis showed the dephosphorylated furanosides **11a** and **11b** and **12a** and **12b** with over 94% in the nucleoside pool, which corresponds to a change of the furanoside/pyranoside ratio from an initial 4:1 to 17:1 (Fig. 3C). The formation of phosphorylated pyranosides **17** are only a minor side reaction. We found no discrimination between α- and β-anomers during the phosphorylation. The furanoside enrichment is best explained by the presence of a primary hydroxyl group in the furanosides which is absent in the pyranosides. The enrichment of 5′-nucleoside monophosphates and diphosphates under these one-pot conditions establishes a further

chemical selection step that favors the furanosides as the components of RNA. We further characterized the structures of the phosphorylated nucleosides and confirmed the formation of the 5′-α- and 5′-β-cytidine mono- and diphosphates (**13a**, **13b**, and **14a**, **14b**; α-/β-CMP and α-/β-CDP) (fig. S8). Additional analysis allowed identification of α,β-UDP **16a** and **16b** (fig. S9). 5′-Pyrophosphates are the dominating species within the diphosphorylated nucleoside mixture (fig. S8a).

Compatible formation of pyrimidine and purine RNA nucleosides

We next investigated if the prebiotically plausible pyrimidine and purine nucleoside pathways are compatible with each other so that they can be connected with the goal to form all Watson-Crick building blocks in the same environment, driven solely by wet-dry cycles. The purine synthesis (*18*) requires as the initial step a reaction of malononitrile **18** with sodium nitrite to give (hydroxyimino)malononitrile **19**. Because malononitrile **18** can be also generated from cyanoacetylene **1**, as shown by Eschenmoser (*35*), pyrimidines and purines can be traced back to the same chemical root (Fig. 4). Compound **19** forms an organic salt with amidines **20** to give nitroso-pyrimidines **21** and, upon reduction and formylation, FaPys (**22** to **25**). The latter can react with ribose **9** to give ribosylated FaPy **26** and then purine nucleosides **27** to **29** (Fig. 1A) (*18*). To investigate how the chemical conditions needed for pyrimidine formation from the urea-isoxazole **8** would affect purine formation, we reacted **8** and the FaPy compounds **22** and **23** with ribose **9** under dry-down conditions. We performed the reaction under identical conditions but in separate reaction vials (Fig. 4). Under these conditions, formation of all four Watson-Crick nucleosides, cytidine **11,** uridine **12**, adenosine **27**, and guanosine **28**, were detected.

We next investigated if pyrimidines and purines can form simultaneously in the same environment (Fig. 5A). For this experiment, we mixed the starting materials cyanoacetylene **1**, hydroxylurea **3**, (hydroxyimino)malononitrile **19**, and amidine **20** under slightly basic conditions (pH ~10). Analysis of the mixture indeed showed formation of **4** with 86% yield, despite the presence of **19** and **20**. It is surprising that the N-OH functionality of compound **19** does not interfere with the formation of **4**. Compound **4** is a liquid that can enrich from a water solution by dry-down, owing to its high boiling point (228°C). Compound **4** can act as a solvent to facilitate the formation of **21** from the reaction of **19** with **20** under milder conditions (50°C to 100°C instead of 126°C), in contrast with results from a previous experiment (*18*). The next step requires reduction and formylation of **21** to the FaPy intermediate, but this step cannot be performed in the presence of the isoxazole. Addition of a water mixture eventually containing urea **5** leads to spontaneous precipitation of **21**. The supernatant containing **4** and **5** can flow away. The water-insoluble **21**, if brought into contact with dilute formic acid and Zn (found in Earth's crust), reacts immediately to form the compounds **22** and **24** with Zn^{2+} as a side product (Fig. 5A and fig. S10a). These reaction products are water-soluble and can potentially recombine with **4** and **5**. The side product Zn^{2+} can then catalyze the reaction of **4** in the presence of **5** to give *N*-isoxazolyl urea **8** in the presence of **22** and **24** (Fig. 5A and fig. S10b). This leads to the formation of the pyrimidine and purine precursors **8**, **22**, and **24**, which can be transformed into the purine and pyrimidine nucleosides. In this scenario, intermediate **4** of the pyrimidine pathway helps formation of the purine precursor **21**, while Zn^{2+} as a side product of the purine pathway mediates formation of the pyrimidine precursor **8** in a mutually synergistic way, driven by wet-dry cycles.

We combined **8** with different FaPy intermediates and investigated if they reacted in a one-pot scenario with ribose **9** to finally give the purine and pyrimidine nucleosides. To examine this, we dissolved a mixture of **8**, **22**, **25**, ribose **9**, and boric acid and warmed the mixture to 95°C for 14 hours, allowing for slow evaporation of water. The solid material was then taken up with a slightly basic solution containing Fe^{2+} (0.0005 equiv.) and DTT (1.5 equiv.), and we allowed the mixture to warm to 95°C. HPLC-MS analysis proved that these conditions simultaneously provided the purine and pyrimidine nucleosides with cytidine (**11a** to **11d**) and adenosine (**27**) as the

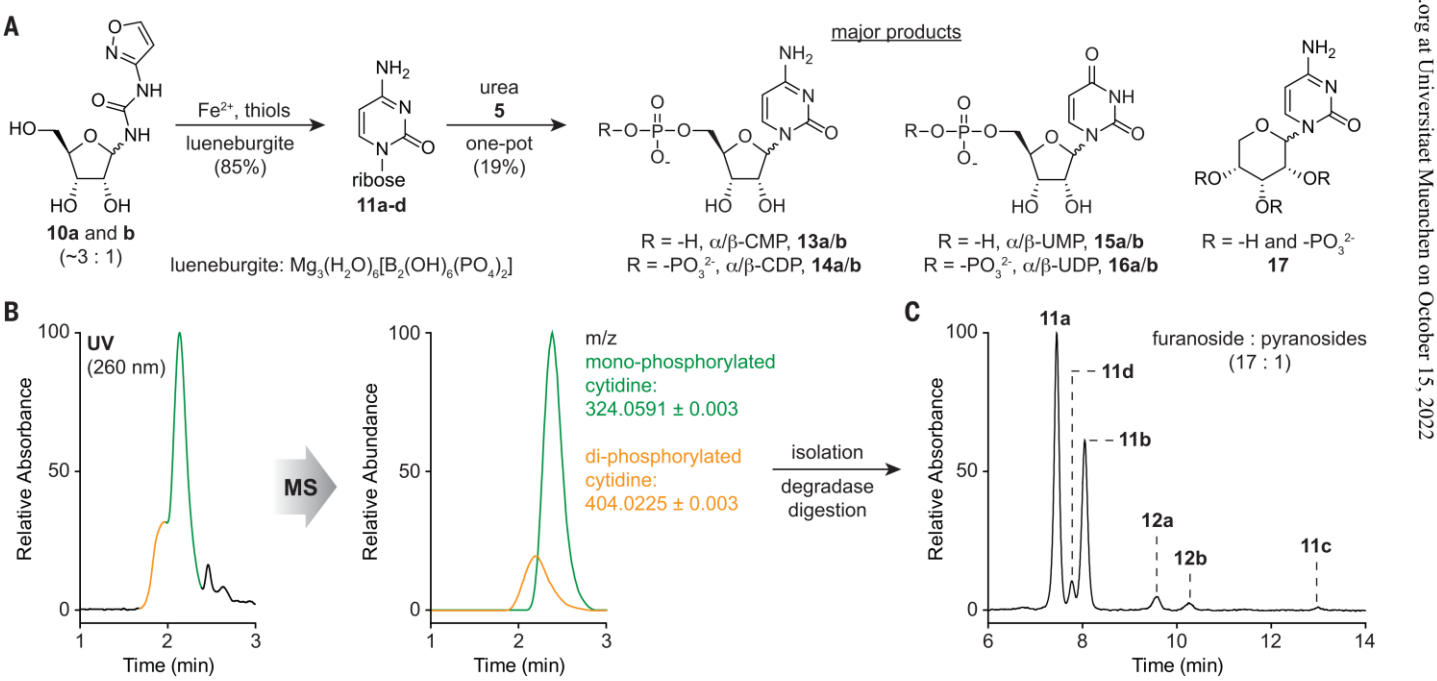

Fig. 3. One-pot nucleotide formation reaction. (**A**) One-pot synthesis of cytidine and uridine 5′-mono- and 5′-diphosphates (**13a** and **13b** to **16a** and **16b**) after urea addition to the reaction mixture and allowing the mixture to dry-down at 85°C for 20 hours. **a**/**b** represent the α- and β-anomers, respectively. (**B**) LC-MS analysis of the corresponding nucleotide peaks with UV and MS detection and isolation of the formed nucleotides from the prebiotic reaction, followed by an enzymatic removal of the phosphate groups. (**C**) HPLC analysis of the dephosphorylated product mixture showing predominant formation of α- and β-cytidine **11a** and **11b**.

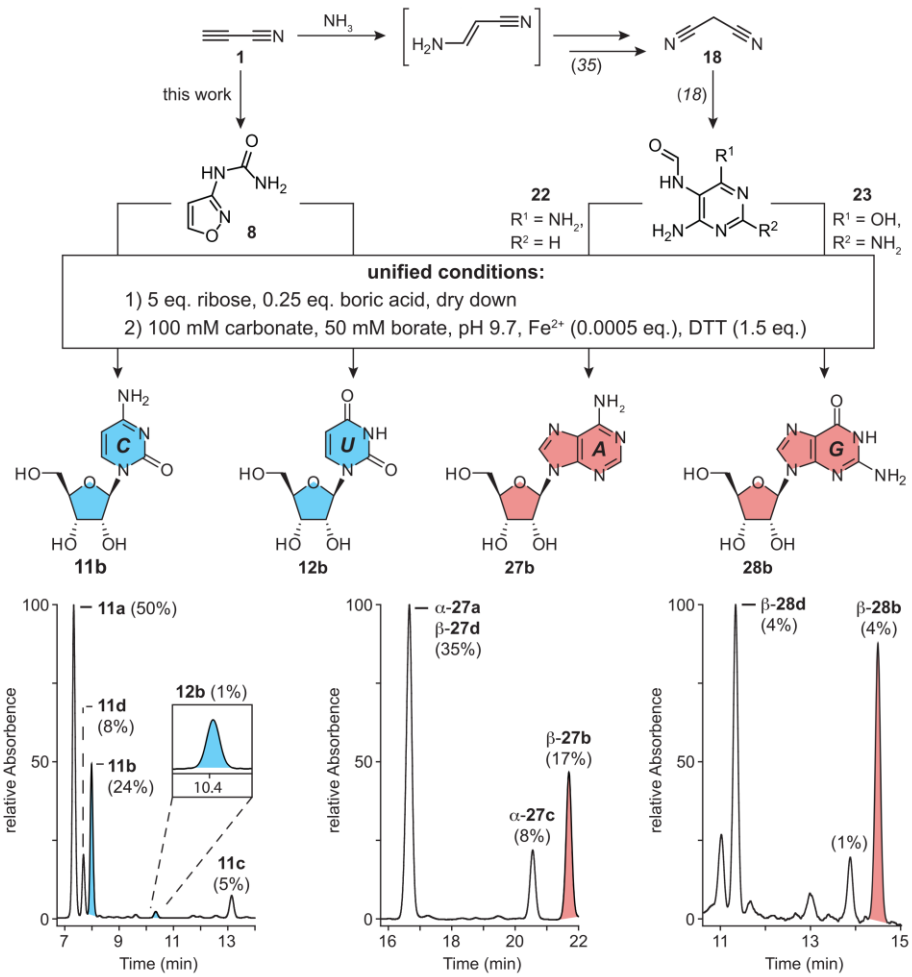

Fig. 4. Formation of all four Watson-Crick RNA building blocks in identical but parallel reactions. C (**11b**), U (**12b**), A (**27b**), and G (**28b**) are formed under the same conditions separately from **8**, **22**, and **23**. HPLC results are shown with a detection at 260 nm. The nucleosides are labeled as follows: **a** = α-furanosyl; **b** = β-furanosyl; **c** = α-pyranosyl; **d** = β-pyranosyl. Canonical pyrimidine and purine RNA building blocks are labeled in blue and red, respectively.

main products. Diaminopurine nucleosides (DA; **29**), which hydrolyze to guanosine **28**, form in this one-pot reaction as well (Fig. 5A, chromatogram). We noted additional formation of double-ribosylated adenine (rib_2-A). Furthermore, the nucleoside **28** was created in this scenario when we used **23** (R^1 = OH, R^2 = NH_2) as the starting material, but the yields were lower.

Discussion

Ribose-based RNA and the four canonical nucleosides, A, G, C, and U, are central to modern life and to prebiotic hypotheses, such as the "RNA world," in which RNA strands replicated and evolved to give increasingly complex chemical systems (*4*). Whether such RNAs were directly assembled from the canonical nucleotides (A, C, G, and U bases) or if they evolved from a simpler proto-RNA system is unclear (*36*).

Here we show that a reaction network toward the purine and pyrimidine RNA building blocks can be established, starting from simple atmospheric or volcanic molecules. Molecular complexity is generated by wet-dry cycles that can drive the chemical transformations. Therefore, any environment that was able to provide wet-dry phases might have been a suitable place for the origin of RNA building blocks. Our geochemical model assumes that chemistry took place in several basins that were needed to locally separate intermediates. We also needed one or two streams of water in our system to allow exchange of soluble molecules (Fig. 5B). Intermediates might precipitate upon fluctuations of physico-chemical parameters, allowing for the separation of soluble and insoluble materials (e.g., **4** and **21**). After further reactions, which reestablish solubility, the compounds can be recombined (Fig. 5B). For our scenario we need to assume that the early Earth provided environmental conditions that fluctuated between slightly acidic (pH 3), potentially caused by acidic rain (SO_2, NO_x), or basic (pH 10) caused by carbonates. Even though most of the chemistry described here was performed at elevated temperatures, the reactions also occur at lower temperatures, but with substantially longer reaction times. We can assume that temperatures fluctuated on the early Earth just like today due to day-night or seasonal cycles. Such fluctuations would certainly have brought about wet-dry cycles, akin to modern droughts and rain. The geophysical requirements needed for the reported chemistry, including elevated temperatures, could have existed in geothermal fields or at surface hydrothermal vents, which are plausible geological environments on early Earth.

Our proposed chemical pathways toward pyrimidines and purines begin with cyanoacetylene **1**, which could have formed in surface hydrothermal vents (*13*). Reaction of **2**, **3**, or **6** with **1** is the starting point for the pyrimidines, but if **1** reacts instead with ammonia, a pathway to malononitrile **18** as the precursor for purine synthesis is possible (Fig. 4) (*35*). Another key molecule for the synthesis of purines and pyrimidines is NO_2^-, which is needed to nitrosate malononitrile **18** to **19** (*18*). NO_2^- is also crucial for the formation of hydroxylamine in the presence of HSO_3^-, which is formed from volcanic SO_2 (*27*). The concentration of NO_2^- that is reachable in a prebiotic setting is under debate, but it is speculated that the most likely place for its accumulation is in shallow ponds, as needed for our scenario (*17*). In general, the limited stability of NO_2^- would not be an issue, provided that it is rapidly captured by HSO_3^- upon its formation. Our model assumes a surface environment, where molecules such as NO_2^-, HSO_3^-, or urea **5** could have been delivered by rain after their formation in the atmosphere (Fig. 5B) (*25*, *37*). Our chemistry shows that robust reaction networks can be established that allow all key intermediates to be generated efficiently from relatively complex mixtures, followed by their physical enrichment or separation on the basis of their solubility in water. Wet-dry cycles govern the formation of purine and pyrimidine RNA building blocks in a scenario depicted in Fig. 5B. Of course, we will be unable to definitively prove that the described scenario indeed took place on early Earth, but the reported chemistry shows that, under plausible prebiotic conditions, mutually synergistic reaction pathways can be established in which the intermediates along one pathway help the chemistry of the other. In such a scenario, we show that the key building blocks of life can be created without the need for sophisticated isolation and purification procedures of reaction intermediates that are common in traditional organic chemistry.

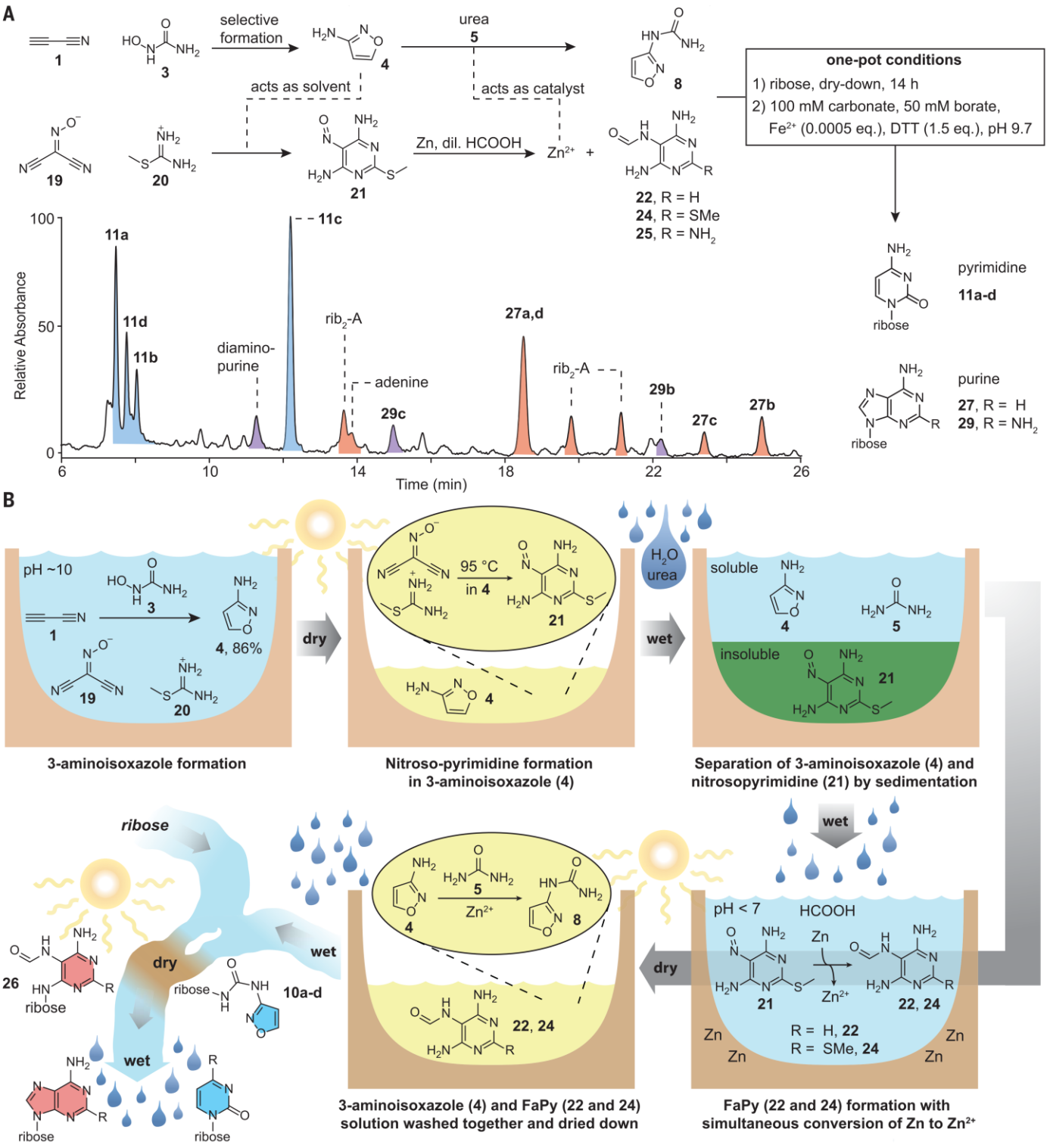

Fig. 5. Unified chemical scenario for the formation of purine and pyrimidine nucleosides. (**A**) Depiction of the connected reaction pathways to pyrimidine and purine nucleosides, together with the HPLC analysis (260 nm) of the final reaction mixtures. Nucleosides are labeled as follows: **a** = α-furanosyl; **b** = β-furanosyl; **c** = α-pyranosyl; **d** = β-pyranosyl. (**B**) Proposed geochemical scenario for the simultaneous synthesis of purine and pyrimidine nucleosides, driven by wet-dry cycles. In yellow, the solvent is 3-aminoisoxazole (**4**), which can be enriched from an aqueous solution due to its high boiling point (228°C). 2-(Methylthio)-5-nitrosopyrimidine-4,6-diamine (**21**) is a general precursor for adenosine and guanosine (*18*). Compounds **8**, **22**, and **24** are accessible in the same pot, and they can react with ribose to the RNA nucleosides in a one-pot reaction.

The concurrent formation of pyrimidine and purine nucleosides in the network can be traced to just a few key starting molecules, such as cyanoacetylene **1**, NH_3, NH_2OH **2** (or the disulfonate **6**), HCN, urea **5**, formic acid, and isocyanate, plus salts such as nitrites, carbonates, and borates. Metals such as Zn or Fe and their ions play an important role in our chemistry, consistent with their proposed involvement in early metabolic cycles (*23*, *38*). In particular, iron-sulfur surfaces needed for pyrimidine formation have been discussed as platforms for early prebiotic chemistry (*15*, *34*, *39*). The 5′-(di)phosphorylation is integrated into our pathway if phosphate minerals such as lüneburgite or struvite (figs. S11 to S13) are present. It remains unclear, however, how ribose or any other carbohydrate, such as glycerol or threose, that is needed to form the backbone of RNA or pre-RNA could have formed selectively (*29*, *40*). Sugars such as ribose can be produced nonselectively in a formose-like reaction, which is possible in a variety of different physico-chemical environments (*32*, *41*–*43*).

REFERENCES AND NOTES

1. J. A. Doudna, T. R. Cech, *Nature* **418**, 222–228 (2002).
2. D. P. Horning, G. F. Joyce, *Proc. Natl. Acad. Sci. U.S.A.* **113**, 9786–9791 (2016).
3. J. Attwater, A. Raguram, A. S. Morgunov, E. Gianni, P. Holliger, *eLife* **7**, e35255 (2018).
4. W. Gilbert, *Nature* **319**, 618 (1986).
5. M. W. Powner, B. Gerland, J. D. Sutherland, *Nature* **459**, 239–242 (2009).
6. S. Becker *et al*., *Science* **352**, 833–836 (2016).
7. H.-J. Kim, S. A. Benner, *Proc. Natl. Acad. Sci. U.S.A.* **114**, 11315–11320 (2017).
8. S. Stairs *et al*., *Nat. Commun.* **8**, 15270 (2017).
9. R. Saladino *et al*., *Proc. Natl. Acad. Sci. U.S.A.* **112**, E2746–E2755 (2015).
10. J. F. Kasting, *Science* **259**, 920–926 (1993).
11. R. M. Hazen, *Am. J. Sci.* **313**, 807–843 (2013).
12. E. D. Swanner *et al*., *Earth Planet. Sci. Lett.* **390**, 253–263 (2014).
13. P. B. Rimmer, O. Shorttle, *Life* **9**, 12 (2019).
14. W. Martin, J. Baross, D. Kelley, M. J. Russell, *Nat. Rev. Microbiol.* **6**, 805–814 (2008).
15. E. Camprubi, S. F. Jordan, R. Vasiliadou, N. Lane, *IUBMB Life* **69**, 373–381 (2017).
16. S. A. Benner, H.-J. Kim, E. Biondi, in *Prebiotic Chemistry and Chemical Evolution of Nucleic Acids*, C. Menor-Salván, Ed. (Springer International Publishing, Cham, 2018), pp. 31–83.
17. S. Ranjan, Z. R. Todd, P. B. Rimmer, D. D. Sasselov, A. R. Babbin, *Geochem. Geophys. Geosyst.* **20**, 2021–2039 (2019).
18. S. Becker *et al*., *Nat. Commun.* **9**, 163 (2018).
19. P. Thaddeus, *Philos. Trans. R. Soc. Lond. B Biol. Sci.* **361**, 1681–1687 (2006).
20. R. A. Sanchez, J. P. Ferris, L. E. Orgel, *Science* **154**, 784–785 (1966).
21. B. H. Patel, C. Percivalle, D. J. Ritson, C. D. Duffy, J. D. Sutherland, *Nat. Chem.* **7**, 301–307 (2015).
22. H. Kofod, B. Wickberg, A. Kjær, *Acta Chem. Scand.* **7**, 274–279 (1953).
23. K. B. Muchowska, S. J. Varma, J. Moran, *Nature* **569**, 104–107 (2019).
24. V. S. Airapetian, A. Glocer, G. Gronoff, E. Hébrard, W. Danchi, *Nat. Geosci.* **9**, 452–455 (2016).
25. H. J. Cleaves, J. H. Chalmers, A. Lazcano, S. L. Miller, J. L. Bada, *Orig. Life Evol. Biosph.* **38**, 105–115 (2008).
26. D. P. Summers, S. Chang, *Nature* **365**, 630–633 (1993).
27. S. Ranjan, Z. R. Todd, J. D. Sutherland, D. D. Sasselov, *Astrobiology* **18**, 1023–1040 (2018).
28. G. K. Rollefson, C. F. Oldershaw, *J. Am. Chem. Soc.* **54**, 977–979 (1932).
29. G. F. Joyce, *Nature* **418**, 214–221 (2002).
30. D. M. Fialho *et al*., *Org. Biomol. Chem.* **16**, 1263–1271 (2018).
31. H.-J. Kim *et al*., *Angew. Chem. Int. Ed.* **55**, 15816–15820 (2016).
32. A. Ricardo, M. A. Carrigan, A. N. Olcott, S. A. Benner, *Science* **303**, 196–196 (2004).
33. M. Kijima, Y. Nambu, T. Endo, *J. Org. Chem.* **50**, 1140–1142 (1985).
34. G. Wächtershäuser, *Microbiol. Rev.* **52**, 452–484 (1988).
35. U. Trinks, A. Eschenmoser, ETH Zurich (1987); doi: 10.3929/ethz-a-000413538.
36. R. Krishnamurthy, *Isr. J. Chem.* **55**, 837–850 (2015).
37. J. Liebig, F. Wöhler, *Ann. Phys.* **96**, 369–400 (1830).
38. M. Preiner *et al*., *bioRxiv* 682955 (2019).
39. C. Bonfio *et al*., *Nat. Catal.* **1**, 616–623 (2018).
40. J. S. Teichert, F. M. Kruse, O. Trapp, *Angew. Chem. Int. Ed.* **58**, 9944–9947 (2019).
41. J. Kofoed, J.-L. Reymond, T. Darbre, *Org. Biomol. Chem.* **3**, 1850–1855 (2005).
42. C. Meinert *et al*., *Science* **352**, 208–212 (2016).
43. K. Usami, A. Okamoto, *Org. Biomol. Chem.* **15**, 8888–8893 (2017).

ACKNOWLEDGMENTS

We thank J. Kampmann for x-ray diffraction measurements and S. Balasubramanian for supporting S.B. during the revision of the manuscript. **Funding:** Deutsche Forschungsgemeinschaft (DFG) provided financial support via the programs SFB1309 (TP-A4), SFB749 (TP-A4), SPP-1784, GRK2062/1, and CA275/11-1, the Excellence Cluster EXC114, the European Research Council (ERC) under the European Union's Horizon 2020 research and innovation program (grant agreement EPiR 741912), and the Volkswagen Foundation (Initiative "Life": EcoRib). H.O. thanks the European Commission for a Marie Sklodowska-Curie postdoctoral fellowship (PRENUCRNA). **Author contributions:** T.C. designed and supervised research; S.B. helped to design the study, S.B., J.F., S.W., and H.O. performed the experiments. C.S., M.R., and A.C. supported the synthesis and MS quantification, K.I. performed biochemical studies, and T.A. helped to design the synthesis. T.C., S.B., J.F., and S.W. analyzed data. T.C. and S.B. wrote the manuscript and designed the figures. **Competing interests:** The authors declare no competing interests. **Data and materials availability:** The x-ray crystallographic data for isoxazoleurea **8** are deposited in the CCDC under accession number 1889652. All other data needed to support the conclusions of this manuscript are included in the main text and supporting material.

SUPPLEMENTARY MATERIALS

science.sciencemag.org/content/366/6461/76/suppl/DC1
Materials and Methods
Figs. S1 to S13
References (*44*–*51*)

8 March 2019; resubmitted 21 June 2019
Accepted 21 August 2019
10.1126/science.aax2747

Science

Unified prebiotically plausible synthesis of pyrimidine and purine RNA ribonucleotides

Sidney BeckerJonas FeldmannStefan WiedemannHidenori OkamuraChristina SchneiderKatharina IwanAntony CrispMartin RossaTynchtyk AmatovThomas Carell

Science, 366 (6461), • DOI: 10.1126/science.aax2747

Conditions right for making nucleosides

In the absence of biological catalysts and metabolism, can atmospheric and geochemical processes provide the substrates and conditions required for production of biological molecules? Becker *et al.* devised an abiotic synthetic scheme that allows for accumulation of both purine and pyrimidine nucleoside mono- and diphosphates (see the Perspective by Hud and Fialho). A key starting material for this chemistry, hydroxylamine and/or hydroxylamine disulfonate, can form under plausible early atmospheric conditions. Cycles between wet and dry conditions provide the environments necessary to complete formation of purine and pyrimidine bases essentially in one pot.

Science, this issue p. 76; see also p. 32

Science (ISSN 1095-9203) is published by the American Association for the Advancement of Science. 1200 New York Avenue NW, Washington, DC 20005. The title *Science* is a registered trademark of AAAS.

4. Unveröffentlichte Arbeiten

4.1 Ein einheitliches Konzept zur präbiotischen Entstehung von Pyrimidinnukleosiden

J. Feldmann†, M. K. Skaanning†, M. Lommel, P. Mayer, and T. Carell.‡

Prolog

Als Bausteine für RNA, DNA und Kofaktoren sind Pyrimidinnukleoside wichtige Biomoleküle heutiger Lebewesen. Phylogenetische Studien lassen vermuten, dass bereits LUCA ein umfangreiches Set verschiedenster Pyrimidinnukleoside besaß. Zu deren präbiotischen Entstehung finden sich in der Literatur mehrere Reaktionswege, welche sich in ihren Bedingungen, Ausgangsverbindungen und Nukleosidierungsstrategien unterscheiden. Welcher dieser Wege präbiotisch am plausibelsten ist, lässt sich nicht pauschal beantworten. Vielmehr bietet jeder Weg eigene Vorteile sowie Nachteile. Im nachfolgenden Manuskript wurden die unterschiedlichen Pyrimidinsynthesen zu einem gemeinsamen Syntheseweg fusioniert, um die Vorteile der unterschiedlichen Ansätze zu einen. So bietet das neue Modell den Vorteil einer indirekten Nukleosidierung, welche den schrittweisen Aufbau des Furanoserings *in situ* ermöglicht und folglich nicht auf freie Ribose angewiesen ist. Zudem kann Cyanoacetylen als reaktive Ausgangsverbindung bereits im ersten Schritt abreagieren, was potenziellen Zersetzungs- bzw. Nebenreaktionen entgegenwirkt. Von zentraler Bedeutung ist Kupfer(I/II), da es sowohl die Anreicherung von 3-Aminoisoxazol erlaubt als auch dessen Folgereaktion katalysiert.

Autorenbeitrag

Entwicklung des Gesamtkonzepts sowie eines neuen Synthesewegs zu Anhydrocytidin. Synthese neuer 3-Aminoisoxazol-Metall-Komplexe. Erhebung, Auswertung und Interpretation von Daten.

---

† Die Autoren haben zu gleichen Teilen zum Manuskript beigetragen

‡ Für ergänzende Informationen siehe Anhang II

A Unifying Concept for the Prebiotic Formation of RNA Pyrimidine Nucleosides

Abstract

The question of how nucleosides might have formed as essential precursor molecules on the early Earth is one of the many challenges associated with the origin of life. In this context, the prebiotic synthesis of pyrimidine nucleosides is controversially discussed. For the pyrimidines, two at first glance contradictory prebiotically plausible reaction pathways have been proposed, based on either oxazole or isoxazole chemistry. Here we show that these two reaction sequences can be merged under prebiotically reasonable conditions, suggesting that both pathways could have co-existed and possibly interacted. The key precursor 3-aminoisoxazole was found to react with the key intermediate of the oxazole route (ribo-2-(methylthio)oxazoline), to give a ribo-isoxazole-oxazoline hybrid structure, which collapses upon reductive N-O bond cleavage to the nucleoside cytidine. The data suggest that different, interacting prebiotically plausible chemical pathways may have created the key molecules of life on the early Earth.

Introduction

Life is a complex phenomenon that rests on the availability of a large number of building blocks such as amino acids, nucleosides, and molecules that can build cell walls and establish complex metabolic networks. The question of how all these "molecules of life" could have formed in the absence of an efficient biosynthetic machinery at the dawn of life is one of the greatest scientific challenges.[194] The first steps towards life required the formation of higher order structures from molecules that must have formed in the abiotic environment on the early Earth.[42] These molecules then learned to perform peptide synthesis.[108] *Urey* and *Miller*, for example, simulated putative early Earth conditions and found that amino acids can form by lightening through an atmosphere composing of H_2, H_2O, CH_4, and NH_3.[19, 41] Since then, scientists have been trying to unravel chemical networks that could lead to the formation of the building blocks of life under prebiotically plausible conditions. In this contexts, particular attention was and is given to pathways that can generate amino acids,[26] establish potential early metabolic pathways,[195] or lead to the formation of purine and pyrimidine nucleosides[27-28]. Particularly, the question of how the pyrimidine nucleosides could have formed under

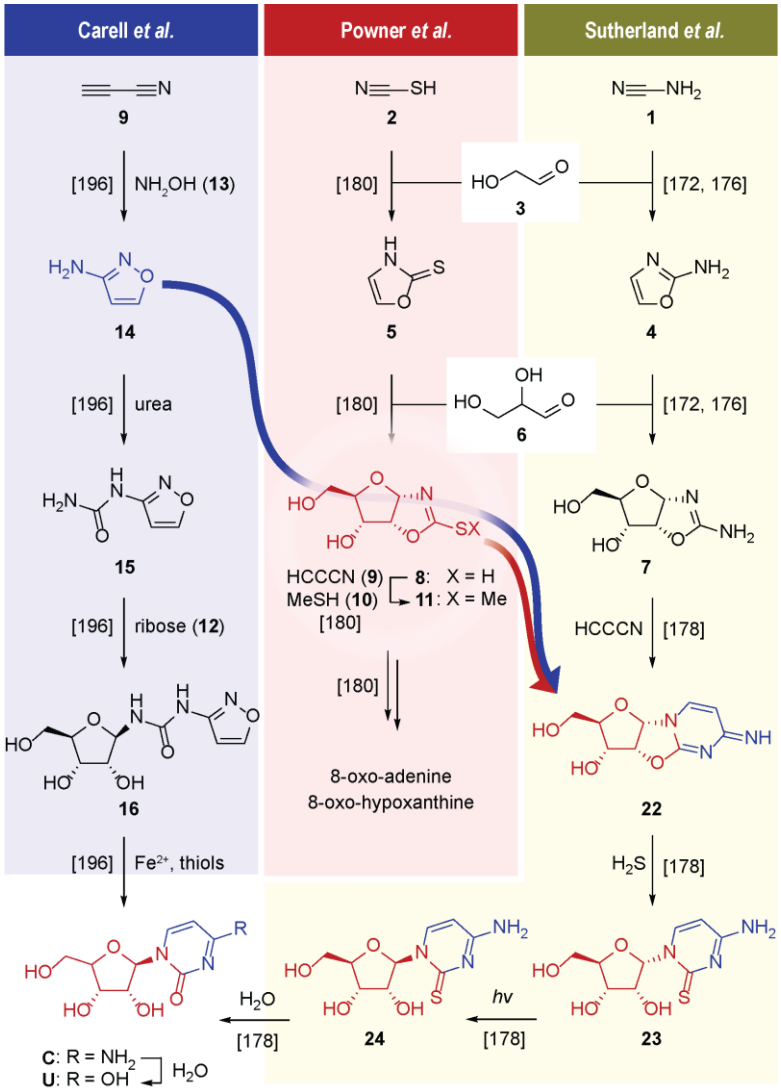

Figure 2: Depiction of the *Sutherland*, *Powner*, and *Carell* pathways to pyrimidines and 8-oxo-purines, respectively, together with a schematic presentation of the link between the pathways.

plausible early Earth condition has been a long-standing question. Based on the chemistry proposed by *Orgel* and co-workers,[169] *Sutherland* and *Powner* (Figure 2) reported in seminal pieces of work that cyanamide (**1**) or thiocyanic acid (**2**) can react with glycolaldehyde (**3**) to give either 2-aminooxazole (**4**)[172, 176] or 2-thiooxazole (**5**)[180]. These precursors were found to react with glyceraldehyde (**6**) to ribo-2-aminooxazoline **7**[172, 176] or ribo-2-thiooxazoline **8**[180], respectively. Ribo-2-aminooxazoline **7** is suggested to have reacted directly with cyanoacetylene (**9**) to form pyrimidine nucleosides.[178] In addition, methylation of ribo-2-thiooxazoline **8** via cyanoacetylene (**9**) and methanethiol (**10**) to ribo-2-(methylthio)oxazoline **11** could have initiated the formation of 8-oxopurine nucleosides under early Earth conditions.[180] The reported pathways have the advantage that they do not require free ribose (**12**) for producing nucleosides. The selective formation of ribose (**12**) under early Earth conditions is intensively investigated,[76] but still under debate. A potential hurdle of the pathways is the need for reactive cyanoacetylene (**9**) at a late stage of the synthesis, which as has a half-life of only 11d in an aqueous environment (pH 9, 30 °C).[141, 150]

Carell and co-workers discovered that cyanoacetylene (**9**) can be directly trapped already in the first step of the isoxazole pathway with hydroxylamine (NH_2OH, **13**), to give 3-aminoisoxazole (**14**), which reacts with urea and ribose (**12**) via **15** to isoxazole ribopyranosides and furanosides **16**.[196] Subsequent cleavage of the central N-O bond (via thiols and Fe^{2+}) allows the molecule to collapse to cytidine (**C**) and upon hydrolysis to uridine (**U**).[196] While this pathway avoids late-stage reaction with cyanoacetylene (**9**) it has the caveat that it depends on the availability of free ribose (**12**).

Here we investigated if the two seemingly incompatible oxazole and isoxazole pathways can be combined to give pyrimidine nucleosides without the need for ribose and late-stage addition of cyanoacetylene (**9**).

Results and Discussion

To establish a combined pathway, we recapitulated that the reaction of thiocyanate (**2**) with glycolaldehyde (**3**) to 2-thiooxazole (**5**), and reaction of **5** with glyceraldehyde (**6**) provides ribo-2-thiooxazole **8**.[180] Upon deviating from the reported methylation step, we found that methylation is possible starting with *N*-methylurea (**17**), which forms from cyanate (**18**) and methylamine (**19**) (Figure 3a).[168] Nitrosation of **17** (via NO_2^-) generates *N*-methyl-*N*-nitrosourea (**20**), which under basic conditions spontaneously decomposes to diazomethane,[168] which allows selective methylation of the thiol functionality in 25% yield (Figure 3b).

Reaction of cyanoacetylene (**9**) at the beginning of the reaction sequence with hydroxylamine (**13**) generates 3-aminoisoxazole (**14**). We now discovered that **14** reacts with ribo-2-(methylthio) oxazoline **11** under Cu^+-catalysis. The reaction proceeds both step wise and under one pot conditions. In in the two-step reaction, ribo-*N*-isoxazolyl-2-aminooxazoline **21** is obtained in 6% yield. Subsequent cleavage of the isoxazole N-O bond with thiols, catalyzed by Cu^+ (*vide infra*), then generated the anhydro nucleoside **22**, which gives cytidine along known pathways via **23** and **24**.[178] The chromatogram depicted in Figure 3c show the efficient conversion of the Sutherland/Powner intermediate with the Carell isoxazole intermediate to the joined structure **22**. The one-pot reaction is more efficient! When we mixed the ribo-2-(methylthio)oxazoline **11** with 3-aminoisoxazole (**14**), we observed under Cu^+-catalysis and slightly acidic conditions (5% AcOH) formation of the anhydro nucleoside in 38% yield.

The combined pathway reported here avoids the need for late stage cyanoacetylene and ribose. A potential problem in this context could be that the ribo-2-(methylthio)oxazoline **11**

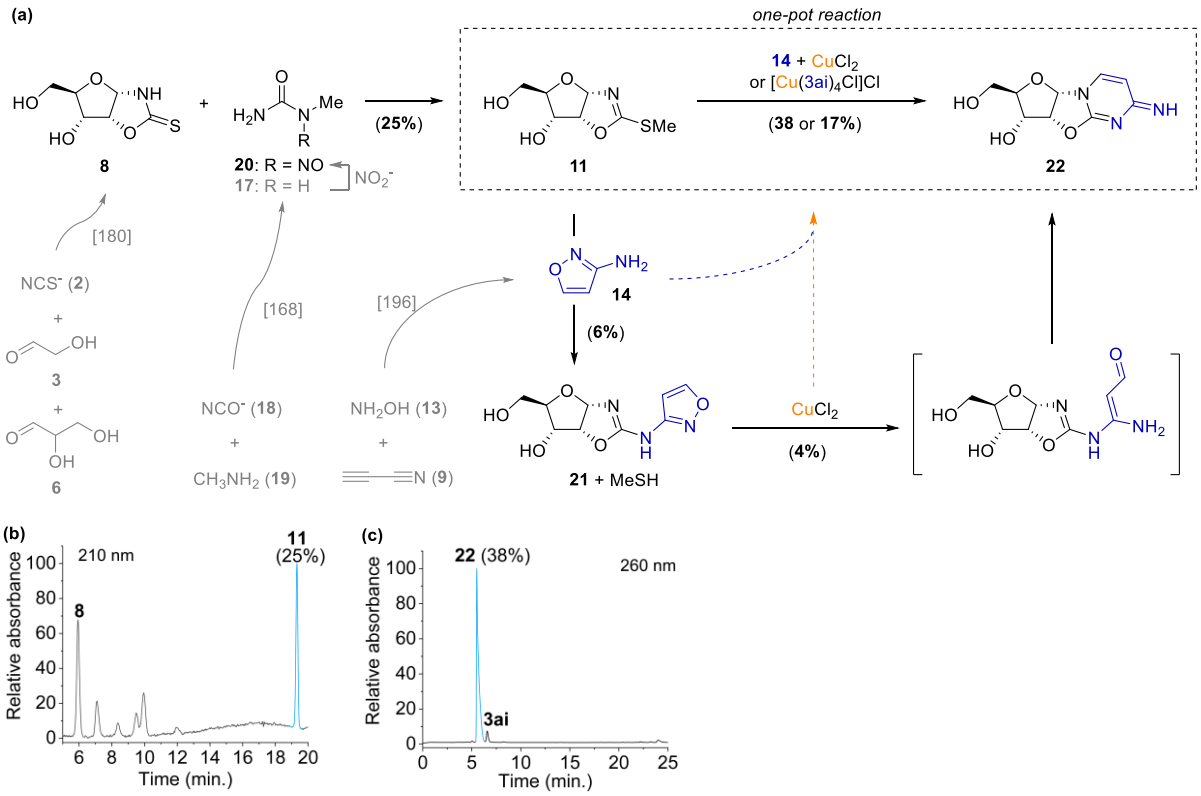

Figure 3: a) Reaction sequence that generates precursor molecules of cytidine upon merging of the Sutherland-Powner and Carell pathways; HPL-chromatogram for (b) the methylation of ribo-2-thiooxazoline 8 to ribo-2-(methylthio)oxazoline 11 and (c) its conversion to ribo-anhydro cytidine 22.

reacts with other nucleophiles in the absence of a 3-aminoisoxazole (**14**), which would waste starting materials. The formation of 3-aminoisoxazole (**14**) requires cyanoacetylene (**9**), and it is assumed that this compound is formed only in traces, so that the 3-aminoisoxazole is also present only in trace amounts. A potential solution to the problem could be an enrichment process that allows formation of 3-aminoisoxazole (**14**) deposits. We therefore investigated the interaction of 3-aminoisoxazole (**14**) with different bivalent metal ions (Ca^{2+}, Co^{2+}, Ni^{2+}, Cu^{2+}, and Zn^{2+}), some of which were prebiotically very abundant (Co^{2+} and Ni^{2+}).[197] We found that 3-aminoisoxazole (**14**) forms stable complexes in the presence of each metal ion, which crystallize from solution (Figure 4). This broad possibility for the deposition and accumulation of 3-aminoisoxazole (**14**) supports the joined pathway discovered here. Next, we performed an experiment mixing all the above-mentioned metal salts in the presence of 3-aminoisoxazole (**14**), and to our delight, we observed that the Cu^{2+} complex ($[Cu(3ai)_4Cl]Cl$) forms first. Since Cu^{2+} is considered a prebiotically less abundant metal ion and its exact concentrations are questionable,[197] it is remarkable that 3-aminoisoxazole (**14**) enables Cu^{2+} enrichment.

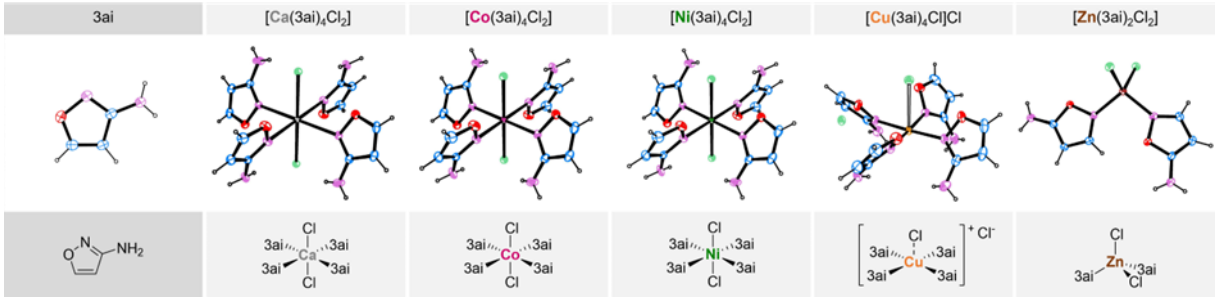

Figure 4: Crystal structures of 3-aminoisoxazole (3ai, 14) and its complexes with various M^{2+} ions. In an experiment with a mixture of M^{2+} salts, the Cu^{2+} complex precipitates first.

This observation further supports the plausibility of the chemistry reported here, since Cu^{+} it is needed to catalyze the N-O bond opening to initiate the reaction cascade to cytidine (Figure 3). To demonstrate that the enriched complex ($[Cu(3ai)_4Cl]Cl$) can be directly used for the one-pot reaction, we mixed the isolated crystals with ribo-2-(methylthio)oxazoline **11** under slightly acidic conditions (5% AcOH). After one day at 25°C, anhydro nucleoside **22** was indeed obtained in 17% yield, showing that both the organic and inorganic parts of the deposit were chemically available.

Conclusion

The currently proposed prebiotically plausible pathways to pyrimidine nucleosides depend on oxazole[172, 176, 178, 180] or isoxazole[196] intermediates, some of which form in one-pot reactions driven by wet-dry cycles. If we assume that prebiotic chemistry took place in warm, shallow ponds, as already assumed by Charles Darwin,[198] early chemical transformations on Earth were probably largely unsynchronized, so that all starting molecules and all intermediates were present in a reaction environment at the same time. In such a scenario, we must assume that multiple reactions proceeded with intensive chemical interactions between individual pathways. Such a scenario can be partially circumvented by extending the concept to interconnected shallow ponds where different chemical processes occur in different ponds, and where pond contents may mix at certain times due to flooding or geological activity. It is not unrealistic that in such a scenario, either ribose or cyanoacetylene formed in a separate pond and entered a pond where the other chemistry occurred. But even in scenarios with multiple ponds, we must assume that different reaction pathways occurred simultaneously.

Here we show that the two pathways that have been proposed for the formation of pyrimidine nucleosides under plausible early Earth conditions, both of which have their specific advantages and disadvantages, can be merged into a unified pathway. The result show that many nucleosides are accessible, which are, in this sense, privileged prebiotic molecules formed under a variety of conditions. There are many routes to nucleosides, and they appear to be interconnected.

4.2 Die Entstehung von Biomolekülen unter frühen Erdbedingungen

J. Feldmann†, S. Wiedemann†, S. Becker, and T. Carell.‡

Prolog

Für die Entstehung des Lebens war die Bildung von Aminosäuren und Nukleosiden auf der frühen Erde unabdingbar. Verschiedene Hypothesen wurden aufgestellt, welche die Bildung dieser molekularen Bausteine aus primitiven Vorläufermolekülen beschreiben. Als zentrale Schlüsselmoleküle gelten vor allem reaktive Nitrile wie Blausäure, Cyanamid und Cyanoacetylen, welche sich in ausreichenden Mengen unter stark reduzierenden Bedingungen bilden. Die frühe Erdatmosphäre war jedoch nur schwach reduzierend und die Bildung reaktiver Nitrile unter diesen Bedingungen ineffizient. Dies stellt die Plausibilität vieler etablierten Hypothesen in Frage. Das nachfolgende Manuskript beschreibt einen Syntheseweg, welcher die systematische Bildung reaktiver Nitrile unter schwach reduzierenden Bedingungen erlaubt. Als Stickstoffquelle dient Hydroxylamin, während Formaldehyd und komplexere Aldehyde als Kohlenstoffquelle fungieren. Die Bildung von Aldoximen und eine anschließende Dehydratisierung liefern verschiedene Nitrile als reaktive Ausgangsverbindungen. Von diesen ausgehend wurden neue Synthesewege entwickelt, welche den Zugang zu Aminosäuren, Purin- und Pyrimidinbasen ermöglichen.

Autorenbeitrag

Entwicklung des Gesamtkonzepts sowie neuer Synthesewege zu Aminosäuren, Pyrimidin- und Purinbasen. Optimierung der Synthesen von Pyrimidin- und Purinbasen unter präbiotisch plausiblen Bedingungen. Erhebung, Auswertung und Interpretation von Daten.

---

† Die Autoren haben zu gleichen Teilen zum Manuskript beigetragen

‡ Für ergänzende Informationen siehe Anhang III

The Origin of Biomolecules Under Early Earth Conditions

Abstract

Life on Earth has started with the formation of biomolecules such as amino acids and nucleosides, which subsequently condensed to give proteins and oligonucleotides. The formation of the building blocks of life required the presence of reactive starting materials on the early Earth, which are currently thought to have been HCN, together with a set of small nitriles such as cyanoacetylene, cyanamide and malononitrile. The formation of these starting materials in significant amounts under plausible early Earth conditions is a major unsolved problem. Here, we analyzed the formation of starting materials for life from simple nitrogen-containing inorganics and formaldehyde that can form on an early Earth surrounded by a weakly reducing atmosphere, composed of CO_2, N_2, H_2O, and SO_2. In contrast to the generally accepted models, which involve highly reducing atmospheric conditions, we detected the formation of aldoximes and of complex nitriles, which can start diverse reaction networks that lead to amino acids as well as pyrimidine and purine nucleosides. The uncovered chemistry provides a comprehensive roadmap from inorganic matter to molecules of life and shows that hydroxylamine and aldoximes can be considered signature molecules for life in the universe.

Introduction

The origin of life on Earth required as the initial step the formation of nucleosides and amino acids as the essential building blocks for nucleic acids and proteins.[16, 26-28] Chemical reactions towards nucleosides and amino acids, however, need reactive starting materials, which must have been present on the early Earth in significant amounts. The current chemical models suggest that nitriles such as hydrogen cyanide (**1**, HCN), cyanamide (**2**), cyanoacetylene (**3**), dicyan (**4**), and malononitrile (**5**) could have served as these reactive precursors on the early Earth (Figure 5A).[16, 26-28] Despite the central importance of these molecules for the current concepts of how life could have emerged, their efficient formation under early Earth conditions is an unsolved problem. While molecules such as **1**–**5** are known to form predominantly in a hydrogen, methane and ammonia containing atmosphere,[16, 78, 132, 149, 199-201] it is currently assumed that such a highly reducing atmosphere may have never existed on the early Earth.

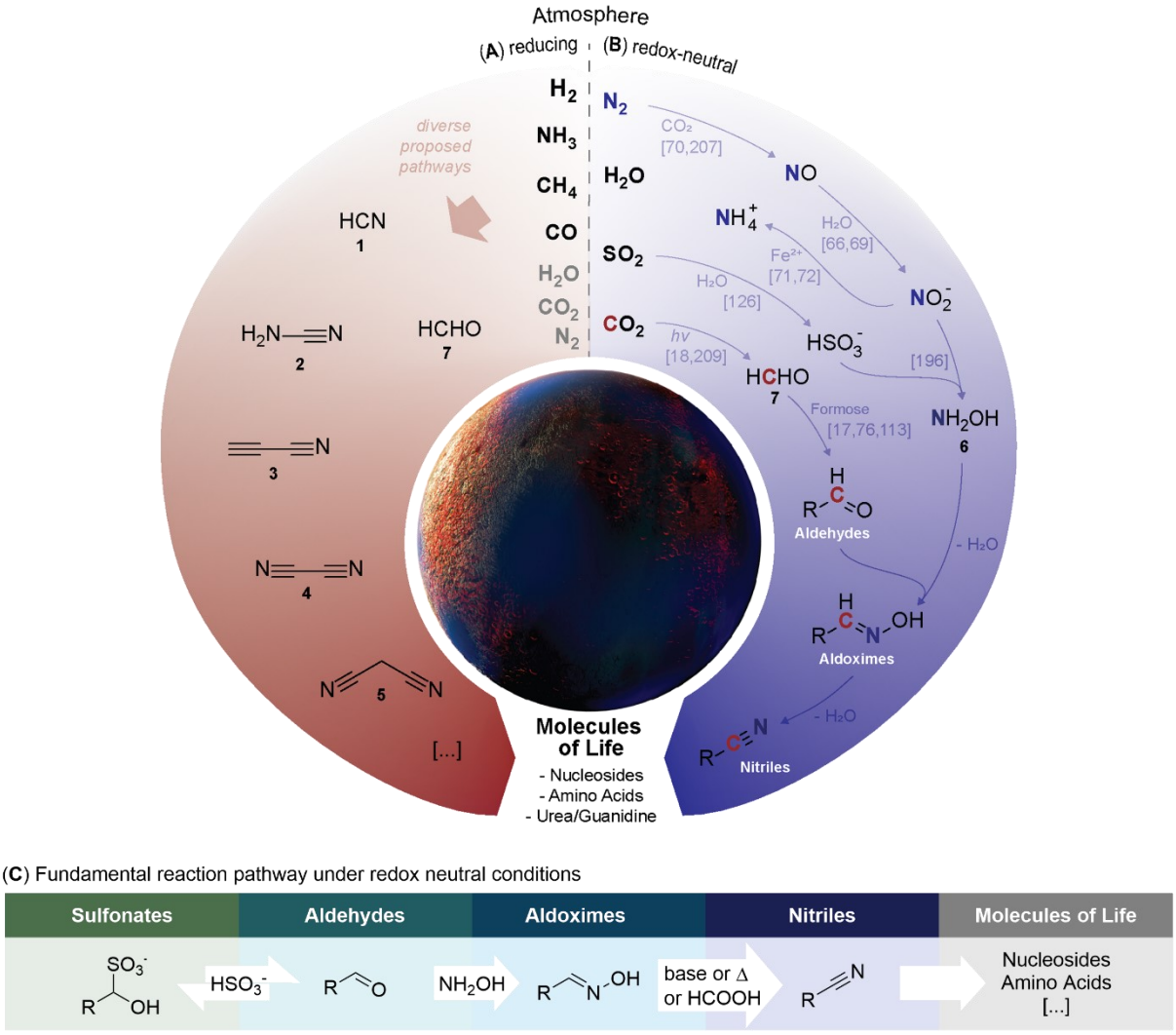

(C) Fundamental reaction pathway under redox neutral conditions

Figure 5: Depiction of the two alternative feedstock-providing early Earth models. (A) The reductive scenario shows the currently accepted model of how HCN (1) and the feedstock molecules 2–5 needed for the synthesis of amino acids and nucleosides could have formed. (B) The neutral scenario is based on the idea that the early Earth atmosphere had a redox neutral atmosphere, which was capable of producing nitrogen oxides and aldehydes. These molecules react to give aldoximes and, upon water elimination, nitriles with a balanced reactivity from which amino acids and nucleosides are available. (C) Fundamental chemistry concept for the origin of biomolecules in a redox neutral, early Earth atmosphere.

All data that are currently available suggest a Hadean atmosphere that was weakly reducing and composed of CO_2, N_2, H_2O, and SO_2.[61, 65, 202-203] Under these conditions, the resilient formation of feedstock molecules such as **1**–**5** is unlikely or even impossible.[64, 77]

The enigma around the fundamental reactions that once allowed life to form is currently tackled with concepts that suggest a temporary, potentially only local, shift of the atmosphere into a H_2-rich state, induced, e.g., by iron core impactors.[64, 79-80] Alternatively, it is discussed that HCN (**1**) may have formed by aerodynamic ablation of carbonaceous chondrites.[91] An attractive model suggests that such sporadically formed HCN (**1**) could have been captured and enriched by soluble Fe^{2+} in the form of ferrocyanides, from where it could have been liberated to fuel prebiotic reactions.[93, 204-205] While these concepts offer potential solutions for the HCN (**1**) supply problem, the durable formation of the other essential nitriles **2**–**5** in larger quantities remains difficult.[64, 77]

Here, we describe chemical pathways that can take place under plausible early Earth conditions, using reactions under a plausible redox neutral atmosphere (Figure 5B). The discovered pathways involve first the formation of nitrogen-containing inorganics by lightning and UV-irradiation, to furnish a set of complex aldoximes, which can further react to complex nitrile organics. From these feedstock molecules amino acids and pyrimidine or purine nucleosides are readily available (Figure 5C).

Formation of nitriles under weakly reducing conditions

The inorganic chemical network that allows the fixation of nitrogen atoms in a redox neutral atmosphere is shown in Fig. 1B. It is well established that lightning and UV-irradiation through a CO_2, N_2, H_2O, and SO_2 atmosphere generates extensive amounts of nitrogen oxide (NO), which further reacts to give the inorganic nitrate (NO_3^-), and nitrite (NO_2^-).[66, 69-70, 78, 206-208] In the presence of (aqueous) Fe^{2+}, which was abundant on the early Earth, it is likely these molecules were partially reduced to NH_3.[71-72] The atmospheric component SO_2, which originated in large quantities from volcanic activity, is known to react with water to give bisulfite (HSO_3^-), which reacts with NO_2^- as a reductant to give hydroxylamine disulfonate[196]. This molecule slowly hydrolyzes to hydroxylamine (**6**) and sulfate.[196] Another major component of the hadean atmosphere, CO_2, provides formaldehyde (**7**, H_2CO),[18, 75, 209]upon lightning and UV irradiation and continues to react to yield more complex aldehydes[18, 67, 75-76, 209-212] including glycolaldehyde (**8a**),[18, 67, 75-76, 209] and malondialdehyde (**9**)[210, 213]. Glycolaldehyde (**8a**), which is a central element of the formose cycle, is the basis for the formation of more complex α-hydroxyaldehydes **8b**–**e**.[17, 76, 109, 113] All of these different aldehydes are rather reactive molecules with consequently limited lifetimes. In the presence of HSO_3^-, however, the aldehydes can

form stable sulfonate deposits. According to Benner, these bisulfite adducts are conceivable storage forms of aldehydes, from which they can be liberated to fuel prebiotic reactions.[126] Our model suggests that these bisulfite adducts and hydroxylamine (**6**) are the major ingredients for prebiotically plausible recipes that enable the formation of biomolecules (Fig. 1C).

Formation of urea, guanidine, and amino acids

To examine how this chemistry could have enabled the formation of amino acids, we systematically reacted various prebiotically reasonable aldehydes (or their bisulfite adducts) with hydroxylamine. We first focused on formaldehyde (**7**), which can be prebiotically stabilized and accumulated upon formation of its bisulfite adduct **10**.[126] While formaldehyde (**7**) is known to form urea (**11**) in the presence of hydroxylamine,[190] we found that the addition of ammonia also provides guanidine (**12**) (Figure 6A). Urea (**11**) and guanidine (**12**) are both key molecules needed for the formation of pyrimidine or purine nucleosides (*vide infra*). We found that the formation of guanidine (**12**) is even possible under prebiotically plausible one-pot conditions.

We next reacted hydroxylamine (**6**) with various α-hydroxyaldehydes that are produced for example by the formose cycle. We tested glycolaldehyde (**8a**),[67, 76] glyceraldehyde (**8b**),[76] lactaldehyde (**8c**),[211-212] and the aldehydes **8d** and **8e** (Figure 6B). Under slightly basic conditions we found that they all form the corresponding aldoximes **13a**–**e** in excellent yields (75%–100%). Again, we observed that the reactions are also possible with the aldehyde bisulfite adducts **14a**–**e** [211-212]. We next subjected the α-hydroxyaldoximes **13a**–**e** to prebiotically plausible wet-dry cycles and noted that all the aldoximes investigated eliminate water quickly to give the corresponding α-hydroxynitriles (**15a**–**c**), again in excellent yields (75%–100%). This reaction sequence can also be performed under one-pot conditions (Figure 6B,C), which furnished the α-hydroxynitriles **15a**–**e** in yields between 20% and 84%. When the hydroxynitriles are brought in contact with ammonia, α-aminonitriles **16a**–**e** form, which are well established precursor molecules for α-amino acids.[20, 179] These results show that the aldoximes **13a**–**e**, which form under redox neutral conditions are efficient precursors for the prebiotic formation of amino acids such as **Gly**, **Ser**, **Ala**, **Val**, and **Phe**. This new route does not exclude

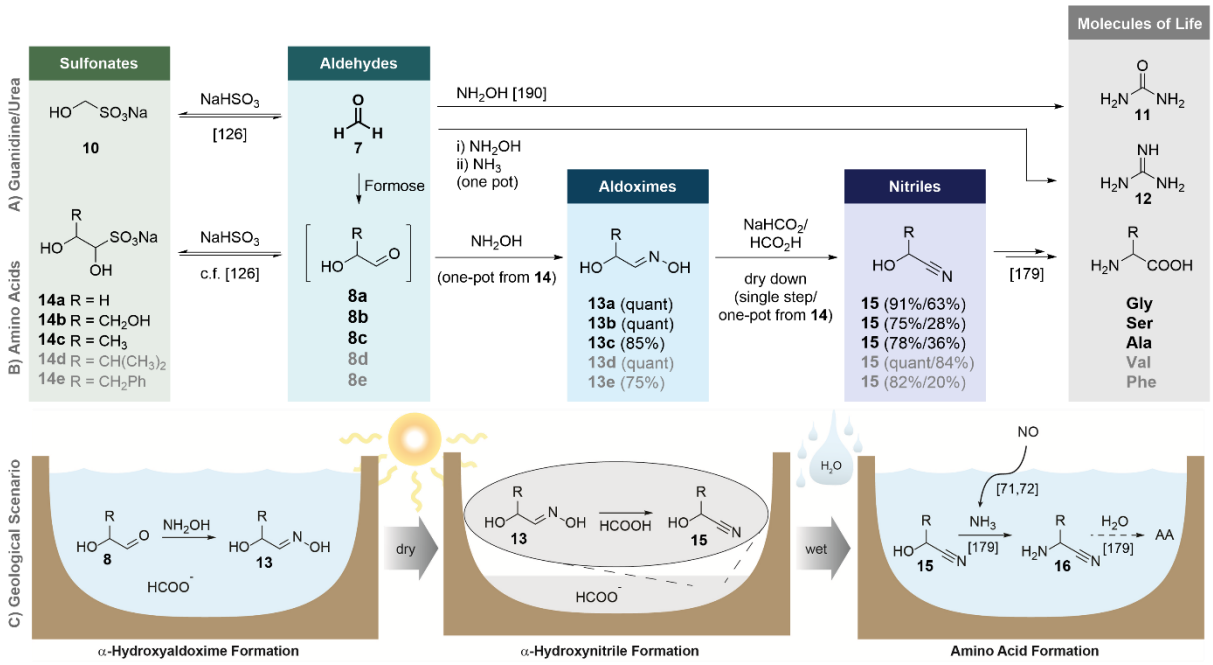

Figure 6: Prebiotic formation of amino acids, urea, and guanidine. (A) Formation of urea (11) and guanidine (12) from formaldehyde (7) and hydroxylamine (6). (B) Formation of amino acids from hydroxylamine (6) and α-hydroxyaldehydes 8 that are stabilizabled as their corresponding bislufite adducts 14. The α-hydroxyaldehydes 8a–c formed from formaldehyde (7) in the formose reaction. The reaction with hydroxylamine (6) followed by elimination of water giving α-hydroxynitriles 15 is possible in (C) one-pot reactions under simple dry down and re-wetting conditions.

amino acid formation by the classical Strecker synthesis,[187, 189-190] but it provides an alternative pathway that does not require HCN and in which the C-atom of the aldehyde is directly converted to the carboxylic acid (without homologization).

Formation of pyrimidine nucleosides

We next investigated how the aldoxime model could create feedstock molecules for the prebiotic formation of pyrimidine RNA nucleosides. To this end we reacted malondialdehyde (**9**), or its bisulfite adduct (**17**), which can be generated from formaldehyde (**7**)[210] or glycolaldehyde (**8a**)[213], with hydroxylamine (**6**) in carbonate solution. We detected rapid formation of the malondialdoxime (**18**), which probably eliminates water under formation of **19**, which then cyclizes to give 5-aminoisoxazole (**20**) in about 70% overall yield (Figure 7A). In the presence of Zn^{2+} or Co^{2+} and cyanate (**21**), which can be derived from urea (**11**)[214] or NO[78], we observed formation of 5-ureaisoxazole (**22**) in about 50% or 18% yield, respectively

(Figure 7B). We found that **22** can subsequently react with ribose **23** (again a product of the formose cycle), to the ribosylated product **24**. The latter forms in this reaction as a mixture of α/β-ribofuranosides **24a**–**b** and pyranosides **24c**–**d**. We observed that if this compound mixture is kept in an aqueous borate[119] buffer, it equilibrates to a mixture composed of **24a** (39%), **24b/d** (21% in total), **24c** (13%), and **22** (26%). In the presence of catalytic amounts of Fe^{2+} and thiols[215-217] the isoxazole N-O bond breaks and the molecules undergo a subsequent cascade reaction that ends with the elimination of ammonia and the formation of uridine (**25**). Uridine is again formed as a mixture of the furanosides **25a** (3%) and **25b** (uridine, 25% in tot.), and the pyranosides **25c** (1%) and **25d** (2%). In a geological scenario (Figure 7C), malondialdehyde (**9**) and hydroxylamine (**6**) provide 5-aminoisoxazole (**20**), which upon influx of cyanate (**21**) and Zn^{2+} (Co^{2+}) followed by a dry-down step generates 5-ureaisoxazole (**22**). If **22** is brought in contact with ribose (**23**) and boric acid it forms in a second dry-down step ribosides **24**, which generates **25** upon recyclization.

Formation of purine nucleosides

We further investigated how the aldoximes could serve as precursor molecules for purine nucleosides. Towards this goal we reacted NO_2^- with malondialdehyde (**9**) to form (hydroxyimino)-malondialdehyde (**26**), which can be stabilized as its bisulfite adduct (**27**) (Figure 7A). We found that **26** reacts with hydroxylamine (**6**) to give (hydroxyimino)malondialdoxime (**28**) in 50% overall yield. A subsequent dry-down step in the presence of guanidinium (**12**) carbonate leads to the crystallization of a salt composed out of nitrile **29** and **12**. When we performed this dry-down process at elevated temperature,[196] formation of nitrosopyrimidine **30** takes place (40% yield). A subsequent hydrolytic reaction furnishes in addition nitrosopyrimidine **31** (90% yield). Both nitroso derivatives are already known precursors for purine nucleosides.[166-167, 196] The nitrosopyrimidine **30** reacts with bisulfite and formic acid to generate the formamidopyrimidine compound FaPy-DA (**32**) in 62% yield. The hydrolysed nitrosopyrimidine **31** forms in the presence of bisufite and formic acid, FaPy-G (**33**, 88% yield). The FaPy-compounds **32** and **33** then react under dry-down conditions with ribose (**23**) to the corresponding ribosides **34** and **35**, which are the direct precursors for the purine nucleosides 2-amino adenosine **36** and guanosine **37** along the recently reported FaPy-pathway.[196] The aldoxime chemistry is compatible with prebiotically plausible, sequential one-pot reactions

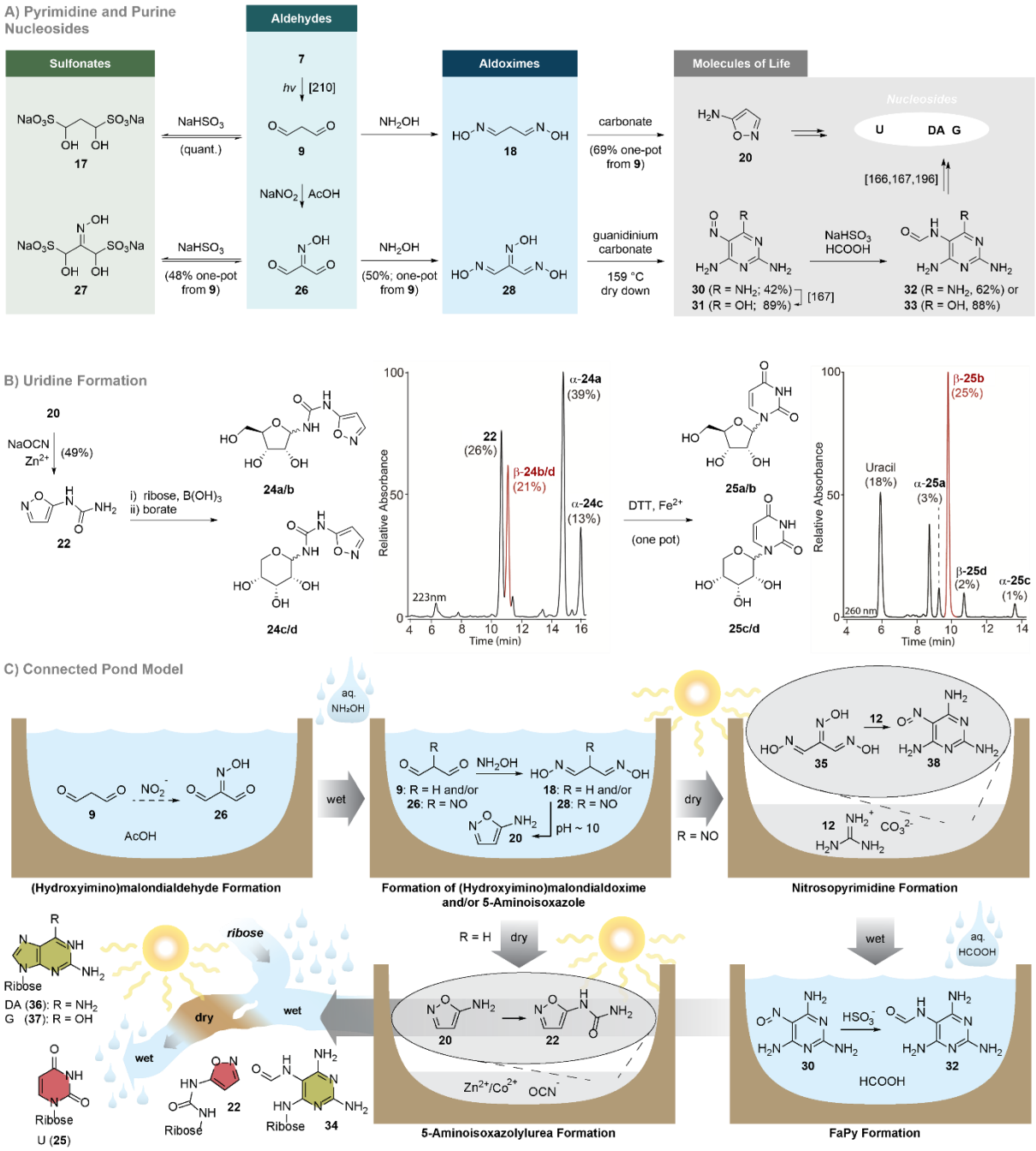

Figure 7: Prebiotic formation of nucleosides. (A) Formation of uridine via 5-aminoisoxazoles (20), respectively, both of which orginate from malondialdehyde (9) and hydroxylamine (6). The purine nucleosides 36 and 37 are formed from nitrosated malondialdehyde (26), hydroxylamine (6), and guanidine (12). (B) Formation of uridine (25) from 5-aminoisoxazoles (20). HPL chromatography reveals the predominant formation of β-furano nucleosides. (C) Connected pond model that postulates the concomitant formation of pyrimidines and purines.

(Figure 7C). Malondialdehyde (**9**) plus NO_2^- and hydroxylamine (**6**) give (hydroxyimino)malondialdoxime (**28**), which can be enriched in a dry-down step. Addition of

guanidinium (**12**), which could plausibly occur by aqueous inundation or flooding and subsequent gentle warming, generates nitrosopyrimidine **30**, which hydrolyzes to **31**[167]. This compound precipitates. Further addition of bisulfite and formic acid, perhaps by similar natural flowing events, allows formation of **32** and **33**, which again precipitate from solution. After influx of ribose (**23**) dissolved in water, followed by a dry-down step and subsequent flooding, the purine nucleosides **36** and **37** can be obtained.[196]

The pyrimidine and purine pathways can also be chemically linked. If malondialdehyde is not completely nitrosated, a mixture of malondialdehyde (**9**) and (hydroxyimino)malondialdehyde (**26**) is formed. Flow-in of a dilute solution of hydroxylamine (**6**) then generates a mixture of the bisaldoxime **18** and the trisaldoxime **28**, which gives 5-aminoisoxazole (**20**) together with **29**. The more NO_2^- is present, the more **26** forms, which allows subsequent formation of the nitrosopyrimidines **30** and **31**, together with the purine nucleosides **36** and **37**. The less NO_2^- is present, the more 5-aminoisoxazole (**20**) forms for the production of uridine (**25**).

Discussion

The currently dominating models of how life may have started on the early Earth assumes that abiotic reactions initially produced amino acids and nucleosides, which then condensed to give functional proteins and information-encoding oligonucleotides.[16, 26-28] For the abiotic formation of these biomolecules reactive starting molecules must have been available on the early Earth.[16, 26-28] In the absence of efficient metabolic pathways, these reactive molecules must have formed in large quantities by sustainable and resilient processes on the Hadean Earth.[26-28] The current models propose HCN (**1**) and small reactive nitriles (**2**–**5**) as the central starting molcules from which life was finally able to emerge.[16, 26-28] Although prebiotically models of how these molecules (**1**–**5**) could have formed exist, they are in disagreement with the current knowledge about the geochemical situation of the early Earth. A particular conflict exists with the fact that the early Earth was surrounded by a redox neutral (CO_2, H_2O, N_2, and SO_2 containing) atmosphere.[61, 65, 202-203] Current chemical knowledge suggests that under these conditions the formation of the compounds (**1**–**5**) is only possible in very small quantities.[64, 77] In addition, the central building blocks for nucleosides, **2**–**5**, are highly reactive with consequently short lifetime, inappropriate for a robust origin of life. We cannot exclude that life indeed formed based on **1**–**5**, potentially under unknown, peculiar conditions in special geological niches. However, a more resilient chemical pathway to create molecules from

which the key building block of life could have formed would certainly provide a better basis for our understanding of how higher moleculer complexity was initially generated.

The idea to search for more robust pathways to complex organic matter under plausible redox neutral early Earth conditions allowed the recent discovery that Urey-Miller experiments with neutral gas mixtures yield amino acids by unresolved mechanisms.[66] It seems that a redox neutral atmosphere that some called chemically unproductive[64] is more versatile than originally thought. Here, we followed the idea that life may have formed under rather weakly reducing atmospheric conditions. We investigated the question of what kind of alternative feedstock molecules could have formed in an "inert" CO_2, H_2O, N_2, and SO_2 atmospheric that has dominated the Hadean eon (Figure 8). We started with considering lightning and UV irradiation through such an atmosphere, which is known to produce NO_x^-[66, 69, 208] as well as CH_2O[18, 75, 209] in large quantities. Calculations predict that the NO_x^- concentration could have reached up to 20 mM levels[70] and also for HSO_3^- it was estimated that concentrations in the millimolar range are plausible.[74] Despite the large uncertainties behind such estimates, the data underpin that NO_x^- and HSO_3^- were robustly formed under early Earth conditions in substantial quantities.[70, 74] If we assume that the formed formaldehyde continued to react (potentially in geochemical niches) to give more complex aldehydes such as malondialdehyde and different □-hydroxyaldehydes, chemical logic predicts a fast and irreversible reaction of all of them with HSO_3^-, which leads to capturing (and storing) these reactive aldehydes as bisulfite adducts. These adducts can then react with hydroxylamine, which is formed from NO_2^- in the presence of HSO_3^-,[196] to generate the corresponding aldoximes in a reaction that is fast and irreversible under ambient pH-conditions. Nitrosation reactions, particularly of malondialdehyde, produces even trialdoximes, such as compound **28**. We observed that these aldoximes rapidly eliminate water under simple early Earth compatible conditions to give a series of complex nitriles. The resulting reaction products are alltogether excellent starting materials for nucleosides and amino acids.

The data presented show that this aldoxime/nitrile chemistry – that can take place under the umbrella of a neutral redox atmosphere – generates the basic ingredients needed for the formation of the most essential biomolecules. Hydroxylamine (**6**), formaldehyde (**7**), SO_2, and water are consequently the central "pillar molecules" that can start chemical reaction networks towards life. It appears that hydroxylamine and aldoximes are molecular markers for places in the universe where life may have originated.[218]

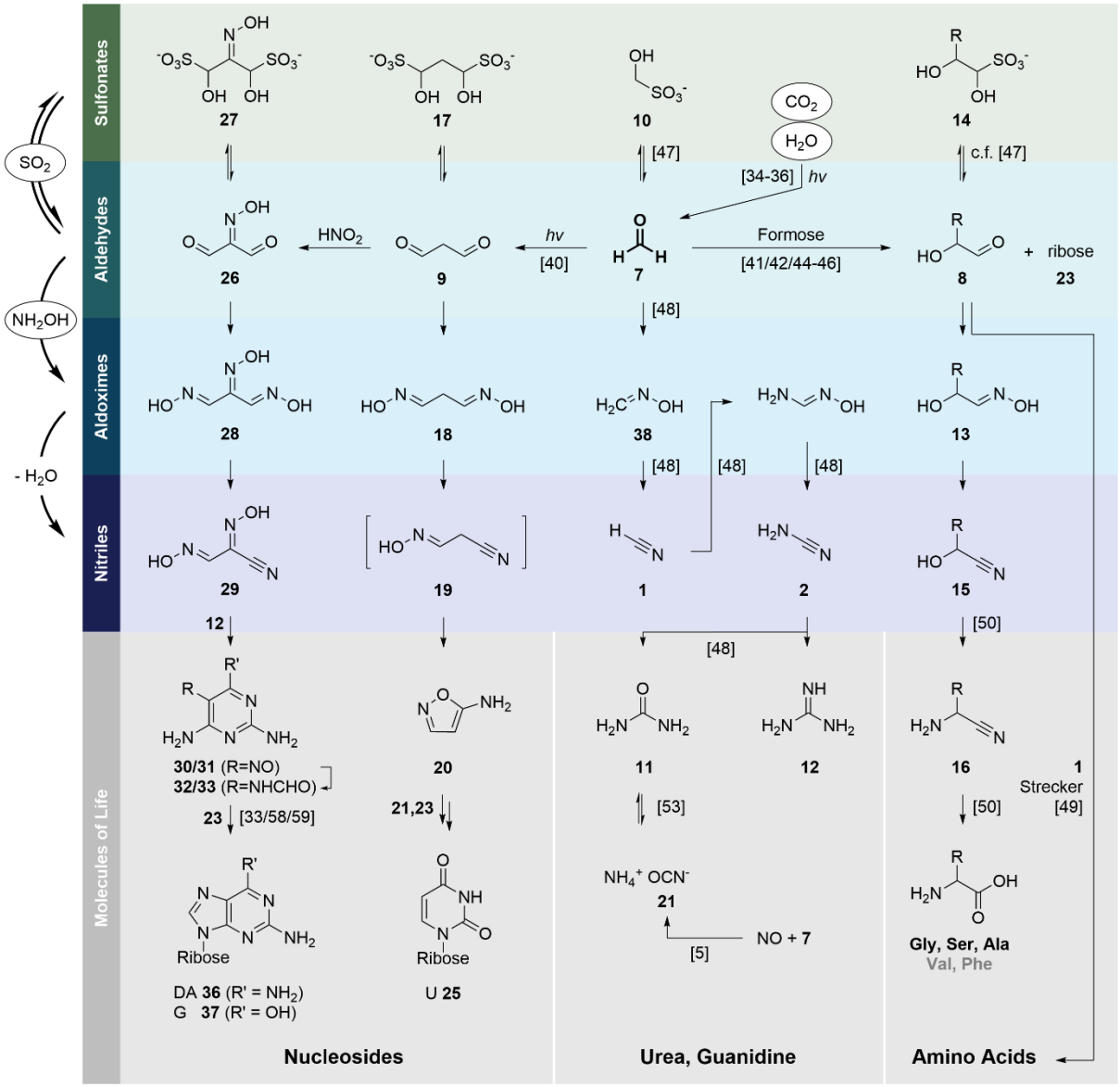

Figure 8: Overview of the prebiotic reaction network. The network operates with formaldehyde-derived aldehydes (stabilized with aqueous SO_2 (HSO_3^-) as their corresponding sulfonates) as the carbon sources. Hydroxylamine (6) (from NO_2^- and SO_3^{2-} in H_2O) allows introduction of N-atoms into organic matter. Aldehydes 26, 9, 7, and 8 can be stabilized as their corresponding α-hydroxysulfonates (27, 17, 10, and 14) and react with hydroxylamine (6) to aldoximes 28, 18, 38, and 13. Subsequent dehydration allows the formation of nitriles 29, 19, 1, and 15, which finally gives access to biomolecules like purines, pyrimidines, guanidine (12), urea (11), and amino acids. The scheme establishes the four molecules SO_2, NH_2OH, CH_2O and H_2O as the key starting molecules to generate the precursors for amino acids, sugars, and nucleosides.

Abkürzungsverzeichnis

A	Adenin, Adenosin
AI	Aminoisoxazol
AICA	4-Aminoimidazol-5-carboxamid
AICN	4-Aminoimidazol-5-carbonitril
AminoPy	Aminopyrimidin
AMN	Aminomalononitril
AS	Aminosäure
°C	Grad Celsius
C	Cytosin, Cytidin
Da	Dalton
DA	2,4-Diaminopurin
DAMN	Diaminomaleonitril
DNA	Desoxyribonukleinsäure
f_{O2}	Sauerstofffugazität
FaPy	Formamidopyrimidin
FMQ	Fayalit-Magnetit/Quarz
G	Guanin, Guanosin
Ga	Jahrmilliarde
HIMN	(Hydroxyimino)malononitrile
LHB	Großes Bombardement
LUCA	letzter allgemeiner gemeinsamer Vorfahr
M	mol · L^{-1}

m^2A	2-Methyladenosin
m^2G	N^2-Methylguanosin
$m^2{}_2G$	N^2,N^2-Dimethylguanosin
m^4C	N^4-Methylcytosin
$m_4{}^2C$	*N*4,*N*4-Dimethylcytosin
Mio.	Million
MNU	*N*-Methyl-*N*-nitrosourea
Mrd.	Milliarde
mRNA	*messenger*-RNA
ms^2A	2-Thiomethyladenosin
NitrosoPy	Nitrosoyprimidin
Nu	Nukleophil
pH	*potentia Hydrogenii*
RNA	Ribonukleinsäure
rRNA	ribosomale RNA
s^4U	4-Thiouracil
Sdp.	Siedepunkt
SMePy	*S*-Methylpyrimidinon
t	Zeit
T	Temperatur, Thymin, Thymidin
$T_{½}$	Halbwertszeit
tRNA	transfer-RNA
U	Uracil, Uridin
UV	ultraviolett

Literaturverzeichnis

[1] Aristotle, *Metaphysics, 983b 8-11*.

[2] J. P. Gardner, J. C. Mather, M. Clampin, R. Doyon, M. A. Greenhouse, H. B. Hammel, J. B. Hutchings, P. Jakobsen, S. J. Lilly, K. S. Long, The james webb space telescope, *Space Sci. Rev.* **2006**, *123*, 485-606.

[3] G. W. Wetherill, Formation of the Earth, *Annu. Rev. Earth Planet Sci.* **1990**, *18*, 205-256.

[4] H. Lammer, A. L. Zerkle, S. Gebauer, N. Tosi, L. Noack, M. Scherf, E. Pilat-Lohinger, M. Güdel, J. L. Grenfell, M. Godolt, Origin and evolution of the atmospheres of early Venus, Earth and Mars, *Astron. Astrophys. Rev.* **2018**, *26*, 1-72.

[5] C. Darwin, Routledge London, **2016**.

[6] N. Shubin, C. Tabin, S. Carroll, Fossils, genes and the evolution of animal limbs, *Nature* **1997**, *388*, 639-648.

[7] E. S. Vrba, Evolution, species and fossils: how does life evolve, *S. Afr. J. Sci.* **1980**, *76*, 61-84.

[8] G. Fox, E. Stackebrandt, R. Hespell, J. Gibson, J. Maniloff, T. Dyer, R. Wolfe, W. Balch, R. Tanner, L. Magrum, The phylogeny of prokaryotes, *Science* **1980**, *209*, 457-463.

[9] C. Woese, The universal ancestor, *Proc. Natl. Acad. Sci. U.S.A.* **1998**, *95*, 6854-6859.

[10] E. V. Koonin, Comparative genomics, minimal gene-sets and the last universal common ancestor, *Nat. Rev. Microbiol.* **2003**, *1*, 127-136.

[11] M. C. Weiss, F. L. Sousa, N. Mrnjavac, S. Neukirchen, M. Roettger, S. Nelson-Sathi, W. F. Martin, The physiology and habitat of the last universal common ancestor, *Nat. Microbiol.* **2016**, *1*, 1-8.

[12] M. Yarus, Getting past the RNA world: the initial Darwinian ancestor, *Cold Spring Harb. Perspect. Med.* **2011**, *3*, a003590.

[13] D. W. Deamer, The first living systems: a bioenergetic perspective, *Microbiol. Mol. Biol. Rev.* **1997**, *61*, 239-261.

[14] J. G. Miller, Living systems: Basic concepts, *Behav. Sci.* **1965**, *10*, 193-237.

[15] J. P. Ferris, L. Orgel, Studies in Prebiotic Synthesis. I. Aminomalononitrile and 4-Amino-5-cyanoimidazole1, 2, *J. Am. Chem. Soc.* **1966**, *88*, 3829-3831.

[16] L. E. Orgel, Prebiotic chemistry and the origin of the RNA world, *Crit. Rev. Biochem. Mol. Biol.* **2004**, *39*, 99-123.

[17] A. Butlerow, Bildung einer zuckerartigen Substanz durch Synthese, *Liebigs Ann.* **1861**, *120*, 295-298.

[18] W. Löb, Studien über die chemische Wirkung der stillen elektrischen Entladung, *Z. Elektrochem. angew. phys. Chem.* **1906**, *12*, 282-312.

[19] S. L. Miller, A production of amino acids under possible primitive earth conditions, *Science* **1953**, *117*, 528-529.

[20] A. Strecker, Ueber die künstliche Bildung der Milchsäure und einen neuen, dem Glycocoll homologen Körper, *Justus Liebigs Annalen der Chemie* **1850**, *75*, 27-45.

[21] J. Oró, Synthesis of adenine from ammonium cyanide, *Biochem. Biophys. Res. Commun.* **1960**, *2*, 407-412.

[22] R. Krishnamurthy, N. V. Hud*, Vol. 120*, ACS Publications, Chem. Rev., **2020**, pp. 4613-4615.

[23] S. A. Sandford, M. Nuevo, P. P. Bera, T. J. Lee, Prebiotic astrochemistry and the formation of molecules of astrobiological interest in interstellar clouds and protostellar disks, *Chem. Rev.* **2020**, *120*, 4616-4659.
[24] D. P. Glavin, A. S. Burton, J. E. Elsila, J. C. Aponte, J. P. Dworkin, The search for chiral asymmetry as a potential biosignature in our solar system, *Chem. Rev.* **2019**, *120*, 4660-4689.
[25] M. A. Pasek, Thermodynamics of prebiotic phosphorylation, *Chem. Rev.* **2019**, *120*, 4690-4706.
[26] M. Frenkel-Pinter, M. Samanta, G. Ashkenasy, L. J. Leman, Prebiotic peptides: Molecular hubs in the origin of life, *Chem. Rev.* **2020**, *120*, 4707-4765.
[27] M. Yadav, R. Kumar, R. Krishnamurthy, Chemistry of abiotic nucleotide synthesis, *Chem. Rev.* **2020**, *120*, 4766-4805.
[28] D. M. Fialho, T. P. Roche, N. V. Hud, Prebiotic syntheses of noncanonical nucleosides and nucleotides, *Chem. Rev.* **2020**, *120*, 4806-4830.
[29] D. G. Blackmond, Autocatalytic models for the origin of biological homochirality, *Chem. Rev.* **2019**, *120*, 4831-4847.
[30] M.-C. Maurel, F. Leclerc, G. Hervé, Ribozyme Chemistry: to be or not to be under high pressure, *Chem. Rev.* **2019**, *120*, 4898-4918.
[31] E. Janzen, C. Blanco, H. Peng, J. Kenchel, I. A. Chen, Promiscuous ribozymes and their proposed role in prebiotic evolution, *Chem. Rev.* **2020**, *120*, 4879-4897.
[32] J. C. Bowman, A. S. Petrov, M. Frenkel-Pinter, P. I. Penev, L. D. Williams, Root of the tree: the significance, evolution, and origins of the ribosome, *Chem. Rev.* **2020**, *120*, 4848-4878.
[33] A. I. Oparin, *Proiskhozhdenie zhizni*, Voennoe Izd. Ministerstva Obrony Sojuza SSR, **1924**.
[34] J. B. S. Haldane, The origin of life, *Rationalist Annual* **1929**, *148*, 3-10.
[35] S. L. Miller, J. W. Schopf, A. Lazcano, Oparin's``Origin of Life'': Sixty Years Later, *J. Mol. Evol.* **1997**, *44*, 351-353.
[36] A. I. Oparin, *Genesis and evolutionary development of life*, Academic Press, **1968**.
[37] A. I. Oparin, The origin of life on the earth, *The origin of life on the earth.* **1957**.
[38] A. Oparin, The origin of life, *New York: MacMillan* **1938**.
[39] H. C. Urey, On the early chemical history of the earth and the origin of life, *Proc. Natl. Acad. Sci. U.S.A.* **1952**, *38*, 351-363.
[40] H. C. Urey, The planets: their origin and development, *Mrs. Hepsa Ely Silliman Memorial Lectures* **1952**.
[41] S. L. Miller, Production of some organic compounds under possible primitive earth conditions1, *J. Am. Chem. Soc.* **1955**, *77*, 2351-2361.
[42] S. J. Mojzsis, in *Prebiotic Chemistry and Life's Origin*, **2022**, pp. 21-76.
[43] K. Zahnle, L. Schaefer, B. Fegley, Earth's earliest atmospheres, *Cold Spring Harb. Perspect. Biol.* **2010**, *2*, a004895.
[44] F. Aston, The rarity of the inert gases on the Earth, *Nature* **1924**, *114*, 786-786.
[45] H. N. Russell, D. H. Menzel, The terrestrial abundance of the permanent gases, *Proc. Natl. Acad. Sci. U.S.A.* **1933**, *19*, 997-1001.
[46] H. Brown, Rare gases and formation of the Earth's atmosphere, *The Atmospheres of the Earth and Planets.* **1952**, 258-266.
[47] P. H. Abelson, Chemical events on the primitive earth, *Proc. Natl. Acad. Sci. U.S.A.* **1966**, *55*, 1365-1372.

[48] H. Holland, *Chemical Evolution of the Atmosphere and Oceans* Princeton, **1984**.
[49] H. D. Holland, *Model for the evolution of the Earth's atmosphere*, Geological Society of America, Boulder, **1962**.
[50] J. H. J. Poole, The evolution of the earth's atmosphere, **1951**, 201-224.
[51] H. Wänke, Constitution of terrestrial planets, *Philos. Trans. Royal Soc. A* **1981**, *303*, 287-302.
[52] C. J. Allegre, G. Manhes, C. Göpel, The age of the Earth, *Geochim. Cosmochim. Acta* **1995**, *59*, 1445-1456.
[53] M. Barboni, P. Boehnke, B. Keller, I. Kohl, B. Schoene, E. Young, K. McKeegan, Early formation of the Moon 4.51 billion years ago, *Sci. Adv.* **2017**.
[54] S. Charnoz, C. Michaut, Evolution of the protolunar disk: Dynamics, cooling timescale and implantation of volatiles onto the Earth, *Icarus* **2015**, *260*, 440-463.
[55] M. D. Norman, L. E. Borg, L. E. Nyquist, D. D. Bogard, Chronology, geochemistry, and petrology of a ferroan noritic anorthosite clast from Descartes breccia 67215: Clues to the age, origin, structure, and impact history of the lunar crust, *Meteorit. Planet. Sci.* **2003**, *38*, 645-661.
[56] C. J. Allegre, J.-P. Poirier, E. Humler, A. W. Hofmann, The chemical composition of the Earth, *Earth Planet. Sci. Lett.* **1995**, *134*, 515-526.
[57] W. F. McDonough, S.-S. Sun, The composition of the Earth, *Chem. Geol.* **1995**, *120*, 223-253.
[58] J. Wade, B. Wood, Core formation and the oxidation state of the Earth, *Earth Planet. Sci. Lett.* **2005**, *236*, 78-95.
[59] D. Stevenson, Models of the Earth's core, *Science* **1981**, *214*, 611-619.
[60] D. J. Frost, C. A. McCammon, The redox state of Earth's mantle, *Annu. Rev. Earth Planet. Sci.* **2008**, *36*, 389-420.
[61] D. Trail, E. B. Watson, N. D. Tailby, The oxidation state of Hadean magmas and implications for early Earth's atmosphere, *Nature* **2011**, *480*, 79-82.
[62] J. W. Delano, Redox history of the Earth's interior since~ 3900 Ma: implications for prebiotic molecules, *Orig. Life Evol. Biosph.* **2001**, *31*, 311-341.
[63] D. Canil, Vanadium in peridotites, mantle redox and tectonic environments: Archean to present, *Earth Planet. Sci. Lett.* **2002**, *195*, 75-90.
[64] S. A. Benner, E. A. Bell, E. Biondi, R. Brasser, T. Carell, H.-J. Kim, S. J. Mojzsis, A. Omran, M. A. Pasek, D. Trail, When Did Life Likely Emerge on Earth in an RNA-First Process?, *ChemSystemsChem* **2020**, *2*, e1900035.
[65] M. M. Hirschmann, Magma ocean influence on early atmosphere mass and composition, *Earth Planet. Sci. Lett.* **2012**, *341*, 48-57.
[66] H. J. Cleaves, J. H. Chalmers, A. Lazcano, S. L. Miller, J. L. Bada, A reassessment of prebiotic organic synthesis in neutral planetary atmospheres, *Orig. Life Evol. Biosph.* **2008**, *38*, 105-115.
[67] C. E. Harman, J. F. Kasting, E. T. Wolf, Atmospheric Production of Glycolaldehyde Under Hazy Prebiotic Conditions, *Orig. Life Evol. Biosph.* **2013**, *43*, 77-98.
[68] K. J. Zahnle, Earth's earliest atmosphere, *Elements* **2006**, *2*, 217-222.
[69] D. P. Summers, B. Khare, Nitrogen fixation on early Mars and other terrestrial planets: experimental demonstration of abiotic fixation reactions to nitrite and nitrate, *Astrobiology* **2007**, *7*, 333-341.

[70] S. Ranjan, Z. R. Todd, P. B. Rimmer, D. D. Sasselov, A. R. Babbin, Nitrogen oxide concentrations in natural waters on early Earth, *Geochem. Geophys. Geosyst.* **2019**, *20*, 2021-2039.

[71] D. P. Summers, Ammonia formation by the reduction of nitrite/nitrate by FeS: ammonia formation under acidic conditions, *Orig. Life Evol. Biosph.* **2005**, *35*, 299-312.

[72] D. P. Summers, S. Chang, Prebiotic ammonia from reduction of nitrite by iron (II) on the early Earth, *Nature* **1993**, *365*, 630-633.

[73] S. A. Benner, H.-J. Kim, E. Biondi, Prebiotic chemistry that could not not have happened, *Life* **2019**, *9*, 84.

[74] S. Ranjan, Z. R. Todd, J. D. Sutherland, D. D. Sasselov, Sulfidic anion concentrations on early earth for surficial origins-of-life chemistry, *Astrobiology* **2018**, *18*, 1023-1040.

[75] H. J. Cleaves, The prebiotic geochemistry of formaldehyde, *Precambrian Res.* **2008**, *164*, 111-118.

[76] H.-J. Kim, A. Ricardo, H. I. Illangkoon, M. J. Kim, M. A. Carrigan, F. Frye, S. A. Benner, Synthesis of carbohydrates in mineral-guided prebiotic cycles, *J. Am. Chem. Soc.* **2011**, *133*, 9457-9468.

[77] G. Schlesinger, S. L. Miller, Prebiotic synthesis in atmospheres containing CH4, CO, and CO2, *J. Mol. Evol.* **1983**, *19*, 383-390.

[78] P. B. Rimmer, S. Rugheimer, Hydrogen cyanide in nitrogen-rich atmospheres of rocky exoplanets, *Icarus* **2019**, *329*, 124-131.

[79] H. Genda, R. Brasser, S. Mojzsis, The terrestrial late veneer from core disruption of a lunar-sized impactor, *Earth Planet. Sci. Lett.* **2017**, *480*, 25-32.

[80] K. J. Zahnle, R. Lupu, D. C. Catling, N. Wogan, Creation and evolution of impact-generated reduced atmospheres of early Earth, *Planet. Sci. J.* **2020**, *1*, 11.

[81] M. Sekiya, K. Nakazawa, C. Hayashi, Dissipation of the rare gases contained in the primordial Earth's atmosphere, *Earth Planet. Sci. Lett.* **1980**, *50*, 197-201.

[82] A. J. Watson, T. M. Donahue, J. C. Walker, The dynamics of a rapidly escaping atmosphere: applications to the evolution of Earth and Venus, *Icarus* **1981**, *48*, 150-166.

[83] O. Abramov, S. J. Mojzsis, Microbial habitability of the Hadean Earth during the late heavy bombardment, *Nature* **2009**, *459*, 419-422.

[84] R. M. Canup, Simulations of a late lunar-forming impact, *Icarus* **2004**, *168*, 433-456.

[85] D. Parkos, A. Pikus, A. Alexeenko, H. J. Melosh, HCN production via impact ejecta reentry during the late heavy bombardment, *J. Geophys. Res. Planets* **2018**, *123*, 892-909.

[86] W. F. Bottke, M. D. Norman, The late heavy bombardment, *Annu. Rev. Earth Planet Sci.* **2017**, *45*, 619-647.

[87] R. Gomes, H. F. Levison, K. Tsiganis, A. Morbidelli, Origin of the cataclysmic Late Heavy Bombardment period of the terrestrial planets, *Nature* **2005**, *435*, 466-469.

[88] P. Boehnke, T. M. Harrison, Illusory late heavy bombardments, *Proc. Natl. Acad. Sci. U.S.A.* **2016**, *113*, 10802-10806.

[89] W. K. Hartmann, Megaregolith evolution and cratering cataclysm models—Lunar cataclysm as a misconception (28 years later), *Meteorit. Planet. Sci.* **2003**, *38*, 579-593.

[90] L. A. Haskin, R. L. Korotev, K. M. Rockow, B. L. Jolliff, The case for an Imbrium origin of the Apollo thorium-rich impact-melt breccias, *Meteorit. Planet. Sci.* **1998**, *33*, 959-975.

[91] K. Kurosawa, S. Sugita, K. Ishibashi, S. Hasegawa, Y. Sekine, N. O. Ogawa, T. Kadono, S. Ohno, N. Ohkouchi, Y. Nagaoka, Hydrogen cyanide production due to mid-size impacts in a redox-neutral N2-rich atmosphere, *Orig. Life Evol. Biosph.* **2013**, *43*, 221-245.

[92] J. E. Coates, N. H. Hartshorne, XC.—Studies on hydrogen cyanide. Part III. The freezing points of hydrogen cyanide–water mixtures, *J. Chem. Soc.* **1931**, 657-665.

[93] A. D. Keefe, S. L. Miller, Was ferrocyanide a prebiotic reagent?, *Orig. Life Evol. Biosph.* **1996**, *26*, 111-129.

[94] J. D. Toner, D. C. Catling, Alkaline lake settings for concentrated prebiotic cyanide and the origin of life, *Geochim. Cosmochim. Acta* **2019**, *260*, 124-132.

[95] H. S. P. Müller, Universität Köln, Molecules in Space, https://cdms.astro.uni-koeln.de/classic/molecules, aufgerufen am 08.09.2022

[96] D. Woon, Interstellar & Circumstellar Molecules, http://www.astrochymist.org/astrochymist_ism.html, aufgerufen am 08.09.2022

[97] M. Araki, Tokyo University of Science Tsukiyama Laboratory, List of interstellar molecules, http://www.astrochymist.org/astrochymist_ism.html, aufgerufen am 08.09.2022

[98] E. Anders, Pre-biotic organic matter from comets and asteroids, *Nature* **1989**, *342*, 255-257.

[99] C. Chyba, C. Sagan, Endogenous production, exogenous delivery and impact-shock synthesis of organic molecules: an inventory for the origins of life, *Nature* **1992**, *355*, 125-132.

[100] D. Whittet, Is extraterrestrial organic matter relevant to the origin of life on Earth?, *Orig. Life Evol. Biosph.* **1997**, 249-262.

[101] M. Pasek, D. Lauretta, Extraterrestrial flux of potentially prebiotic C, N, and P to the early Earth, *Orig. Life Evol. Biosph.* **2008**, *38*, 5-21.

[102] E. Pierazzo, C. Chyba, Amino acid survival in large cometary impacts, *Meteorit. Planet. Sci.* **1999**, *34*, 909-918.

[103] C. F. Chyba, P. J. Thomas, L. Brookshaw, C. Sagan, Cometary delivery of organic molecules to the early Earth, *Science* **1990**, *249*, 366-373.

[104] J. Watson, F. Crick, Genetical implications of the structure of deoxyribonucleic acid, *Nature* **1953**, *171*, 964-967.

[105] W. Gilbert, Origin of life: The RNA world, *Nature* **1986**, *319*, 618-618.

[106] M. Eigen, W. Gardiner, P. Schuster, R. Winkler-Oswatitsch, The origin of genetic information, *Sci. Am.* **1981**, *244*, 88-119.

[107] M. Di Giulio, On the RNA world: evidence in favor of an early ribonucleopeptide world, *J. Mol. Evol.* **1997**, *45*, 571-578.

[108] F. Müller, L. Escobar, F. Xu, E. Węgrzyn, M. Nainytė, T. Amatov, C. Y. Chan, A. Pichler, T. Carell, A prebiotically plausible scenario of an RNA–peptide world, *Nature* **2022**, *605*, 279-284.

[109] A. K. Eckhardt, M. M. Linden, R. C. Wende, B. Bernhardt, P. R. Schreiner, Gas-phase sugar formation using hydroxymethylene as the reactive formaldehyde isomer, *Nat. Chem.* **2018**, *10*, 1141-1147.

[110] A. Butlerow, Formation synthétique d'une substance sucrée, *CR Acad. Sci* **1861**, *53*, 145-147.

[111] O. Loew, Ueber formaldehyd und dessen condensation, *J. Prakt. Chem.* **1886**, *33*, 321-351.

[112] E. Fischer, in *Untersuchungen Über Kohlenhydrate und Fermente (1884–1908)*, Springer, **1909**, pp. 158-161.
[113] R. Breslow, On the mechanism of the formose reaction, *Tetrahedron Lett.* **1959**, *1*, 22-26.
[114] T. Mizuno, A. H. Weiss, in *Adv. Carbohydr. Chem. Biochem., Vol. 29*, Elsevier, **1974**, pp. 173-227.
[115] R. Shapiro, Prebiotic ribose synthesis: a critical analysis, *Orig. Life Evol. Biosph.* **1988**, *18*, 71-85.
[116] D. Müller, S. Pitsch, A. Kittaka, E. Wagner, C. E. Wintner, A. Eschenmoser, G. Ohlofjgewidmet, Chemie von a-Aminonitrilen. Aldomerisierung von Glycolaldehyd-phosphat zu racemischen Hexose-2, 4, 6-triphosphaten und (in Gegenwart von Formaldehyd) racemischen Pentose-2, 4-diphosphaten: rac-Allose-2, 4, 6-triphosphat und rac-Ribose-2, 4-diphosphat sind die Reaktionshauptprodukte, *Helv. Chim. Acta* **1990**, *73*, 1410-1468.
[117] R. Krishnamurthy, G. Arrhenius, A. Eschenmoser, Formation of glycolaldehyde phosphate from glycolaldehyde in aqueous solution, *Orig. Life Evol. Biosph.* **1999**, *29*, 333-354.
[118] R. Krishnamurthy, S. Guntha, A. Eschenmoser, Regioselective α-phosphorylation of aldoses in aqueous solution, *Angew. Chem. Int. Ed.* **2000**, *39*, 2281-2285.
[119] A. Ricardo, M. Carrigan, A. Olcott, S. Benner, Borate minerals stabilize ribose, *Science* **2004**, *303*, 196-196.
[120] S. A. Benner, H.-J. Kim, M. A. Carrigan, Asphalt, water, and the prebiotic synthesis of ribose, ribonucleosides, and RNA, *Acc. Chem. Res.* **2012**, *45*, 2025-2034.
[121] E. S. Grew, J. L. Bada, R. M. Hazen, Borate minerals and origin of the RNA world, *Orig. Life Evol. Biosph.* **2011**, *41*, 307-316.
[122] J. Kofoed, J.-L. Reymond, T. Darbre, Prebiotic carbohydrate synthesis: zinc–proline catalyzes direct aqueous aldol reactions of α-hydroxy aldehydes and ketones, *Org. Biomol. Chem.* **2005**, *3*, 1850-1855.
[123] S. Dong, P. K. Dasgupta, On the formaldehyde-bisulfite-hydroxymethanesulfonate equilibrium, *Atmos. Environ.* **1986**, *20*, 1635-1637.
[124] P. Erik, V. S. Andersen, The formaldehyde-hydrogen sulphite system in alkaline aqueous solution. Kinetics, mechanisms, and equilibria, *Acta Chem. Scand.* **1970**, *24*.
[125] G. L. Kok, S. N. Gitlin, A. L. Lazrus, Kinetics of the formation and decomposition of hydroxymethanesulfonate, *J. Geophys. Res. Atmos.* **1986**, *91*, 2801-2804.
[126] J. Kawai, D. C. McLendon, H.-J. Kim, S. Benner, Hydroxymethanesulfonate from volcanic sulfur dioxide: A “mineral” reservoir for formaldehyde and other simple carbohydrates in prebiotic chemistry, *Astrobiology* **2019**, *19*, 506-516.
[127] D. Ritson, J. D. Sutherland, Prebiotic synthesis of simple sugars by photoredox systems chemistry, *Nat. Chem.* **2012**, *4*, 895-899.
[128] D. J. Ritson, J. D. Sutherland, Synthesis of aldehydic ribonucleotide and amino acid precursors by photoredox chemistry, *Angew. Chem. Int. Ed.* **2013**, *52*, 5845-5847.
[129] J. Xu, D. J. Ritson, S. Ranjan, Z. R. Todd, D. D. Sasselov, J. D. Sutherland, Photochemical reductive homologation of hydrogen cyanide using sulfite and ferrocyanide, *Chem. Commun.* **2018**, *54*, 5566-5569.
[130] E. Fischer, Reduction von säuren der Zuckergruppe, *Ber. Dtsch. Chem. Ges.* **1889**, *22*, 2204-2205.

[131] A. S. Serianni, E. L. Clark, R. Barker, Carbon-13-enriched carbohydrates. Preparation of erythrose, threose, glyceraldehyde, and glycolaldehyde with 13C-enrichment in various carbon atoms, *Carbohydr. Res.* **1979**, *72*, 79-91.

[132] B. H. Patel, C. Percivalle, D. J. Ritson, C. D. Duffy, J. D. Sutherland, Common origins of RNA, protein and lipid precursors in a cyanosulfidic protometabolism, *Nat. Chem.* **2015**, *7*, 301-307.

[133] J. D. Sutherland, The origin of life—out of the blue, *Angew. Chem. Int. Ed.* **2016**, *55*, 104-121.

[134] N. J. Green, J. Xu, J. D. Sutherland, Illuminating life's origins: UV photochemistry in abiotic synthesis of biomolecules, *J. Am. Chem. Soc.* **2021**, *143*, 7219-7236.

[135] J. Oró, Mechanism of synthesis of adenine from hydrogen cyanide under possible primitive Earth conditions, *Nature* **1961**, *191*, 1193-1194.

[136] J. Oró, A. P. Kimball, Synthesis of purines under possible primitive earth conditions: II. Purine intermediates from hydrogen cyanide, *Arch. Biochem. Biophys.* **1962**, *96*, 293-313.

[137] J. P. Ferris, L. Orgel, Aminomalononitrile and 4-Amino-5-cyanoimidazole in Hydrogen Cyanide Polymerization and Adenine Synthesis1, *J. Am. Chem. Soc.* **1965**, *87*, 4976-4977.

[138] M. Levy, S. L. Miller, J. Oró, Production of guanine from NH4CN polymerizations, *J. Mol. Evol.* **1999**, *49*, 165-168.

[139] S. Miyakawa, H. James Cleaves, S. L. Miller, The cold origin of life: A. Implications based on the hydrolytic stabilities of hydrogen cyanide and formamide, *Orig. Life Evol. Biosph.* **2002**, *32*, 195-208.

[140] C. Lowe, M. Rees, R. Markham, Synthesis of complex organic compounds from simple precursors: formation of amino-acids, amino-acid polymers, fatty acids and purines from ammonium cyanide, *Nature* **1963**, *199*, 219-222.

[141] J. P. Ferris, R. A. Sanchez, L. E. Orgel, Studies in prebiotic synthesis: III. Synthesis of pyrimidines from cyanoacetylene and cyanate, *J. Mol. Biol.* **1968**, *33*, 693-704.

[142] R. Shapiro, The prebiotic role of adenine: a critical analysis, *Orig. Life Evol. Biosph.* **1995**, *25*, 83-98.

[143] R. Lohrmann, Formation of urea and guanidine by irradiation of ammonium cyanide, *J. Mol. Evol.* **1972**, *1*, 263-269.

[144] R. A. Sanchez, J. P. Ferbis, L. E. Orgel, Studies in prebiodc synthesis: II. Synthesis of purine precursors and amino acids from aqueous hydrogen cyanide, *J. Mol. Biol.* **1967**, *30*, 223-253.

[145] H. Yamada, T. Okamoto, A one-step synthesis of purine ring from formamide, *Chem. Pharm. Bull.* **1972**, *20*, 623-624.

[146] R. Saladino, C. Crestini, S. Pino, G. Costanzo, E. Di Mauro, Formamide and the origin of life, *Phys. Life Rev.* **2012**, *9*, 84-104.

[147] R. Saladino, C. Crestini, G. Costanzo, R. Negri, E. Di Mauro, A possible prebiotic synthesis of purine, adenine, cytosine, and 4 (3H)-pyrimidinone from formamide: implications for the origin of life, *Bioorg. Med. Chem.* **2001**, *9*, 1249-1253.

[148] R. Saladino, C. Crestini, V. Neri, F. Ciciriello, G. Costanzo, E. Di Mauro, Origin of informational polymers: The concurrent roles of formamide and phosphates, *ChemBioChem* **2006**, *7*, 1707-1714.

[149] R. Sanchez, J. Ferris, L. Orgel, Cyanoacetylene in prebiotic synthesis, *Science* **1966**, *154*, 784-785.

[150] J. Ferris, O. Zamek, A. Altbuch, H. Freiman, Chemial evolution, *J. Mol. Evol.* **1974**, *3*, 301-309.
[151] H. Okamura, S. Becker, N. Tiede, S. Wiedemann, J. Feldmann, T. Carell, A one-pot, water compatible synthesis of pyrimidine nucleobases under plausible prebiotic conditions, *Chem. Commun.* **2019**, *55*, 1939-1942.
[152] M. P. Robertson, S. L. Miller, An efficient prebiotic synthesis of cytosine and uracil, *Nature* **1995**, *375*, 772-774.
[153] K. E. Nelson, M. P. Robertson, M. Levy, S. L. Miller, Concentration by evaporation and the prebiotic synthesis of cytosine, *Orig. Life Evol. Biosph.* **2001**, *31*, 221-229.
[154] L. E. Orgel, Is cyanoacetylene prebiotic?, *Orig. Life Evol. Biosph.* **2002**, *32*, 279-281.
[155] W. D. Fuller, R. A. Sanchez, L. E. Orgel, Studies in prebiotic synthesis: VI. Synthesis of purine nucleosides, *J. Mol. Evol.* **1972**, *67*, 25-33.
[156] W. Fuller, R. Sanchez, L. Orgel, Studies in prebiotic synthesis. VII, *J. Mol. Evol.* **1972**, *1*, 249-257.
[157] A. A. Ingar, R. W. Luke, B. R. Hayter, J. D. Sutherland, Synthesis of cytidine ribonucleotides by stepwise assembly of the heterocycle on a sugar phosphate, *ChemBioChem* **2003**, *4*, 504-507.
[158] G. Zubay, T. Mui, Prebiotic synthesis of nucleotides, *Orig. Life Evol. Biosph.* **2001**, *31*, 87-102.
[159] H.-J. Kim, S. A. Benner, Prebiotic stereoselective synthesis of purine and noncanonical pyrimidine nucleotide from nucleobases and phosphorylated carbohydrates, *Proc. Natl. Acad. Sci. U.S.A.* **2017**, *114*, 11315-11320.
[160] H.-J. Kim, J. Kim, A prebiotic synthesis of canonical pyrimidine and purine ribonucleotides, *Astrobiology* **2019**, *19*, 669-674.
[161] H. Hashizume, B. K. Theng, S. van der Gaast, K. Fujii, Formation of adenosine from adenine and ribose under conditions of repeated wetting and drying in the presence of clay minerals, *Geochim. Cosmochim. Acta* **2019**, *265*, 495-504.
[162] M. Akouche, M. Jaber, M. C. Maurel, J. F. Lambert, T. Georgelin, Phosphoribosyl pyrophosphate: a molecular vestige of the origin of life on minerals, *Angew. Chem. Int. Ed.* **2017**, *56*, 7920-7923.
[163] I. Nam, J. K. Lee, H. G. Nam, R. N. Zare, Abiotic production of sugar phosphates and uridine ribonucleoside in aqueous microdroplets, *Proc. Natl. Acad. Sci. U.S.A.* **2017**, *114*, 12396-12400.
[164] I. Nam, H. G. Nam, R. N. Zare, Abiotic synthesis of purine and pyrimidine ribonucleosides in aqueous microdroplets, *Proc. Natl. Acad. Sci. U.S.A.* **2018**, *115*, 36-40.
[165] W. Traube, Der synthetische Aufbau der Harnsäure, des Santhins, Theobromins, Theophyllins und Caffeïns aus der Cyanessigsäure, *Chem. Ber.* **1900**, *33*, 3035-3056.
[166] S. Becker, I. Thoma, A. Deutsch, T. Gehrke, P. Mayer, H. Zipse, T. Carell, A high-yielding, strictly regioselective prebiotic purine nucleoside formation pathway, *Science* **2016**, *352*, 833-836.
[167] S. Becker, C. Schneider, H. Okamura, A. Crisp, T. Amatov, M. Dejmek, T. Carell, Wet-dry cycles enable the parallel origin of canonical and non-canonical nucleosides by continuous synthesis, *Nat. Commun.* **2018**, *9*, 1-9.
[168] C. Schneider, S. Becker, H. Okamura, A. Crisp, T. Amatov, M. Stadlmeier, T. Carell, Noncanonical RNA nucleosides as molecular fossils of an early Earth—Generation by

prebiotic methylations and carbamoylations, *Angew. Chem. Int. Ed.* **2018**, *57*, 5943-5946.

[169] R. A. Sanchez, L. E. Orgel, Studies in prebiotic synthesis: V. Synthesis and photoanomerization of pyrimidine nucleosides, *J. Mol. Biol.* **1970**, *47*, 531-543.

[170] G. A. O'Donovan, J. Neuhard, Pyrimidine metabolism in microorganisms, *Bacteriol. Rev.* **1970**, *34*, 278-343.

[171] M. W. Powner, J. D. Sutherland, J. W. Szostak, Chemoselective multicomponent one-pot assembly of purine precursors in water, *J. Am. Chem. Soc.* **2010**, *132*, 16677-16688.

[172] C. Anastasi, M. A. Crowe, M. W. Powner, J. D. Sutherland, Direct Assembly of Nucleoside Precursors from Two-and Three-Carbon Units, *Angew. Chem. Int. Ed.* **2006**, *45*, 6176-6179.

[173] A. Cockerill, A. Deacon, R. Harrison, D. Osborne, D. Prime, W. Ross, A. Todd, J. Verge, An improved synthesis of 2-amino-1, 3-oxazoles under basic catalysis, *Synthesis* **1976**, *1976*, 591-593.

[174] M. W. Powner, C. Anastasi, M. A. Crowe, A. L. Parkes, J. Raftery, J. D. Sutherland, On the prebiotic synthesis of ribonucleotides: Photoanomerisation of cytosine nucleosides and nucleotides revisited, *ChemBioChem* **2007**, *8*, 1170-1179.

[175] C. Fernández-García, N. M. Grefenstette, M. W. Powner, Selective aqueous acetylation controls the photoanomerization of α-cytidine-5'-phosphate, *Chem. Commun.* **2018**, *54*, 4850-4853.

[176] M. W. Powner, B. Gerland, J. D. Sutherland, Synthesis of activated pyrimidine ribonucleotides in prebiotically plausible conditions, *Nature* **2009**, *459*, 239-242.

[177] A. W. Schwartz, Phosphorus in prebiotic chemistry, *Philos. Trans. R. Soc. B: Biol. Sci.* **2006**, *361*, 1743-1749.

[178] J. Xu, M. Tsanakopoulou, C. J. Magnani, R. Szabla, J. E. Šponer, J. Šponer, R. W. Góra, J. D. Sutherland, A prebiotically plausible synthesis of pyrimidine β-ribonucleosides and their phosphate derivatives involving photoanomerization, *Nat. Chem.* **2017**, *9*, 303-309.

[179] S. Islam, D.-K. Bučar, M. W. Powner, Prebiotic selection and assembly of proteinogenic amino acids and natural nucleotides from complex mixtures, *Nat. Chem.* **2017**, *9*, 584-589.

[180] S. Stairs, A. Nikmal, D.-K. Bučar, S.-L. Zheng, J. W. Szostak, M. W. Powner, Divergent prebiotic synthesis of pyrimidine and 8-oxo-purine ribonucleotides, *Nat. Commun.* **2017**, *8*, 1-12.

[181] E. T. Parker, H. J. Cleaves, M. P. Callahan, J. P. Dworkin, D. P. Glavin, A. Lazcano, J. L. Bada, Prebiotic Synthesis of Methionine and Other Sulfur-Containing Organic Compounds on the Primitive Earth: A Contemporary Reassessment Based on an Unpublished 1958 Stanley Miller Experiment, *Origins of Life and Evolution of Biospheres* **2011**, *41*, 201-212.

[182] A. P. Johnson, H. J. Cleaves, J. P. Dworkin, D. P. Glavin, A. Lazcano, J. L. Bada, The Miller volcanic spark discharge experiment, *Science* **2008**, *322*, 404-404.

[183] E. T. Parker, H. J. Cleaves, J. P. Dworkin, D. P. Glavin, M. Callahan, A. Aubrey, A. Lazcano, J. L. Bada, Primordial synthesis of amines and amino acids in a 1958 Miller H2S-rich spark discharge experiment, *Proc. Natl. Acad. Sci. U.S.A.* **2011**, *108*, 5526-5531.

[184] S. L. Miller, H. C. Urey, Organic compound synthesis on the primitive Earth: Several questions about the origin of life have been answered, but much remains to be studied, *Science* **1959**, *130*, 245-251.

[185] S. Miyakawa, H. Yamanashi, K. Kobayashi, H. J. Cleaves, S. L. Miller, Prebiotic synthesis from CO atmospheres: implications for the origins of life, *Proc. Natl. Acad. Sci. U.S.A.* **2002**, *99*, 14628-14631.
[186] G. H. Shaw, Earth's atmosphere–Hadean to early Proterozoic, *Geochemistry* **2008**, *68*, 235-264.
[187] J. Oró, A. Kimball, R. Fritz, F. Master, Amino acid synthesis from formaldehyde and hydroxylamine, *Arch. Biochem. Biophys.* **1959**, *85*, 115-130.
[188] F. Tiemann, Ueber aromatische Amidosäuren, *Ber. Dtsch. Chem. Ges.* **1880**, *13*, 381-385.
[189] H. Hatanaka, F. Egami, The formation of amino acids and related oligomers from formaldehyde and hydroxylamine in modified sea mediums related to prebiotic conditions, *Bull. Chem. Soc. Jpn.* **1977**, *50*, 1147-1156.
[190] H. Yanagawa, F. Egami, Formation of molecules of biological interest from formaldehyde and hydroxylamine in a modified sea medium, *J. Biochem.* **1979**, *85*, 1503-1507.
[191] S. Pulletikurti, M. Yadav, G. Springsteen, R. Krishnamurthy, Prebiotic synthesis of α-amino acids and orotate from α-ketoacids potentiates transition to extant metabolic pathways, *Nat. Chem.* **2022**, 1-9.
[192] A. Osumah, R. Krishnamurthy, Diamidophosphate (DAP): A Plausible Prebiotic Phosphorylating Reagent with a Chem to BioChem Potential?, *ChemBioChem* **2021**, *22*, 3001-3009.
[193] J. J. Li, in *Name Reactions*, Springer, **2021**, pp. 53-55.
[194] R. Krishnamurthy, N. V. Hud, Introduction: Chemical Evolution and the Origins of Life, *Chem. Rev.* **2020**, *120*, 4613-4615.
[195] S. Nader, L. Sebastianelli, S. S. Mansy, Protometabolism as out-of-equilibrium chemistry, *Philos. Trans. Royal Soc. A* **2022**, *380*, 20200423.
[196] S. Becker, J. Feldmann, S. Wiedemann, H. Okamura, C. Schneider, K. Iwan, A. Crisp, M. Rossa, T. Amatov, T. Carell, Unified prebiotically plausible synthesis of pyrimidine and purine RNA ribonucleotides, *Science* **2019**, *366*, 76-82.
[197] A. D. Anbar, Elements and evolution, *Science* **2008**, *322*, 1481-1483.
[198] H. Follmann, C. Brownson, Darwin's warm little pond revisited: from molecules to the origin of life, *Naturwissenschaften* **2009**, *96*, 1265-1292.
[199] A. Schimpl, R. M. Lemmon, M. Calvin, Cyanamide formation under primitive Earth conditions, *Science* **1965**, *147*, 149-150.
[200] Y. L. Yung, An update of nitrile photochemistry on Titan, *Icarus* **1987**, *72*, 468-472.
[201] U. Trinks, A. Eschenmoser, ETH Zurich **1987**.
[202] P. A. Sossi, A. D. Burnham, J. Badro, A. Lanzirotti, M. Newville, H. S. C. O'Neill, Redox state of Earth's magma ocean and its Venus-like early atmosphere, *Sci. Adv.* **2020**, *6*, eabd1387.
[203] R. Lupu, K. Zahnle, M. S. Marley, L. Schaefer, B. Fegley, C. Morley, K. Cahoy, R. Freedman, J. J. Fortney, The atmospheres of earthlike planets after giant impact events, *Astrophys. J.* **2014**, *784*, 27.
[204] J. D. Toner, D. C. Catling, Alkaline lake settings for concentrated prebiotic cyanide and the origin of life, *Geochim. Cosmochim. Acta.* **2019**, *260*, 124-132.
[205] D. D. Sasselov, J. P. Grotzinger, J. D. Sutherland, The origin of life as a planetary phenomenon, *Sci. Adv.* **2020**, *6*, eaax3419.

[206] W. Chameides, J. C. Walker, Rates of fixation by lightning of carbon and nitrogen in possible primitive atmospheres, *Orig. Life* **1981**, *11*, 291-302.
[207] D. N. Mvondo, R. Navarro-González, C. P. McKay, P. Coll, F. Raulin, Production of nitrogen oxides by lightning and coronae discharges in simulated early Earth, Venus and Mars environments, *Adv. Space Res.* **2001**, *27*, 217-223.
[208] M. L. Wong, B. D. Charnay, P. Gao, Y. L. Yung, M. J. Russell, Nitrogen oxides in early Earth's atmosphere as electron acceptors for life's emergence, *Astrobiology* **2017**, *17*, 975-983.
[209] J. P. Pinto, G. R. Gladstone, Y. L. Yung, Photochemical Production of Formaldehyde in Earth's Primitive Atmosphere, *Science* **1980**, *210*, 183-185.
[210] M. Halmann, S. Bloch, Glyoxal and malonaldehyde formation by ultraviolet irradiation of aqueous formaldehyde, *BioSystems* **1979**, *11*, 227-232.
[211] S. Stovbun, A. Skoblin, A. Zanin, V. Tverdislov, O. Taran, V. Parmon, Formation of Chiral Structures in Photoinitiated Formose Reaction, *High Energy Chem.* **2018**, *52*, 108-116.
[212] S. Stovbun, A. Skoblin, A. Zanin, V. Tverdislov, O. Taran, V. Parmon, Formation of chiral structures in UV-initiated formose reaction, *Dokl. Phys. Chem.* **2018**, *479*, 57-60.
[213] A. Beeby, D. b. H. Mohammed, J. R. Sodeau, Photochemistry and photophysics of glycolaldehyde in solution, *J. Am. Chem. Soc.* **1987**, *109*, 857-861.
[214] N. Malkina, S. Kazarnovskii, Synthesis of cyanuric acid from urea, *Zh. Priklad. Khim.* **1960**, *34*, 1583-1587.
[215] H. L. Barnes, *Geochemistry of hydrothermal ore deposits*, John Wiley & Sons, **1997**.
[216] S. JW, Isotopic fractionations accompanying sulfur hydrolysis, *Gechem. J.* **2000**, *34*, 95-99.
[217] M. Kusakabe, Y. Komoda, B. Takano, T. Abiko, Sulfur isotopic effects in the disproportionation reaction of sulfur dioxide in hydrothermal fluids: implications for the δ34S variations of dissolved bisulfate and elemental sulfur from active crater lakes, *J. Volcanol. Geotherm. Res.* **2000**, *97*, 287-307.
[218] V. M. Rivilla, J. Martín-Pintado, I. Jiménez-Serra, S. Martín, L. F. Rodríguez-Almeida, M. A. Requena-Torres, F. Rico-Villas, S. Zeng, C. Briones, Prebiotic precursors of the primordial RNA world in space: Detection of NH2OH, *Astrophys. J. Lett.* **2020**, *899*, L28.

Anhang I

science.sciencemag.org/content/366/6461/76/suppl/DC1

Supplementary Materials for

Unified prebiotically plausible synthesis of pyrimidine and purine RNA ribonucleotides

Sidney Becker*, Jonas Feldmann*, Stefan Wiedemann*, Hidenori Okamura, Christina Schneider, Katharina Iwan, Antony Crisp, Martin Rossa, Tynchtyk Amatov, Thomas Carell†

*These authors contributed equally to this work.
†Corresponding author. Email: thomas.carell@lmu.de

Published 4 October 2019, *Science* **366**, 76 (2019)
DOI: 10.1126/science.aax2747

This PDF file includes:

Materials and Methods

General Information

Chemicals were purchased from Sigma-Aldrich, Fluka, ABCR, Carbosynth, TCI or Acros organics and used without further purification. The solvents were of reagent grade or purified by distillation. Chromatographic purification of products was accomplished using flash column chromatography on Merck Geduran Si 60 (40-63 µm) silica gel (normal phase). ^{1}H- and ^{13}C-NMR spectra were recorded on Varian Oxford 200, Bruker ARX 300, Varian VXR400S, Varian Inova 400, Bruker AMX 600 and Bruker AVIIIHD 400 spectrometers and calibrated to the residual solvent peak. Multiplicities are abbreviated as follows: s = singlet, d = doublet, t = triplet, q = quartet, m = multiplet, br = broad. High-resolution ESI spectra were obtained on the mass spectrometer Thermo Finnigan LTQ FT-ICR. IR measurements were performed on Perkin Elmer Spectrum BX FT-IR spectrometer with a diamond-ATR (Attenuated Total Reflection) setup. Melting points were measured on a Büchi B-540 device. For preparative HPLC purification a Waters 1525 binary HPLC Pump in combination with a Waters 2487 Dual Absorbance Detector was used, with a Nucleosil 100-7 C18 reversed phase column. The prebiotic reactions were analyzed by LC-ESI-MS on a Thermo Finnigan LTQ Orbitrap XL and were chromatographed by a Dionex Ultimate 3000 HPLC system. All chromatographic separations except for nucleotides were performed on an Interchim Uptisphere120 3HDO C18 column with a flow of 0.15 ml/min and a constant column temperature of 30 °C. Eluting buffers were buffer A (2 mM $HCOONH_4$ in H_2O (pH 5.5)) and buffer B (2 mM $HCOONH_4$ in H2O/MeCN 20/80 (pH 5.5)). The gradient for isoxazole containing compounds and pyrimidine nucleosides was 0 → 20 min, 0% → 4% buffer B. The gradient for purine nucleosides was 0 → 45 min, 0% → 15% buffer B. Chromatographic separation for nucleotides were performed on a YMC-Triart C18 column with a flow of 0.20 ml/min and a constant column temperature of 40 °C. Eluting buffers were buffer A (10 mM NH_4HCO_3 and 5 mM dibutylamine in H_2O (pH 9.1)) and buffer B (MeCN). The gradient was 0 → 10 min, 0% → 20%; 10 → 20 min, 20% → 20% buffer B. The elution was monitored at 223 nm and 260 nm (Dionex Ultimate 3000 Diode Array Detector). The chromatographic eluent was directly injected into the ion source without prior splitting. Ions were scanned by use of a positive polarity mode over a full-scan range of m/z 80-500 with a resolution of 30000. Nucleotides were scanned by use of a negative polarity mode over a full-scan range of m/z 120-1000 with a resolution of 30000. The synthetic standards for the co-injection experiments were synthesized in our lab (see synthetic procedures or according to reported literature (*6*)) or purchased. XRD measurements were performed on a STOE powder diffractometer in transmission geometry (Cu-Kα1, λ = 1.5406 Å) with a step size of 2°2θ (30 seconds per step) and equipped with a position-sensitive Mythen-1K detector. The X-ray intensity data was measured at a temperature of 100 K on a Bruker D8 Venture TXS system equipped with a multilayer mirror optics monochromator and a Mo Kα rotating-anode X-ray tube (λ = 0.71073 Å). The frames were integrated with the Bruker SAINT software package using a narrow-frame algorithm. Data were corrected for absorption effects using the Multi-Scan method (SADABS). The structures were solved and refined using the Bruker SHELXTL software package.

Degradase digestion

Isolated nucleotides in 42 µL H_2O were digested as follows: 10X DNA Degradase™ Reaction Buffer (5 µL), together with 8 U DNA Degradase Plus™ (2 µL, Zymo Research) and 3.5 U of Benzonase® Nuclease (1 µL, Merck, purity >90%) was added and the mixture was incubated at 37 °C for 2 h. The sample was directly analysed by LC-MS according to the general information.

Apyrase digestion

Isolated nucleotides in 17.6 µL H_2O were digested as follows: 10X Apyrase reaction buffer (2 µL, NEB) was added together with 0.2 U of apyrase (0.4 µL, NEB). The mixture was incubated at 30 °C for 2 h. The sample was directly analysed by LC-MS according to the general information.

Synthetic Procedures

Hydroxylammonium chloride (2)

A solution of potassium hydroxylamine disulfonate **6** (269 mg, 1.00 mmol, 1.0 eq) (*28*) in 100 mM aq. HCl (10 mL) was shaken at 850 rpm and 90 °C for 2 h in an Eppendorf ThermoMixer®. The reaction mixture was treated with $BaCl_2$ (489 mg, 2.00 mmol, 2.0 eq) and left for 5 min at 90 °C to precipitate the formed sulfates. The resulting suspension was filtered, and the filtrate was lyophilized to afford a white residue, which was extracted with EtOH (3 x 5 mL). After removing the solvent *in vacuo*, hydroxylammonium chloride **2** was identified *via* ^{1}H-NMR (Fig. S1).

Note: Under neutral conditions, hydrolysis of hydroxylamine disulfonate proceeds over a much longer period of time (*28*, *44*).

^{1}H NMR (400 MHz, DMSO-d_6) δ 10.32 (s, 3H), 10.11 (s, 1H).

((2-Cyanovinyl)oxy)(sulfonato)sulfamate (7) *via* hydroxylamine disulfonate (6)

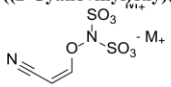

Prebiotically from SO_2 and NO_2^-:

$NaNO_2$ (2.76 g, 40.0 mmol, 1.0 eq) and $Na_2S_2O_5$ (4.18 g, 22.0 mmol, 0.55 eq) were dissolved in H_2O (150 mL). SO_2 was passed through the solution under stirring, while the temperature increased from 25 °C to about 35 °C. When a pH of 3 was reached, the gas injection was stopped and 700 µL of the reaction mixture were transferred into a microcentrifuge tube. After the successive addition of aq. Na_2CO_3 (300 µL, 1 M) and cyanoacetylene (6.26 µL, 100 µmol), the mixture was shaken at 25 °C and 850 rpm for 60 min in an Eppendorf ThermoMixer®. For quantification, a sample of 100 µL was treated with aq. 14.3 mM NaOAc (350 µL, as internal standard) and D_2O (50 µL). NMR spectroscopy (Fig. S2a) revealed the formation of (Z)-((2-cyanovinyl)oxy)(sulfonato)-sulfamate (**7**, 88%).

From hydroxylamine disulfonate:

To a solution of Na_2CO_3 (106 mg, 1.00 mmol, 2.2 eq.) and **6** (121 mg, 450 µmol, 1.0 eq) in H_2O (5 mL) was added cyanoacetylene (31.3 µL, 500 µmol, 1.1 eq.). The mixture was shaken at 25 °C and 850 rpm for 40 min in an Eppendorf ThermoMixer®. The mixture was neutralized with aq. 2 M HCl (500 µL) and lyophilized to obtain crude (*Z*)-((2-cyanovinyl)oxy)(sulfonato)sulfamate (**7**) as identified *via* NMR (Fig. S2b). Note: Compound **6** was synthesized according to literature (*28*).

^{1}H NMR (400 MHz, D_2O) δ 7.38 (d, *J* = 7.0 Hz, 1H), 4.91 (d, *J* = 7.0 Hz, 1H). **^{13}C NMR** (101 MHz, D_2O) δ 160.35, 115.47, 74.52. **HRMS** (ESI-): calc.: $[C_3H_3N_2O_7S_2]^-$ 242.9387, found: 242.9386 $[M\text{-}H]^-$.

General procedure for the formation of 3-aminoisoxazole (4) under prebiotic conditions

From hydroxyurea:

To a mixture of a divalent metal salt (13.6 mg $ZnCl_2$ or 23.8 mg $CoCl_2 \cdot 6\,H_2O$, 100 µmol, 1.0 eq.), Na_2CO_3 (42.4 mg, 400 µmol, 4.0 eq.), urea (24.0 mg, 400 µmol, 4.0 eq.), hydroxylurea (8.0 mg, 105 µmol, 1.1 eq.) in H_2O (1 mL) was added cyanoacetylene (6.26 µL, 100 µmol, 1.0 eq.). The mixture was shaken at 25 °C and 850 rpm for 2 h in an Eppendorf ThermoMixer®. A sample (10 µL) was taken and diluted with H_2O (990 µL) to 1 mL for LC-MS analysis (5 µL injection volume). Compound **4** was formed in 88% (Zn^{2+}) and 83% (Co^{2+}) yield, respectively. The yield was determined by LC-MS measurement with the calibration curve prepared using commercially available 3-aminoisoxazole. For the confirmation of the structural integrity, the reaction mixture was extracted with diethylether, dried over $MgSO_4$, concentrated and the crude residue purified by flash column chromatography (CH_2Cl_2:MeOH = 20:1). The NMR spectrum of the isolated compound was identical to that of a commercial sample.

From SO_2 and NO_2^-:

$NaNO_2$ (2.76 g, 40.0 mmol, 1.0 eq) and $Na_2S_2O_5$ (4.18 g, 22.0 mmol, 0.55 eq) were dissolved in H_2O (150 mL). SO_2 was passed through the solution under stirring, while the temperature increased from 25 °C to about 35 °C. When a pH of 3 was reached, the gas injection was stopped and 700 µL of the reaction mixture were transferred into a microcentrifuge tube. After the successive addition of aq. Na_2CO_3 (300 µL, 1 M) and cyanoacetylene (6.26 µL, 100 µmol), the mixture was shaken at 25 °C and 850 rpm for 60 min in an Eppendorf ThermoMixer®. To accelerate hydrolysis (*44*), 900 µL of the reaction mixture were acidified with aq. conc. HCl (100 µL) and shaken at 50 °C and 850 rpm for 60 min in an Eppendorf ThermoMixer®. Compound **4** was formed in 63% yield. The yield was determined by LC-MS measurement with the calibration curve prepared using commercially available 3-aminoisoxazole.

From hydroxylamine:

To a mixture of $ZnCl_2$ (6.8 mg, 50 µmol, 0.5 eq), Na_2CO_3 (26.5 mg, 250 µmol, 2.5 eq), urea (12.0 mg, 200 µmol, 2.0 eq), 40% wt hydroxylamine (6.32 µL, 0.105 mmol, 1.1 eq) in H_2O (1 mL) was added cyanoacetylene (6.26 µL, 100 µmol, 1.0 eq). The mixture

was shaken at 25 °C and 850 rpm for 3.5 h in an Eppendorf ThermoMixer®. A sample (10 µL) was taken and diluted with H_2O (990 µL) to 1 mL for LC-MS analysis (5 µL injection volume). Compound **4** was formed in 17% yield. The yield was determined by LC-MS measurement with the calibration curve prepared using commercially available 3-aminoisoxazole.

^{1}H NMR (400 MHz, DMSO-d_6) δ 8.32 (d, J = 1.7 Hz, 1H, HC5), 5.88 (d, J = 1.7 Hz, 1H, HC4), 5.57 (s, 2H, NH_2). **^{13}C NMR** (101 MHz, DMSO-d_6) δ 163.76 (C5), 158.73 (C3), 97.71 (C4).

***N*-isoxazolyl-urea (8)**

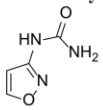

Prebiotic Synthesis from **4**:

To a solution of urea (120 mg, 2.00 mmol, 4.0 eq.) and a divalent metal salt (68 mg $ZnCl_2$ or 119 mg $CoCl_2 \cdot 6\ H_2O$; 0.5 mmol, 1.0 eq.) in H_2O (500 µL) was added 3-aminoisoxazole (36.9 µL, 500 µmol, 1.0 eq.). The mixture was shaken at 850 rpm and 95 °C for 2 d in an Eppendorf ThermoMixer® open to the air to allow water to evaporate. The resulting residue was dissolved in H_2O to a final volume of 1 mL. A sample (10 µL) was taken and diluted with H_2O (2000 x) for LC-MS analysis (5 µL injection volume). Compound **8** was formed in 88% (Zn^{2+}), 68% (Co^{2+}) and 25% (no metal) yield, respectively. The yield was determined by LC-MS measurement with the calibration curve prepared using synthetic *N*-isoxazolyl-urea.

For prebiotic enrichment, five replicates of the aforementioned reaction were prepared using $ZnCl_2$. The crude products were combined and resuspended in H_2O (50 mL). After treatment with K_2CO_3 (2.76 g, 20 mmol, 4.0 eq.) in H_2O (10 mL), the resulting suspension was mixed and centrifuged at 5000 rpm for 5 min. The supernatant was transferred into a 100 mL beaker and left at RT for 5 d to allow for crystallization by concentration. Crystallized *N*-Isoxazolyl-urea (348 mg, 2.74 mmol, 55%) was collected and analyzed by X-ray spectroscopy.

One-pot prebiotic synthesis from **1**:

To a mixture of a divalent metal salt (13.6 mg $ZnCl_2$ or 23.8 mg $CoCl_2 \cdot 6\ H_2O$; 100 µmol, 1.0 eq.), Na_2CO_3 (42.4 mg, 400 µmol, 4.0 eq.), urea (24.0 mg, 400 µmol, 4.0 eq.), hydroxylurea (8.0 mg, 105 µmol, 1.1 eq.) in H_2O (1 mL) was added cyanoacetylene (6.26 µL, 100 µmol, 1.0 eq.). The suspension was shaken at 25 °C and 850 rpm for 2 h in an Eppendorf ThermoMixer®. The mixture was neutralized with conc. aq. HCl (70.4 µL) and left to equilibrate for several minutes at 95 °C to adjust the pH to ~6-7. The resulting solution was shaken at 95 °C and 850 rpm for 2 d in an Eppendorf ThermoMixer® open to the air to allow water to evaporate. The resulting residue was dissolved in H_2O to a final volume of 1 mL. A sample (10 µL) was taken and diluted with H_2O (990 µl) to 1 mL for LC-MS analysis (5 µL injection volume). Compound **8** was formed in 56% (Zn^{2+}) and 40% (Co^{2+}) yield, respectively. The yield was determined by LC-MS measurement with the calibration curve prepared using synthetic *N*-isoxazolyl-urea.

Synthetic reference:

3-aminoisoxazole (1.14 g, 1.00 ml, 13.5 mmol) was dissolved in dry THF (20 ml) under inert atmosphere at 0°C. 2,2,2-trichloroacetylisocyanate (2.45 g, 1.61 ml, 13.5 mmol) was slowly added to the solution and the reaction was stirred at rt for 2 h. The reaction was quenched with MeOH (10 ml) and the solvent removed *in vacuo*. After co-evaporation with EtOH (2 x 20 ml) the product was obtained as a colorless solid (3.44 g, 12.6 mmol, 93 %). The crude product (3.12 g, 11.4 mmol) was dissolved in methanolic ammonia (10 mL, 7 M) and stirred for 1.5 h at rt. MeOH (20 mL) und EtOH (20 mL) were added to the reaction to obtain a clear solution. Et_2O (40ml) was added to the clear solution to precipitate the product. The crude product was filtered off and was subsequently dissolved in H_2O (20 ml). After filtering through celite, the solvent was removed by freeze-drying to obtain the product as a colorless solid (1.16 g, 9.15 mmol, 80%).

mp: 175 °C. **^{1}H NMR** (400 MHz, DMSO-d_6) δ (ppm) = 9.41 (s, 1H, HN4), 8.65 (d, ^3J = 1.7 Hz, 1H, HC5), 6.70 (d, ^3J = 1.7 Hz, 1H, HC4), 6.28 (s, 2H, NH_2).**^{13}C NMR** (101 MHz, DMSO-d_6) δ (ppm) = 159.4 (C5), 158.6 (C3), 154.6 (CO), 98.2 (C4). **HRMS** (ESI+): calc.: $[C_4H_6N_3O_2]^+$ 128.0455, found: 128.0455 $[M+H]^+$. **IR** (cm^{-1}): $\tilde{\nu}$ = 3486 (vw), 3389 (w), 3259 (vw), 3179 (w), 3194 (w), 3033 (w), 2958 (w), 1752 (m), 1730 (m), 1686 (w), 1631 (w), 1592 (vs), 1537 (w), 1486 (m), 1416 (s), 1378 (s), 1343 (w), 1298 (vw), 1284 (w), 1123 (m), 1070 (w), 1039 (vw), 981 (vw), 928 (w), 891 (w), 797 (s), 756 (vs), 654 (w).

Formation of 3-aminoisoxazole 4 in the presence of 19 and 20

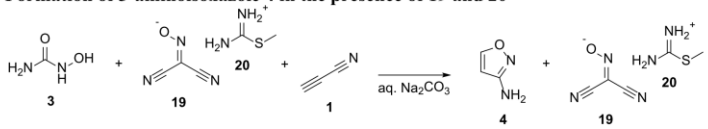

3 19 1 4 19 20

To a solution of the methylthioamidine **20** salt of (hydroxyimino)malononitrile **19** (9.3 mg, 50 µmol, 0.5 eq), Na_2CO_3 (26.5 mg, 250 µmol, 2.5 eq.), and hydroxylurea **3** (8.0 mg, 0.11 µmol, 1.1 eq.) in H_2O (1 mL) was added cyanoacetylene (6.26 µL, 100 µmol, 1.0 eq). The mixture was left at rt for 10 min. A sample (10 µL) was taken and diluted with H_2O (990 µL) to 1 mL for LC-MS analysis (5 µL injection volume). Compound **4** was formed in 86% yield. The yield was determined by LC-MS measurement with the calibration curve prepared using commercially available 3-aminoisoxazole.

Prebiotically linked syntheses of pyrimidine (8) and purine (22,24) precursors (see Fig. 5 and Fig. S10)

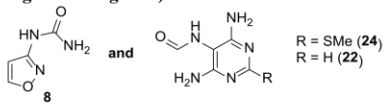

8

(A) Formation of 2-(methylthio)-5-nitrosopyrimidine-4,6-diamine **21**

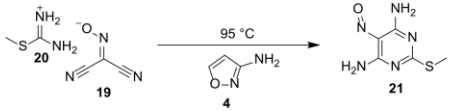

The methylthioamidine salt of (hydroxyimino)malononitrile (130 mg, 0.7 mmol, 0.5 eq.) was suspended in 3-amino-isoxazole (103 µL, 1.39 mmol, 1 eq.) and shaken at 95 °C and 850 rpm for 3 h in an Eppendorf ThermoMixer®. To the reaction mixture was added an aq. solution of urea (4 eq. in 1 mL H_2O). The reaction mixture was filtered, the residue was washed with H_2O (1 mL) and dried to afford crude 2-(methylthio)-5-nitroso-pyrimidine-4,6-diamine **21** (57 mg, 0.31 mmol, 45%). The filtrate was kept for the formation of **8**.

(B) Formation of formamidopyrimidine **22** and **24**

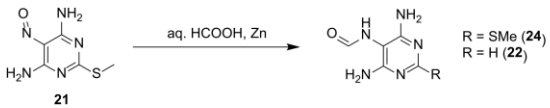

The intermediate **21** (46 mg, 0.25 mmol, 1.0 eq) was suspended in aq. HCOOH (4.5%, 2.5 mL) in the presence of elementary Zn powder (65 mg, 1.0 mmol, 4.0 eq). The reaction mixture was stirred at 70 °C in a sealed 15 mL Ace pressure tube for 4 h. After cooling to rt, the mixture was diluted with H_2O (2.5 mL) and filtered. The filtrate was analysed by LC-MS (see Fig. 5b) and was used for the formation of **8** in the next step.

(C) Formation of isoxazolyl-urea **8**

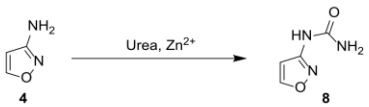

The filtrate from (B) was transferred into a conical glass tube containing the filtrate of (A). The solution was left at 95 °C for 2d in the oven open to the air to allow water to evaporate. After cooling to rt, the resulting solid was suspended in H_2O (10 mL). A sample (100 µL) was taken and diluted with H_2O (10 x) for LC-MS analysis (5 µL injection volume). FaPyA (**22**), FaPyms^{2}A (**24**) and *N*-isoxazolyl-urea (**8**), were observed as main products (see Fig. 5c).

***N*-isoxazolyl-*N'*-ribosyl-urea (10a-d)**

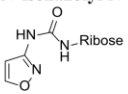

Prebiotic synthesis:

N-isoxazolylurea (6.4 mg, 0.05 mmol) was thoroughly ground up with ribose (37.5 mg, 0.25 mmol, 5 eq.) and boric acid (0.8 mg, 0.013 mmol, 0.25 eq.). The mixture was heated overnight in an oven at 95 °C. Alternatively the reaction can also be performed by a dry-down method, where a solution of *N*-isoxazolylurea (500 ul, 0.05 mmol, 100 mM) is mixed with a ribose (83 µl, 0.25 mmol, 3 M) and boric acid (25 ul, 0.013 mmol, 500 mM) solution. The mixture was kept in an oven for 20 h at 95 °C. The sample was dissolved in H_2O (2 ml) and analyzed by LC-MS. To confirm the structural integrity, the different isomers were isolated by reversed phase HPLC in pure form.

Synthetic reference:

1-*O*-acetyl-2,3,5-tri-*O*-benzoyl-β-D-ribofuranose (17.0 g, 33.8 mmol) was dissolved in dry DCM (300 ml) under inert atmosphere. $TiCl_4$ (4.46 mL, 40.7 mmol) was added and stirred for 2 h at rt. H_2O (250 ml) was added and filtered through celite. The organic layer was separated and the aqueous phase was extracted with DCM (3 x 100 ml). The combined organic layers were washed with sat. NaCl (300 ml), dried over $MgSO_4$, filtered and the solvent was removed *in vacuo*. The crude product was dissolved in dry toluene (300 ml) and AgNCO (6.25 g, 41.6 mmol) was added. After refluxing for 2.5 h, the reaction mixture was filtered through celite and washed with dry toluene. To the clear solution was added 3-aminoisoxazole (3 ml, 40.6 mmol) and stirred for 16 h at rt. The solvent was removed *in vacuo* and the product purified by flash column chromatography (DCM:MeOH 50:1). The product was dissolved in methanolic ammonia (330 ml, 7 M) and stirred for 18 h at rt. The solvent was removed *in vacuo* and the product purified by flash column chromatography (DCM:MeOH 17:3 → 4:1). The product was obtained as a colorless foam and contained a 3:1 mixture of the α- and β-furanoside (4.87 g, 18.8 mmol, 56%). The α- and β-furanosides were isolated in pure form by reversed phase HPLC to confirm the structural integrity.

α-furanosyl-isomer 10a

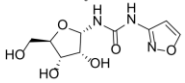

mp: (131 °C).^{1}**H NMR** (400 MHz, DMSO-d_6) δ (ppm) = 9.85 (s, 1H, NH), 8.66 (d, ^3J = 1.7 Hz, 1H, HC5), 7.24 (d, ^3J = 9.5 Hz, 1H, C1'NH), 6.73 (d, ^3J = 1.8 Hz, 1H, HC4), 5.50 (dd, ^3J = 9.5, 4.4 Hz, 1H, HC1'), 5.41 (br, 1H, C3'OH), 5.03 (br, 1H, C2'OH), 4.66 (br, 1H, C5'OH), 3.92 (t, ^3J = 4.4 Hz, 1H, HC2'), 3.87 (dd, ^3J = 6.6, 4.5 Hz, 1H, HC3'), 3.71 (ddd, J = 6.5, 4.9, 3.1 Hz, 1H, HC4'), 3.49 (dd, ^2J = 11.7 Hz, ^3J = 3.1 Hz, 1H, H_aC5'), 3.39-3.35 (m, 1H, H_bC5'). ^{13}**C NMR** (101 MHz, DMSO-d_6) δ (ppm) = 159.5 (C5), 158.4 (C3), 153.3 (CO), 98.3 (C4), 81.9 (C4'), 80.6 (C1'), 71.1 (C3'), 70.1 (C2'), 61.6 (C5'). **HRMS** (ESI+): calc.: $[C_9H_{14}N_3O_6]^+$ 260.0877, found: 260.0877 $[M+H]^+$. **IR**

(cm^{-1}): $\tilde{\nu}$ = 3852 (w), 3820 (w), 3648 (w), 3283 (w)m 1843 (vw), 1771 (w), 1717 (m), 1699 (s), 1652 (vs), 1634 (s), 1575 (m), 1558 (vs), 1539 (vs), 1506 (vs), 1456 (s), 1436 (m), 1418 (m), 1032 (m), 971 (m).

β-furanosyl-isomer 10b

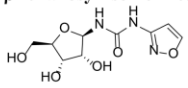

mp: 120 °C (decomp.).**^{1}H NMR** (400 MHz, DMSO-d_6) δ(ppm) = 9.63 (s, 1H, NH), 8.67 (d, ^3J = 1.7 Hz, 1H, HC5), 7.13 (d, ^3J = 9.5 Hz, 1H, C1'NH), 6.74 (d, ^3J = 1.7 Hz, 1H, HC4), 5.20 (dd, ^3J = 9.5, 5.4 Hz, 1H, HC1'), 5.12 – 4.68 (m, 3H, C2'OH, C3'OH and C5'OH), 3.85 (t, ^3J = 4.6 Hz, 1H, HC3'), 3.71 (t, ^3J = 5.4 Hz, 1H, HC2'), 3.67 (q, ^3J = 4.2 Hz, 1H, HC4'), 3.45 (dd, ^2J = 11.7 Hz, ^3J = 4.0 Hz, 1H, H_aC5'), 3.42 – 3.39 (m, 1H, H_bC5').**^{13}C NMR** (101 MHz, DMSO-d_6) δ(ppm) = 159.6 (C5), 158.3 (C3), 153.4 (CO), 98.3 (C4), 84.4 (C1'), 83.5 (C4'), 74.3 (C2'), 70.3 (C3'), 61.8 (C5'). **HRMS** (ESI+): calc.: $[C_9H_{13}NaN_3O_6]^+$ 282.0697, found: 282.0696 $[M+Na]^+$. **IR** (cm^{-1}): $\tilde{\nu}$ = 3268 (m), 1677 (m), 1599 (s), 1537 (vs), 1478 (s), 1403 (m), 1228 (m), 999 (vs), 893 (s), 777 (vs).

α-pyranosyl-isomer (10c)

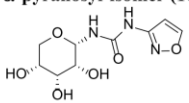

mp: 190 °C. **^{1}H NMR** (400 MHz, DMSO-d_6) δ(ppm) = 9.97 (s, 1H, NH), 8.67 (d, ^3J = 1.8 Hz, 1H, HC5), 7.47 (d, ^3J = 9.1 Hz, 1H, C1'NH), 6.74 (d, ^3J = 1.8 Hz, 1H, HC4), 5.25 – 4.87 (m, 4H, HC1', C2'OH, C3'OH, C5'OH), 3.70 (t, ^3J = 2.8 Hz, 1H, HC3'), 3.64 – 3.44 (m, 4H, HC2', HC4', H_aC5', H_bC5'). **^{13}C NMR** (101 MHz, DMSO-d_6) δ(ppm) = 159.5 (C5), 158.4 (C3), 153.4 (CO), 98.4 (C4), 77.9 (C1'), 69.4 (C3'), 69.3 (C4'), 68.4 (C5') 67.6 (C2'). **HRMS** (ESI+): calc.: $[C_9H_{13}N_3O_6]^+$ 260.0877, found: 260.0877 $[M+H]^+$. **IR** (cm^{-1}): $\tilde{\nu}$ = 3090 (vw), 2363 (m), 2271 (w), 1956 (w), 1700 (vs), 1683 (s), 1652 (s), 1823 (w), 1732 (w), 1700 (vs), 1683 (s), 1652 (s), 1609 (w), 1559 (m), 1509 (m), 1456 (s), 707 (w), 680 (m), 656 (s).

β-pyranosyl-isomer (10d)

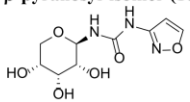

mp: 175 °C (decomp.). **^{1}H NMR** (400 MHz, DMSO-d_6) δ(ppm) = 9.46 (s, 1H, NH), 8.68 (d, ^3J = 1.8 Hz, 1H, HC5), 6.89 (d, ^3J = 9.1 Hz, 1H, C1'NH), 6.74 (d, ^3J = 1.8 Hz, 1H, HC4), 4.90 (t, ^3J = 9.1 Hz, 1H, HC1'), 4.84 (d, ^3J = 3.6 Hz, 1H, C3'OH), 4.82 (d, J = 7.4 Hz, 1H, C2'OH), 4.69 (d, ^3J = 6.5 Hz, 1H, C4'OH), 3.88 (q, J = 2.8 Hz, 1H, HC3'), 3.55 – 3.47 (m, 1H, HC4'), 3.47 – 3.37 (m, 2H, H_aC5', H_bC5'), 3.18 (ddd, J = 9.1, 7.4, 2.8 Hz, 1H, HC2'). **^{13}C NMR** (101 MHz, DMSO-d_6) δ(ppm) = 159.7 (C5), 158.3 (C3), 153.6 (CO), 98.3 (C4), 77.5 (C1') 70.9 (C3'), 69.9 (C2'), 67.0 (C4'), 64.1 (C5'). **HRMS** (ESI+): calc.: $[C_9H_{13}N_3O_6]^+$ 260.0877, found: 260.0877 $[M+H]^+$. **IR** (cm^{-1}): $\tilde{\nu}$ = 3314 (m), 2871 (vw), 1941 (vw), 1705 (vs), 1598 (w), 1540 (vs), 1476 (w), 1432 (vw), 1336 (vw), 1282 (m), 1266 (w), 1208 (w), 1168 (m), 1139 (m), 1088 (w), 1065(m), 1035 (vs), 1004 (m), 950 (s), 916 (w), 886 (m), 804 (m), 789 (vs), 744 (w), 706 (m).

Prebiotic formation of pyrimidine nucleosides and nucleotides

General procedure nucleoside formation

The reactions were handled under inert atmosphere. All solutions were degassed for 1 h with argon before use. A solution of ribose isoxazole **10a**/**b** as a 3:1 mixture (25.9 mg, 0.1 mmol, 1 eq.) in 75 mM Na_2CO_3 (0.5 ml) was added to a mixture of mineral (1 eq.), dithiol (1.5 eq.) and Fe^{2+} source (0.5 eq.) in a 15 ml falcon tube. The tube was sealed with a PTFE sealing tape and shaked for 4 h at 100°C in an Eppendorf ThermoMixer®. After cooling to rt, it was centrifuged and a sample (10 µL) was removed and diluted with H_2O to 1 ml. This diluted sample was used for LC-MS analysis according to the general information.

The different minerals, thiols and iron sources used are stated in the main text. Monothiols were used with 3 eq. As water soluble Fe^{2+} salt we used ammonium iron(II) sulfate hexahydrate in a range of 0.001-0.0001 eq. Reactions without minerals were performed in a different buffer (100 mM Na_2CO_3, 50 mM boric acid, pH 9.7).

General procedure for one-pot nucleotide formation

The above described procedure was used for nucleoside formation. Lüneburgite or struvite (0.1 mmol, 1 eq.) were used as minerals, DTT (23.1 mg, 0.15 mmol, 1.5 eq.) and FeS_2 (6.0 mg, 0.05 mmol, 0.5 eq.) were used as thiol and Fe^{2+} source. After nucleoside formation we added solid urea (240 mg, 4 mmol, 40 eq.) and in case of struvite additionally oxalic acid (0.30 mmol, 3.0 eq.). The mixture was heated to 65 °C until the urea was fully dissolved. The sample was well suspended by vortexing and a sample (25 µL) was transferred into a 2 ml Eppendorf tube. The sample was kept at 85 °C for 20 h in an Eppendorf ThermoMixer® open to the air to allow water to evaporate. The dried sample was taken up in H_2O (1 ml) and analyzed for nucleotides by LC-MS analysis according to the general information.

Formation of purine nucleosides compatible to pyrimidine nucleoside formation

For purine nucleoside synthesis, FaPyA **22** or FaPyG **23** (0.05 mmol, 1eq.) was thoroughly ground up with ribose (37.5 mg, 0.25 mmol, 5 eq.) and boric acid (0.80 mg, 0.013 mmol, 0.25 eq.), identical to the N-isoxazolyl-urea ribosylation. The mixture was heated overnight in an oven at 95 °C. The resulting ribosides were heated at 100 °C in sealed 2 ml Eppendorf tubes under the following conditions: 100 mM Na_2CO_3, 50 mM boric acid, pH 9.7, 1.5 eq. DTT and 0.0005 eq. ammonium iron(II) sulfate hexahydrate. The following reaction times and concentrations were used: FaPyA (3d, 25 mM), FaPyG (2d, 6.25 mM).

Formation of purine and pyrimidine nucleoside in an one-pot reaction

For one-pot nucleoside synthesis of purines and pyrimidines, solutions of **8** (400 µl, 100 mM, 40 µmol, 1.0 eq), FaPyA (400 µl, 50 mM, 20 µmol, 0.5 eq.), FaPyDA (400 µL, 50 mM, 20 µmol, 0.5 eq.), ribose (267 µL, 3 M, 800 µmol, 20 eq.) and boric acid (48.0 uL, 500 mM, 24 µmol, 0.6 eq.) were heated at 95 °C for 14 h in a dry down reaction. The formed residue containing **10** and **26** was dissolved in a basic buffer (1.6 mL, 100 mM Na_2CO_3 and 50 mM Borate) and degased in a 15 mL Falcon tube with argon. To the degassed reaction mixture (500 µl) was added soluble Fe^{2+} (0.0005 eq.) and DTT (2.8 mg, 18.2 µmol, 1.5 eq.). The tube was sealed with a PTFE sealing tape and shaked for 4 h at 100 °C in an Eppendorf ThermoMixer®. After 4 h a carbonate solution (0.5 mL, 500 mM) was added and the reaction continued for another 20 h. After cooling to rt, it was centrifuged and a sample (20 µL) was removed and diluted with H_2O to 0.5 ml. This diluted sample was used for LC-MS analysis according to the general information.

(1R,2R,3R,4S)-tetrahydro-2H-pyran-2,3,4,5-tetrayl tetraacetate (30)

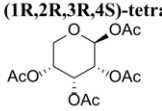

D-ribose (5.00 g, 33.3 mmol) was dissolved in pyridine (20 mL) and cooled to 0°C in an ice water bath. Acetic anhydride (20 ml, 212 mmol) was added and stirred at 0°C overnight. The mixture was poured into ice cold water (200 ml). The solid was filtered off and the crude product was crystallized from a mixture of MeOH and H_2O to obtain the pure product as colorless crystals (5.22 g, 16.4 mmol, 49%).

^{1}H NMR (400 MHz, $CDCl_3$) δ (ppm) = 6.02 (d, ^3J = 4.8 Hz, 1H, HC1), 5.47 (t, ^3J = 3.4 Hz, 1H, HC3), 5.19 – 5.11 (m, 1H, HC4), 5.05 – 5.00 (m, 1H, HC2), 4.01 (dd, ^2J = 12.4 Hz, ^3J = 3.4 Hz, 1H, H_aC5), 3.90 (dd, ^2J = 12.4 Hz, ^3J = 5.7 Hz, 1H, H_bC5), 2.12 (s, 3H, CH_3), 2.09 (s, 3H, CH_3), 2.09 (s, 3H, CH_3), 2.08 (s, 3H, CH_3). **^{13}C NMR** (101 MHz, $CDCl_3$) δ (ppm) = 170.0 (CO), 169.9 (CO), 169.6 (CO), 168.9 (CO), 91.0 (C1), 67.40 (C2), 66.3 (C3), 66.2 (C4), 62.8 (C5), 21.0 (CH_3), 20.9 (CH_3), 20.8 (CH_3), 20.8 (CH_3).

(1'R,2'R,3'R,4'S)-2-(2,4-Dioxo-3,4-dihydropyrimidin-1(2H)-yl)tetrahydro-2H-pyran-3,4,5-triyl triacetate (31)

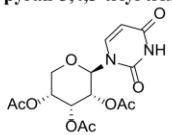

Uracil (269 mg, 2.40 mmol) was suspended in dry MeCN (14 ml) under inert atmosphere. The mixture was refluxed and bis(trimethylsilyl)acetamid (1.26 mL, 1.05 mg, 5.15 mmol) was added. After the mixture became clear, a solution containing tetraacetyl-β-D-ribose **30** (636 mg, 2.00 mmol, 0.8 eq.) and TMSOTf (0.54 mL ,667 mg, 3.00 mmol) in dry MeCN was added. The reaction was further refluxed for 8 h. After cooling to rt, the reaction was quenched with sat. $NaHCO_3$ (20 ml) and the aqueous phase

extracted with EtOAc (5 x 25 ml). The combined organic layers were dried over $MgSO_4$, filtered and the solvent removed *in vacuo*. The crude product was purified by flash column chromatography (DCM/MeOH 97:3) to obtain the pure compound as a yellowish solid (655 mg, 1.77 mmol, 89%).

mp: 164 °C. **^{1}H NMR** (400 MHz, DMSO-d_6) δ (ppm) = 11.47 (s, 1H, HN3), 7.90 (d, ^3J = 8.2 Hz, 1H, HC6), 5.85 (d, ^3J = 9.7 Hz, 1H, HC1'), 5.70 (dd, ^3J = 8.1 Hz, ^4J = 1.5 Hz, 1H, HC5), 5.66 – 5.63 (m, 1H, HC3'), 5.49 (dd, ^3J = 9.8, 3.1 Hz, 1H, HC2'), 5.23 – 5.15 (m, 1H, HC4'), 3.99 – 3.92 (m, 1H, H_aC5'), 3.85 (dd, ^2J = 11.0 Hz, ^3J = 5.5 Hz, 1H, H_bC5'), 2.19 (s, 3H, CH_3), 1.98 (s, 3H, CH_3), 1.92 (s, 3H, CH_3). **^{13}C NMR** (101 MHz, DMSO-d_6) δ (ppm) = 170.0 (CO), 169.3 (CO), 169.0 (CO), 162.8 (C4), 150.6 (C2), 140.7 (C6), 102.7 (C5), 77.7 (C1'), 67.7 (C3'), 66.5 (C2'), 65.5(C4'), 62.7 (C5'), 20.5 (CH_3), 20.5 (CH_3), 20.3 (CH_3). **HRMS** (ESI+): calc.: $[C_{15}H_{19}N_2O_9]^+$ 371.1090, found: 371.1085 $[M+H]^+$. **IR** (cm^{-1}): $\tilde{\nu}$ = 3066 (vw), 2822 (vw), 2360 (vw), 1747 (s), 1692 (s), 1453 (w), 1371 (s), 1305 (w), 1212 (vs), 1163 (m), 1121 (w), 1079 (s), 1041 (s), 986 (m), 952 (m), 882 (w), 813 (m), 771 (w), 718 (w).

β-D-Ribopyranosyl-uradine (12d)

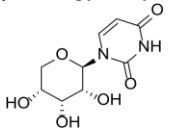

Nucleoside **31** (56 mg, 0.151 mmol) was dissolved in methanolic ammonia (4 ml, 1 M) and stirred for 19 h at rt. The solvent was removed *in vacuo* and the crude product was purified by flash column chromatography (DCM/MeOH 4:1) to obtain the pure product as a colorless solid (28.0 mg, 0.115 mmol, 76%). For LC-MS measurements, a fraction of the product was further purified by reversed phase HPLC.

mp: 220 °C (decomp.). **^{1}H NMR** (599 MHz, DMSO-d_6) δ (ppm) = 11.25 (s, 1H, HN3), 7.66 (d, ^3J = 8.1 Hz, 1H, HC6), 5.60 (d, ^3J = 8.1 Hz, 1H, HC5), 5.58 (d, ^3J = 9.4 Hz, 1H, HC1'), 5.11 (br, 1H, OH), 5.09 (br, 1H, OH), 4.84 (br, 1H, OH), 3.97 (d, ^3J = 3.2 Hz, 1H, HC3'), 3.68 (d, J = 9.5 Hz, 1H, HC2'), 3.63 (ddd, ^3J = 7.4, 6.0, 2.3 Hz, 1H, HC4'), 3.58 – 3.53 (m, 2H, H_aC5', H_bC5'). **^{13}C NMR** (101 MHz, DMSO-d_6) δ (ppm) = 163.0 (C4), 151.1 (C2), 141.4 (C6), 101.67 (C5), 79.6 (C1'), 71.2 (C3'), 67.6 (C2'), 66.4 (C4'), 65.2 (C5'). **HRMS** (ESI+): calc.: $[C_9H_{13}N_2O_6]^+$ 245.0768, found: 245.0768 $[M+H]^+$. **IR** (cm^{-1}): $\tilde{\nu}$ = 3347 (w), 2357 (vw), 2336 (vw), 1675 (vs), 1363 (w), 1391 (w), 1272 (m), 1250 (m), 1197 (m), 1084 (vs), 1042 (vs), 975 (m), 918 (w), 859 (w), 813 (m), 779 (w), 689 (m), 667 (m).

(1'R,2'S,3'S,4'R)-6-(2,4-Dioxo-3,4-dihydropyrimidin-1(2H)-yl)-2,2-dimethyltetrahydro-4H-[1,3]dioxolo[4,5-c]pyran-7-yl acetate (32)

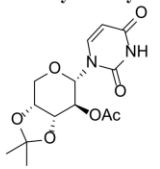

Uracil (224 mg, 2.00 mmol, 1.00 eq.) was suspended in dry MeCN (16 ml) under inert atmosphere. Bis(trimethylsilyl)acetamid (1.26 ml, 1.05 g, 5.00 mmol, 2.50 eq.) was added and stirred at 40 °C until the mixture became clear. TMSOTf (0.50 ml, 0.62 mg, 2.80 mmol, 1.40 eq.) was added. 1,2-O-acetate-3,4-O-isopropylidene-D-arabinose (*6*) (716 mg, 2.60 mmol, 1.30 eq.) was separately dissolved in dry MeCN (5 ml) and slowly added to the reaction mixture within 30 min. After stirring 2 h at 40 °C, the reaction was quenched with sat. $NaHCO_3$ (20 ml) and extracted with DCM (3 x 25 ml). The combined organic layers were washed with sat. NaCl (30 ml), dried over Na_2SO_4, filtered and the solvent removed *in vacuo*. The product was purified by flash column chromatography (iHex/acetone, 7:3 → 1:1) to yield the product as a colorless solid (565 mg, 1.73 mmol, 87%).

mp: 225 °C; **^{1}H NMR** (400 MHz, $CDCl_3$) δ (ppm) = 8.54 (s, 1H, HN3), 7.43 (d, ^3J = 8.2 Hz, 1H, HC6), 5.78 (dd, ^3J = 8.2 Hz, ^4J 2.3 Hz, 1H, HC5), 5.56 (d, ^3J = 9.4 Hz, 1H, HC1'), 5.10 (dd, ^3J = 9.4, 7.0 Hz, 1H, HC3'), 4.40 (d, ^2J = 13.9 Hz, 1H, H_aC5'), 4.34 (dd, J = 7.1, 5.4 Hz, 1H,HC2'), 4.31 – 4.26 (m, 1H, HC4'), 3.98 (dd, ^2J = 13.9, 2.4 Hz, 1H, H_b5'), 2.06 (s, 3H, CH_3), 1.59 (s, 3H, CH_3), 1.39 (s, 3H, CH_3). **^{13}C NMR** (101 MHz, $CDCl_3$) δ (ppm) = 170.0 (CO), 162.5 (C4), 150.4 (C2), 139.9 (C6), 110.8 (C_q), 103.3 (C5), 80.4 (C1'), 76.5 (C2'), 73.3 (C4'), 71.1 (C3'), 66.3 (C5'), 27.9 (CH_3), 26.2 (CH_3), 20.8 (CH_3). **HRMS** (ESI+): calc.: $[C_{14}H_{19}N_2O_7]^+$ 327.1187, found: 327.1188 $[M+H]^+$. **IR** (cm^{-1}): $\tilde{\nu}$ = 2985 (vw), 2882 (vw), 2359 (vw), 2053 (vw), 1741 (m), 1711 (s), 1675 (vs), 1470 (w), 1426 (w), 1375 (m), 1296 (m), 1249 (m), 1218 (vs), 1170 (w), 1130 (s), 1051 (vs), 967 (w), 889 (w), 847 (m), 797 (m), 761 (w), 686 (w).

1-((1'R,2'S,3'S,4'R)-7-Hydroxy-2,2-dimethyltetrahydro-4H-[1,3]dioxolo[4,5-c]pyran-6-yl)pyrimidine-2,4(1H,3H)-dion (33)

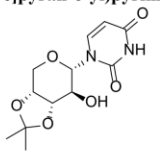

Nucleoside **32** (355 mg, 1.09 mmol) was dissolved in methanolic ammonia (14 ml, 1 M) and kept at rt for 20 h. The solvent was removed *in vacuo* and the crude product was purified by flash column chromatography (DCM/MeOH, 92:8) to obtain the product as colorless solid (284 mg, 1.00 mmol, 92%).

mp: 220 °C (decomp.). **^{1}H NMR** (400 MHz, DMSO-d_6) δ (ppm) = 11.36 (s, 1H, HN3), 7.65 (d, ^3J = 8.1 Hz, 1H, HC6), 5.64-5.59 (m, 2H, HC5, HO), 5.26 (d, ^3J = 9.7 Hz, 1H, HC1'), 4.23 – 4.18 (m, 1H, HC4'), 4.15 (d, ^2J = 13.5 Hz, 1H, H_aC5'), 4.11 (dd, ^3J = 7.0, 5.5 Hz, 1H, HC3'), 3.92 (dd, ^2J = 13.5 Hz, ^3J = 2.6 Hz, 1H, H_bC5'), 3.71 – 3.63 (m, 1H, HC2'), 1.49 (s, 4H, CH_3), 1.29 (s, 4H, CH_3). **^{13}C NMR** (101 MHz, DMSO-d_6) δ (ppm) = 163.0 (C4), 151.0 (C2), 141.3 (C6), 108.7 (C_q), 102.0 (C5), 81.9 (C1'), 79.1 (C3'), 73.3 (C4'), 69.7 (C2'), 65.3 (C5'), 28.0 (CH_3), 26.2 (CH_3). **HRMS** (ESI+): calc.: $[C_{12}H_{17}N_2O_6]^+$ 285.1081, found: 285.1082 $[M+H]^+$. **IR** (cm^{-1}): $\tilde{\nu}$ = 3378 (w), 2989 (w), 2888 (vw), 2827 (vw), 2360 (vw), 1678 (vs), 1623 (m), 1469 (w), 1416 (w), 1392 (m), 1372 (m), 1336 (w), 1288 (m), 1275 (w), 1249 (s), 1216 (s), 1202 (s), 1167 (w), 1138 (s), 1108 (m), 1086 (vs), 1046 (s), 1022 (m), 975 (m), 958 (m, 936 (w), 874 (s), 846 (s), 826 (m), 796 (m), 780 (w), 761 (s), 732 (m), 684 (m).

1-((1'R,2'R,3'S,4'R)-7-Hydroxy-2,2-dimethyltetrahydro-4H-[1,3]dioxolo[4,5-c]pyran-6-yl)pyrimidine-2,4(1H,3H)-dion (34)

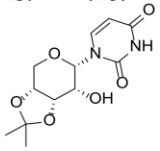

Nucleoside **33** (150 mg, 0.53 mmol) was dissolved in DCM (8 ml) together with Dess-Martin Periodinan (336 mg, 0.79 mmol) and $NaHCO_3$ (89 mg, 1.06 mmol). The reaction mixture was reacted for 2 h at 45 °C and quenched with solid $Na_2S_2O_3$ (0.55 g) together with sat. $NaHCO_3$ (5 ml). It was rigorously stirred until the organic phase became clear. The organic layer was separated and the aqueous layer was extracted with DCM (5 x 15 ml) and EtOAc (5 x 20 ml). The combined organic layers were dried over $MgSO_4$, filtered and the solvent removed *in vacuo*. The crude product was dissolved in a mixture of DCM/EtOAc/MeOH (2:1:1, 10 mL) and $NaBH_4$ (35 mg, 0.93 mmol) was added. The mixture was stirred for 1 h at 0 °C. The solvent was removed *in vacuo*. The residue was dissolved in EtOAc (20 ml) and washed with sat. NaCl (30 ml). The aqueous phase was extracted with EtOAc (8 x 25 ml). The combined organic layers were dried over $MgSO_4$, filtered and the solvent removed *in vacuo*. The crude product was purified by flash column chromatography (DCM/MeOH, 96:4) to obtain the product as a colorless solid (60 mg, 0.21 mmol, 40%).

mp: 205 °C (decomp.). **^{1}H NMR** (400 MHz, DMSO-d_6) δ (ppm) = 11.32 (s, 1H, HN3), 7.79 (d, ^3J = 8.1 Hz, 1H, HC6), 5.64 (d, ^3J = 3.0 Hz, 1H, HC1'), 5.56 (d, ^3J = 8.1 Hz, 1H, HC5), 5.40 (d, ^3J = 5.9 Hz, 1H, OH), 4.34 (dd, ^3J = 6.7, 4.5 Hz, 1H, HC3'), 4.24 – 4.19 (m, 1H, HC4'), 4.06 (dd, ^2J = 12.6 Hz, ^3J = 3.1 Hz, 1H, H_aC5'), 3.95 (dd, ^2J = 12.7 Hz, ^3J = 3.9 Hz, 1H, H_bC5'), 3.91 – 3.87 (m, 1H, HC2'), 1.46 (s, 3H, CH_3), 1.30 (s, 3H, CH_3). **^{13}C NMR** (101 MHz, DMSO-d_6) δ (ppm) = 163.2 (C4), 150.3 (C2), 143.2 (C6), 109.1 (C_q), 100.0 (C5), 80.2 (C1'), 72.8 (C3'), 70.8 (C4'), 65.4 (C5'), 64.60 (C2'), 26.0 (CH_3), 25.5. (CH_3). **HRMS** (ESI+): calc.: $[C_{12}H_{17}N_2O_6]^+$ 285.1081, found: 285.1081 $[M+H]^+$. **IR** (cm^{-1}): $\tilde{\nu}$ = 2989 (vw), 2890 (vw), 2359 (vw), 2215 (vw), 1708 (s), 1674

(vs), 1454 (w), 1425 (w), 1381 (m), 1211 (s), 1155 (m), 1126 (s), 1084 (s), 1064 (vs), 1042 (vs), 991 (w), 882 (w), 846 (m), 814 (m), 763 (m), 737 (m), 678 (w).

α-D-Ribopyranosyl-Uracil (α-p-U, 12c)

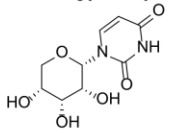

Nucleoside **34** was dissolved in 70% acetic acid (5 ml) and stirred for 5 h at 60 °C. The solvent was removed *in vacuo* and remaining AcOH was co-evaporated with EtOH (2 x 30 ml) and MeCN (3 x 30 ml). The crude product was purified by flash column chromatography (DCM/MeOH 88:12) to obtain the product as white solid (32.0 mg, 0.151 mmol, 83%). For LC-MS measurements, a fraction of the product was further purified by reversed phase HPLC.

mp: 243 °C (decomp.) **^{1}H NMR** (599 MHz, DMSO-d_6) δ (ppm) = 11.34 (s, 1H, HN3), 7.70 (d, ^3J = 8.2 Hz, 1H, HC6), 5.57 (d, ^3J = 8.1 Hz, 1H, HC5), 5.47 (d, ^3J = 1.2 Hz, 1H, HC1'), 5.27 (br, 1H, C2'OH), 5.17 – 5.12 (br, 1H, C3'OH), 5.10 (br, 1H, C4'OH), 3.96 (dd, ^2J = 12.4 Hz, ^3J = 1.6 Hz, 1H, H_aC5'), 3.75 (d, ^2J = 12.2 Hz, 1H, H_bC5'), 3.72 (d, ^3J = 7.4 Hz, 1H, HC2'), 3.70 – 3.66 (m, 2H, HC3', HC4'). **^{13}C NMR** (101 MHz, DMSO-d_6) δ (ppm) = 163.1 (C4), 150.0 (C2), 142.5 (C6), 100.1 (C5), 81.6 (C1'), 70.9 (C2'), 70.3 (C5'), 68.6 (C4'), 67.2 (C3'). **HRMS** (ESI+): calc.: $[C_9H_{13}N_2O_6]^+$ 245.0768, found: 245.0768 $[M+H]^+$. **IR** (cm^{-1}): $\tilde{\nu}$ =3359 (w), 3295 (w), 2934 (vw), 1769 (vw), 1716 (w), 1692 (m), 1665 (s), 1461 (m), 1432 (w), 1398 (w), 1385 (w), 1373 (w), 1322 (vw), 1295 (m), 1251 (m), 1195 (w), 1159 (w), 1110 (m), 1084 (vs), 996 (w), 968 (w), 911 (w), 889 (w), 834 (w), 818 (s), 769 (vs), 714 (s), 670 (s).

Synthesis pathway for α-furanosyl-uridine

(1'S,2'R,3'S,4'R)-2-amino-5-(hydroxymethyl)-3a,5,6,6a-tetrahydrofuro[2,3-d]oxazol-6-ol (35)

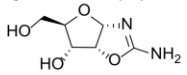

D-Ribose (14.4 g, 96 mmol) and cyanamide (8.06 g, 192 mmol) were dissolved in aqueous ammonia (16 ml, 1M) in a pressure tube. The mixture was heated at 30 °C until the solution became clear. The reaction was further stirred at rt until a precipitate started to form. The reaction was heated for 30 min at 60 °C and the solvent removed *in vacuo*. The residue was taken up in hot MeOH (32 ml) and filtrated immediately. The warm filtrate was kept at -20 °C overnight. The yellowish solid was filtered off and washed with MeOH and Et_2O to obtain the pure product as a colorless solid (12.6 g, 72.3 mmol, 75%) (*45*).

The analytical data is in agreement with reported literature (*46*).

^{1}H NMR (400 MHz, DMSO-d_6) δ(ppm) = 6.14 (d, ^3J = 1.8 Hz, 2H), 5.57 – 5.12 (m, 1H), 4.29 (dd, ^3J = 18.4, 1.9 Hz, 2H), 2.00 – 1.78 (m, 2H), 1.74 – 1.66 (m, 1H), 1.51 – 1.29 (m, 2H). **^{13}C NMR** (101 MHz, DMSO-d_6) δ(ppm) = 164.0, 98.1, 80.9, 77.8, 71.1, 60.4.

(1'S,2'R,3'S,4'R)-3-Hydroxy-2-(hydroxymethyl)-2,3,3a,9a-tetrahydro-6H-furo[2',3':4,5]oxazolo[3,2-a]pyrimidin-6-on (36)

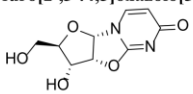

Compound **35** (10.0 g, 75.4 mmol) and methyl propiolate (9.60 g, 9.65 mL, 114 mmol) were dissolved in H_2O (130 mL) and stirred at 100 °C for 30 min. The solvent was removed *in vacuo* and the residue taken up in hot MeOH (65 ml). The solution was filtered hot and the filtrate kept at -20 °C for 48 h. The formed yellow crystals were filtered off to obtain the pure product (6.21 g, 27.5 mmol, 48%).(*47*) The analytical data is in agreement with reported literature (*47*).

^{1}H NMR (400 MHz, DMSO-d_6) δ(ppm) = 7.85 (d, ^3J = 7.4 Hz, 1H), 6.20 (d, ^3J = 5.3 Hz, 1H), 5.88 (d, ^3J = 7.4 Hz, 1H), 5.77 (d, ^3J = 6.8 Hz, 1H), 5.23 (t, ^3J = 5.4 Hz, 1H), 4.91 – 4.86 (m, 1H), 4.05 (ddd, ^3J = 9.1, 6.8, 5.4 Hz, 1H), 3.69 (ddd, ^2J = 12.3 Hz, ^3J = 4.9, 2.0 Hz, 1H), 3.56 (ddd, ^3J = 9.2, 5.0, 1.9 Hz, 1H), 3.50 – 3.42 (m, 1H). **^{13}C NMR** (101 MHz, DMSO-d_6) δ(ppm) = 171.2, 160.8, 137.0, 108.9, 88.7, 81.5, 80.8, 69.7, 59.5.

α-furanosyl-uradine (12a)

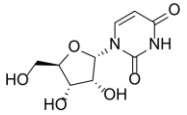

Compound **36** (1.0 g, 4.40 mmol) dissolved in aqueous HCl (2.2 ml, 0.2 M) was refluxed for 2 h. The solvent was removed *in vacuo* and the residue was taken up in H_2O. The solution was neutralized until pH ~6 with Dowex 1X8. It was filtered and the resin was washed with H_2O. The filtrate was freeze dried to obtain the product as a colorless powder (1.02 g, 4.18 mmol, 95%). For LC-MS analysis, a small fraction of the product was further purified by reversed phase HPLC.

mp: 202 °C (decomp.). **^{1}H NMR** (400 MHz, DMSO-d_6) δ(ppm) = 11.18 (s, 1H, HN3) 7.61 (d, ^3J = 8.1 Hz, 1H, HC6), 6.01 (d, ^3J = 4.6 Hz, 1H, HC1'), 5.56 (d, ^3J = 8.1 Hz, 1H, HC5), 5.49 (br, 1H, OH), 5.12 (br, 1H, OH), 4.80 (d, ^3J = 9.0 Hz, 1H, OH), 4.16 (t, ^3J = 4.5 Hz, 1H, HC2'), 4.06 – 3.98 (m, 2H, HC3', HC4'), 3.58 (dd, ^2J = 12.0 Hz, ^3J = 2.7 Hz, 1H, H_aC5), 3.42 (dd, ^2J = 12.2 Hz, ^3J = 4.1 Hz, 1H, H_bC5). **^{13}C NMR** (101 MHz, DMSO-d_6) δ(ppm) = 163.3 (C4), 150.6 (C2), 142.8 (C6), 99.8 (C5), 85.1 (C1'), 84.0 (C4'), 70.4 (C3'), 70.3 (C2'), 61.2 (C7). **HRMS** (ESI+): calc.: $[C_9H_{13}N_2O_6]^+$ 245.0768, found: 245.0768 $[M+H]^+$. **IR** (cm^{-1}): $\tilde{\nu}$ = 3301 (w), 3058 (w), 2930 (w), 2805 (vw), 2342 (vw), 1659 (vs), 1463 (m), 1394 (m), 1269 (s), 1197 (m), 1096 (s), 1037 (vs), 1021 (vs), 990 (s), 927 (m), 857 (m), 806 (s), 763 (s), 718 (m).

Synthesis of α-furanosyl-cytidine(1'S,2'R,3'S,4'R)-2-(acetoxymethyl)-5-(2,4-dioxo-3,4-dihydropyrimidin-1(2H)-yl)tetrahydrofuran-3,4-diyl diacetate (37)

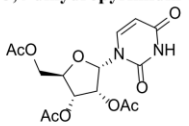

Compound **12a** (500 mg, 2.05 mmol) was dissolved in pyridine (5 ml) and acetic anhydride (5 ml) at 0 °C. The mixture was reacted for 18 h and the solvent removed *in vacuo*. It was co-evaporated with MeCN (20 ml). The residue was purified by flash column chromatography (DCM/MeOH 97:3) to afford the product as a colorless solid (611 mg, 1.65 mmol, 80%).

mp: 70 °C. **^{1}H NMR** (400 MHz, DMSO-d_6) δ(ppm) = 11.38 (s, 1H, HN3), 7.65 (d, ^3J = 8.2 Hz, 1H, HC6), 6.34 (d, ^3J = 4.7 Hz, 1H, HC1'), 5.64 (d, ^3J = 8.2 Hz, HC5), 5.54 (t, ^3J = 4.7 Hz, 1H, HC2'), 5.35 (dd, ^3J = 6.2, 5.1 Hz, 1H, HC3'), 4.66 – 4.60 (m, 1H, HC4'), 4.26 (dd, ^2J = 12.2 Hz, ^3J = 3.4 Hz, 1H, H_aC5'), 4.16 (dd, ^2J = 12.2 Hz, ^3J = 5.7 Hz, 1H, H_bC5'), 2.06 (s, 3H, CH_3), 2.03 (s, 3H, CH_3), 1.97 (s, 3H, CH_3). **^{13}C NMR** (101 MHz, DMSO-d_6) δ(ppm) = 170.1 (CO), 169.4 (CO), 168.8 (CO), 163.1 (C4), 150.2 (C2), 141.0 (C6), 100.9 (C5), 83.5 (C1'), 78.8 (C4'), 70.6 (C3') 69.8 (C2'), 63.1 (C5'), 20.6 (CH_3), 20.4 (CH_3), 20.1 (CH_3). **HRMS** (ESI+): calc.: $[C_{15}H_{18}N_2NaO_9]^+$ 393.0905, found: 393.0904 $[M+Na]^+$. **IR** (cm^{-1}): $\tilde{\nu}$ = 3059 (vw), 2159 (vw), 1743 (s), (1682 (vs), 1455 (w), 1371 (m), 1211 (vs), 1109 (s), 1075 (m), 1030 (s), 944 (w), 902 (w), 813 (m), 766 (w), 714 (w), 674 (vw).

α-furanosyl-cytidine (11a)

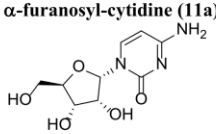

Compound **37** (100 mg, 0.27 mmol) was dissolved in dry DCM. It was added Et_3N (105 µL, 78.1 mg, 0.77 mmol), DMAP (6.00 mg, 0.05 mmol) and 2,4,6-TIPBS (164 mg, 0.54 mmol) and stirred for 20 h at rt. The reaction was quenched with sat. aqueous ammonia (6 ml) and further stirred for 3 h at rt. The solvent was removed *in vacuo* and residual water co-evaporated with MeCN (2 x 25 ml). The residue was purified by flash column chromatography (DCM/MeOH 88:12) and reversed phase HPLC to afford the product as a colorless solid (15 mg, 0.06 mmol, 23%)

mp: 190 °C. **^{1}H NMR** (400 MHz, DMSO-d_6) δ(ppm) = 7.52 (d, ^3J = 7.4 Hz, 1H, HC6), 7.05 (br, 1H, H_aN), 6.96 (br, 1H, H_bN), 6.01 (d, ^3J = 3.7 Hz, 1H, HC1'), 5.66 (d, ^3J = 7.4 Hz, 1H, HC5), 5.27 (s, 1H, OH), 4.97 (s, 1H, OH), 4.77 (s, 1H, OH), 4.07 – 4.01 (m, 2H, HC2', HC3'), 3.98 – 3.92 (m, 1H, HC4'), 3.61 (dd, ^2J = 12.1 Hz, ^3J = 2.6 Hz, 1H, HaC5'), 3.42 (dd, ^2J = 12.2 Hz, ^3J = 4.6 Hz, 1H, HbC5').**^{13}C NMR** (101 MHz, DMSO-d_6) δ(ppm) = 165.6 (C4), 155.2 (C2), 143.1 (C6), 92.3 (C5), 85.6 (C1'), 83.1 (C4'), 70.6 (C2'), 70.1 (C3'), 61.1 (C5'). **HRMS** (ESI+): calc.: $[C_9H_{14}N_3O_5]^+$ 244.0928,

found: 244.0927 $[M+H]^+$. **IR** (cm^{-1}): $\tilde{\nu}$ = 3267 (w), 2360 (vs), 2222 (s), 1842 (m), 1589 (m), 1311 (w), 1210 (w), 1033 (m), 793 (m), 668 (vs).

Synthesis of α-pyranosyl-cytidine 4-amino-1-((1'R,2'S,3'S,4'R)-7-hydroxy-2,2-dimethyltetrahydro-4H-[1,3]dioxolo[4,5-c]pyran-6-yl)pyrimidin-2(1H)-on (38)

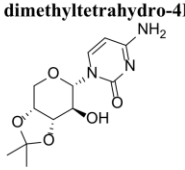

Compound **32** (143 mg, 0.44 mmol) was dissolved in dry DCM (9 ml). It was added triethylamine (118 mg, 162 ml, 1.60 mmol), DMAP (8 mg, 0.07 mmol, 0.15 eq.) and 2,4,6-TIPBS (265 mg, 0.88 mmol). The mixture was reacted for 72 h at rt and quenched with sat. ammonia in H_2O (3 ml). The reaction was further stirred for 5 h at rt. The solvent was removed *in vacuo* und residual H_2O was co-evaporated with MeCN (2 x 25 ml). The crude mixture was purified by flash column chromatography (DCM/MeOH 12:1 → 4:1, containing 0.1% Et_3N) to obtain the product as a white solid (67 mg, 0.21 mmol, 48%).

mp: 210 °C (decomp.). **^{1}H NMR** (400 MHz, DMSO-d_6) δ(ppm) = 7.54 (d, ^3J = 7.5 Hz, 1H, HC6), 7.23 (br, 1H, H_aN), 7.11 (br, 1H, H_bN), 5.71 (d, ^2J = 7.4 Hz, 1H, HC5), 5.41 (d, ^3J = 6.4 Hz, 1H, OH), 5.36 (d, ^3J = 9.8 Hz, 1H, HC1'), 4.22 – 4.18 (m, 1H, HC4'), 4.14 – 4.07 (m, 2H, H_aC5', HC3'), 3.85 (dd, ^2J = 13.6 Hz, ^3J = 2.5 Hz, 1H, H_bC5'), 3.67 – 3.57 (m, 1H, HC3'), 1.48 (s, 3H, CH_3), 1.29 (s, 3H, CH_3). **^{13}C NMR** (101 MHz, DMSO-d_6) δ(ppm) = 165.4 (C4), 155.5 (C2), 141.7 (C6), 108.5 (C_q), 94.2 (C5), 82.3 (C1'), 79.4 (C3'), 73.3 (C4'), 69.9 (C2'), 65.2 (C5'), 28.0 (CH_3), 26.2 (CH_3). **HRMS** (ESI+): calc.: $[C_{12}H_{18}N_3O_5]^+$ 284.1240, found: 284.1241 $[M+H]^+$. **IR** (cm^{-1}): $\tilde{\nu}$ = 3326 (w), 2932 (w), 2819 (vw), 2360 (vw), 1660 (vs), 1525 (vw), 1465 (m), 1395 (m), 1270 (s), 1203 (m), 1096 (s), 1039 (vs), 1022 (s), 928 (w), 869 (m), 808 (s), 763 (m), 719 (m).

α-pyranosyl-cytidine (11c)

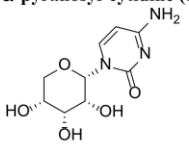

Compound **38** (35 mg, 0.12 mmol) was dissolved in MeCN (5.5 ml). Dess-Martin-Periodinan (104 mg, 0.25 mmol) was added and the reaction mixture was stirred for 3.5 h at rt. The reaction was quenched with $Na_2S_2O_3$ (500 mg) und $NaHCO_3$ (100 mg) and further stirred for 10 min. The mixture was filtered and the solvent removed *in vacuo*. The crude keto product was dissolved in DCM (3 mL), EtOAc (1.5 mL) und MeOH (1.5 mL). $NaBH_4$ (20 mg, 0.529 mmol) was added and stirred for 2.5 h at rt. The solvent

was removed *in vacuo*. The crude product was dissolved in 70% acetic acid (5 ml) and stirred for 5 h at 60 °C. The solvent was removed *in vacuo* and co-evaporated with EtOH (2 x 30 ml) and MeCN (3 x 30 ml). The crude mixture was purified by reversed phase HPLC to obtain the product as colorless solid (7.0 mg, 0.029 mmol, 24 %).

mp: 194 °C (decomp.). **^{1}H NMR** (400 MHz, DMSO-d_6) δ(ppm) = 7.61 (d, ^3J = 7.4 Hz, 1H, HC6), 7.18 (br, 1H, H_aN), 7.02 (br, 1H, H_bN), 5.67 (d, ^3J = 7.4 Hz, 1H, HC5), 5.47 (s, 1H, HC1‘), 5.13 (d, ^3J = 6.0 Hz, 1H, OH), 5.10 (d, ^3J = 5.8 Hz, 1H, OH), 5.07 (d, ^3J = 7.7 Hz, 1H, OH), 3.95 (dd, ^2J = 12.2 Hz, ^3J = 1.8 Hz, 1H, H_aC5‘), 3.75 – 3.63 (m, 4H, HC2, HC3, HC4, H_bC5‘).**^{13}C NMR** (101 MHz, DMSO-d_6) δ(ppm) = 165.5 (C4), 154.4 (C2), 143.1 (C6), 92.5 (C5), 82.3 (C1‘), 70.6 (C2‘), 70.3 (C5‘), 68.7 (C4‘), 67.4 (C3‘). **HRMS** (ESI+): calc.: $[C_9H_{14}N_3O_5]^+$ 244.0928, found: 244.0927 $[M+H]^+$. **IR** (cm^{-1}): $\tilde{\nu}$ = 3217 (w), 2360 (vw), 1891 (vw), 1645 (s), 1598 (m), 1525 (w), 1481 (m), 1405 (m), 1299 (m), 1203 (m), 1158 (m), 1084 (vs), 1015 (s), 987 (s), 902 (m), 833 (m), 780 (vs), 752 (s), 668 (vs).

Synthesis of β-pyranosyl-cytidine (11d)

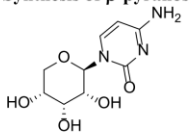

Nucleoside **31** (50.0 mg, 0.135 mmol) was dissolved in dry DCM. It was added NEt_3 (27.3 mg, 37.4 µL, 0.270 mmol), DMAP (1.7 mg, 0.014 mmol, 0.1 eq.) and 2,4,6-TIPBS (61.5 mg, 0.203 mmol) and stirred for 17 h at rt. The reaction was quenched with sat. ammonia in H_2O. The solvent was removed *in vacuo* and residual water was co-evaporated with MeCN (4 x 20 ml). The crude product was purified by reversed phase HPLC to obtain the pure product as a colorless solid (15 mg, 0.062 mmol, 46%).

mp: 180 °C. **^{1}H NMR** (599 MHz, DMSO-d_6) δ(ppm) = 7.54 (d, ^3J = 7.4 Hz, 1H, HC6), 7.16 (br, 1H, H_aN), 7.05 (br, 1H, H_bN), 5.70 (d, ^3J = 9.6 Hz, 1H, HC1’), 5.68 (d, J = 7.5 Hz, 1H, HC5), 5.01 (d, ^3J = 3.5 Hz, 1H, OH), 4.83 (d, ^3J = 7.2 Hz, 1H, OH), 4.78 (br, 1H, OH), 3.96 (s, 1H, HC3’), 3.64 – 3.57 (m, 2H, HC4’, HC2’), 3.54 (d, ^2J = 10.2 Hz, 1H, H_aC5’), 3.50 (dd, ^2J = 10.3 Hz, ^3J = 5.0 Hz, 1H, H_bC5’). **^{13}C NMR** (101 MHz, DMSO-d_6) δ(ppm) = 165.3 (C4), 155.7 (C2), 141.8 (C6), 93.9 (C5), 79.8 (C1’), 71.2 (C3’), 68.0 (C2’), 66.7 (C4’), 65.2 (C5’). **HRMS** (ESI+): calc.: $[C_9H_{14}N_3O_5]^+$ 244.0928, found: 244.0927 $[M+H]^+$. **IR** (cm^{-1}): $\tilde{\nu}$ = 3426 (w), 3210 (m), 2922 (w), 1640 (vs), 1596 (vs), 1526 (m), 1489 (vs), 1400 (m), 1387 (m), 1368 (m), 1322 (w), 1300 (m), 1281 (m), 1269 (m), 1242 (m), 1224 (m), 1204 (s), 1132 (s), 1115 (m), 1094 (s), 1076 (s), 1039 (vs), 1018 (s), 991 (s), 970 (m), 800 (m), 781 (s), 660 (vs).

Synthesis of lüneburgite: $Mg_3(H_2O)_6[B_2(OH)_6(PO_4)_2]$

The synthesis was performed according to literature (*48*). Magnesium oxide (1 g, 25 mmol), dimagnesiumphosphate trihydrate (8.1 g, 46.5 mmol) and boric acid (9.2 g, 149 mmol) were refluxed in H_2O (200 ml) for 4 days. After cooling to rt, the colorless solid was filtered off to afford the product (9.5 g, 19.2 mmol, 83%). The mineral was analysed by XRD measurement to confirm the correct product (see Fig. S10).

Synthesis of struvite: $MgNH_4PO_4$ x $6H_2O$

The synthesis was performed according to literature (*49*). A solution of $(NH_4)_2PO_4$ (50 mL, 1 M, 50 mmol) was added to a solution of $MgCl_2$ (50 mL, 1M, 50 mmol). The mixture was stirred for 15 min at room temperature. The solid was filtered off and washed with water to afford the product as a white solid (8.1 g). The mineral was analysed by XRD measurement to confirm the correct product (see Fig. S11).

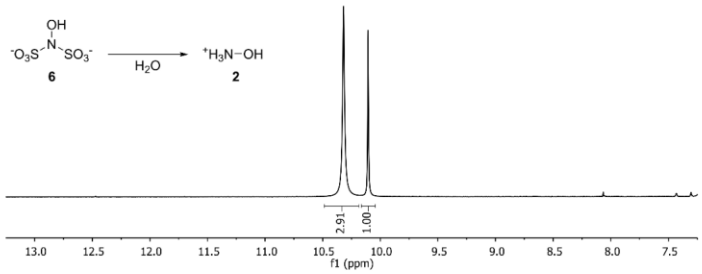

Fig. S1.

Hydrolysis of hydroxylamine disulfonate (**6**) affords hydroxylamine (**2**) as reveald by ^{1}H-NMR. Detailed information can be found in the aforementioned synthetic procedure.

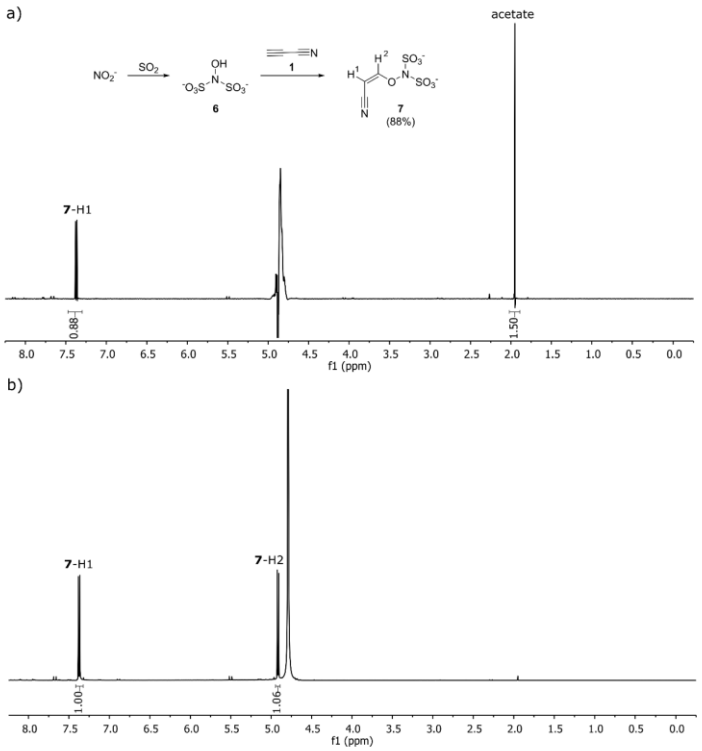

Fig. S2.

^{1}H NMR analysis for the formation of *cis*-**7**. a) Treatment of an aqueous nitrite solution with SO_2 afforded **6**, which further reacted with **1** to give adduct **7**. Detailed information can be found in the aforementioned procedure. ^{1}H-NMR spectroscopy in H_2O/D_2O (9:1) reveals formation *cis*-**7** (88%). Quantification was achieved using sodium acetate (0.5 eq) as reference standard. b) Since water suppression interferes with the H-2 signal of the cis-**7** isomer, we isolated and spectroscopically characterized the compound in D_2O.

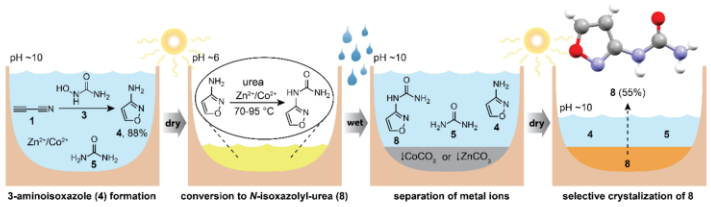

Fig. S3.

Plausible prebiotic scenario for the one-pot formation and enrichment of isoxazolylurea **8**.

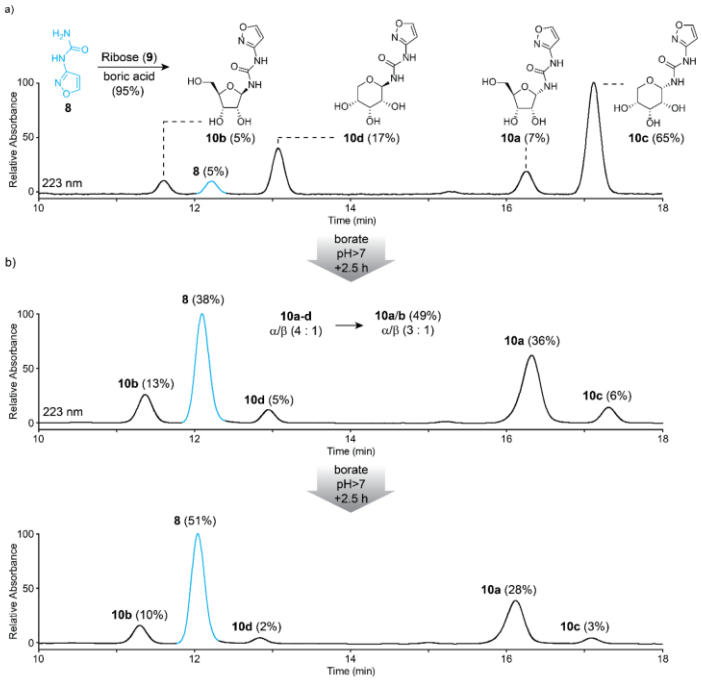

Fig. S4.

LC-MS analysis for the formation of **10a-d**. The UV-chromatograms at 223 nm are shown. a) Boric acid catalysed ribosylation of **8** affords the four expected α and β-anomers of isoxazolyl-urea as furanoside **10 a,b** or pyranoside **10c,d**. b) The mixture obtained in a) was heated in 125 mM borax at 95 °C for 2.5 h. Isomerization is also possible at lower temperature but with longer reaction time. The pyranoside products (**10c** and **d**) are converted into the furanoside products (**10a** and **b**). Further reaction gives **10a** and **b** as the only ribosides with only trace amounts of the pyranosides **10c** and **d** after 5 h.

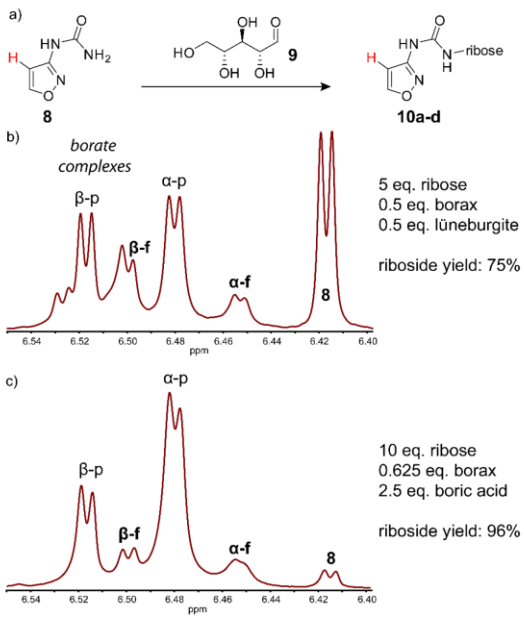

Fig. S5.

^{1}H-NMR in D_2O after **8** was reacted with ribose under different conditions. The ribosylated product **10a-d** is obtained as a mixture of α- and β-anomers as either furanoside (f) or pyranoside (p). The ^{1}H-NMR signals observed correspond to the proton labelled in red. The yields are relative to the starting material **8**. a) reaction scheme. b) the slightly basic conditions are expected to give borate complexes that are overlapping with the free nucleosides. c) more acidic conditions lead to higher degree of glycosylation and no borate complexes.

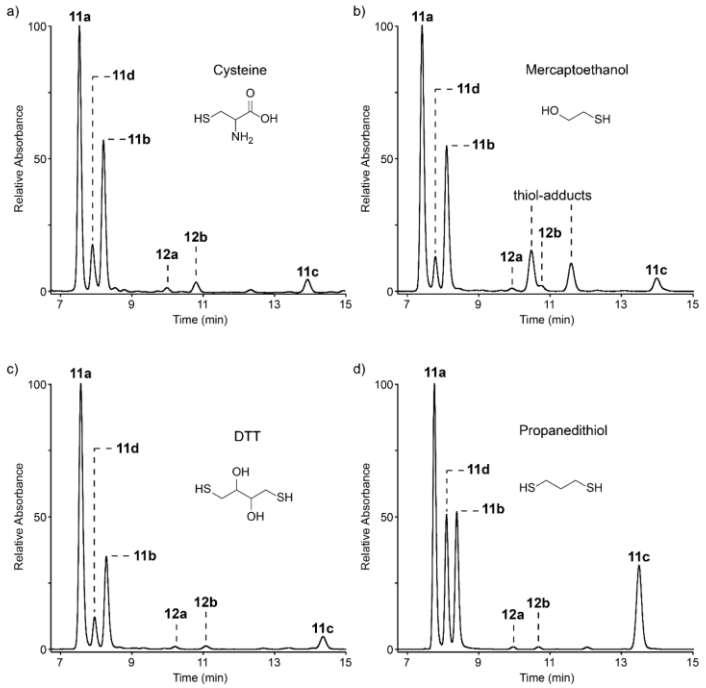

e)

thiol	11a	11b	11c	11d	12a	12b
cysteine	37.2%	22.9%	3.2%	6.1%	0.5%	1.4%
mercaptoethanol	30.8%	18.2%	1.7%	2.6%	0.3%	0.4%
DTT	54.7%	19.8%	2.8%	5.4%	0.7%	1.0%
propanedithiol	26.0%	12.2%	11.0%	10.9%	0.2%	0.1%

Fig. S6.

Cytidine **11a-d** and uridine **12a/b** formation in the presence of different thiols. All reductions were performed with 0.001 eq. of soluble Fe^{2+} in 100 mM sodium carbonate, 50 mM borate buffer (pH 9.7). Reduction in the presence of different thiols: a) cysteine, b) mercaptoethanol, c) dithiothreitol (DTT) and d) propanedithiol. e) table with calculated yields for **11a-d** and **12a/b**. For mercaptoethanol the overall yield is significantly lower, probably due to formation of thiol-adducts as labeled in b).

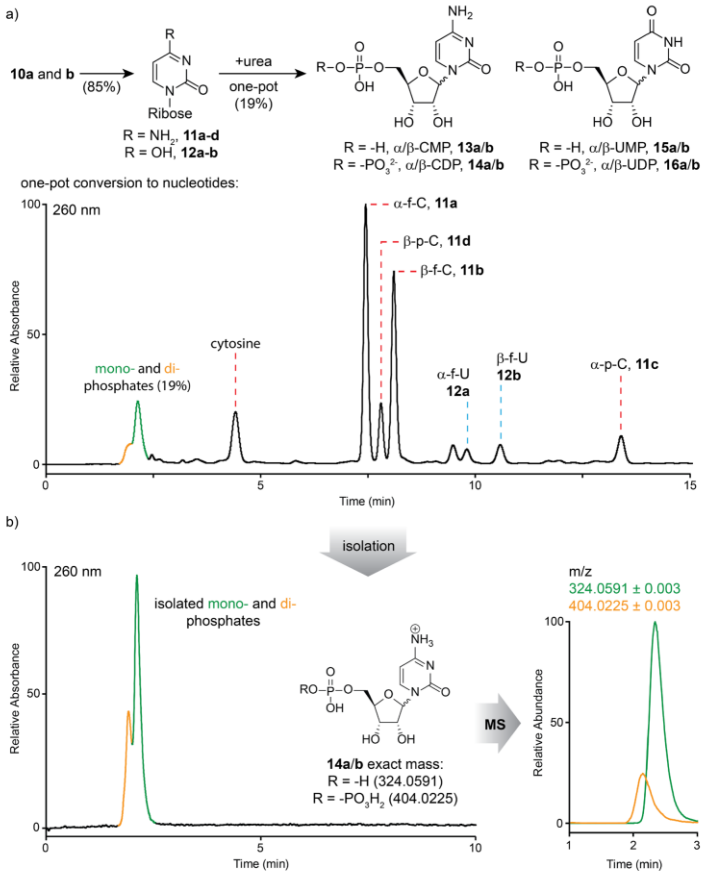

Fig. S7.

Prebiotic nucleotide synthesis in the presence of lueneburgite. a) Reaction scheme and full UV-chromatogram after nucleotide formation. An extract was shown in Fig. 5b in the main text. The yield was calculated relative to all cytidine isomers. The mono- (green) and di-phosphate (orange) peaks are highlighted. b) UV-chromatogram and corresponding mass (ESI+) for the isolated nucleotides.

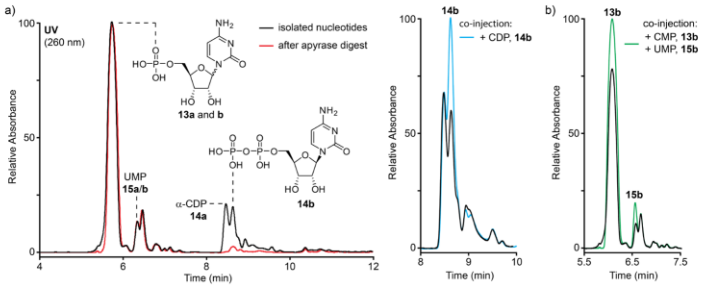

Fig. S8.

Confirmation of nucleotide structures from a prebiotic sample. a) LC-MS separation of phosphorylated nucleosides, isolated from a prebiotic reaction. The products were compared with a sample treated with apyrase. The di-phosphorylated peaks are clearly depleted in the treated sample (red line), proving the formation of pyrophosphates (left panel). Co-injection with 5'-cytidine-di-phosphate (**14b**, β-CDP) clearly confirmed formation of α- and β-CDP (right panel) . b) Co-injection of 5'-cytidine and 5'-uridine-mono-phosphate (**13b** and **15b**, β-CMP and β-UMP) confirmed the formation of **13b** and **15b**. The peaks represent mixtures of the inseparable α- and β-anomers.

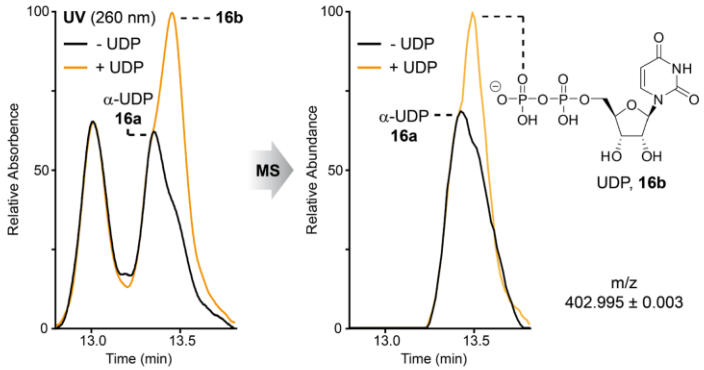

Fig. S9.

Co-injection study for β-5'-uridine-di-phosphate **16b**. For this experiment we used the same buffers as stated in the general information, but a different gradient: 0 → 15 min, Buffer B 0% → 10%. Co-injection was followed by UV and MS detection with commercially available material.

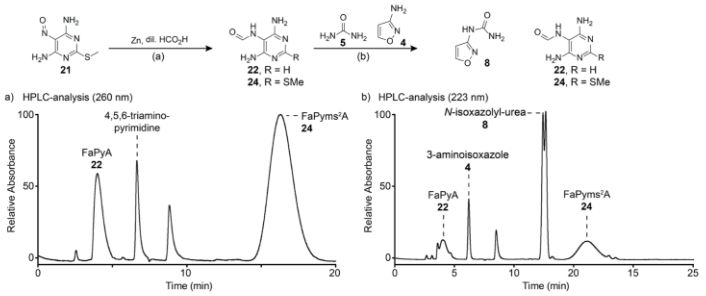

Fig. S10

Prebiotically linked syntheses of pyrimidine (**8**) and purine (**22**, **24**) precursors (detailed information can be found in the aforementioned procedure). a) prebiotically formed nitrosopyrimidine **21** was converted to **22** and **24** in the presence of Zn and dil. formic acid. The HPL-chromatogram of the reaction products is shown. b) The reaction from a) was directly used and a solution containing **4** and **5** was added. Upon dry-down the formation of **8** was observed in the presence of **22** and **24**. The HPL-chromatogram of the resulting products is shown.

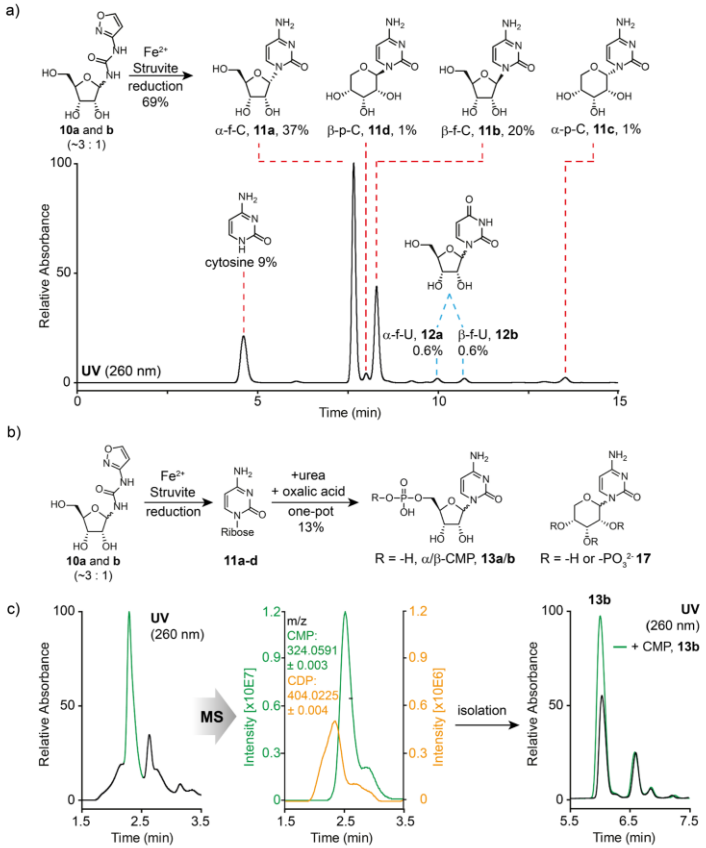

Fig. S11.

Formation of pyrimidine nucleotides from isoxazolylurea-ribosides with struvite. a) LC-MS analysis of pyrimidine nucleoside formation from compound **10a**/**b** in the presence of struvite. The UV-chromatogram at 260 nm is shown. The reduction of the isoxazole moiety in **10a**/**b** furnished the α and β-anomers as pyranoside (p) and furanside (f) isomers of cytidine (C, **11a-d**) or uridine (U, **12a/b**). b) One-pot Synthesis of cytidine mono- and di-phosphates (**13a**/**b**-**14a**/**b**) with struvite after urea and oxalic acid was added to the reaction mixture shown in (a) and letting the mixture dry-down at 85°C for 20 h. c) LC-MS analysis of the corresponding nucleotide peaks and isolation from the prebiotic reaction. Co-injection studies confirmed formation of CMP (**13a**/**b**). The α- and β-anomers of CMP were not separable and therefore the UV peaks represent a mixture of both anomers.

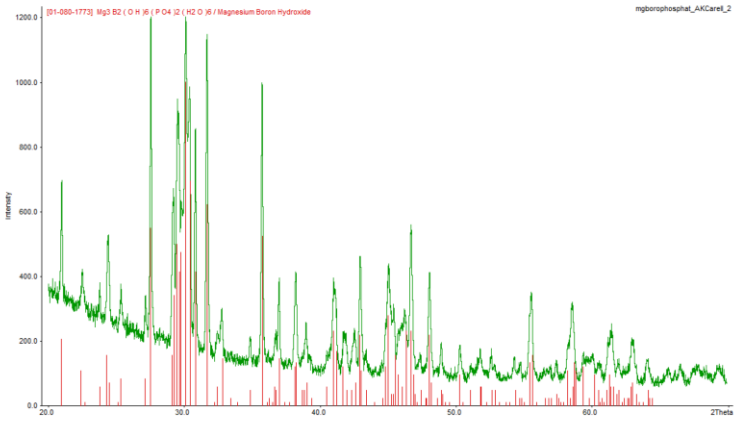

Fig. S12.

XRD measurement of synthetic lueneburgite (green) and comparison with database values (red).

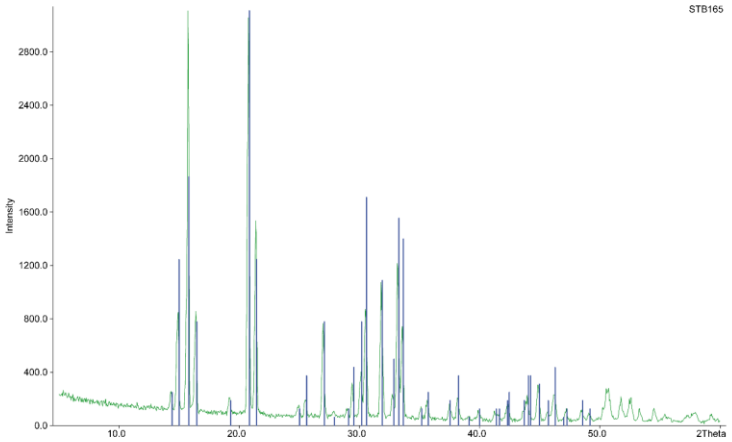

Fig. S13.

XRD measurement of synthetic struvite (green) and comparison with database values (blue).

References and Notes

1. J. A. Doudna, T. R. Cech, The chemical repertoire of natural ribozymes. *Nature* **418**, 222–228 (2002). doi:10.1038/418222a Medline

2. D. P. Horning, G. F. Joyce, Amplification of RNA by an RNA polymerase ribozyme. *Proc. Natl. Acad. Sci. U.S.A.* **113**, 9786–9791 (2016). doi:10.1073/pnas.1610103113 Medline

3. J. Attwater, A. Raguram, A. S. Morgunov, E. Gianni, P. Holliger, Ribozyme-catalysed RNA synthesis using triplet building blocks. *eLife* **7**, e35255 (2018). doi:10.7554/eLife.35255 Medline

4. W. Gilbert, Origin of life: The RNA world. *Nature* **319**, 618 (1986). doi:10.1038/319618a0

5. M. W. Powner, B. Gerland, J. D. Sutherland, Synthesis of activated pyrimidine ribonucleotides in prebiotically plausible conditions. *Nature* **459**, 239–242 (2009). doi:10.1038/nature08013 Medline

6. S. Becker, I. Thoma, A. Deutsch, T. Gehrke, P. Mayer, H. Zipse, T. Carell, A high-yielding, strictly regioselective prebiotic purine nucleoside formation pathway. *Science* **352**, 833–836 (2016). doi:10.1126/science.aad2808 Medline

7. H.-J. Kim, S. A. Benner, Prebiotic stereoselective synthesis of purine and noncanonical pyrimidine nucleotide from nucleobases and phosphorylated carbohydrates. *Proc. Natl. Acad. Sci. U.S.A.* **114**, 11315–11320 (2017). doi:10.1073/pnas.1710778114 Medline

8. S. Stairs, A. Nikmal, D.-K. Bučar, S.-L. Zheng, J. W. Szostak, M. W. Powner, Divergent prebiotic synthesis of pyrimidine and 8-oxo-purine ribonucleotides. *Nat. Commun.* **8**, 15270 (2017). doi:10.1038/ncomms15270 Medline

9. R. Saladino, E. Carota, G. Botta, M. Kapralov, G. N. Timoshenko, A. Y. Rozanov, E. Krasavin, E. Di Mauro, Meteorite-catalyzed syntheses of nucleosides and of other prebiotic compounds from formamide under proton irradiation. *Proc. Natl. Acad. Sci. U.S.A.* **112**, E2746–E2755 (2015). doi:10.1073/pnas.1422225112 Medline

10. J. F. Kasting, Earth's early atmosphere. *Science* **259**, 920–926 (1993). doi:10.1126/science.11536547 Medline

11. R. M. Hazen, Paleomineralogy of the Hadean Eon: A preliminary species list. *Am. J. Sci.* **313**, 807–843 (2013). doi:10.2475/09.2013.01

12. E. D. Swanner, N. J. Planavsky, S. V. Lalonde, L. J. Robbins, A. Bekker, O. J. Rouxel, M. A. Saito, A. Kappler, S. J. Mojzsis, K. O. Konhauser, Cobalt and marine redox evolution. *Earth Planet. Sci. Lett.* **390**, 253–263 (2014). doi:10.1016/j.epsl.2014.01.001

13. P. B. Rimmer, O. Shorttle, Origin of Life's Building Blocks in Carbon- and Nitrogen-Rich Surface Hydrothermal Vents. *Life* **9**, 12 (2019). doi:10.3390/life9010012 Medline

14. W. Martin, J. Baross, D. Kelley, M. J. Russell, Hydrothermal vents and the origin of life. *Nat. Rev. Microbiol.* **6**, 805–814 (2008). doi:10.1038/nrmicro1991 Medline

15. E. Camprubi, S. F. Jordan, R. Vasiliadou, N. Lane, Iron catalysis at the origin of life. *IUBMB Life* **69**, 373–381 (2017). doi:10.1002/iub.1632 Medline

16. S. A. Benner, H.-J. Kim, E. Biondi, in *Prebiotic Chemistry and Chemical Evolution of Nucleic Acids*, C. Menor-Salván, Ed. (Springer International Publishing, Cham, 2018), pp. 31–83.

17. S. Ranjan, Z. R. Todd, P. B. Rimmer, D. D. Sasselov, A. R. Babbin, Nitrogen Oxide Concentrations in Natural Waters on Early Earth. *Geochem. Geophys. Geosyst.* **20**, 2021–2039 (2019). doi:10.1029/2018GC008082

18. S. Becker, C. Schneider, H. Okamura, A. Crisp, T. Amatov, M. Dejmek, T. Carell, Wet-dry cycles enable the parallel origin of canonical and non-canonical nucleosides by continuous synthesis. *Nat. Commun.* **9**, 163 (2018). doi:10.1038/s41467-017-02639-1 Medline

19. P. Thaddeus, The prebiotic molecules observed in the interstellar gas. *Philos. Trans. R. Soc. Lond. B Biol. Sci.* **361**, 1681–1687 (2006). doi:10.1098/rstb.2006.1897 Medline

20. R. A. Sanchez, J. P. Ferris, L. E. Orgel, Cyanoacetylene in prebiotic synthesis. *Science* **154**, 784–785 (1966). doi:10.1126/science.154.3750.784 Medline

21. B. H. Patel, C. Percivalle, D. J. Ritson, C. D. Duffy, J. D. Sutherland, Common origins of RNA, protein and lipid precursors in a cyanosulfidic protometabolism. *Nat. Chem.* **7**, 301–307 (2015). doi:10.1038/nchem.2202 Medline

22. H. Kofod, B. Wickberg, A. Kjær, On the Isomerism of Hydroxyurea. I. Kinetics of the Reaction between Hydroxylammonium Ion and Cyanate Ion. *Acta Chem. Scand.* **7**, 274–279 (1953). doi:10.3891/acta.chem.scand.07-0274

23. K. B. Muchowska, S. J. Varma, J. Moran, Synthesis and breakdown of universal metabolic precursors promoted by iron. *Nature* **569**, 104–107 (2019). doi:10.1038/s41586-019-1151-1 Medline

24. V. S. Airapetian, A. Glocer, G. Gronoff, E. Hébrard, W. Danchi, Prebiotic chemistry and atmospheric warming of early Earth by an active young Sun. *Nat. Geosci.* **9**, 452–455 (2016). doi:10.1038/ngeo2719

25. H. J. Cleaves, J. H. Chalmers, A. Lazcano, S. L. Miller, J. L. Bada, A reassessment of prebiotic organic synthesis in neutral planetary atmospheres. *Orig. Life Evol. Biosph.* **38**, 105–115 (2008). doi:10.1007/s11084-007-9120-3 Medline

26. D. P. Summers, S. Chang, Prebiotic ammonia from reduction of nitrite by iron (II) on the early Earth. *Nature* **365**, 630–633 (1993). doi:10.1038/365630a0 Medline

27. S. Ranjan, Z. R. Todd, J. D. Sutherland, D. D. Sasselov, Sulfidic Anion Concentrations on Early Earth for Surficial Origins-of-Life Chemistry. *Astrobiology* **18**, 1023–1040 (2018). doi:10.1089/ast.2017.1770 Medline

28. G. K. Rollefson, C. F. Oldershaw, The reduction of nitrites to hydroxylamine by sulfites. *J. Am. Chem. Soc.* **54**, 977–979 (1932). doi:10.1021/ja01342a019

29. G. F. Joyce, The antiquity of RNA-based evolution. *Nature* **418**, 214–221 (2002). doi:10.1038/418214a Medline

30. D. M. Fialho, K. C. Clarke, M. K. Moore, G. B. Schuster, R. Krishnamurthy, N. V. Hud, Glycosylation of a model proto-RNA nucleobase with non-ribose sugars: Implications for

the prebiotic synthesis of nucleosides. *Org. Biomol. Chem.* **16**, 1263–1271 (2018). doi:10.1039/C7OB03017G Medline

31. H.-J. Kim, Y. Furukawa, T. Kakegawa, A. Bita, R. Scorei, S. A. Benner, Evaporite Borate-Containing Mineral Ensembles Make Phosphate Available and Regiospecifically Phosphorylate Ribonucleosides: Borate as a Multifaceted Problem Solver in Prebiotic Chemistry. *Angew. Chem. Int. Ed.* **55**, 15816–15820 (2016). doi:10.1002/anie.201608001 Medline

32. A. Ricardo, M. A. Carrigan, A. N. Olcott, S. A. Benner, Borate minerals stabilize ribose. *Science* **303**, 196–196 (2004). doi:10.1126/science.1092464 Medline

33. M. Kijima, Y. Nambu, T. Endo, Reduction of cyclic compounds having nitrogen-oxygen linkage by dihydrolipoamide-iron(II). *J. Org. Chem.* **50**, 1140–1142 (1985). doi:10.1021/jo00207a052

34. G. Wächtershäuser, Before enzymes and templates: Theory of surface metabolism. *Microbiol. Rev.* **52**, 452–484 (1988). Medline

35. U. Trinks, A. Eschenmoser, ETH Zurich (1987; doi:10.3929/ethz-a-000413538).

36. R. Krishnamurthy, On the Emergence of RNA. *Isr. J. Chem.* **55**, 837–850 (2015). doi:10.1002/ijch.201400180

37. J. Liebig, F. Wöhler, Untersuchungen über die Cyansäure. *Ann. Phys.* **96**, 369–400 (1830). doi:10.1002/andp.18300961102

38. M. Preiner *et al*., A hydrogen dependent geochemical analogue of primordial carbon and energy metabolism. *bioRxiv* 682955 (2019).

39. C. Bonfio, E. Godino, M. Corsini, F. Fabrizi de Biani, G. Guella, S. S. Mansy, Prebiotic iron–sulfur peptide catalysts generate a pH gradient across model membranes of late protocells. *Nat. Catal.* **1**, 616–623 (2018). doi:10.1038/s41929-018-0116-3

40. J. S. Teichert, F. M. Kruse, O. Trapp, Direct Prebiotic Pathway to DNA Nucleosides. *Angew. Chem. Int. Ed.* **58**, 9944–9947 (2019). doi:10.1002/anie.201903400 Medline

41. J. Kofoed, J.-L. Reymond, T. Darbre, Prebiotic carbohydrate synthesis: Zinc-proline catalyzes direct aqueous aldol reactions of α-hydroxy aldehydes and ketones. *Org. Biomol. Chem.* **3**, 1850–1855 (2005). doi:10.1039/b501512j Medline

42. C. Meinert, I. Myrgorodska, P. de Marcellus, T. Buhse, L. Nahon, S. V. Hoffmann, Ll. S. d'Hendecourt, U. J. Meierhenrich, Ribose and related sugars from ultraviolet irradiation of interstellar ice analogs. *Science* **352**, 208–212 (2016). doi:10.1126/science.aad8137 Medline

43. K. Usami, A. Okamoto, Hydroxyapatite: Catalyst for a one-pot pentose formation. *Org. Biomol. Chem.* **15**, 8888–8893 (2017). doi:10.1039/C7OB02051A Medline

44. S. Naiditch, D. M. Yost, The Rate and Mechanism of the Hydrolysis of Hydroxylamine Disulfonate Ion. *J. Am. Chem. Soc.* **63**, 2123–2127 (1941). doi:10.1021/ja01853a028

45. D. H. Shannahoff, R. A. Sanchez, 2,2-Anhydropyrimidine nucleosides. Novel syntheses and reactions. *J. Org. Chem.* **38**, 593–598 (1973). doi:10.1021/jo00943a040 Medline

46. R. M. Davidson, E. White, S. A. Margolis, B. Coxon, Synthesis of nitrogen-15-labeled 2-amino(glycofurano)oxazolines via glycosylamine intermediates. *Carbohydr. Res.* **116**, 239–254 (1983). doi:10.1016/0008-6215(83)88113-0

47. R. U. Lemieux, T. L. Nagabhushan, B. Paul, Relationship of 13C to Vicinal 1H Coupling to the Torsion Angle in Uridine and Related Structures. *Can. J. Chem.* **50**, 773–776 (1972). doi:10.1139/v72-120

48. W. Berdesinski, Synthetische Darstellung von Lüneburgit. *Naturwissenschaften* **38**, 476–477 (1951). doi:10.1007/BF00622085

49. V. V. Vol'khin, D. A. Kazakov, G. V. Leont'eva, Y. V. Andreeva, E. A. Nosenko, M. Y. Siluyanova, Synthesis of struvite (MgNH4PO4·6H2O) and its use for sorption of nickel ions. *Russ. J. Appl. Chem.* **88**, 1986–1996 (2015). doi:10.1134/S10704272150120149

Anhang II

A Unifying Concept for the Prebiotic Formation of RNA Pyrimidine Nucleosides

Table of Contents

Materials and Methods

Chemicals were purchased from Sigma-Aldrich, Fluka, ABCR, Carbosynth, TCI or Acros organics and used without further purification. The solvents were of reagent grade or purified by distillation. Reactions and chromatography fractions were monitored by qualitative thin-layer chromatography (TLC) on silica gel F_{254} TLC plates from Merck KGaA. Chromatographic purification was performed on Silicagel 60 (40-63 µm) silica gel from Macherey-Nagel. ^{1}H- and ^{13}C-NMR spectra were recorded on a Bruker AVIIIHD 400 (400 MHz) spectrometer and calibrated to the residual solvent peak. Multiplicities are abbreviated as follows: s = singlet, d = doublet, t = triplet, q = quartet, m = multiplet. High-resolution ESI spectra were obtained on the mass spectrometer Thermo Finnigan LTQ FT-ICR. IR measurements were performed on Perkin Elmer Spectrum BX FT-IR spectrometer with a diamond-ATR (Attenuated Total Reflection) setup. Melting points were measured on a Büchi B-540 device. For preparative HPLC purification a Agilent 1260 Infinity II system was used with a Machery-Nagel VP 250/32 C18 RP column. The prebiotic reactions were analyzed by LC-ESI-MS on a Thermo Finnigan LTQ Orbitrap XL and were chromatographed by a Dionex Ultimate 3000 HPLC system. All chromatographic separations were performed on an Interchim Uptisphere120 3HDO C18 column with a flow of 0.15 ml/min and a constant column temperature of 30 °C. Eluting buffers were buffer A (2 mM $HCOONH_4$ in H_2O (pH 5.5)) and buffer B (2 mM $HCOONH_4$ in H_2O/MeCN 20/80 (pH 5.5)). The elution was monitored at 223, 243 and 260 nm (Dionex Ultimate 3000 Diode Array Detector). The chromatographic eluent was directly injected into the ion source without prior splitting. The synthetic standards for the co-injection experiments were synthesized in our lab according to reported literature or purchased. The X-ray intensity data of the metal complexes were measured on a Bruker D8 Venture TXS system equipped with a multilayer mirror monochromator and a Mo-*K*α rotating anode X-ray tube (λ = 0.71073 Å). The frames were integrated with the Bruker SAINT software package.[1] Data were corrected for absorption effects using the Multi-Scan method (SADABS).[2] For the ligand, an Oxford Xcalibur3 diffractometer with a CCD area detector was employed for data collection using Mo-*K*α radiation. The data collection and reduction were carried out using the CRYSALISPRO software.[3] The structures were solved and refined using the Bruker SHELXTL Software Package.[4] All C-bound hydrogen atoms have been calculated in ideal geometry riding on their parent atoms while the N-bound hydrogen atoms have been refined freely. The figures have been drawn at the 50% ellipsoid probability level.[5] Crystallographic data have been deposited with the Cambridge Crystallographic Data Centre, CCDC, 12 Union Road, Cambridge CB21EZ, UK. Copies of the data can be obtained free of charge on quoting the depository numbers CCDC-2217036 (ligand),

CCDC-2216042 (Ca), CCDC-2216043 (Co), CCDC-2216044 (Ni), CCDC-2216045 (Cu), and CCDC-2216046 (Zn) (https://www.ccdc.cam.ac.uk/structures/).

Synthetic Procedures

Ribo-2-thiooxazoline (8)

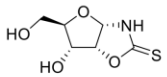

Synthesized using a protocol adapted from known literature protocol.[6] In a round-bottomed flask, D-ribose (8.00 g, 53.3 mmol, 1.0 eq.) was dissolved in water (8 mL) followed by addition of KCN (10.35 g, 106.6 mmol, 2.0 eq.). The reaction mixture was cooled to 0 °C before dropwise addition of conc. HCl (9.8 mL, 117.4 mmol, 2.20 eq.). Subsequently, the reaction mixture stirred for 40 min at 0 °C before heated to 80 °C for 30 min. The solvent was then removed in vacuo and the product was purified by flash column chromatography (0-5% MeOH in EtOH) affording ribo-2-thiooxazoline (7.10 g, 37.1 mmol, 70%).

^{1}H NMR (400 MHz, Deuterium Oxide) δ 5.90 (d, *J* = 5.4 Hz, 1H), 5.31 (t, *J* = 5.4 Hz, 1H), 4.21 (dd, *J* = 9.1, 5.4 Hz, 1H), 3.95 – 3.91 (m, 1H), 3.78 – 3.69 (m, 2H). **^{13}C NMR** (101 MHz, Deuterium Oxide) δ 190.43, 88.22, 85.11, 78.51, 70.12, 59.16. **HRMS** (ESI-): calc.: $[C6H8NO4S]^-$ 190.0180, found: 190.0180 $[M-H]^-$.

Ribo-2-(methylthio)oxazoline (11)

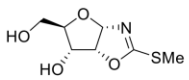

Synthesized using a protocol adapted from known literature protocol.[7] NaOH (950 mg, 23.8 mmol, 1.14 eq.) and **8** (4.00 g, 20.9 mmol, 1.0 eq.) were added to a solution of EtOH (160mL) and water (85 mL) followed by dropwise addition of iodomethane (1.50 mL, 24.1 mmol, 1.15 eq.). The reaction mixture was stirred for 60 min at rt. before removal of the solvent *in vacuo*. Flash column chromatography (0-10% MeOH in DCM) was performed to obtain ribo-2-(methylthio) oxazoline (2.40 g, 11.7 mmol, 56%).

^{1}H NMR (400 MHz, Deuterium Oxide) δ 5.95 (d, *J* = 5.3 Hz, 1H), 5.05 (t, *J* = 5.4 Hz, 1H), 4.16 (dd, *J* = 9.5, 5.6 Hz, 1H), 3.89 (dd, *J* = 12.8, 2.4 Hz, 1H), 3.69 (dd, *J* = 12.8, 4.7 Hz, 1H), 3.51 (ddd, *J* = 9.5, 4.7, 2.3 Hz, 1H), 2.48 (s, 3H). **^{13}C NMR** (101 MHz, Deuterium Oxide) δ 174.9, 98.0, 83.2, 77.9, 70.3, 59.3, 13.7. **HRMS** (ESI+): calc.: $[C7H12NO4S]^+$ 206.0482, found: 206.0483 $[M+H]^+$.

Ribo-*N*-isoxazolyl-2-aminooxazoline (21)

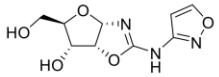

Ribo-2-(methylthio)oxazoline (**11**) (540mg, 2.63 mmol, 1.0 eq.), 3-aminoisoxazole (390 µL, 5.28 mmol, 2.0 eq.), and dichloroacetic acid (2.7 mL, 32.9 mmol, 12.5 eq.) were dissolved in MeCN (24 mL). The reaction mixture was allowed to stir at 70 °C for 4 h. Hereafter, the reaction mixture was cooled to rt. and poured into water. The aqueous phase was washed with EtOAc and concentrated in vacuo. Flash column chromatography (5-12% MeOH in DCM) was performed to obtain ribo-*N*-isoxazolyl-2-aminooxazoline (432 mg, 1.8 mmol, 68%).

^{1}H NMR (400 MHz, Deuterium Oxide) δ 8.41 (d, *J* = 1.8 Hz, 1H), 6.33 (s, 1H), 5.89 (d, *J* = 5.1 Hz, 1H), 5.20 (t, *J* = 5.3 Hz, 1H), 4.18 (dd, *J* = 9.5, 5.3 Hz, 1H), 3.91 (dd, *J* = 12.7, 2.3 Hz, 1H), 3.82 (ddd, *J* = 9.5, 4.7, 2.2 Hz, 1H), 3.71 (dd, *J* = 12.7, 4.7 Hz, 1H). **^{13}C NMR** (101 MHz, Deuterium Oxide) δ 164.1, 160.2†, 101.5, 88.5*, 81.7*, 78.0, 69.9, 59.3. **HRMS** (ESI+): calc.: $[C9H12N3O5]^+$ 242.0771, found: 242.0772 $[M+H]^+$. †Small shoulder peak observed *Low intensity

***N*-Methyl-*N*-nitrosourea (20)**

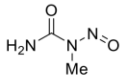

Compound **20** was synthesized according to known literature protocol.[8]

Ribo-anhydro cytidine (22)

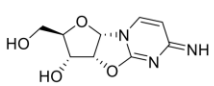

Compound **22** was synthesized according to known literature protocol.[7, 9]

Prebiotic Procedures

Prebiotic synthesis of compound 11

LC-MS grade water (2.5 mL) and $NaHCO_3$ (22.0 mg, 262 µmol) were added to a pressure tube together with ribo-2-thiooxazoline (**8**) (5.0 mg, 26 µmol). Subsequently, *N*-methyl-*N*-nitrosourea (**20**) (67.4 mg, 655 µmol) was added to the reaction mixture and the pressure tube was capped with a seal. The reaction mixture was heated to 55 °C in an oil bath. After 5 h, the reaction mixture was cooled to 0 °C in an ice bath and *N*-methyl-*N*-nitrosourea (**20**) (67.4 mg, 655 µmol) was added. The pressure tube was again capped with a seal, heated to 55 °C, and stirred for another 19 h. The yield of compound **11** (25 %) was determined by LC-ESI-MS according to the calibration curve Figure S7**.**

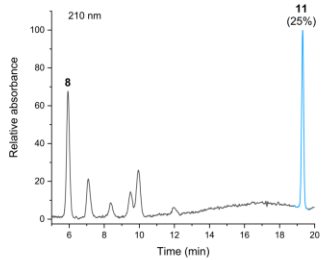

Figure S1. HPL-chromatogram for the synthesis of **11**.

Prebiotic synthesis of compound 21

Compound **11** (10.0 mg, 48.7 µmol, 1 eq) and 3-aminoisoxazole (7.2 µL, 98 µmol, 2 eq) were added to a solution of AcOH (25 µL) and LC-MS grade water (467.8 µL). The reaction mixture was stirred at 25 °C for 24 h. The yield of compound **21** (6%) was determined by LC-ESI-MS according to the calibration curve Figure S8.

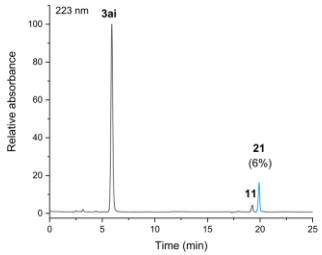

Figure S2. HPL-chromatogram for the synthesis of **21**.

Prebiotic synthesis of compound 22

Compound **21** (6.1 mg, 26 µmol), sodium thiolmethoxide (3.5 mg, 51 µmol), and $CuCl_2$ (0.3 mg, 3 µmol) were added to an aqueous solution of AcOH (5 %V/V, 80 µL). The reaction mixture was stirred at 25 °C for 24 h. The yield of compound **22** (4%) was determined by LC-ESI-MS according to the calibration curve Figure S9.

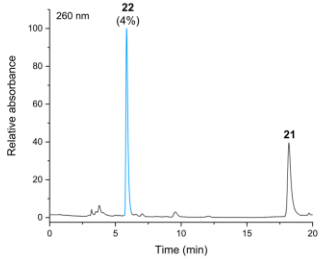

Figure S3. HPL-chromatogram for the synthesis of **22**.

Prebiotic one-pot synthesis of compound 22

Compound **11** (10.0 mg, 48.7 µmol) and 3-aminoisoxazole (7.2 µL, 98 µmol) were added to a degassed solution of $CuCl_2$ (0.6 mg, 5 µmol) in aqueous AcOH (5 %V/V, 153 µL). The reaction mixture was stirred under inert conditions at 25 °C for 24 h. The yield of compound **22** (38 %) was determined by LC-ESI-MS according to the calibration curve Figure S9.

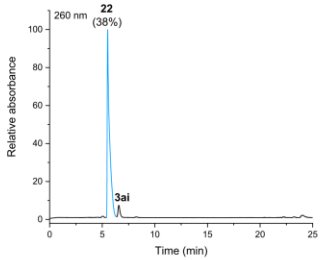

Figure S4. HPL-chromatogram for one-pot synthesis of compound **22**.

Prebiotic one-pot synthesis of compound 22 using $[Cu(3ai)_4Cl]Cl$

The crystal $[Cu(3ai)_4Cl]Cl$ (2.3 mg, 4.8 µmol) and compound **11** (10.0 mg, 48.7 µmol) were added to an aqueous solution of AcOH (5 %V/V, 160 µL). The reaction mixture was stirred at 25 °C for 24 h. The yield of compound **22** (17 %) was determined by LC-ESI-MS according to the calibration curve Figure S9.

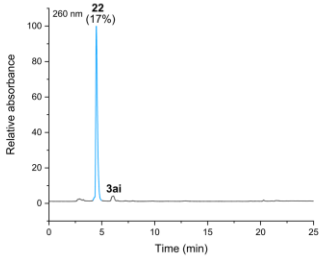

Figure S5. HPL-chromatogram for the synthesis of **22** with the crystal $[Cu(3ai)_4Cl]Cl$.

Formation of Metal Complexes

Tetra(3-aminoisoxazole)dichlorocalcium(II) ([Ca(3ai)$_4$Cl$_2$])

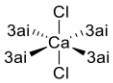

A solution of $CaCl_2$ (111 mg, 1.00 mmol, 1.0 eq) and 3-aminoisoxazole (95%; 311 µL, 4.0 eq) in H_2O (10 mL) was left at r.t. for 4 w and [Ca(3ai)$_4$Cl$_2$] (128 mg, 287 µmol, 29 %) was obtained as colorless crystals.

IR (cm^{-1}): $\tilde{\nu}$ = 3389 (m), 3306 (m), 1615 (s), 1584 (m), 1498 (m), 1449 (s), 1151 (m), 1113 (w), 1055 (m), 998 (m), 914 (m), 886 (m), 771 (m), 707 (m), 697 (m). **EA:** Calc. (found) for $C_{12}H_{16}CaCl_2N_8O_4$: C, 32.22 (31.82); H, 3.61 (3.54); N, 25.05 (24.94). **Crystallographic data:** Figure S17**.**

Tetra(3-aminoisoxazole)dichlorocobalt(II) ([Co(3ai)$_4$Cl$_2$])

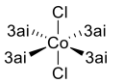

A solution of $CoCl_2 \cdot 6\ H_2O$ (238 mg, 1.00 mmol, 1.0 eq) and 3-aminoisoxazole (95%; 311 µL, 4.0 eq) in H_2O (10 mL) was left at r.t. for 4 w and [Co(3ai)$_4$Cl$_2$] (462 mg, 991 µmol, quant.) was obtained as pink crystals.

IR (cm^{-1}): $\tilde{\nu}$ = 3377 (m), 3286 (m), 1618 (m), 1508 (m), 1445 (s), 1459 (w), 1118 (w), 1056 (m), 999 (w), 914 (m), 890 (m), 774 (s), 708 (m), 696 (m). **EA:** Calc. (found) for $C_{12}H_{16}Cl_2CoN_8O_4$: C, 30.92 (30.58); H, 3.46 (3.20); N, 24.04 (23.98). **Crystallographic data:** Figure **S18.**

Tetra(3-aminoisoxazole)dichloronickel(II) ([Ni(3ai)$_4$Cl$_2$])

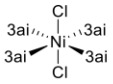

A solution of $NiCl_2 \cdot 6\ H_2O$ (238 mg, 1.00 mmol, 1.0 eq) and 3-aminoisoxazole (95%; 311 µL, 4.0 eq) in H_2O (10 mL) was left at r.t. for 4 w and [Ni(3ai)$_4$Cl$_2$] (465 mg, 998 µmol, quant.) was obtained as bright green crystals.

IR (cm^{-1}): $\tilde{\nu}$ = 3384 (m), 3291 (m), 1620 (s), 1508 (m), 1453 (m), 1162 (w), 1120 (w), 1058 (w), 999 (w), 921 (m), 893 (m), 775 (s), 708 (w). **EA:** Calc. (found) for $C_{12}H_{16}Cl_2N_8NiO_4$: C, 30.94 (31.05); H, 3.46 (3.44); N, 24.05 (23.96). **Crystallographic Data:** Figure S19**.**

Tetra(3-aminoisoxazole)chlorocopper(II) chloride ([Cu(3ai)$_4$Cl]Cl)

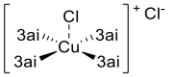

A solution of $CuCl_2$ (134 mg, 1.00 mmol, 1.0 eq) and 3-aminoisoxazole (95%; 311 µL, 4.0 eq) in H_2O (10 mL) was left at r.t. for 4 w and [Cu(3ai)$_4$Cl]Cl (367 mg, 780 µmol,78 %) was obtained as a dark green crystal.

IR (cm^{-1}): $\tilde{\nu}$ = 3433 (w), 3315 (m), 3131 (m), 1615 (s), 1580 (s), 1501 (s), 1456 (s), 1126 (m), 1052 (m), 1010 (m), 948 (s), 895 (s), 797 (s), 712 (m), 695 (m). **EA:** Calc. (found) for $C_{12}H_{16}Cl_2CuN_8O_4$: C, 30.62 (30.44); H, 3.43 (3.22); N, 23.80 (23.65). **Crystallographic data**: Figure S20.

Di(3-aminoisoxazole)dichlorozinc(II) ([Zn(3ai)$_2$Cl$_2$])

A solution of $ZnCl_2$ (136 mg, 1.00 mmol, 1.0 eq) and 3-aminoisoxazole (95%; 156 µL, 2.0 eq) in H_2O (10 mL) was left at r.t. for 4 w and [Zn(3ai)$_2$Cl$_2$] (272 mg, 893 µmol, 89 %) was obtained as colorless crystals.

IR (cm^{-1}): $\tilde{\nu}$ = 3493 (w), 3351 (m), 3313 (m), 3143 (w), 3076 (w), 1621 (s), 1588 (s), 1511 (m), 1453 (s), 1151 (m), 1057 (m), 1007 (m), 950 (m), 891 (s), 785 (s), 777 (s), 703 (m). **EA:** Calc. (found) for $C_6H_8Cl_2N_4O_2Zn$: C, 23.67 (23.70); H, 2.65 (2.68); N, 18.40 (18.60). **Crystallographic Data**: Figure S21.

Selective enrichment of [Cu(3ai)$_4$Cl]Cl

A solution of $CaCl_2$ (111 mg, 1.00 mmol, 1.0 eq), $CoCl_2 \cdot 6\ H_2O$ (238 mg, 1.00 mmol, 1.0 eq), $NiCl_2 \cdot 6\ H_2O$ (238 mg, 1.00 mmol, 1.0 eq), $CuCl_2$ (134 mg, 1.00 mmol, 1.0 eq), $ZnCl_2$ (272 mg, 1.00 mmol, 2.0 eq) and 3-aminoisoxazole (95%; 156 µL, 2.0 eq) in H_2O (50 mL) was left at r.t. to allow water to evaporate. During evaporation, dark green crystals formed. After the mixture was concentrated to about 2.5 mL, the crystals were collected and detected as [Cu(3ai)$_4$Cl]Cl (243 mg, 512 µmol, 51 %).

Figure S6. Concentrated reaction mixture with crystallized [Cu(3ai)4Cl]Cl.

Calibration Curves

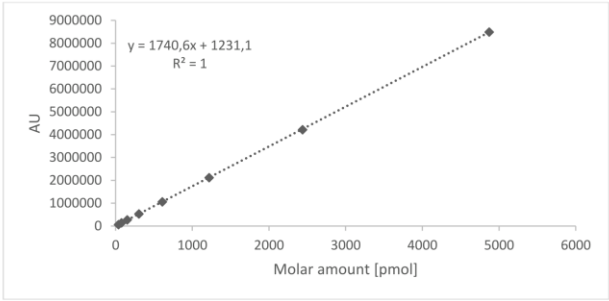

Figure S7. Calibration curve of ribo-2-(methylthio)oxazoline (**11**) (λ_{max} = 210 nm).

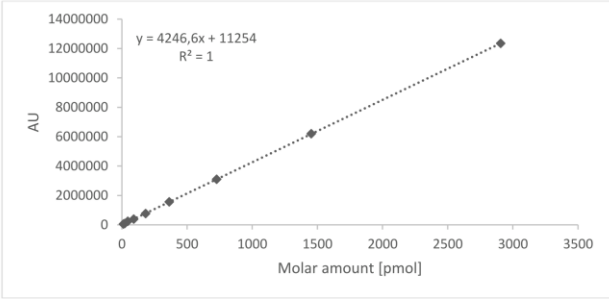

Figure S8. Calibration curve of ribo-*N*-isoxazolyl-2-aminooxazoline (**21**) (λ_{max} = 223 nm).

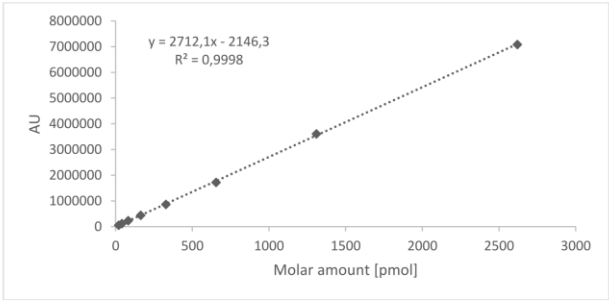

Figure S9 Calibration curve of ribo-anhydro cytidine (22) (λ_{max} = 260 nm).

NMR Spectra

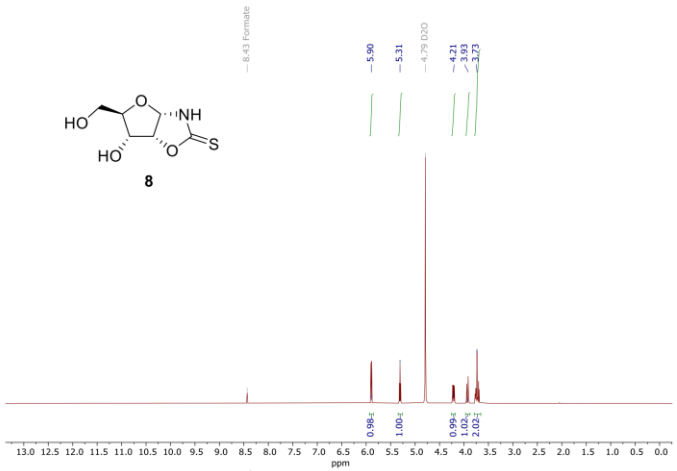

Figure S10. ^{1}H NMR of ribo-2-thiooxazoline (8).

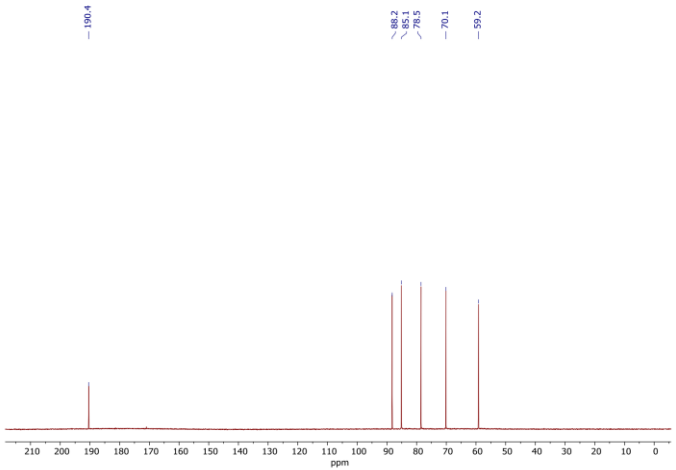

Figure S11. ^{13}C NMR of ribo-2-thiooxazoline (8).

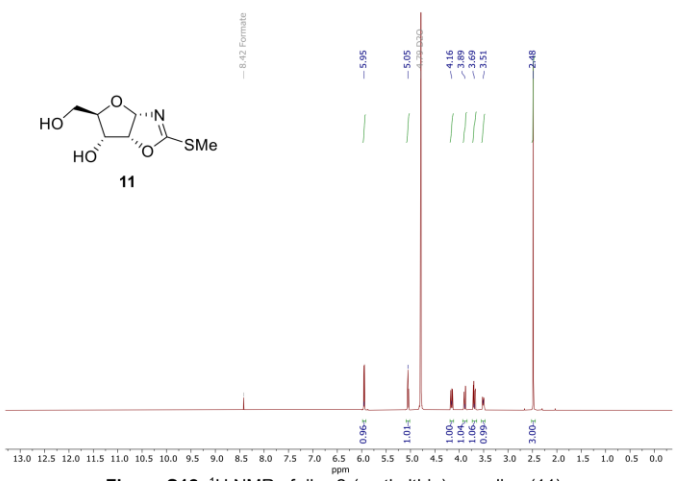

Figure S12. ^{1}H NMR of ribo-2-(methylthio)oxazoline (11).

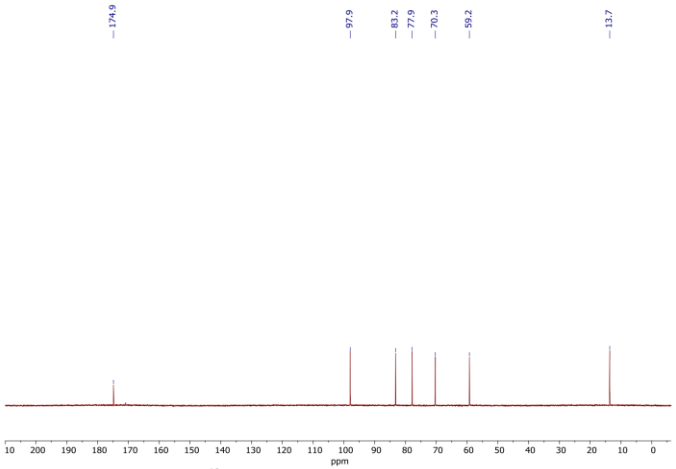

Figure S13. ^{13}C NMR of ribo-2-(methylthio)oxazoline (11).

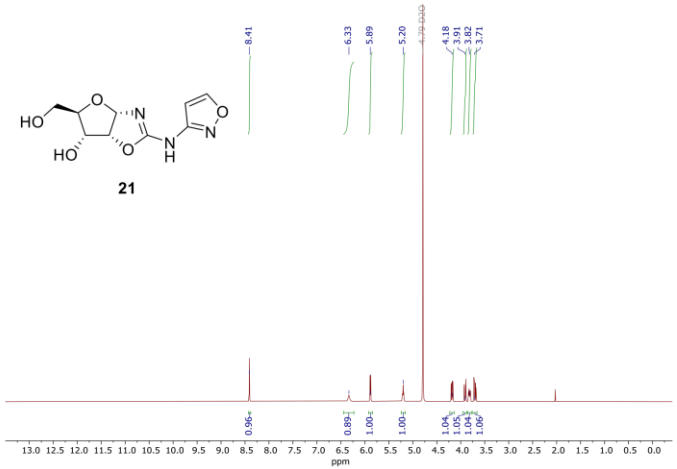

21

Figure S14. [1]H NMR of ribo-*N*-isoxazolyl-2-aminooxazoline (21).

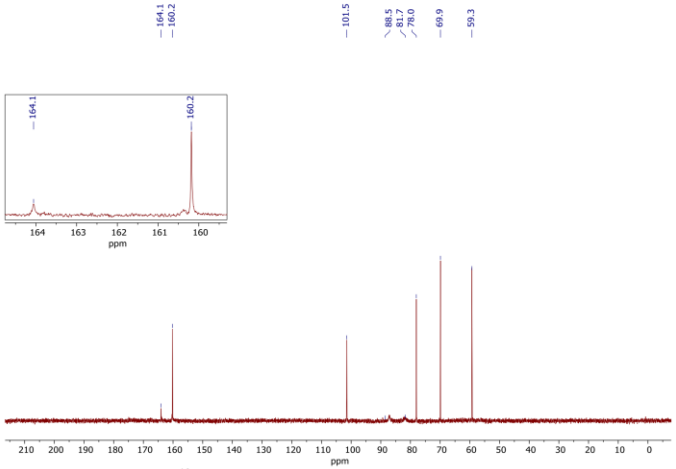

Figure S15. [13]C NMR of ribo-*N*-isoxazolyl-2-aminooxazoline (21).

Crystallographic Data

Figure S16. Crystal structure of 3-aminoisoxazole (**14**).

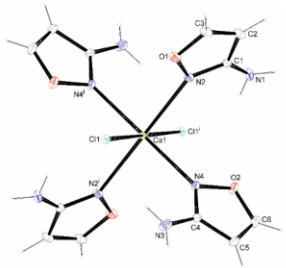

Figure S17. Crystal structure of $[Ca(3ai)_4Cl_2]$.[1]

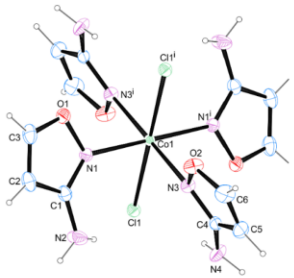

Figure S18. Crystal structure of $[Co(3ai)_4Cl_2]$.[2]

[1] Symmetriecode: i = 1-x, 1-y, 1-z.
[2] Symmetriecode: i = 1-x, 1-y, 1-z.

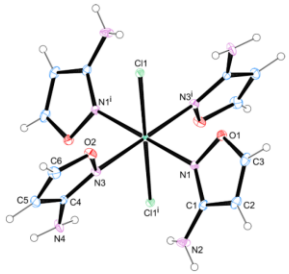

Figure S19. Crystal structure of $[Ni(3ai)_4Cl_2]$.[3]

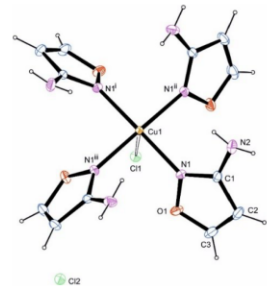

Figure S20. Crystal structure of $[Cu(3ai)_4Cl_2]$.[4]

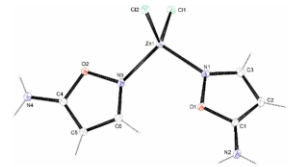

Figure S21. Crystal structure of $[Zn(3ai)_2Cl_2]$.

[3] Symmetriecode: i = 1-x, 1-y, 1-z.
[4] Symmetriecode: i = 0.5–x, 0.5–y, z; ii = y, 0.5–x, z; iii = 0.5–y, x, z.

Table S1. Crystallographic data of **14**

	14
Formula	$C_3H_4N_2O$
FW [g mol^{-1}]	84.08
Crystal system	monoclinic
Space group	P21/c (No. 14)
Color / Habit	colorless plate
Size [mm]	0.50 x 0.30 x 0.08
a [Å]	7.3422(11)
b [Å]	6.6530(7)
c [Å]	8.4735(12)
α [°]	90
β [°]	110.674(16)
γ [°]	90
V [Å^3]	387.26(10)
Z	4
$\rho_{calc.}$ [g cm^{-3}]	1.442
μ [mm^{-1}]	0.112
F(000)	176
$\lambda_{MoK\alpha}$ [Å]	0.71073
T [K]	100
θ Min-Max [°]	2.965, 25.242
Dataset	-9: 9 ; -8: 9 ; -10: 11
Reflections collected	5270
Independent refl.	983
R_{int}	0.0506
Observed reflections	807
Parameters	71
R_1 (obs)[a]	0.0356
wR_2 (all data)[b]	0.0950
S[c]	1.053
Resd. dens [e Å^{-3}]	-0.168, 0.244
Device type	Oxford Xcalibur3
Solution	SHELXT
Refinement	SHELXL-2018
Absorption correction	multi-scan

[a] $R_1 = \Sigma||F_0|-|F_c||/\Sigma|F_0|$. [b] $wR_2 = [\Sigma[w(F_0^2-F_c^2)^2]/\Sigma[w(F_0)^2]]^{1/2}$; $w = [\sigma c^2(F_0^2)+(xP)^2+yP]^{-1}$ and $P=(F_0^2+2F_c^2)/3$. [c] $S = \{\Sigma[w(F_o^2-F_c^2)^2]/(n-p)\}^{1/2}$ (n = number of reflections; p = total number of parameters).

Table S2. Crystallographic data of **[Ca(3ai)$_4$Cl$_2$]**, **[Co(3ai)$_4$Cl$_2$]**, and **[Ni(3ai)$_4$Cl$_2$]**

	[Ca(3ai)$_4$Cl$_2$]	**[Co(3ai)$_4$Cl$_2$]**	**[Ni(3ai)$_4$Cl$_2$]**
net formula	$C_{12}H_{16}CaCl_2N_8O_4$	$C_{12}H_{16}Cl_2CoN_8O_4$	$C_{12}H_{16}Cl_2N_8NiO_4$
M_r/g mol^{-1}	447.31	466.16	465.94
crystal size/mm	0.100 × 0.090 × 0.080	0.120 × 0.090 × 0.070	0.110 × 0.060 × 0.020
T/K	108.(2)	173.(2)	173.(2)
radiation	MoKα	MoKα	MoKα
diffractometer	'Bruker D8 Venture	'Bruker D8 Venture	'Bruker D8 Venture
crystal system	monoclinic	monoclinic	monoclinic
space group	'P 1 21/n 1'	'P 1 21/n 1'	'P 1 21/n 1'
a/Å	9.1871(3)	8.8917(9)	8.8716(10)
b/Å	11.1368(3)	10.9489(12)	10.9306(11)
c/Å	9.3197(3)	9.1220(10)	9.1304(10)
α/°	90	90	90
β/°	90.7900(10)	90.686(4)	90.664(4)
γ/°	90	90	90
V/Å^3	953.45(5)	888.00(16)	885.33(17)
Z	2	2	2
calc. density/g cm^{-3}	1.558	1.743	1.748
μ/mm^{-1}	0.646	1.306	1.437
absorption correction	Multi-Scan	Multi-Scan	Multi-Scan
transmission factor	0.93–0.95	0.85–0.91	0.89–0.97
refls. measured	16996	15150	15009
R_{int}	0.0348	0.0447	0.0475
mean σ(*I*)/*I*	0.0247	0.0331	0.0326
θ range	3.092–28.282	3.219–28.278	2.957–27.483
observed refls.	2096	2050	1897
x, *y* (weighting	0.0163, 0.6048	0.0265, 0.4961	0.0224, 0.5411
hydrogen refinement	H(C) constr, H(N) refall	mixed	mixed
refls in refinement	2361	2198	2030
parameters	140	140	140
restraints	0	0	0
$R(F_{obs})$	0.0242	0.0250	0.0246
$R_w(F^2)$	0.0616	0.0677	0.0630
S	1.090	1.072	1.075
shift/error$_{max}$	0.001	0.001	0.001
max electron density/e	0.335	0.334	0.348
min electron density/e	−0.279	-0.306	−0.451

Table S3. Crystallographic data of **[Cu(3ai)$_4$Cl]Cl** and **[Zn(3ai)$_2$Cl$_2$]**

	[Cu(3ai)$_4$Cl]Cl	**[Zn(3ai)$_2$Cl$_2$]**
net formula	$C_{12}H_{16}Cl_2CuN_8O_4$	$C_6H_8Cl_2N_4O_2Zn$
M_r/g mol^{-1}	470.77	304.43
crystal size/mm	0.060 × 0.050 × 0.030	0.040 × 0.030 × 0.030
T/K	173.(2)	110.(2)
radiation	MoKα	MoKα
diffractometer	'Bruker D8 Venture	'Bruker D8 Venture
crystal system	tetragonal	orthorhombic
space group	'P 4/n'	'P b c a'
a/Å	12.8511(17)	9.1479(8)
b/Å	12.8511(17)	13.2969(9)
c/Å	5.4910(7)	17.8319(14)
α/°	90	90
β/°	90	90
γ/°	90	90
V/Å^3	906.8(3)	2169.0(3)
Z	2	8
calc. density/g cm^{-3}	1.724	1.864
μ/mm^{-1}	1.537	2.742
absorption correction	Multi-Scan	Multi-Scan
transmission factor	0.91–0.95	0.85–0.92
refls. measured	20463	21652
R_{int}	0.0585	0.0471
mean σ(*I*)/*I*	0.0251	0.0256
θ range	3.711–28.276	2.934–27.482
observed refls.	1054	2089
x, *y* (weighting	0.0253, 0.4888	0.0191, 2.1288
hydrogen refinement	mixed	H(C) constr, H(N) refall
refls in refinement	1127	2478
parameters	71	152
restraints	0	0
$R(F_{obs})$	0.0225	0.0233
$R_w(F^2)$	0.0610	0.0590
S	1.115	1.108
shift/error$_{max}$	0.001	0.001
max electron density/e	0.279	0.357
min electron density/e	−0.446	−0.440

References

[1] A. Bruker, *Inc. Madison, Wisconsin, USA* **2012**.
[2] G. M. Sheldrick, *University of Göttingen, Germany* **1996**.
[3] O. D. L. CrysAlisPRO (Version 171.33.41), 2009.
[4] G. M. Sheldrick, *Acta Cryst. A* **2015**, *71*, 3-8.
[5] L. J. Farrugia, *J. Appl. Crystallogr.* **2012**, *45*, 849-854.
[6] a) J. Girniene, *Carbohydr. Res* **2003**, *338*, 711-719; b) J. Girniene, D. Gueyrard, A. Tatibouët, A. Sackus, P. Rollin, *Tetrahedron Lett.* **2001**, *42*, 2977-2980.
[7] S. Stairs, A. Nikmal, D.-K. Bučar, S.-L. Zheng, J. W. Szostak, M. W. Powner, *Nat. Commun.* **2017**, *8*, 1-12.
[8] Z. Huang, X. Huang, B. Li, C. Mou, S. Yang, B.-A. Song, Y. R. Chi, *J. Am. Chem. Soc.* **2016**, *138*, 7524-7527.
[9] M. W. Powner, B. Gerland, J. D. Sutherland, *Nature* **2009**, *459*, 239-242.

Author Contributions

T.C. supervised the research and wrote the original draft. J.F. designed the study, J.F., M.K.S, and M.L. performed the experiments, M.L. and P.M. generated the x-ray crystallographic data.

Anhang III

The Origin of Biomolecules Under Early Earth Conditions

Materials and Methods

General Information

Chemicals were purchased from Sigma-Aldrich, Fluka, ABCR, Carbosynth, TCI or Acros organics and used without further purification. The solvents were of reagent grade or purified by distillation. Chromatographic purification of products was accomplished using flash column chromatography on Merck Geduran Si 60 (40-63 µm) silica gel (normal phase). ^{1}H- and ^{13}C-NMR spectra were recorded on Bruker ARX 300, Varian VXR400S, Varian Inova 400, Bruker AMX 600 and Bruker AVIIIHD 400 spectrometers and calibrated to the residual solvent peak. Multiplicities are abbreviated as follows: s = singlet, d = doublet, t = triplet, q = quartet, m = multiplet, br = broad. High-resolution ESI spectra were obtained on the mass spectrometer Thermo Finnigan LTQ FT-ICR. IR measurements were performed on Perkin Elmer Spectrum BX FT-IR spectrometer with a diamond-ATR (Attenuated Total Reflection) setup. Melting points were measured on a Büchi B-540 device. For preparative HPLC purification a Waters 1525 binary HPLC Pump in combination with a Waters 2487 Dual Absorbance Detector was used, with a Nucleosil 100-7 C18 reversed phase column. The prebiotic reactions were analyzed by LC-ESI-MS on a Thermo Finnigan LTQ Orbitrap XL and were chromatographed by a Dionex Ultimate 3000 HPLC system. All chromatographic separations were performed on an Interchim Uptisphere120 3HDO C18 column with a flow of 0.15 ml/min and a constant column temperature of 30 °C. Eluting buffers were buffer A (2 mM $HCOONH_4$ in H_2O (pH 5.5)) and buffer B (2 mM $HCOONH_4$ in H2O/MeCN 20/80 (pH 5.5)). The gradient for isoxazole or pyrimidine nucleosides containing compounds and nucleosides was 0 → 25 min, 0% → 10% buffer B. The gradient for samples containing pyrimidine- and purine nucleosides was 0 → 10 min, 0% → 2%, 10 → 40 min, 2% → 10% buffer B. The elution was monitored at 223 nm, 243 nm and 260 nm (Dionex Ultimate 3000 Diode Array Detector). The gradient for one-pot guanidine formation was was 0 → 30 min, 40% → 80%, buffer B. The eluation was monitored at 260nm, 223nm, 230nm and 225nm. The chromatographic eluent was directly injected into the ion source without prior splitting. Ions were scanned by use of a positive polarity mode over a full-scan range of m/z 80-500 with a resolution of 30000. The synthetic standards for the co-injection experiments were synthesized in our lab according to reported literature[1-8] or purchased. The X-ray intensity data were measured on a Bruker D8 Venture TXS system equipped with a multilayer mirror monochromator and a Mo Kα rotating anode X-ray tube (λ = 0.71073 Å). The frames were integrated with the Bruker SAINT software package.[9] Data

were corrected for absorption effects using the Multi-Scan method (SADABS).[10] The structure was solved and refined using the Bruker SHELXTL Software Package.[11] All C-bound hydrogen atoms have been calculated in ideal geometry riding on their parent atoms while the N-bound hydrogen atoms have been refined freely. The figures have been drawn at the 50% ellipsoid probability level.[12]

Purine Nucleosides

Malondialdehyde (9)

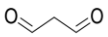

Synthetic reference:

Monohydrate sodium salt of **9***:* In a modified procedure of Grabowski and Autrey,[3] an emulsion of 1,1,3,3-tetraethoxypropane (95% purity; 115 mL, 450 mmol, 1.0 eq) in 1 M aq. HCl (40 mL) was stirred vigorously at r.t. for 90 min. The pH was adjusted to 12 with 5 M aq. NaOH (~ 50 mL) and acetone (750 mL) was added under stirring to allow precipitation. The mixture was stirred at 0 °C for 1.5 h and filtered. The residue was washed with acetone (100 mL) and dried under hv for 1 h to obtain a yellowish solid (25.2 g). The crude product was suspended in H_2O (30 mL) and vigorously stirred at r.t. for 20 min. After filtration, the residue was washed with acetone (100 mL) and dried under hv for 1 h to obtain an off-white powder (9.95 g). The crude product was again suspended in H_2O (9 mL) and vigorously stirred at r.t. for 20 min. After filtration, the residue was washed with acetone (100 mL) and dried under hv for 5 d to obtain the pure monohydrate sodium salt of malondialdehyde (3.36 g, 30.0 mmol, 7%) as a white powder. A 1 M aq. stock solution was prepared and stored aliquoted at -20 °C.

mp: 245 °C. **^{1}H-NMR** (400 MHz, D_2O) δ 8.62 (d, J = 10.1 Hz, 2H, CHO), 5.28 (t, J = 10.1 Hz, 1H, CH^-). **^{13}C-NMR** (101 MHz, D_2O) δ 192.9 (CHO), 109.5 (CH^-). **IR** (cm^{-1}): $\tilde{\nu}$ = 3334 (w), 2774 (w), 1718 (w), 1581 (s), 1365 (s), 1268 (s), 1164 (s), 1020 (m), 852 (w), 838 (m), 813 (s), 799 (w). **HRMS** (ESI^-): calc.: $[C_3H_3O_2]^-$ 71.0139, found: 71.0137. **Elemental analysis:** Calc. (found) for $C_3H_5NaO_3$: C, 32.16 (31.65); H, 4.50 (4.46); Na, 20.52 (20.49).

Sodium 1,3-dihydroxypropane-1,3-disulfonate (17)

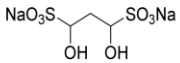

Synthetic reference:

An emulsion of 1,1,3,3-tetraethoxypropane (2.5 mL g, 10.0 mmol, 1.0 eq) in H_2O (2.0 mL) and aq. 2 M HCl (1.0 mL) was stirred vigorously at r.t. for 90 min. A solution of $NaHSO_3$ (2.08 g, 20.0 mmol, 2.0 eq) in H_2O (5 mL) was added dropwise and the resulting suspension was stirred at r.t. for 20 min. After filtration, the residue was washed with EtOH and Et_2O, and dried under high vacuum. Sodium 1,3-dihydroxypropane-1,3-disulfonate (**17**; 2.77 g, 9.89 mmol, quant.) was obtained as a white solid.

NMR analysis revealed a diastereomeric ratio of *dr* = 60 (*R*,*R* and *S*,*S*) : 40 (*meso*).

^{1}H-NMR (400 MHz, D_2O) δ 4.66 (dd, *meso*, *J* = 8.0, 5.1 Hz, 2H, CH), 4.58 (dd, *R*,*R* and *S*,*S*, *J* = 8.1, 5.4 Hz, 2H, CH), 2.57 (dt, *meso*, *J* = 14.7, 5.1 Hz, 1H, CH_2), 2.26 (dd, *R*,*R* and *S*,*S*, *J* = 8.1, 5.4 Hz, 2H, CH_2), 2.07 (dt, *meso*, *J* = 14.7, 8.0 Hz, 1H, CH_2). **^{13}C-NMR** (101 MHz, D_2O) δ 81.17 (*meso*, CH), 79.99 (*R*,*R* and *S*,*S*, CH), 34.39 (*meso*, CH_2), 33.30 (*R*,*R* and *S*,*S*, CH_2). **IR** (cm^{-1}): $\tilde{\nu}$ = 3541 (w), 3432 (w), 3325 (w), 1645 (mw), 1276 (w), 1181 (s), 1099 (m), 1049 (m), 1026 (s), 990 (w), 949 (w), 884 (w), 750 (w), 660 (m). **HRMS** (ESI^-): calc.: $[C_3H_6NaO_8S_2]^-$ 256.9407, found: 256.9406.

Prebiotic formation from malondialdehyde (**9**):

A solution of malondialdehyde (**9**) sodium salt monohydrate (40.0 mM) and $NaHSO_3$ (100 mM, 2.5 eq.) in H_2O (1.0 mL) was acidified with 2 M aq. HCl to pH 5.5. The solution was incubated at 25 °C and 500 rpm under a nitrogen flow to allow water to evaporate. After evaporation to dryness, the remaining solid was taken up in D_2O (1 mL) and analyzed by NMR spectroscopy using sodium acetate as an internal standard. The yield of sodium 1,3-dihydroxypropane-1,3-disulfonate (**17**) was found to be quantitative (Figure S1).

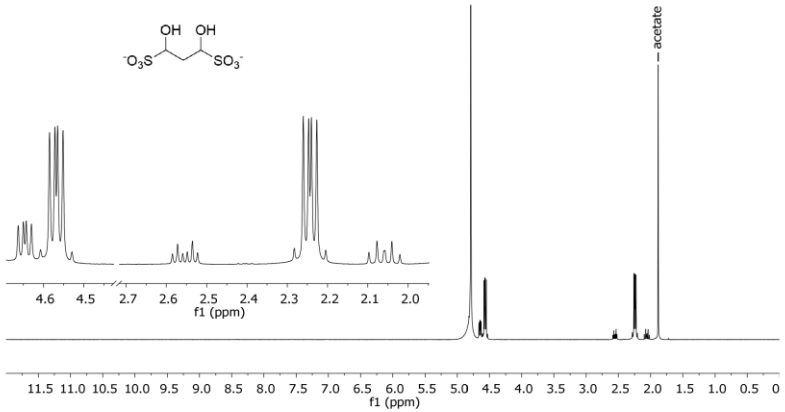

Figure S1: ^{1}H-NMR spectrum (400 MHz, D_2O, 0.0–12.0 ppm) of prebiotically enriched 1,3-dihydroxypropane-1,3-disulfonate (**17**).

Sodium 1,3-dihydroxy-2-(hydroxyimino)propane-1,3-disulfonate (27)

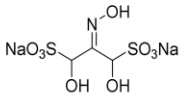

Synthetic reference:

An emulsion of 1,1,3,3-tetraethoxypropane (12.0 mL, 50.0 mmol, 1.0 eq) in 1 M aq. HCl (60 mL, 60 mmol, 1.2 eq) was stirred vigorously at r.t. for 2 h. The reaction mixture was treated with a solution of NaOAc · 3 H_2O (8.16 g, 60.0 mmol, 1.2 eq) in H_2O (20 mL) at 0 °C to adjust the pH to 2.5. A solution of $NaNO_2$ (4.14 mg, 60.0 mmol, 1.2 eq) in H_2O (10 mL) was added dropwise at 0 °C and the mixture was stirred at r.t. for 60 min. The reaction mixture was extracted with EtOAc (2 x 70 mL). The combined org. phases were treated with a solution of $NaHSO_3$ (10.4 g, 100 mmol, 2.2 eq) in H_2O (100 mL) and the emulsion was stirred vigorously at r.t. for 30 min. The aqueous phase was lyophilized to afford the crude product (6.40 g) in the presence of inorganic salts as an off-white powder.

NMR analysis revealed a diastereomeric ratio of *dr* = 67 (*R*,*R* and *S*,*S*) : 33 (*R*,*E*,*S* and *R*,*Z*,*S*).

^{1}H-NMR (400 MHz, D_2O) δ 5.93 (s, *R*,*R* and *S*,*S*, 1H, CH), 5.59 (s, *R*,*E*,*S* and *R*,*Z*,*S*, 1H, CH), 5.47 (s, *R*,*R* and *S*,*S*, 1H, CH), 5.33 (s, *R*,*E*,*S* and *R*,*Z*,*S*, 1H, CH). **^{13}C-NMR** (101 MHz, D_2O) δ 150.85 (*R*,*R* and *S*,*S*, CNOH), 149.34 (*R*,*E*,*S* and *R*,*Z*,*S*, CNOH), 82.80 (*R*,*E*,*S* and *R*,*Z*,*S*, CH), 82.25 (*R*,*E*,*S* and *R*,*Z*,*S*, CH), 79.44 (*R*,*R* and *S*,*S*, CH), 76.58 (*R*,*R* and *S*,*S*, CH). **IR** (cm^{-1}): $\tilde{\nu}$ = 3252 (w), 1634 (w), 1184 (s), 1036 (s), 863 (m).

Prebiotic formation:

A solution of malondialdehyde (**9**) sodium salt monohydrate (40.0 mM) and $NaNO_2$ (50.0 mM) in dil. AcOH (1% in H_2O; 1 mL) was incubated at r.t. and 500 rpm for 30 min. The mixture was then treated with $NaHSO_3$ (100 mM) and incubated at r.t. and 500 rpm for 30 min. For prebiotic enrichment, the reaction mixture was left at 25 °C and 500 rpm under a nitrogen flow to allow water to evaporate. After evaporation to dryness, the remaining solid was taken up in D_2O and quantified by NMR spectroscopy using maleic acid (MA) as internal standard (Figure S2). The yield was found to be 48%.

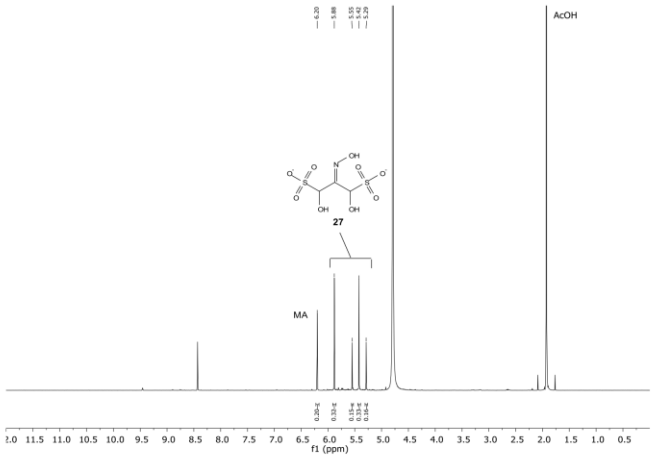

Figure S2: ^{1}H-NMR spectrum (400 MHz, D_2O, 0.0–12.0 ppm) of prebiotically enriched 1,3-dihydroxy-2-(hydroxyimino)propane-1,3-disulfonate (**27**).

(Hydroxyimino)malondialdoxime (28)

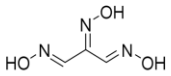

Synthetic reference:

An emulsion of 1,1,3,3-tetraethoxypropane (47.9 mL, 200 mmol, 1.0 eq) in 1 M aq. HCl (220 mL, 220 mmol, 1.1 eq) was stirred vigorously at r.t. for 30 min. The yellowish mixture was cooled to 0 °C and treated with a solution NaOAc · 3 H_2O (29.9 g, 220 mmol, 1.1 eq.) in H_2O (80 mL). A solution of $NaNO_2$ (15.2 g, 220 mmol, 1.1 eq.) in H_2O (40 mL) was added dropwise at 0 °C and the mixture was stirred at r.t. for 45 min. After the addition of NH_2OH (50% in H_2O; 27.0 mL, 440 mmol, 2.2 eq), the orange solution was stirred at r.t. for 60 min and 0 °C for another 60 min, during which a precipitate formed. The reaction mixture was filtered, and the residue was washed with H_2O. After drying under vacuum, (hydroxyimino)malondialdoxime (**28**; 12.6 g, 96.1 mmol, 48%) was obtained as a beige solid.

^{1}H-NMR (400 MHz, DMSO-d_6) δ 12.21 (s, 1H, OH), 11.92 (s, 1H, OH), 11.54 (s, 1H, OH), 8.14 (s, 1H, CH), 7.79 (s, 1H, CH). **^{13}C-NMR** (101 MHz, DMSO-d_6) δ 146.02 (C2), 144.07 (CH), 139.00 (CH). **IR** (cm^{-1}): $\tilde{\nu}$ = 3197 (m), 1474 (w), 1438 (w), 1392 (w), 1322 (w), 1279 (m), 1046 (m), 970 (s), 932 (s), 762 (m), 728 (s). **HRMS** (ESI^+): calc.: $[C_3H_6N_3O_3]^+$ 132.0404, found: 132.0406.

Prebiotic formation:

A solution of malondialdehyde (**9**) sodium salt monohydrate (40.0 mM) and $NaNO_2$ (50.0 mM) in dil. AcOH (1% in H_2O; 1 mL) was incubated at r.t. and 500 rpm for 30 min. The mixture was then treated with NH_2OH **7** (100 mM) and incubated at r.t. and 500 rpm for 30 min. The reaction was monitored via ^{1}H-NMR (Figure S3). For prebiotic enrichment, the reaction mixture was left at 25 °C and 500 rpm under a nitrogen flow to allow water to evaporate. After evaporation to dryness, the remaining solid was taken up in D_2O and quantified by NMR spectroscopy using maleic acid (MA) as internal standard (Figure S4). The yield was found to be 50%.

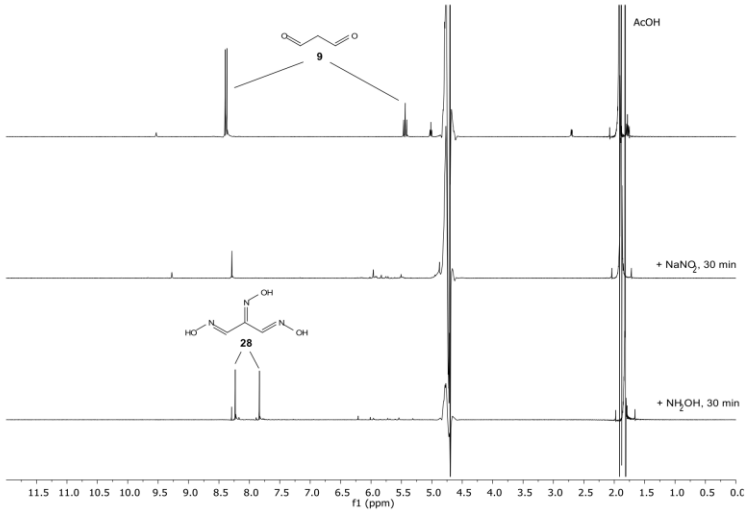

Figure S3: Conversion of malondialdehyde (**9**) to (hydroxyimino)malondialdoxime (**28**). ^{1}H-NMR spectra (400 MHz, D_2O, 0.0–12.0 ppm) before the addition of sodium nitrite (top); 30 min after the addition of sodium nitrite (middle); and 30 min after the addition of hydroxylamine (bottom).

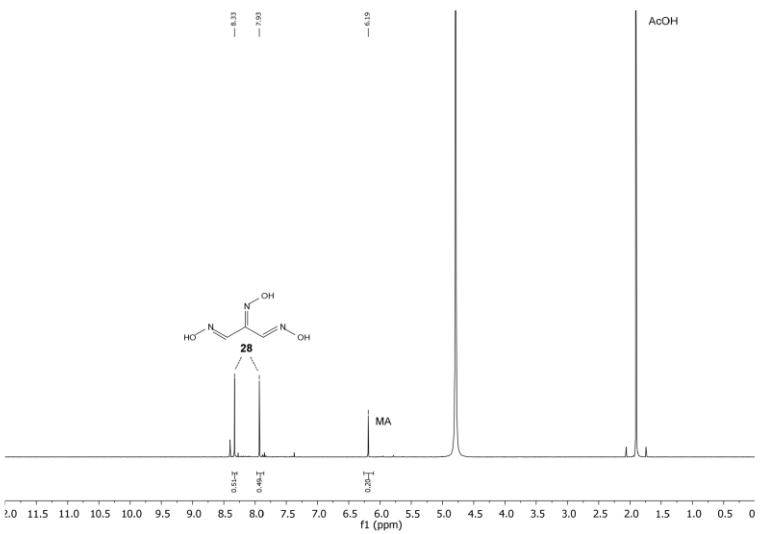

Figure S4: ^{1}H-NMR spectrum (400 MHz, D_2O, 0.0–12.0 ppm) of prebiotically enriched (hydroxyimino)malondialdoxime (**28**).

Guanidinium (12) salt of *N*-hydroxy-2-(hydroxyimino)acetimidoyl cyanide (29)

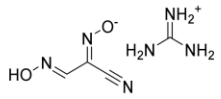

Prebiotic formation:

(Hydroxyimino)malondialdoxime (**28**; 3.93 g, 30.0 mmol, 1.0 eq) and guanidinium (**12**) carbonate (2.70 g, 30.0 mmol, 1.0 eq) were dissolved in H_2O (150 mL) in a 200 mL beaker at 60 °C. The solution was kept at 60 °C under an N_2 flow until the mixture was concentrated to 30 mL. The reaction mixture was placed in a fridge for 1 week open to the air. The orange crystals formed were filtered off to give the monohydrate of the desired salt (2.91 g, 15.3 mmol, 51%).

^{1}H-NMR (400 MHz, DMSO-d_6) δ 8.15 (s, 1H, CH), 7.12 (s, 6H, guanidinium). **^{13}C-NMR** (101 MHz, DMSO-d_6) δ 157.94 (guanidinium), 148.53 (CH), 126.15 (C2), 114.14 (CN). **IR** (cm^{-1}): $\tilde{\nu}$ = 3417 (m), 3350 (m), 3127 (m), 2210 (m), 1661 (s), 1575 (m), 1429 (s), 1256 (m), 1132 (s), 970 (s), 924 (s), 802 (s), 676 (s). **Crystallographic data**: Figure S29.

5-Nitrosopyrimidine-2,4,6-triamine (30)

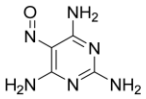

Prebiotic formation:

A suspension of (hydroxyimino)malondialdoxime (**28**; 65.5 mg, 500 µmol, 1.0 eq) and guanidinium (**12**) carbonate (90.1 mg, 500 µmol, 1.0 eq) in H_2O (500 µL) was left at 159 °C* for 20 min open to the air to allow water to evaporate. The residue was taken up in H_2O (3 mL) and the red solids were collected and dried to give 5-nitrosopyrimidine-2,4,6-triamine (32 mg, 208 µmol, 42%). The ^{1}H-NMR spectrum is shown in Figure S5.

^{1}H-NMR (400 MHz, DMSO-d_6) δ 10.25 (s, 1H, NH), 8.15 (s, 1H, NH), 7.81 – 7.67 (m, 1H, NH), 7.35 (s, 1H, NH), 7.20 (s, 2H, NH_2). **^{13}C-NMR** (101 MHz, DMSO-d_6) δ 166.11, 164.91, 151.02, 137.62. **IR** (cm^{-1}): $\tilde{\nu}$ = 1624 (s), 1520 (s), 1370 (s), 1253 (m), 1160 (s), 994 (m), 785 (s), 752 (m). **HRMS** (EI): calc.: [$C_4H_6N_6O$] 154.0603, found: 154.0599.

*) Melting point of the guanidine salt of (hydroxyimino)malononitrile.[2]

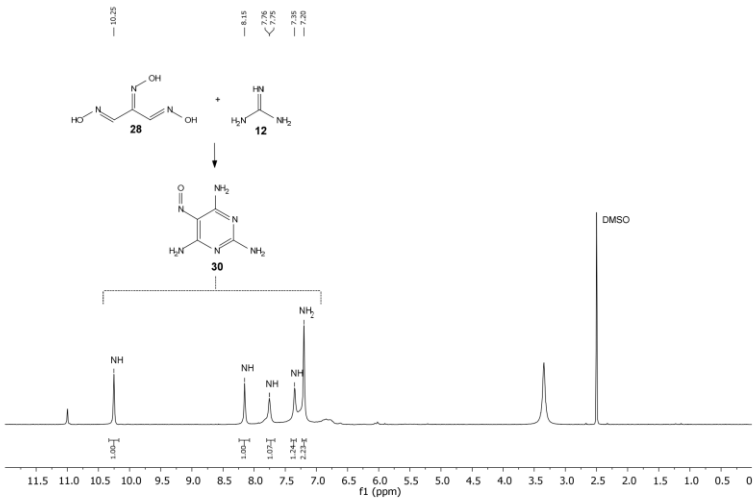

Figure S5: ^{1}H-NMR spectrum (400 MHz, DMSO-*d*6, 0.0–12.0 ppm) of prebiotically enriched 5-nitrosopyrimidine-2,4,6-triamine (**30**).

***N*-(2,4,6-Triaminopyrimidin-5-yl)formamide (FaPyDA; 32)**

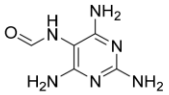

Prebiotic formation:

A suspension of 5-nitrosopyrimidine-2,4,6-triamine[2] (**30**; 231 mg, 1.50 mmol, 1.0 eq) and $NaHSO_3$ (312 mg, 3.00 mmol, 2.0 eq) in dil. HCOOH (5% in H_2O; 30 mL) was stirred at 90 °C for 10 h. The reaction mixture was evaporated to dryness and the residue taken up in H_2O (50 mL). The pH was adjusted to 8 by adding K_2CO_3. The mixture was concentrated (to about 1/10 of the volume) and left at r.t. for 5 days. The orange crystals formed were filtered off to give the *N*-(2,4,6-triaminopyrimidin-5-yl)formamide (**32**; 157 mg, 934 µmol, 62%).

^{1}H-NMR (400 MHz, DMSO-d_6) δ 8.60 (s, *cis*, 1H; NH), 8.08 (d, *trans*, J = 11.9 Hz, 1H; NH), 8.04 (s, *cis*, 1H; CHO), 7.69 (d, *trans*, J = 11.5 Hz, 1H; CHO), 5.74 (s, *trans*, 2H; C2NH_2), 5.56 (s, *trans*, 4H; C4NH_2 and C6NH_2), 5.55 (s, *cis*, 4H; C4NH_2 and C6NH_2), 5.46 (s, *cis*, 2H; C2NH_2). **^{13}C-NMR** (101 MHz, DMSO-d_6) δ 166.56 (*trans*, CHO), 166.33 (*trans*, C4 and C6), 161.67 (*cis*, CHO), 161.18 (*trans*, C2), 161.13 (*cis*, C2), 161.07 (*cis*, C4 and -C6), 160.11(*cis*, C4 and C6), 86.75 (*trans*, C5), 86.57 (*cis*, C5). **HRMS** (ESI^+): calc.: $[C_5H_9N_6O]^+$ 169.0832, found: 169.0833.

***N*-(2,4-Diamino-6-oxo-1,6-dihydropyrimidin-5-yl)formamide (FaPyG; 33)**

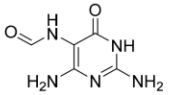

Prebiotic formation:

A suspension of 2,6-diamino-5-nitrosopyrimidin-4-ol[2] (**31**; 233 mg, 1.50 mmol, 1.0 eq) and $NaHSO_3$ (312 mg, 3.00 mmol, 2.0 eq) in dil. HCOOH (5% in H_2O; 30 mL) was stirred at 90 °C for 10 h. The reaction mixture was evaporated to dryness and the residue taken up in H_2O (50 mL). The pH was adjusted to 8 by adding K_2CO_3. The mixture was concentrated to about 1/10

of the volume. The orange solids were filtered off to give the *N*-(2,4-diamino-6-oxo-1,6-dihydropyrimidin-5-yl)formamide (**33**; 224 mg, 1.32 mmol, 88%).

^{1}H-NMR (400 MHz, DMSO-d_6) δ 10.32 (s, *cis*/trans, 2H; N_{arom}), 8.49 (d, *cis*, *J* = 1.6 Hz, 1H; NH), 7.99 (d, *cis*, *J* = 1.6 Hz, 1H; CHO), 7.85 (d, *trans*, *J* = 11.7 Hz, 1H; NH), 7.72 (d, *trans*, *J* = 11.7 Hz, 1H; CHO), 6.40 (s, *trans*, 2H; $C2NH_2$), 6.31 (s, *cis*, 2H; $C2NH_2$), 6.00 (s, *trans*, 2H; $C4NH_2$), 5.77 (s, *cis*, 2H; $C4NH_2$). **^{13}C-NMR** (101 MHz, DMSO-d_6) δ 166.90, 161.52, 160.70, 160.66, 160.01, 159.53, 153.56, 153.39, 88.66, 88.54. **HRMS** (ESI^+): calc.: $[C_5H_6N_5O_2]^-$ 168.0527, found: 168.0527.

Pyrimidine Nucleosides

Malondialdoxime (15)

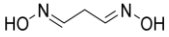

Synthetic reference:

In a modified procedure of Betke and Gröger,[4] a solution of hydroxylammonium chloride (12.2 g, 176 mmol, 4.0 eq.) in H_2O (40 mL) was degassed with argon. 1,1,3,3-Tetraethoxypropane (11.0 mL g, 44.0 mmol, 1.0 eq) was added and the resulting emulsion was stirred vigorously at 40 °C for 30 min. After cooling to r.t., Na_2CO_3 (9.33 g, 88.0 mmol, 2.0 eq) was added portion-wise under stirring. The suspension was stirred for 30 min at r.t., left at 0 °C for 1 h and filtered. The residue was washed with H_2O and dried under high vacuum to afford malondialdoxime (**15**; 1.94 g, 19.0 mmol, 43%) as a white solid.

mp: 137 °C. **^{1}H-NMR** (400 MHz, DMSO-d_6) δ 11.05 (s, 2H, OH), 6.78 (t, *J* = 5.3 Hz, 2H, CH), 3.19 (t, *J* = 5.3 Hz, 2H, CH_2). **^{13}C-NMR** (101 MHz, DMSO-d_6) δ 145.03 (CH), 22.69 (CH_2). **IR** (cm^{-1}): $\tilde{\nu}$ = 3082 (m), 3040 (m), 2850 (m), 1661 (m), 1489 (w), 1435 (s), 1400 (m), 1343 (w), 1321 (s), 1253 (m), 1048 (w), 971 (w), 946 (s), 928 (s), 860 (m), 784 (s), 748 (s), 677 (s). **HRMS** (ESI^+): calc.: $[C_3H_7N_2O_2]^+$ 103.0502, found: 103.0503.

Prebiotic formation:

For the prebiotic formation of malondialdoxime see page 18 (one-pot formation of 5-aminoisoxazole (**20**) from malondialdehyde (**9**).

5-Aminoisoxazole (20)

Prebiotic formation from malondialdoxime (**15**):

A solution of malondialdoxime (**15**; 40.0 mM) and Na_2CO_3 (5 eq.) in H_2O (2 mL) was incubated at 50 °C and 500 rpm for 4 h. The reaction was monitored via NMR (Figure S6). After 4 h, a sample (10 µL) was taken and diluted with H_2O (990 µL) for LC-MS analysis (injection volume: 10 µL). 5-Aminoisoxazole (**20**) was formed in 63% yield. The yield was determined by LC-MS measurements with the calibration curve prepared using synthetically produced 5-aminoisoxazole.

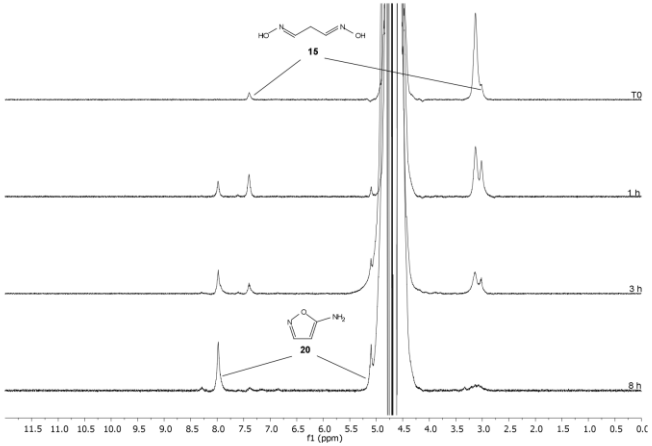

Figure S6: Conversion of malondialdoxime (**15**) to 5-aminoisoxazole (**20**). ^{1}H-NMR spectra (400 MHz, D_2O, 0.0–12.0 ppm) before the addition of hydroxylamine (top); as well as 1 after the addition of hydroxylamine.

Prebiotic one-pot formation from malondialdehyde (**9**):

A solution of malondialdehyde (**9**) sodium salt monohydrate (40.0 mM), Na_2CO_3 (5 eq.) and NH_2OH (2.5 eq.) in H_2O (2 mL) was incubated at 50 °C and 500 rpm for 8 h. The reaction was monitored via NMR (Figure S7). After 8 h, a sample (10 µL) was taken and diluted with H_2O (990 µL) for LC-MS analysis (injection volume: 10 µL). 5-Aminoisoxazole (**20**) was formed in 69% yield. The yield was determined by LC-MS measurements with the calibration curve prepared using synthetically produced 5-aminoisoxazole.

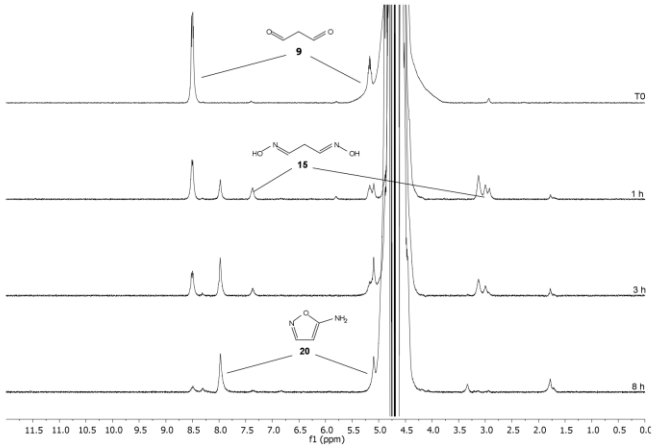

Figure S7: Conversion of malondialdehyde (**9**) to 5-aminoisoxazole (**20**). ^{1}H-NMR spectra (400 MHz, D_2O, 0.0–12.0 ppm) before the addition of hydroxylamine (top); as well as 1 after the addition of hydroxylamine.

Prebiotic one-pot formation from bisulfite-stabilized malondialdehyde (**17**) and enrichment:

A solution of malondialdehyde (**9**) sodium salt monohydrate (40.0 mM) and $NaHSO_3$ (2.5 eq.) in H_2O (1.0 mL) and the pH was adjusted to 5.5 with 2 M aq. HCl. The solution was incubated at 25 °C and 500 rpm under a nitrogen flow to allow water to evaporate. After evaporation to dryness, the remaining solid together with Na_2CO_3 (200 mM, 5 eq.) and NH_2OH (100 mM, 2.5 eq.) was dissolved in H_2O (1 mL). The suspension was incubated at 50 °C and 500 rpm for 4 h. A sample (10 µL) was taken and diluted with H_2O (990 µL) for LC-MS analysis (injection volume: 10 µL). 5-Aminoisoxazole (**20**) was formed in 65% yield. The yield was determined by LC-MS measurements with the calibration curve prepared using synthetically produced 5-aminoisoxazole (**20**). For prebiotic enrichment, the above-mentioned reaction mixture was left at 25 °C and 500 rpm under a nitrogen flow to allow water to evaporate. After evaporation to dryness, the remaining solid was taken up in D_2O (1 mL) and analyzed by NMR spectroscopy (Figure S8).

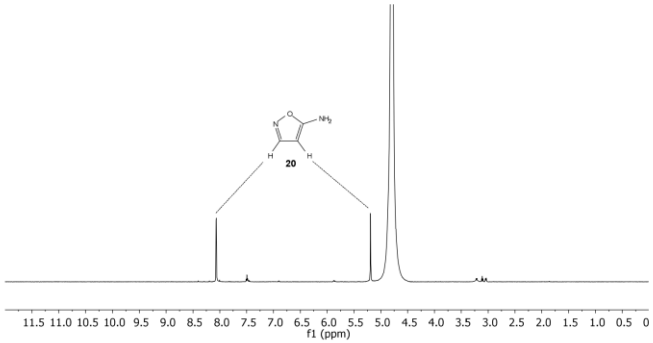

Figure S8: ^{1}H-NMR spectrum (400 MHz, D2O, 0.0–12.0 ppm) of prebiotically enriched 5-aminoisoxazole (**20**).

Prebiotic one-pot formation of **28**, **29**, and **20** from malondialdehyde (**9**):

A solution of malondialdehyde (**9**) sodium salt monohydrate (40.0 mM) and $NaNO_2$ (50.0 mM) in dil. AcOH (1% in H_2O; 1 mL) was incubated at 25 °C and 500 rpm for 30 min. The mixture was treated with NH_2OH (**6**; 5 eq), basified with Na_2CO_3 to pH 10.5 and incubated at 500 rpm and 25 °C for 1 h or at 50 °C for 4 h. The reactions were monitored via ^{1}H-NMR (Figure S9) revealing the formation of (hydroxyimino)malondialdoxime (**28**), *N*-hydroxy-2-(hydroxyimino)acetimidoyl cyanide (**29**), and 5-aminoisoxazole (**20**).

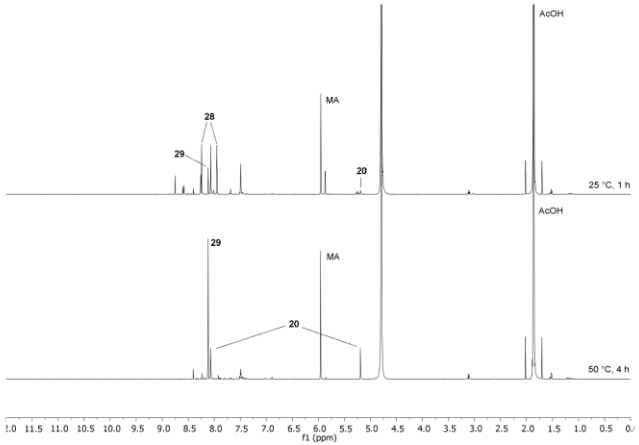

Figure S9: Conversion of malondialdehyde (**9**) to (hydroxyimino)malondialdoxime (**28**), *N*-hydroxy-2-(hydroxyimino)acetimidoyl cyanide (**29**), and 5-aminoisoxazole (**20**). ^{1}H-NMR spectra (400 MHz, D_2O, 0.0-12.0 ppm) monitoring the second reaction step after 1 h at 25 °C (top) and after 4 h at 50 °C (bottom). Maleic acid (MA) was used as an internal standard.

Synthetic reference:

Hydroxylamine (**6**; 50 wt% in H_2O; 10.2 g, 9.40 mL, 153 mmol, 1.1 eq) was added to 3-ethoxyacrylonitrile, mixture of *cis* and *trans,* (13.2 g, 14.0 mL, 136 mmol 1.00 eq) and stirred for 2 h at 65 °C. The crude product was purified by flash column chromatography (isohexan/EtOAc 3:2) to obtain the product (**20**; 5.92 g, 70.3 mmol, 52%) as slightly yellowish needles. For LC-MS measurements, a fraction of the product was further purified by reversed phase HPLC. The NMR spectrum of the isolated compound was identical to that of a commercial sample.

Crystallographic data: Figure S30.

1-(Isoxazol-5-yl)urea (22)

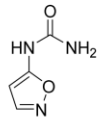

Prebiotic formation:

A solution of 5-aminoisoxazole (**20**; 10 µL, 10 µmol, 1 M, 1.0 eq) was added to a mixture of NaOCN (**21**; 2.60 mg, 40 µmol, 4.0 eq) and $ZnSO_4 \cdot 7\ H_2O$ (11.5 mg, 40 µmol, 4.0 eq.). The mixture was shaken at 65 °C and 450 rpm for 14 h in an Eppendorf ThermoMixer® open to the air to allow water to evaporate. The resulting residue was dissolved in water to a finale volume of 2 mL. A sample (100 µL) was taken and diluted with water (900 µL) to 1 mL for LCMS analysis (4 µL injection volume). Compound **22** was formed in 49% yield. The yield was determined by LC-MS measurement with the calibration curve prepared using synthetically produced 1-(isoxazol-5-yl)urea (**22**; Figure S10).

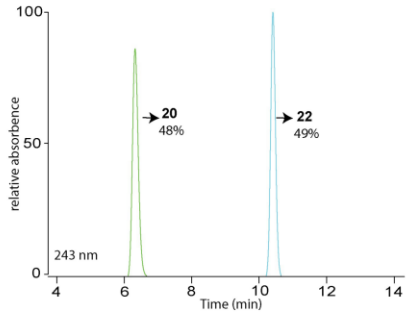

Figure S10: LCMS diagram for the formation of **22** from **20**.

Prebiotic formation with Co^{2+}:

A solution of 5-aminoisoxazole (**20**; 10 µL, 10 µmol, 1 M, 1.0 eq) was added to a mixture of NaOCN (**21**; 2.60 mg, 40 µmol, 4.0 eq) and $CoSO_4 \cdot 7\ H_2O$ (11.2 mg, 40 µmol, 4.0 eq.). The mixture was shaken at 65 °C and 450 rpm for 25 h in an Eppendorf ThermoMixer® open to the air to allow water to evaporate. The resulting residue was dissolved in water to a finale volume of 2 mL. A sample (100 µL) was taken and diluted with water (900 µL) to 1 mL for LCMS analysis (4 µL injection volume). Compound **22** was formed in 18% yield.

Prebiotic purification:

A solution of 5-aminoisoxazole (**20**; 100 µL, 100 µmol, 1 M, 1.0 eq) was added to a mixture of NaOCN (**27**; 26.0 mg, 400 µmol, 4.0 eq) and $ZnSO_4 \cdot 7\ H_2O$ (115 mg, 400 µmol, 4.0 eq.). The mixture was shaken at 65 °C and 450 rpm for 14 h in an Eppendorf ThermoMixer® open to the air to allow water to evaporate. The residue was dissolved in water (10 mL) and Na_2CO_3 (42.4 mg, 400 µmol, 4.0 eq.). The precipitate was filtered off and the filtrate was transferred into a 250 mL baker and left at RT for 7 days to allow for crystallization by concentration. The supernatant was removed and the formed solid residue was dissolved in D_2O.

22 (0.8 mg, 6.3 µmol, 6.5%) has been identified by comparison of the **^{1}H-NMR** spectra with synthetic material and the yield determined by 1,4-dioxane as internal standard (Figure S11).

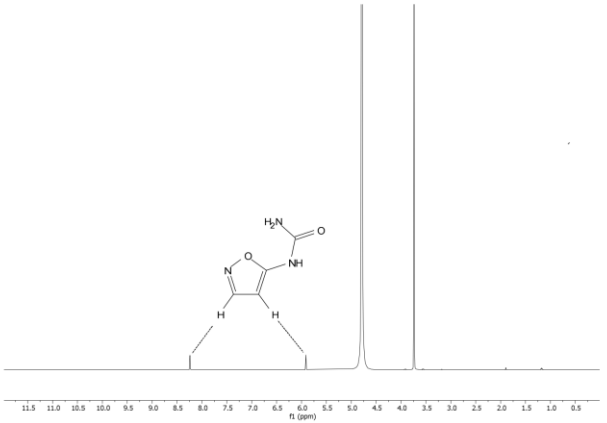

Figure S11: ^{1}H-NMR spectrum (400 MHz, D2O, 0.0–12.0 ppm) of prebiotically enriched 5-isoxazolylurea (**22**). The peak at 3.74 ppm refers to 1,4-dioxane, which has been used as an internal standard.

Synthetic reference:

5-Aminoisoxazole (**20**; 2.00 g, 23.8 mmol, 1.1 eq) was dissolved in MeCN (28 mL) under inert atmosphere. The reaction mixture was cooled down to 0 °C and trichloro acetylisocyanate (3.98 g, 2.50 mL, 21.1 mmol, 1.0 eq) was slowly added. The ice bath was removed and the reaction mixture stirred for 1.5 h at rt. The reaction was quenched with methanol (15 mL) and the solvents removed *in vacuo*. After co-evaporation with EtOH (2 x 25 ml) the residue was dissolved in methanolic ammonia (28 mL, 2 M) and stirred for 1.5 h at rt. The solvent was removed *in vacuo* and the crude product purified by flash column chromatography (DCM/MeOH 24:1). Product **22** (2.36 g, 18.6 mmol, 88%) was obtained as a white solid.

mp: 165 °C. **^{1}H-NMR** (400 MHz, DMSO-d_6) δ (ppm) = 10.05 (s, 1H, HN), 8.26 (d, ^3J = 1.9 Hz, 1H, HC3), 6.25 (s, 2H, H_2N), 5.88 (d, ^3J = 1.9 Hz, 1H, HC4). **^{13}C-NMR** (101 MHz, DMSO-d_6) δ (ppm) = 162.7 (C5), 152.9 (CO), 152.0 (C3), 84.1 (C4). **HRMS** (ESI$^-$): calc.: $[C_4H_4N_3O_2]^-$ 126.0309, found: 126.0309 [M-H]$^-$. **IR** (cm^{-1}): $\tilde{\nu}$ = 3464 (w), 3261 (w), 3195 (m), 3021 (w), 1734 (vs), 1699 (m), 1568 (vs), 1560 (vs), 1373 (s), 1326 (s), 1240 (m), 1189 (s), 1122 (m), 1045 (s), 980 (w), 911 (s), 864 (m), 853 (m), 805 (m), 770 (s). **Crystallographic data**: Figure S31.

Phenyl isoxazol-5-ylcarbamate (39)

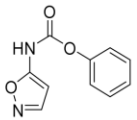

5-Aminoisoxazol (**20**; 6.00 g, 71.4 mmol, 1.00 eq.) was dissolved in dry MeCN (120 mL) and dry pyridine (5.48 g, 5.60 mL, 69.4 mmol, 0.97 eq.) under inert atmosphere. The reaction mixture was cooled down to 0 °C and phenyl chloroformate (13.6 g, 9.00 mL, 86.8 mmol, 1.22 eq.) was added dropwise. The ice bath was removed and the reaction mixture stirred for 15 h at rt. Water (120 mL) was added and the reaction mixture put in a refrigerator overnight. The formed precipitate was filtered off and washed with cold water to give the product (**39**; 9.63 g, 47.1 mmol, 66 %) as a yellow solid.

mp 195 °C. **^{1}H-NMR** (400 MHz, $CDCl_3$) δ (ppm) = 8.18 (dd, ^3J = 1.9, 0.8 Hz, 1H, HC3), 7.82 (s, 1H, NH), 7.46 – 7.39 (m, 2H, HCph3), 7.33 – 7.26 (m, 1H, HCph4), 7.22 – 7.18 (m, 2H, HCph2), 6.19 (s, 1H, HC4). **^{13}C-NMR** (101 MHz, $CDCl_3$) δ (ppm) = 160.2 (C5), 152.2 (C3), 150.2 (CO), 149.5 (Cph1), 129.8 (Cph3), 126.6 (Cph4), 121.4 (Cph2), 87.2 (C4). **HRMS** (ESI$^-$): calc.: $[C_{10}H_7N_2O_3]^-$ 203.0462, found: 203.0460 [M-H]$^-$. **IR** (cm^{-1}): $\tilde{\nu}$ = 3203 (vw), 3003 (vw), 1760 (s), 1612 (m), 1560 (s), 1494 (m), 1476 (m), 1340 (w), 1246 (s), 1221 (m), 1190 (vs), 1030 (m), 995 (w), 916 (s), 781 (s), 715 (s), 686 (vs).

1-(Isoxazol-5-yl)-*N'*-ribosyl-urea (24a-d)

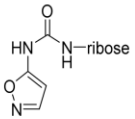

Prebiotic formation:

A solution of **22** (500 ul, 0.05 mmol, 100 mM) was mixed with ribose (**23**; 125 µl, 0.25 mmol, 2 M) and boric acid (50 ul, 0.025 mmol, 500 mM). The mixture was kept in an oven for 14 h at 80 °C. The sample was dissolved in H_2O (1 ml) and a sample (10 µL) was taken and diluted with water (990 µL) to 1 mL for LCMS analysis (4 µL injection volume). To confirm the structural integrity, the different pyrano-isomers **24c+d** were isolated by reversed phase HPLC in pure form.

Prebiotic formation and rearrangement:

A solution of **22** (500 ul, 0.05 mmol, 100 mM) is mixed with ribose (**23**; 83.3 µl, 0.25 mmol, 3 M) and boric acid (50 ul, 0.035 mmol, 500 mM). The mixture was kept in an oven for 14 h at 95 °C. The residue was dissolved in an aqueous borax solution (1.00 mL, 500 mM) and shaken for 3 h at 750 rpm at 75°C in an Eppendorf ThermoMixer®. A sample (10 µL) was taken and diluted with water (990 µL) to 1 mL for LCMS analysis (4 µL injection volume; Figure S12). The second reaction can be performed at different conditions to result different ratios for α/β and furano/pyrano isomers. When the glycosylation reaction is dissolved in an aqueous borax buffer (4.00 mL, 500 mM). A sample of 1 mL was taken from this solution and shaken for 1 h

at 750 rpm at 75°C in an Eppendorf ThermoMixer®. A sample (40 µL) was taken and diluted with water (960 µL) to 1 mL for LCMS analysis (4 µL injection volume; Figure S13).

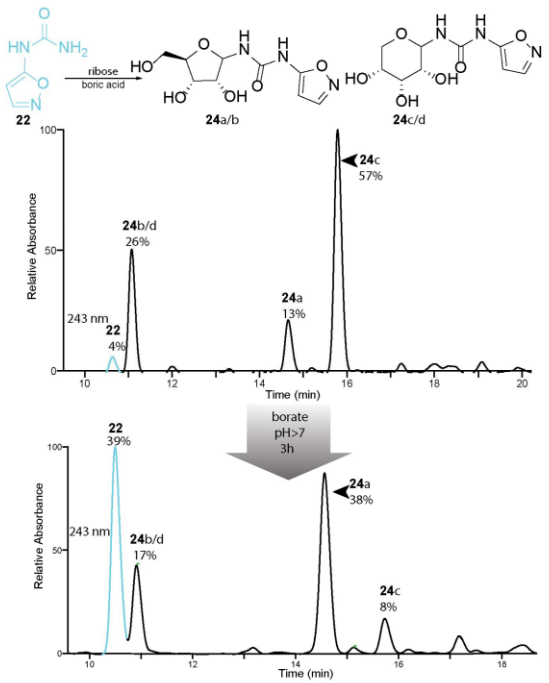

Figure S12: LC-MS analysis for the formation of **24a-d**. The UV-chromatograms at 243 nm are shown. The β-anomers **24b/d** could not be separated. a) Boric acid catalyzed ribosylation of **22** affords the four expected α and β anomers of isoxazolyl-urea ribosides **24a-d**. b) The mixture obtained in a) was heated in 500 mM borax at 75 °C for 3 h. The pyranoside products (**24c/d**) are converted into the furanoside products (**24a/b**), which was observed for the α-anomers and expected to happen for the β-anomers.

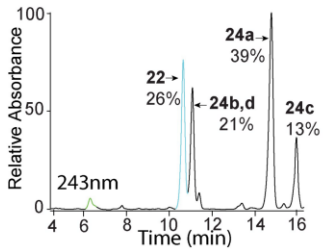

Figure S13: LC-MS analysis for the formation of **24a-d** under different conditions in the stereo-inversion step.

Synthetic reference:

β-D-Ribofuranosyl azide, 2,3,5-tribenzoate[6] (7.07 g, 14.5 mmol, 1.0 eq) was dissolved in THF (40 mL) and Pd/C (25 mg) was added. The mixture stirred for 19 h at rt under a H_2 atmosphere. It was filtered over celite 454 and the solvent removed *in vacuo*. The residue was dissolved in dry MeCN (120 mL) together with **39** (3.26 g, 16.0 mmol, 1.1 eq) under inert atmosphere. It was stirred for 72 h at rt and for additional 48 h at 45 °C. The solvent was removed *in vacuo* and the residue purified by flash column chromatography (DCM/MeOH 99/1 →49/1). The product was dissolved in methanolic ammonia (84 mL, 2 M) and stirred for 14 h at rt. The solvent was removed *in vacuo* and the residue purified by flash column chromatography (DCM/MeOH 9/1). Not completely deprotected fractions were collected and stirred in methanolic ammonia (42 mL, 2 M) for 16 h, The solvent was removed *in vacuo* and the residue purified by flash column chromatography (DCM/MeOH 9/1).

The products were combined to give the product (645 mg, 2.49 mmol, 17%) as a yellowish foam in a 2.25:1 mixture of α- and β-furanosides. The isomers were separated by reversed phase HPLC to confirm the structural integrity for the different furano-compounds **24a/b**.

α-Furanosyl-isomer 24a

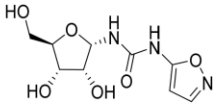

^{1}H-NMR (400 MHz, DMSO-d_6) δ (ppm) = 10.54 (s, 1H, NH), 8.33 (d, ^{3}J = 2.0 Hz, 1H, HC3), 7.07 (d, ^{3}J = 9.5 Hz, 1H, C1'NH), 5.95 (d, ^{3}J = 1.9 Hz, 1H, HC4), 5.50 – 5.44 (m, 2H, HC1', C2'OH), 5.10 (d, ^{3}J = 5.8 Hz, 1H, C3'OH), 4.70 (t, ^{3}J = 5.7 Hz, 1H, C5'OH), 3.94 (q, ^{3}J = 4.7 Hz, 1H, HC2'), 3.88 (td, ^{3}J = 6.0, 4.6 Hz, 1H, HC3'), 3.72 (ddd, ^{3}J = 6.2, 4.8, 3.2 Hz, 1H, HC4'), 3.48 (ddd, ^{3}J = 11.8, 5.5, 3.3 Hz, 1H, H_aC5'), 3.40 – 3.29 (m, 1H, H_bC5'). **^{13}C-NMR** (101 MHz, DMSO-d_6) δ (ppm) = 162.3 (C5), 152.1 (C3), 151.5 (CO), 84.4 (C4), 823 (C4'), 80.5 (C1'), 71.1 (C3'), 70.1 (C2'), 61.6 (C5')

β-furanosyl-isomer 24b

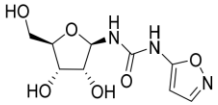

^{1}H-NMR (400 MHz, DMSO-d_6) δ (ppm) = 8.42 (s, 1H, NH), 8.31 (d, ^{3}J = 1.9 Hz, 1H, HC3), 8.16 (d, ^{3}J = 9.3 Hz, 1H, C1'NH), 5.95 (d, ^{3}J = 1.9 Hz, 1H, HC4), 5.20 (dd, ^{3}J = 9.3, 5.1 Hz, 1H, HC1'), 3.87 (t, ^{3}J = 4.7 Hz, 1H HC3'), 3.77 (t, ^{3}J = 5.1 Hz, 1H. HC2'), 3.66 (q, ^{3}J = 4.3 Hz, 1H, HC4'), 3.46 (dd, ^{3}J = 11.7, 4.0 Hz, 1H, H_aC5'), 3.38 (dd, J = 11.7, 4.7 Hz, 1H. H_bC5'). **^{13}C-NMR** (101 MHz, DMSO-d_6) δ (ppm) = 162.8 (C5), 152.3 (CO), 151.9 (C3), 84.8 (C1'), 84.4 (C4), 83.5 (C4'), 74.1 (C2'), 70.5 (C3'), 62.1 (C5').

α-pyranosyl-isomer 24c

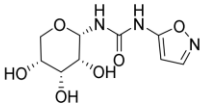

^{1}H-NMR (400 MHz, DMSO-d_6) δ (ppm) = 8.40 (s, 1H, NH), 8.33 (d, ^{3}J = 1.9 Hz, 1H, HC3), 7.48 (d, ^{3}J = 9.0 Hz, 1H, C1'NH), 5.95 (d, ^{3}J = 1.9 Hz, 1H, HC4), 5.02 (dd, ^{3}J = 8.9, 3.3 Hz, 1H, HC1'), 3.74 (t, J = 2.7 Hz, 1H, HC3'), 3.60 – 3.52 (m, 3H, HC2', HC4', H_aC5'), 3.35 – 3.31 (m, 1H, H_bC5'). **^{13}C-NMR** (101 MHz, DMSO-d_6) δ (ppm) = 162.5 (C5), 152.0 (C3), 151.8 (CO), 84.4 (C4) , 77.7 (C1'), 69.8 (C3'), 68.8 (C4'), 67.4 (C2'), 61.6 (C5').

β-pyranosyl-isomer 24d

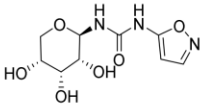

^{1}H-NMR (400 MHz, DMSO-d_6) δ (ppm) =8.41 (s, 1H, NH), 8.32 (d, ^{3}J = 1.9 Hz, 1H, HC3), 7.67 (d, ^{3}J = 8.9 Hz, 1H, HC1'NH), 5.95 (d, ^{3}J = 1.8 Hz, 1H, HC4), 4.89 (t, ^{3}J = 8.9 Hz, 1H, HC1'), 3.88 (q, ^{3}J = 2.7 Hz, 1H, HC3'), 3.49 (ddt, ^{3}J = 11.8, 6.5, 2.3 Hz, 1H, HC4'), 3.46 – 3.34 (m, 2H, H_aC5', H_bC5'), 3.23 (dd, ^{3}J = 8.9, 2.7 Hz, 1H, HC2'). **^{13}C-NMR** (101 MHz, DMSO-d_6) δ (ppm) = 163.1 (C5), 152.8 (CO), 152.4 (C3), 84.8 (C4), 78.2 (C1'), 71.2 (C3'), 70.1 (C2'), 67.5 (C4'), 64.6 (C5').

Prebiotic formation from 1-(isoxazol-5-yl)-N'-ribosyl-urea **24a/b**:

The reaction was handled under inert atmosphere. All solutions were degassed for 1 h with argon before usage. A solution of ribose isoxazole **24a**/**b** as a 2.25:1 mixture (25.9 mg, 0.1 mmol, 1.0 eq.) in water (0.5 ml) was added to a mixture of sodium carbonate (5.3 mg, 0.05 mmol, 0.5 eq.), DTT (23.1 mg, 1.5 mmol, 1.5 eq.) and FeS_2 (6.0 mg, 0.5 mmol, 0.5eq.) in a 15 ml falcon tube. The tube was sealed with a PTFE sealing tape and shaken for 4 h at 750 rpm at 100 °C in an Eppendorf ThermoMixer®. After cooling to rt, it was centrifuged and a sample (10 µL) was removed and diluted with H_2O (990 µL) to 1 ml. This diluted sample was used for LC-MS (4 µL) analysis according to the general information (Figure S14). The mechanism of the ring opening and the following rearrangement to uridine is shown in (Figure S15).

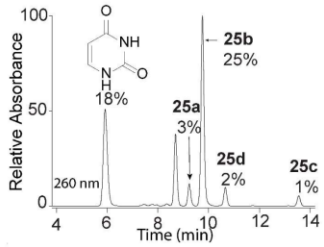

Figure S14: LC-MS analysis for the formation of **25a-d** starting from **24a/b**.

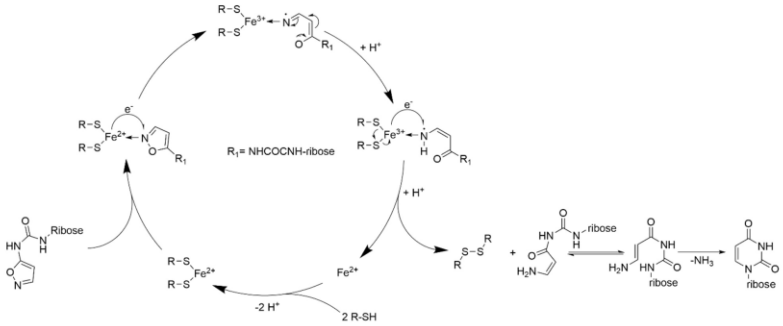

Figure S15: Mechanism for the Fe^{2+} catalyzed ring opening of **24** and the following rearrangement to form uridine nucleosides **25**.

Prebiotic one-pot formation from **22**:

The second step was handled under inert atmosphere. For this step solutions were degassed for 1 h with argon before usage. A solution of **22** (500 µl, 0.05 mmol, 100 mM) is mixed with ribose (**23**; 83 µl, 0.25 mmol, 3 M) and boric acid (25 µl, 0.013 mmol, 500 mM). The mixture was kept in an oven for 14 h at 95 °C. The residue was dissolved in 75 mM Na_2CO_3 (0.5 mL, pH 10) and added to DTT (11.6 mg, 0.075 mmol, 1.5 eq). An $(NH_4)_2Fe(SO_4)_2$ solution (10 µL, 0.075 µmol, 0.001 eq, 7.5 mM) was added and the mixture sealed with a PTFE sealing tape and shaken for 4 h at 750 rpm at 100°C in an Eppendorf ThermoMixer®. After cooling to rt, it was centrifuged and a sample (10 µL) was removed and diluted with H_2O (990 µL) to 1 ml. This diluted sample was used for LC-MS analysis according to the general information (4 µL injection volume; Figure S16).

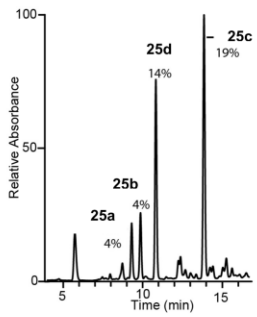

Figure S16: LC-MS analysis for the formation of **25a-d** and uracil in a one-pot reaction from **22**.

Guanidine (12)

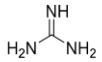

Prebiotic one-pot formation:

In a further developed procedure of Egami,[13] hydroxylamine (**6**; 50 wt% in H_2O, 306 µL, 5.00 mmol, 2.0 eq), formaldehyde (**7**; 37 wt%, 249 µL, 2.50 mMol, 1.0 eq.) and KCl (105 mg) were dissolved in H_2O (4 mL) and the resulting solution heated for 4d at 95 °C in a sealed pressure tube. After cooling to room temperature sat. aqueous ammonia (3 ml) was added and stirred for additional 60 h. The reaction mixture was freeze dried and the residue benzyloxycarbonyl-(Cbz)-protected with benzyl chloroformate[7] for analytical reasons. The crude reaction mixture was freeze dried again and dissolved in H_2O (6 mL) and MeCN (4 mL). A sample (200uL) has been taken and diluted with H_2O (480 µL) and MeCN (320 µL) for LCMS analysis (16 µL injection volume; Figure S17). Di-Cbz-protected guanidinie was formed and identified by comparison with authentic di-Cbz-protected guanidinie[7]. In the LCMS data also a quite big peak for mono-Cbz-protected guanidine (Figure S18) appeared and therefore no yields for total guanidine synthesis were determined. The Cbz protection was performed, since guanidine could not be detected by MS or UV during LCMS spectroscopy. However, the presence of residual unprotected guanidine **12** cannot be excluded. The amount of the protecting reagent (benzyl chloroformate) was calculated assuming a quantitative conversion of formaldehyde (**7**) to **12**.

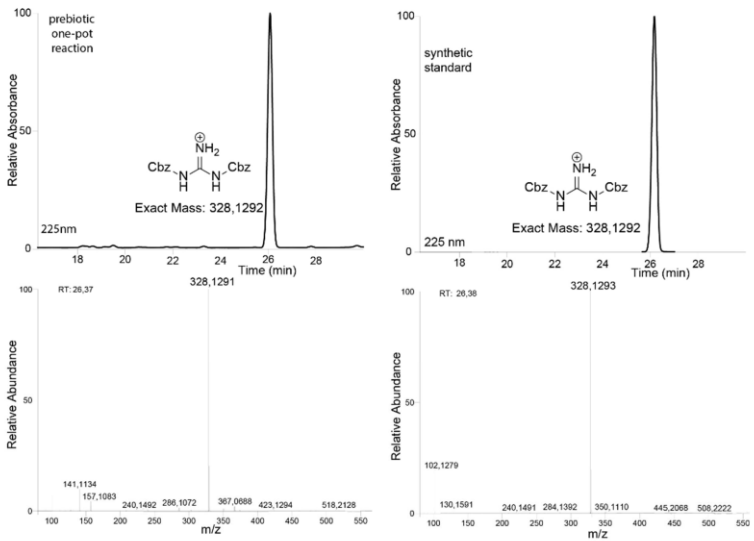

Figure S17: Comparison of the LCMS spectra of the one-pot formation and subsequent Cbz-protection of guanidine (left top) in comparison with an authentic synthetized standard[7] (right top). On the bottom the measured mass spectra at the time the di-Cbz-protected guanidinie 23 elutes (RT) for the corresponding UV-measurement.

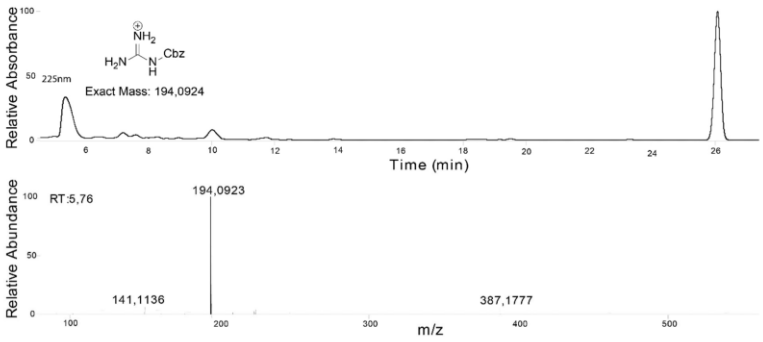

Figure S18: (Top) LCMS spectra of the one-pot synthesis of guanidine and subsequent Cbz-protection. The the (di-Cbz)-protected guanidinie 23 can be seen at 26 min retention time again. Additionally, the peak for the mono (Cbz)-protected product can be seen at 5 to 6 min and on the bottom the corresponding mass spectra for this peak. The mass corresponds to the expected product placed in the top part.

Amino Acids

Synthesis of Sulfonates

Sodium 1,2-dihydroxyethane-1-sulfonate (14a)

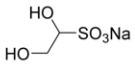

1,4-Dioxan-2,5-diol (300 mg, 2.50 mmol, 0.5 eq.) was dissolved in H_2O (1.0 mL) and 2M HCl (100 µL). A solution of $NaHSO_3$ (520 mg, 5.00 mmol, 1.0 eq.) in H_2O (2.5 mL) was added dropwise and the reaction mixture was stirred for 1h at room temperature. MeCN (10 mL) was added and formed precipitates were filtered off. The solvents were removed *in vacuo*. The residue was taken up in MeOH, filtered and the solvent removed *in vacuo* and the residue dried under high vacuum. The product was obtained as a white solid (720 mg, 4.39 mmol, 88%).

^{1}H-NMR (400 MHz, D_2O) δ 4.49 (dd, *J* = 8.2, 3.2 Hz, 1H, CH), 4.00 (dd, *J* = 12.1, 3.2 Hz, 1H, CH_2a), 3.71 (dd, *J* = 12.1, 8.2 Hz, 1H, CH_2b). **^{13}C-NMR** (101 MHz, D_2O) δ 83.72, 61.28. **IR** (cm^{-1}): $\tilde{\nu}$ = 3331 (w), 2359 (vw), 1343 (w), 1263 (m), 1178 (s), 1132 (m), 1079 (s), 1045 (vs), 989 (m), 894 (m), 703 (s). **HRMS** (ESI^-): calc.: $[C_2H_5O_5S]^-$ 140.9863, found: 140.9862.

Sodium 1,2,3-trihydroxypropane-1-sulfonate (14b)

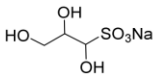

3,6-Dihydroxy-1,4-dioxan-2,5-dimethanol (450 mg, 2.5 mmol, 0.5 eq.) was dissolved in H_2O (1.0 mL) and 2M HCl (100 µL). A solution of $NaHSO_3$ (520 mg, 5.00 mmol, 1.0 eq.) in H_2O (2.5 mL) was added dropwise and the reaction mixture was stirred for 20 min at room temperature. MeCN (10 mL) was added and formed precipitates were filtered off. The solvents were removed *in vacuo*. The residue was taken up in MeOH, filtered and the precipitate dried under high vacuum. The product was obtained as a colorless oil (quantitative yield).

NMR analysis revealed an isomeric ratio of = 59 (*R*,*R* and *S*,*S*) : 41 (*R*,*S* and *S*,*R*).

^{1}H-NMR (400 MHz, D_2O) δ 4.44 (d, *R*,*S* and *S*,*R*, *J* = 6.1 Hz, 1H, SO_3CH), 4.41 (d, *R*,*R* and *S*,*S*, *J* = 3.1 Hz, 1H, SO_3CH), 4.11 (ddd, *R*,*R* and *S*,*S* *J* = 6.8, 5.3, 3.1 Hz, 1H, CH), 3.99 (m, *R*,*S* and *S*,*R*, 1H), 3.88 (dd, *R*,*S* and *S*,*R*, *J* = 12.1, 2.8 Hz, 1H, CH_2a), 3.75 – 3.70 (m, *R*,*S* and *S*,*R*,1H, CH_2b), 3.68 (dd, *R*,*R* and *S*,*S* *J* = 9.4, 6.1 Hz, 2H, CH_2). **^{13}C-NMR** (101 MHz, D_2O) δ 83.99 (*R*,*S* and *S*,*R*, SO_3CH), 82.12 (*R*,*R* and *S*,*S*, SO_3CH), 71.13 (*R*,*S* and *S*,*R*, CH) 70.20 (*R*,*R* and *S*,*S*, CH), 62.28 (*R*,*R* and *S*,*S*,CH_2)s, 61.87 (*R*,*S* and *S*,*R*, CH_2). **IR** (cm^{-1}): $\tilde{\nu}$ = 3375 (m), 2961 (vw), 1643 (vw), 1409 (w), 1174 (vs), 1068 (m), 1029 (vs), 703 (m). **HRMS** (ESI^-): calc.: $[C_3H_7O_6S]^-$ 170.9969, found: 170.9968.

Sodium 1,2-dihydroxypropane-1-sulfonate (14c)

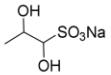

1,1-Dimethoxy-2-propanol (601 mg, 5.00 mmol, 1.0 eq.) was dissolved in H_2O (1.0 mL) and 2M HCl (500 µL) and stirred for 90 min at room temperature. A solution of $NaHSO_3$ (520 mg, 5.00 mmol, 1.0 eq.) in H_2O (2.5 mL) was added dropwise and the reaction mixture was stirred for 20 min. Isopropanol (15 mL) was added and formed precipitates were filtered off. The solvents were removed *in vacuo*. The residue was taken up in isopropanol, filtered and the precipitate dried under high vacuum. The product was obtained as a white solid (338 mg, 1.90 mmol, 38%).

NMR analysis revealed a mixture of isomers, but the signals are overlapping except for the signal at the carbon linked to the sulfonate, therefore the structures could not be assigned.

^{1}H-NMR (400 MHz, D_2O) δ 4.37 (m, 1H, SO_3CH), 4.22 – 4.20 (m, 1H, SO_3CH), 4.20 – 4.13 (m, 1H, CH), 1.27 (m, 3H, CH_3). **^{13}C-NMR** (101 MHz, D_2O) δ 86.37 (SO_3CH), 85.87 (SO_3CH), 66.81 (CH), 66.40 (CH), 18.73 (CH_3), 16.27 (CH_3). **IR** (cm^{-1}): $\tilde{\nu}$ = 3406 (m), 2974 (w), 1631 (w), 1379 (w), 1261 (m), 1191 (vs), 1136 (vs), 1112 (s), 1044 (vs), 1014 (s), 937 (m), 856 (m), 791 (w), 703 (m). **HRMS** (ESI^-): calc.: $[C_3H_7O_5S]^-$ 155.0020, found: 155.0019.

Sodium 1,2-dihydroxy-3-methylbutane-1-sulfonate (14d)

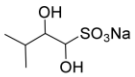

1,1-dimethoxy-3-methylbutan-2-ol[8] (741 mg, 5.00 mmol, 1.0 eq) was dissolved in H_2O (1.0 mL) and 2M HCl (500 µL) and stirred for 90 min at room temperature. A solution of $NaHSO_3$ (520 mg, 5.00 mmol, 1.0 eq.) in H_2O (2.5 mL) was added dropwise and the reaction mixture was stirred for 20 min. The formed precipitated was filtered off and dried under high vacuum. The product (183 mg, 1.23 mmol, 25%) was obtained as a white solid.

NMR analysis revealed an isomeric ratio of = 76 (*R*,*R* and *S*,*S*) : 24 (*R*,*S* and *S*,*R*).

^{1}H-NMR (400 MHz, D_2O) δ 4.91 (d, *R*,*R* and *S*,*S*, *J* = 5.5 Hz, 1H, SO_3CH), 4.17 (d, *R*,*S* and *S*,*R*, *J* = 4.3 Hz, 1H, SO_3CH), 3.73 (m, *R*,*S* and *S*,*R*, 1H, CH), 3.21 (t, *R*,*R* and *S*,*S*, *J* = 5.2 Hz, 1H, CH), 2.20 (pd, *R*,*S* and *S*,*R*, *J* = 6.9, 4.3 Hz, 1H, $(CH_3)_2CH$), 1.90-1.75 (m, *R*,*R* and *S*,*S*, 1H, $(CH_3)_2CH$), 1.00 (d, *J* = 6.9 Hz, 6H, CH_3), 0.92 – 0.83 (m, 6H, CH_3). **^{13}C-NMR** (101 MHz, D_2O) δ 93.29 (*R*,*S* and *S*,*R*, SO_3CH), 90.09 (*R*,*R* and *S*,*S*, SO_3CH), 81.02 (*R*,*S* and *S*,*R*, CH), 78.23 (*R*,*R* and *S*,*S*, CH), 29.29 (*R*,*S* and *S*,*R*, $(CH_3)_2CH$), 28.89 (*R*,*R* and *S*,*S*, $(CH_3)_2CH$), 18.62 (*R*,*R* and *S*,*S*, CH_3a) 18.01 (*R*,*S* and *S*,*R*, CH_3a) 15.83 (*R*,*S* and *S*,*R*, CH_3b), 15.67 (*R*,*R* and *S*,*S*, CH_3b). **IR** (cm^{-1}): $\tilde{\nu}$ = 3381 (w), 3321 (vw), 2961 (vw), 1641 (vw), 1257 (w), 1189 (vs), 1135 (m), 1067 (s), 1040 (vs), 969 (m), 838 (w), 752 (m), 701 (m). **HRMS** (ESI^-): calc.: $[C_5H_{11}O_5S]^-$ 183.0333, found: 183.0332.

Sodium 1,2-dihydroxy-3-phenylpropane-1-sulfonate (14e)

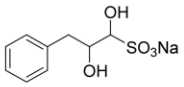

1,1-dimethoxy-3-phenylpropan-2-ol[8] (981 mg, 5.00 mmol, 1.0 eq) was dissolved in H_2O (1.0 mL) and 2M HCl (500 µL) and stirred for 2h at room temperature. A solution of $NaHSO_3$ (520 mg, 5.00 mmol, 1.0 eq.) in H_2O (2.5 mL) was added dropwise and the reaction mixture was stirred for 40 min at room temperature. MeCN (20 mL) was added and formed precipitates were filtered off. The solvents were removed *in vacuo*. The residue was taken up in isopropanol,

filtered and the solvent removed *in vacuo*. The residue was dried under high vacuum. The product was obtained as a colorless oil (982 mg, 3.86 mmol, 77%).

No mixture of isomers could be distinguished.

^{1}H-NMR (400 MHz, DMSO-d$_6$): δ 7.32 – 7.14 (m, 5H, CH_{phenyl}), 4.77 (d, *J* = 6.0 Hz, 1H, CHOH), 4.09 (d, *J* = 5.6 Hz, 1H, SO_3CH), 3.63 (dtd, *J* = 9.0, 5.8, 2.8 Hz, 1H, CH), 3.41 (s, 1H, SO_3CHOH), 2.80 (dd, *J* = 13.9, 2.8 Hz, 1H, CH_2a), 2.58 – 2.48 (m, 1H, CH_2b). **^{13}C-NMR (100 MHz DMSO-d$_6$):** δ 140.08 (C_{phenyl}), 129.92 (CH_{phenyl}), 128.34 (CH_{phenyl}), 126.12 (CH_{phenyl}), 107.14 (SO_3CH), 71.75 (CH), 38.36 (CH_2). **IR** (cm^{-1}): $\tilde{\nu}$ = 3449 (vw), 2993 (vw), 2832 (vw), 1453 (w), 1168 (s), 1128 (vs), 1056 (vs), 967 (vs), 750 (m), 699 (vs), 695 (s). **HRMS** (ESI^-): calc.: $[C_9H_{11}O_5S]^-$ 231.0333, found: 231.0333.

Synthesis of Oximes

2-Hydroxyacetaldehyde oxime (13a)

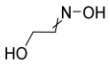

Prebiotic formation:

A 1 M solution of the sulfonate **14a** (100 µL, 0.10 mmol, 1.0 eq) in D_2O was mixed with hydroxylamine (**7**; 50 wt% in H_2O; 7.66 uL, 8.26 mg, 0.125 mmol, 1.25 eq), Na_2CO_3(53 mg, 0.50 mmol, 5.0 eq.) and D_2O (892 uL). The reaction mixture was shaken at 50 °C at 450 rpm for 4 h in an Eppendorf ThermoMixer®. The reaction mixture was analyzed by NMR spectroscopy using maleic acid as an internal standard. The yield of sodium 2-hydroxyacetaldehyde oxime (**13a**) was found to be quantitative (Figure S19).

NMR analysis revealed an isomeric ratio of 70 (*Z*) : 30 (*E*).

Synthetic reference:

In a 50 mL Falcon-tube added with a stirring bar, 1,4-dioxane-2,5-diol (1.20 g, 10.0 mmol, 0.5 eq.) was dissolved in water (7.55 mL). After adding hydroxylamine (**7**; 50 wt% in H_2O; 2.64 g, 2.45 mL, 40.0 mmol, 2.0 eq.), the white suspension was stirred for 1 hour at room temperature. After the clear solution was lyophilized, 2-hydroxyacetaldehyde oxime (**13a**) was obtained as a colorless oil (0.99 g, 13.2 mmol, 66%).

NMR analysis revealed an isomeric ratio of 7 (*Z*) : 93 (*E*).

^{1}H-NMR (400 MHz, D_2O) δ = 7.44 (t, *Z*, *J* = 5.1 Hz, 1H, CH), 6.84 (t, *E*, *J* = 3.8 Hz, 1H, CH), 4.31 (d, *E*, *J* = 3.9 Hz, 2H, CH_2), 4.08 (d, *Z*, *J* = 5.2 Hz, 2H, CH_2). **^{13}C-NMR** (101 MHz, D_2O) δ = 151.6 (*Z*, CH), 151.2 (*E*, CH), 58.4 (*E*, CH_2), 55.6 (*Z*, CH_2). **IR** (cm^{-1}): $\tilde{\nu}$ = 3243 (s), 2882 (w), 1635 (w), 1447 (m), 1282 (m), 1224 (w), 1104 (w), 1046 (s), 989 (vs), 931 (vs), 690 (vs). **HRMS** (ESI^+) calc.: $[C_2H_5NO_2]^+$ 76.0354, found: 76.0391.

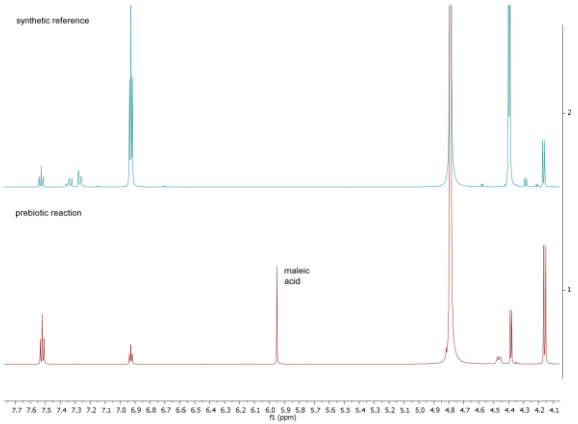

Figure S19: ^{1}H-NMR spectrum (400 MHz, D_2O, 4.1–7.7 ppm) of prebiotically and synthetically produced 2-hydroxyacetaldehyde oxime (**13a**). The *E*/*Z* ratio strongly varies depending on the synthetic conditions.

2,3-Dihydroxypropanal oxime (13b)

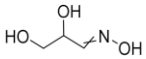

Prebiotic formation:

A 1M solution of sulfonate **14b** (100 µL, 0.10 mmol, 1.0 eq) in D_2O was mixed with hydroxylamine (**7**; 50 wt% in H_2O; 7.66 uL, 8.26 mg, 0.125 mmol, 1.25 eq), Na_2CO_3 (53 mg, 0.50 mmol, 5.0 eq.) and D_2O (892 uL). The reaction mixture was shaken at 50 °C at 450 rpm for 4 h in an Eppendorf ThermoMixer®. The reaction mixture was analyzed by NMR spectroscopy using maleic acid as an internal standard. The yield of sodium 2-hydroxyacetaldehyde oxime (**13b**) was found to be quantitative (Figure S20).

NMR analysis revealed an isomeric ratio of 84 (*Z*) : 16 (*E*).

Synthetic reference:

In a 2 ml Eppendorf tube 3,6-bis(hydroxymethyl)-1,4-dioxane-2,5-diol (180 mg, 1 mmol, 0.5 eq.) was dissolved in water (755 µL). After adding hydroxylamine (**7**; 50 wt% in H_2O; 264 mg, 245 µL, 4.00 mmol, 2.0 eq.), the resulting white suspension was shaken at 1000 rpm in an Eppendorf shaker for 1 hour. After lyophilization 2,3-dihydroxypropanal oxime (**13b**; 65.0 mg, 0.619 mmol, 31%) was obtained as colorless oil.

NMR analysis revealed an isomeric ratio of 76 (*Z*) : 24 (*E*).

^{1}H-NMR (400 MHz, D_2O) δ = 7.44 (d, *Z*, *J* = 5.9 Hz, 1H, HONCH), 6.79 (t, *E*, *J* = 5.7 Hz, 1H, HONCH), 4.87 (td, *E*, *J* = 5.8, 3.9 Hz, 1H, CH), 4.29 (td, *Z*, *J* = 6.0, 4.9 Hz, 1H, CH), 3.67 (d, *E*, *J* = 4.8 Hz, 2H, CH_2), 3.65 (d, *Z*, *J* = 6.0 Hz, 2H, CH_2). **^{13}C-NMR** (101 MHz, D_2O) δ = 152.2 (*E*, HONCH), 151.6 (*Z*, HONCH), 69.2 (*Z*, CH), 65.7 (*E*, CH), 63.1 (*Z*, CH_2), 62.3 (*E*, CH_2). **IR** (cm^{-1}): $\tilde{\nu}$ = 3248 (s), 2883 (m), 1607 (vw), 1416 (m), 1284 (m), 1210 (w), 1077 (s), 1031 (vs), 924 (vs), 873 (vs). **HRMS** (ESI^+) $[C_3H_7NO_3]^+$ calc.: 106.0459, found: 106.0498.

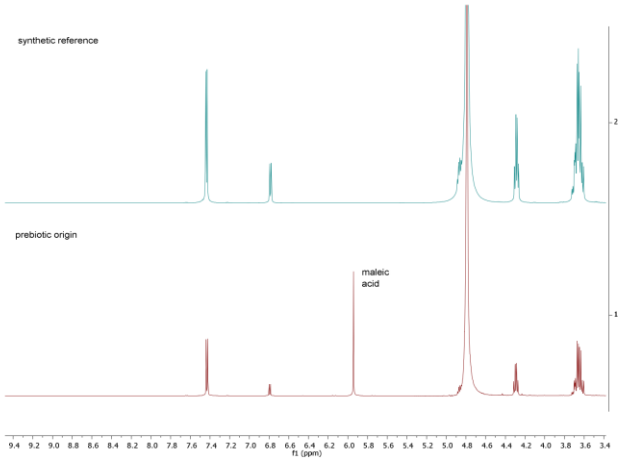

Figure S20: ^{1}H-NMR spectrum (400 MHz, D_2O, 3.4–9.4 ppm) of prebiotically and synthetically produced 2,3-dihydroxypropanal oxime (**13b**).

2-Hydroxypropanal oxime (13c)

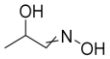

Prebiotic formation:

A 1M solution of the sulfonate **14c** (100 µL, 0.10 mmol, 1.0 eq) in D_2O was mixed with hydroxylamine (**7**; 50 wt% in H_2O; 7.66 uL, 8.26 mg, 0.125 mmol, 1.25 eq), Na_2CO_3 (53 mg, 0.50 mmol, 5.0 eq.) and D_2O (892 uL). The reaction mixture was shaken at 50 °C at 450 rpm for 4 h in an Eppendorf ThermoMixer®. The reaction mixture was analyzed by NMR spectroscopy using maleic acid as an internal standard. The yield of sodium 2-hydroxyacetaldehyde oxime (**13c**) was found to be 85% (Figure S21).

NMR analysis revealed an isomeric ratio of 85 (*Z*) : 15 (*E*).

Synthetic reference:

1,1-dimethoxypropan-2-ol (1.11 g, 10.0 mmol, 1.0eq.) was dissolved in water (10 mL). After the addition of DOWEX 50WX 8 (2.50 g), it was stirred at 50 °C for 3 h. DOWEX was filtered off, hydroxylamine solution 50 wt% in H_2O (755 mg, 700 µL, 11.4 mmol, 1.14 eq.) was added to the filtrate and the solution was stirred for 1.5 hours at room temperature. After lyophilization the crude product was purified by column chromatography (DCM/MeOH: 9:1) to obtain the product (303 mg, 3.39 mmol, 34%) as a colorless oil.

NMR analysis revealed an isomeric ratio of 76 (*Z*) : 24 (*E*).

^{1}H-NMR (400 MHz, D_2O) δ = 7.43 (d, *Z*, *J* = 6.0 Hz, 1H, HONCH), 6.81 (d, *E*, J = 5.8 Hz, 1H, HONCH), 4.98-4.88 (m, 1H, CH), 4.41-4.36 (m, 1H, CH), 1.28 (dd, *J* = 6.7, 3.1 Hz, 3H, CH_3). **^{13}C-NMR** (101 MHz, D_2O) δ = 155.8 (*E*, HONCH), 154.7 (*Z*, HONCH), 64.8 (*Z*, CH), 60.9 (*E*, CH), 21.9 (*Z*, CH_3), 18.6 (*E*, CH_3). **IR** (cm^{-1}): $\tilde{\nu}$ = 3270 (w), 2975 (w), 2933 (w), 1643 (w), 1605 (vw), 1447 (m), 1370 (m), 1291 (w), 1218 (s), 1161 (m), 1070 (s), 1027 (vs), 962 (m), 917 (s), 865 (s), 836 (s), 717 (s). **HRMS** (ESI^+) calc.: $[C_3H_7NO_2]^+$ 90.0510, found: 90.0549.

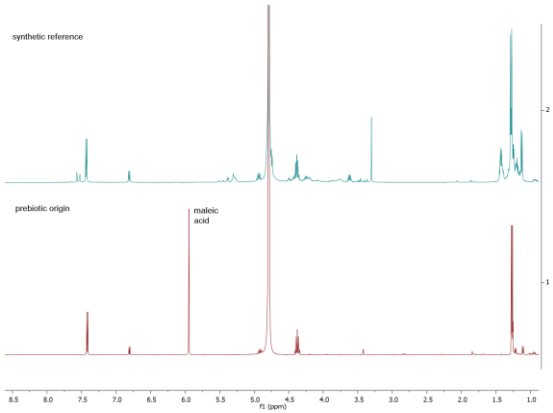

Figure S21: ^{1}H-NMR spectrum (400 MHz, D_2O, 1.0–8.5 ppm) of prebiotically and synthetically produced 2-hydroxypropanal oxime (**13c**).

2-Hydroxy-3-methylbutanal oxime (13d)

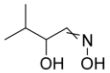

Prebiotic formation:

14d (22.0 mg, 0.10 mmol, 1.0 eq) was dissolved in D_2O (992 uL) together with hydroxylamine (**7**; 50 wt% in H_2O; 7.66 uL, 8.26 mg, 0.125 mmol, 1.25 eq) and Na_2CO_3 (53 mg, 0.50 mmol, 5.0 eq.). The reaction mixture was shaken at 50 °C at 450 rpm for 8 h in an Eppendorf ThermoMixer®. The reaction mixture was analyzed by NMR spectroscopy using maleic acid as an internal standard. The yield of sodium 2-hydroxyacetaldehyde oxime (**14d**) was found to be quantitative (Figure S22).

NMR analysis revealed just one variant of 85 (*Z*) : 15 (*E*).

Synthetic reference:

1,1-Dimethoxy-3-methylbutan-2-ol[8] (1.48 g, 10.0 mmol, 1.0 eq.) was dissolved in H_2O (10 mL). After the addition of DOWEX 50WX 8 (2.50 g), the reaction mixture was stirred at 50 °C for 4 h. DOWEX was filtered off, hydroxylamine solution 50 wt% in H_2O (755 mg, 700 µL, 11.4 mmol, 1.14 eq.) was added to the filtrate and the solution was stirred for 1h at room temperature. The crude product was purified by column chromatography (DCM/MeOH = 9/1) to obtain the product (468 mg, 3.99 mmol, 40%) as a yellowish solid.

NMR analysis revealed just one isomer.

^{1}H-NMR (400 MHz, D_2O) δ = 7.43 (d, *Z*, *J* = 7.1 Hz, 1H, HONCH), 6.70 (d, *E*, *J* = 6.8 Hz, 1H, HONCH), 4.48 (t, *E*, *J* = 6.8 Hz, 1H, CH), 3.91 (t, *Z*, *J* = 7.0 Hz, 1H, CH), 2.65 – 2.51 (m, *E*, 1H, CH), 1.84 (dp, *Z*, *J* = 13.7, 6.9 Hz, 1H, $(CH_3)_2CH$), 0.94 (d, *E*,s *J* = 8.4 Hz, 6H, CH_3). 0.91 (d, *Z*, *J* = 6.7 Hz, 3H, CH_3), 0.85 (d, *Z*, *J* = 6.9 Hz, 3H, CH_3).**^{13}C-NMR** (101 MHz, D_2O) δ = 151.4 (HONCH), 73.2 (CH), 32.4 ($(CH_3)_2CH$), 18.2 (CH_3). **IR** (cm^{-1}): $\tilde{\nu}$ = 3260 (m), 2963 (w), 2920 (m), 2871 (w), 1656 (vw), 1464 (m), 1381 (w), 1369 (w), 1346 (m), 1324 (w), 1304 (w), 1272 (w), 1145 (w), 1125 (w), 1025 (vs), 962 (vs), 945 (vs), 927 (vs), 917 (s), 842 (m), 801 (w), 738 (s). **HRMS** (ESI^+) calc.: $[C_5H_{11}NO_2]^+$ 118.0823, found: 118.0497.

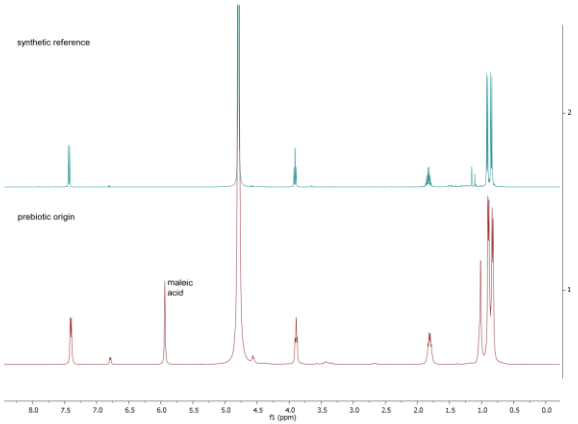

Figure S22: ^{1}H-NMR spectrum (400 MHz, D_2O, 1.0–8.5 ppm) of prebiotically and synthetically produced 2-hydroxy-3-methylbutanal oxime (**13d**).

2-Hydroxy-3-phenylpropanal oxime (13e)

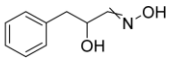

Prebiotic formation:

14e (25.4 mg, 0.10 mmol, 1.0 eq) was dissolved in D_2O (992 uL) together with hydroxylamine (**7**; 50 wt% in H_2O; 7.66 uL, 8.26 mg, 0.125 mmol, 1.25 eq) and Na_2CO_3(53 mg, 0.50 mmol, 5.0 eq.). The reaction mixture was shaken at 50 °C at 450 rpm for 8 h in an Eppendorf ThermoMixer®. The reaction mixture was analyzed by NMR spectroscopy using maleic acid as an internal standard. The yield of sodium 2-hydroxyacetaldehyde oxime (**13e**) was found to be 75% (Figure S23).

NMR analysis revealed an isomeric ratio of 81 (*Z*) : 19 (*E*).

Synthetic reference:

1,1-dimethoxy-3-phenylpropan-2-ol[8] (1.96 g, 10.0 mmol, 1.0 eq) and DOWEX 50WX 8 (5.0 g) were dissolved in H_2O (10 mL) and stirred at room temperature for 3 h. Dowex was filtered of and hydroxylamine 50 wt% in H_2O (1.35 g, 1.25 mL, 20.4 mmol, 2.04 eq) was added and the reaction mixture stirred at room temperature for 90 min. The solvent was removed by freeze drying and the crude product purified through column chromatogarphy (EtOAc/Isohex = 2/3) to yield the product as a yellowish oil (631 mg, 3.82 mmol, 38%).

NMR analysis revealed an isomeric ratio of 76 (*Z*) : 24 (*E*).

^{1}H-NMR (400 MHz, D_2O) δ = 7.45 (d, *Z*, *J* = 6.4 Hz, 1H, HONCH), 7.38 – 7.18 (m, *E*+*Z*, 5H, CH_{phenyl}), 6.79 (d, *E*, *J* = 6.0 Hz, 1H, HONCH), 5.06 (ddd, *E*, *J* = 7.9, 6.0, 5.0 Hz, 1H, CH), 4.45 (dt, *Z*, *J* = 7.4, 6.6 Hz, 1H, CH), 3.03 – 2.82 (m, *E*+*Z*, 2H, CH_2). **^{13}C-NMR** (101 MHz, D_2O) δ = 154.32 (*E*, HONCH), 153.54 (*Z*, HONCH), 137.02 (*E*, C_{phenyl}), 136.68 (*Z*, C_{phenyl}), 129.55 (*Z*, CH_{phenyl}), 129.48 (*E*, CH_{phenyl}), 128.58 (*Z*, CH_{phenyl}), 128.53 (*E*, CH_{phenyl}), 126.77 (*Z*, CH_{phenyl}), 126.75 (*E*, CH_{phenyl}), 69.71 (*Z*, CH), 65.33 (*E*, CH), 40.43 (*Z*, CH_3), 39.03 (*E*, CH_3). **IR** (cm^{-1}): $\tilde{\nu}$ = 3379 (vw), 2930 (w), 2832 (vw), 10603 (vw), 1495 (w), 1453, (m), 1276 (w), 1189 (m), 1128 (s), 1055 (vs), 974 (s), 749 (s), 699 (vs). **HRMS** (ESI^-) calc.: $[C_9H_{10}NO_2]^-$ 164.0717, found: 164.0717

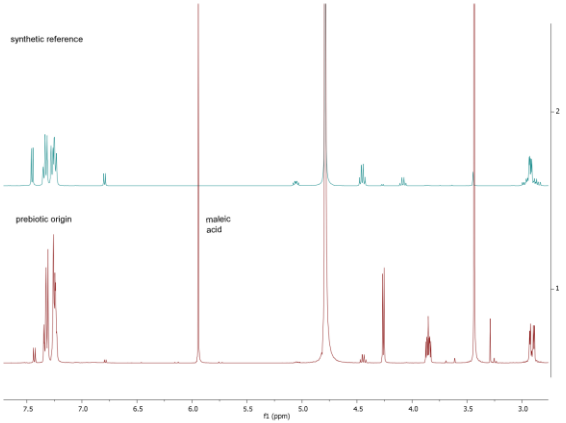

Figure S23: ^{1}H-NMR spectrum (400 MHz, D_2O, 3.0–7.5 ppm) of prebiotically and synthetically produced 2-hydroxy-3-phenylpropanal oxime (**13e**).

Synthesis of α-Hydroxynitriles

2-Hydroxyacetonitrile (15a)

Prebiotic formation from oximes:

A 1 M solution of 2-hydroxyacetaldehyde oxime (**13a**; 50 µL, 0.05 mmol, 1.0 eq.) was mixed with a buffer containing formic acid and NaHCOO (5 M/5 M, 200 µl). The mixture was shaken at 70 °C and 450 rpm for 6 h in an Eppendorf ThermoMixer® open to the air to allow water to evaporate. The residue was dissolved in D_2O and the solution was analyzed by NMR spectroscopy using maleic acid as an internal standard (0.5 eq.). The product was identified by comparison of the NMR with a commercial sample and the yield was determined to be 91% (Figure S24).

Prebiotic one-pot formation from sulfonates:

A 1 M solution of sodium 1,2-dihydroxyethane-1-sulfonate (**14a**; 100 µL, 0.1 mmol, 1.0 eq.) was mixed with Na_2CO_3 (26.5 mg, 0.25 mmol, 2.5 eq) and water (392 µL). To the resulting solution hydroxylamine (**7**; 50 wt% in H_2O; 7.66 uL, 8.26 mg, 0.125 mmol, 1.25 eq.) was added and it was shaken at 50 °C and 450 rpm for 4 h in an Eppendorf ThermoMixer®. A formic acid and NaHCOO containing buffer (10 M/10 M, 300 µl) was added to the reaction mixture and it was shaken at 70 °C and 450 rpm for 24 h in an Eppendorf ThermoMixer® open to the air to allow water to evaporate. The residue was dissolved in D_2O and the solution was analyzed by NMR spectroscopy using maleic acid as an internal standard (0.5 eq.). The product was identified by comparison of the NMR with a commercial sample and the yield determined to be 63% (Figure S24).

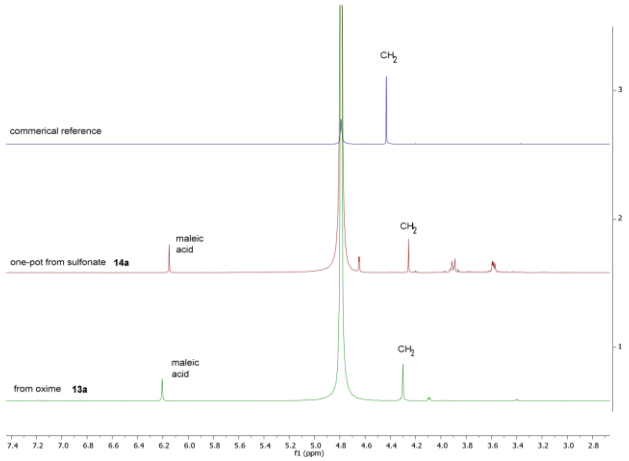

Figure S24: ^{1}H-NMR spectrum (400 MHz, D_2O, 2.8–7.4 ppm) for the prebiotic synthesis of 2-hydroxyacetonitrile (**15a**) from sulfonate **14a** (middle) and oxime **13a** (bottom) and the commercial reference (top).

2,3-Dihydroxypropanenitrile (15b)

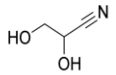

Prebiotic formation from oximes:

A 500 mM solution of 2,3-dihydroxypropanal oxime (**13b**; 100 µL, 0.05 mmol, 1.0 eq.) was mixed with a buffer containing formic acid and NaHCOO (5 M/5 M, 200 µl). The mixture was shaken at 70 °C and 450 rpm for 6 h in an Eppendorf ThermoMixer® open to the air to allow water to evaporate. The residue was dissolved in D_2O and the solution was analyzed by NMR spectroscopy using maleic acid as an internal standard (0.5 eq.). The product was identified by comparison of the NMR with a synthetic reference and the yield was determined to be 75% (Figure S25).

Prebiotic one-pot formation from sulfonate:

A 1M solution of sodium 1,2,3-trihydroxypropane-1-sulfonate (**14b**; 50 µL, 0.05 mmol, 1.0 eq.) was mixed with 2 M Na_2CO_3 in H_2O (50 µL, 0.10 mmol, 2.0 eq) and water (46 µL). To the resulting solution hydroxylamine (**7**; 50 wt% in H_2O; 3.83 uL, 4.13 mg, 0.063 mmol, 1.25 eq.) was added and it was shaken at 50 °C and 450 rpm for 4 h in an Eppendorf ThermoMixer®. A formic acid and NaHCOO containing buffer (6 M/4 M, 275 µl) was added to the reaction mixture and it was shaken at 50 °C and 450 rpm for 28 h in an Eppendorf ThermoMixer® open to the air to allow water to evaporate. The residue was dissolved in D_2O and the solution was analyzed by NMR spectroscopy using maleic acid as an internal standard (0.5 eq.). The product was identified by comparison of the NMR with the synthetic standard and the yield determined to be 28% (Figure S25).

Synthetic reference:

1,4-Dioxane-2,5-diol (1.88 g, 15.7 mmol, 1.0 eq.) was dissolved in water (100 mL). After the addition of potassium cyanide (2.45 g, 37.6 mmol, 2.4 eq.), the reaction batch was adjusted with 2 M hydrochloric acid to pH 3-4. The reaction mixture was stirred for 4 h at room temperature. The solution was degassed with N_2 for 2 h to remove remaining hydrocyanic acid. The water was removed by rotary evaporation and the residue was dissolved in isopropanol (100 mL). The resulting white suspension was filtered, and the solvent was removed from the filtrate by rotary evaporation. 2,3-dihydroxypropanenitrile (**15b**; 2.28 g, 26.2 mmol, 84 %) was obtained as brown oil.

^{1}H-NMR (400 MHz, D_2O) δ = 4.67 (t, J = 4.8 Hz, 1H, CH), 3.79 (d, J = 4.8 Hz, 2H, CH_2). **^{13}C-NMR** (101 MHz, D_2O) δ = 117.6 (CN), 62.6 (CH), 61.7 (CH_2). **IR** (cm^{-1}): $\tilde{\nu}$ =3290 (m), 2943 (w), 2653 (w), 2247 (w), 1770 (vw), 1667 (vw), 1516 (vw), 1417 (w), 1323 (w), 1230 (w), 1204 (w), 1148 (w), 1094 (vs), 1056 (vs), 1007 (s), 935 (w), 900 (m), 873 (w), 819 (m), 701 (s).

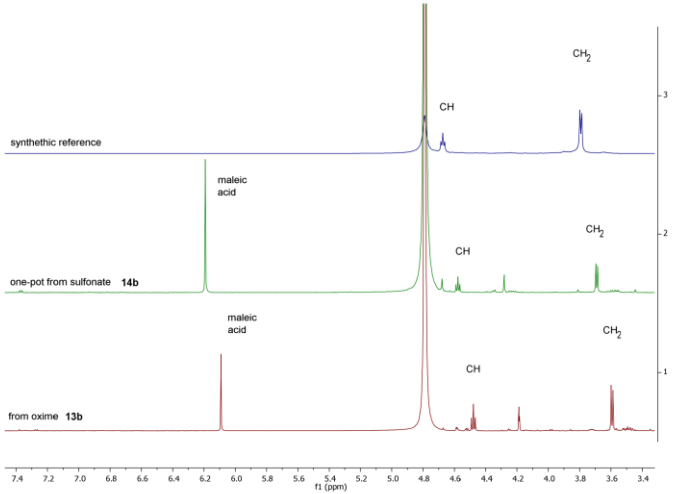

Figure S25: ^{1}H-NMR spectrum (400 MHz, D_2O, 3.4–7.4 ppm) for the synthesis of 2-hydroxyacetonitrile (**15b**) from sulfonate **14b** (middle) and oxime **13b** (bottom) and the synthetic standard (top).

2-Hydroxypropanenitrile (15c)

Prebiotic origin from oximes:

A 500 mM solution of 2-hydroxypropanal oxime (**15c**; 100 µL, 0.10 mmol, 1.0 eq.) was mixed with a buffer containing formic acid and NaHCOO (5 M/5 M, 250 µl). The mixture was shaken at 50 °C and 450 rpm for 48 h in an Eppendorf ThermoMixer® open to the air to allow water to evaporate. The residue was dissolved in D_2O and the solution was analyzed by NMR spectroscopy using maleic acid as an internal standard (0.5 eq.). The product was identified by comparison of the NMR with a commercial sample and the yield was determined to be 78% (Figure S26).

Prebiotic one-pot formation from sulfonates:

A 1M solution of sodium 1,2-dihydroxypropane-1-sulfonate (**14c**; 50 µL, 0.05 mmol, 1.0 eq.) was mixed with an aqueous 2 M Na_2CO_3 solution (50 µL, 0.10 mmol, 2.0 eq) and water (46 µL). To the resulting solution hydroxylamine (**7**; 50 wt% in H_2O; 3.83 uL, 4.13 mg, 0.063 mmol, 1.25 eq.) was added and it was shaken at 50 °C and 450 rpm for 4 h in an Eppendorf ThermoMixer®. A formic acid and NaHCOO containing buffer (6 M/4 M, 330 µl) was added to the reaction mixture and it was shaken at 50 °C and 450 rpm for 48 h in an Eppendorf ThermoMixer® open to the air to allow water to evaporate. The residue was dissolved in D_2O and the solution was analyzed by NMR spectroscopy using maleic acid as an internal standard (0.5 eq.). The product was identified by comparison of the NMR with a commercial sample and the yield determined to be 36% (Figure S26).

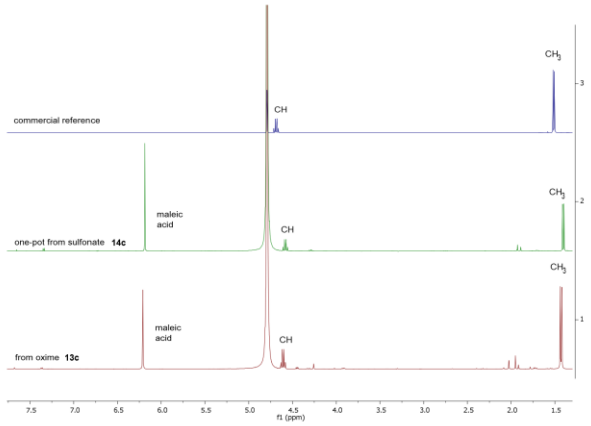

Figure S26: ^{1}H-NMR spectrum (400 MHz, D_2O, 1.5–7.5 ppm) for the synthesis of 2-hydroxypropanenitrile (**15c**) from sulfonate **14c** (middle), oxime **13c** (bottom) and the synthetic standard (top).

2-Hydroxy-3-methylbutanenitrile (15d)

Prebiotic formation from oximes:

2-Hydroxy-3-methylbutanal oxime (**13d**; 5.9 mg, 0.05 mmol, 1.0 eq.) was mixed with a buffer containing formic acid and NaHCOO (10 M/10 M, 200 µl). The mixture was shaken at 50 °C and 450 rpm for 72 h in an Eppendorf ThermoMixer® open to air to allow water to evaporate. The residue was dissolved in D_2O and the solution was analyzed by NMR spectroscopy using maleic acid as an internal standard (0.5 eq.). The product was identified by comparison of the NMR with a synthetic reference and the yield was determined to be quantitative (Figure S27).

Prebiotic one-pot formation from sulfonates:

Sodium 1,2-dihydroxy-3-methylbutane-1-sulfonate (**14d**; 20.6 mg, 0.10 mmol, 1.0 eq.) was mixed with 2 M Na_2CO_3 in H_2O (100 µL, 0.20 mmol, 2.0 eq.) and water (92 µL). To the resulting solution hydroxylamine (**7**; 50 wt% in H_2O; 7.88 uL, 8.26 mg, 0.125 mmol, 1.25 eq.) was added and it was shaken at 50 °C and 450 rpm for 4 h in an Eppendorf ThermoMixer®. A formic acid and NaHCOO containing buffer (6 M/4 M, 500 µl) was added to the reaction mixture and it was shaken at 70 °C and 450 rpm for 18 h in an Eppendorf ThermoMixer® open to the air to allow water to evaporate. The residue was dissolved in D_2O and the solution was analyzed by NMR spectroscopy using maleic acid as an internal standard (0.5 eq.). The product was identified by comparison of the NMR with the synthetic standard and the yield determined to be 84% (Figure S27).

Synthetic reference:

Isobutyraldehyde (1.00 g, 1.27 mL, 13.9 mmol, 1.0 eq.) was dissolved in H_2O (10 mL) and Et_2O (17 mL), KCN (2.53 g, 38.8 mmol, 2.8 eq.) was added and the reaction mixture vigorously stirred overnight. The phases were separated and the aqueous phase extracted with Et_2O (3 x 20 mL). The combined organic layers were dried over $MgSO_4$, filtered and the solvent removed *in vacuo*. The crude product was purified by column chromatography (DCM /MeOH = 39 /1) to yield 2-hydroxy-3-methylbutanenitrile **15d** (650 mg, 6.56 mmol, 47%) as a colorless liquid.

The NMR data correspond to the literature.[14]

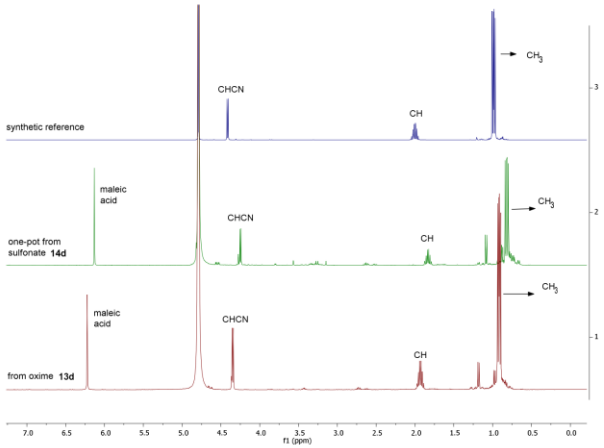

Figure S27: ^{1}H-NMR spectrum (400 MHz, D_2O, 0.4–6.4 ppm) for the synthesis of 2-hydroxy-3-methylbutanenitrile (**15d**) from sulfonate **14d** (middle), oxime **13d** (bottom) and the synthetic standard (top).

2-Hydroxy-3-phenylpropanenitrile (15e)

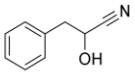

Prebiotic formation from oximes:

2-Hydroxy-3-phenylpropanal oxime (**13e**; 16.5 mg, 0.05 mmol, 1.0 eq.) was mixed with a buffer containing formic acid and NaHCOO (5 M/5 M, 300 µl). The mixture was shaken at 50 °C and 450 rpm for 72 h in an Eppendorf ThermoMixer® open to the air to allow water to evaporate. The residue was dissolved in D_2O and the solution was analyzed by NMR spectroscopy using maleic acid as an internal standard (0.5 eq.). The product was identified by comparison of the NMR with a synthetic reference and the yield was determined to be 82% (Figure S28).

Prebiotic one-pot formation from sulfonates:

Sodium 1,2-dihydroxy-3-phenylpropane-1-sulfonate (**14e**; 12.7 mg, 0.05 mmol, 1.0 eq.) was mixed with 2 M Na_2CO_3 in H_2O (50 µL, 0.10 mmol, 2.0 eq.) and water (46 µL). To the resulting solution hydroxylamine (**7**; 50 wt% in H_2O, 3.84 uL, 4.13 mg, 0.063 mmol, 1.25 eq) was added an it was shaken at 50 °C and 450 rpm for 4 h in an Eppendorf ThermoMixer®. A formic acid and NaHCOO containing buffer (6 M/4 M, 600 µl) was added to the reaction mixture and it was shaken at 70 °C and 450 rpm for 24 h in an Eppendorf ThermoMixer® open to the air to allow water to evaporate. The residue was dissolved in D_2O and the solution was analyzed by NMR spectroscopy using maleic acid as an internal standard (0.5 eq.). The product was identified by comparison of the NMR with the synthetic standard and the yield determined to be 20% (Figure S28).

Synthetic reference:

KCN (650 mg, 10.0 mmol, 1.67 eq.) was dissolved in water (2 mL) and Et_2O (4 mL) and the resulting solution cooled to 0 °C. 2-phenylacetaldehyde (721 mg, 700 µL, 6.00 mmol, 1.0 eq.) and acetic acid (572 µL) were added dropwise to the solution and the reaction mixture stirred for 2h at room temperature. The phases were separated and the aqueous phase extracted with Et_2O (3 x 10 mL), the combined organic layers dried over $MgSO_4$, filtered and the solvent

removed *in vacuo*. The crude product was purified by column chromatography (Isohex/EtOAC = 3/1) to yield the product (733 mg, 4.98 mmol, 83%) as a yellow oily liquid.

^{1}H-NMR (400 MHz, D_2O) δ = 7.34 – 7.22 (m, 5H, CH_{phenyl}), 6.53 (d, J = 6.3 Hz, 1H, HONCH), 4.73 (q, J = 7.0 Hz, 1H, CH), 2.99 (dd, J = 7.1, 2.7 Hz, 2H CH_2). **^{13}C-NMR** (101 MHz, D_2O) δ =135.74 (C_{phenyl}), 129.67 (CH_{phenyl}), 128.29 (CH_{phenyl}), 126.94 (CH_{phenyl}), 121.01 (HONCH), 61.28 (CH), 40.83 (CH). **IR** (cm^{-1}): $\tilde{\nu}$ = 3372 (m), 3030 (vw), 2266 (vw), 1495 (w), 1456 (w), 1419 (w), 1279 (m), 1127 (w), 1080 (m), 1063 (s), 1026 (m), 970 (m), 829 (w), 801 (m), 748 (vs), 700 (vs).

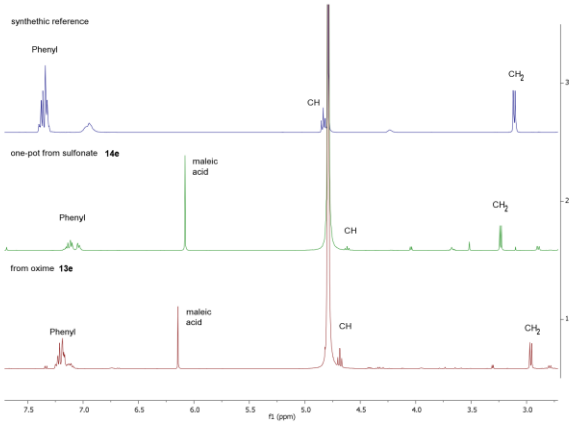

Figure S28: ^{1}H-NMR spectrum (400 MHz, D2O, 3.0–7.5 ppm) for the synthesis of 2-hydroxy-3-phenylpropanenitrile (**15e**) from sulfonate **14e** (middle), oxime **13e** (bottom) and the synthetic standard (top).

Fundamental Reaction Pathways

Formation of NO:[15]

$$CO_2 + h\nu \rightarrow O + CO \quad (1)$$

$$N_2 + O \rightarrow NO + N \quad (2)$$

$$N + CO_2 \rightarrow NO + CO \quad (3)$$

Formation of NO_x^-:[16]

$$2\ CO_2 + N_2 \rightarrow 2\ CO + 2\ NO \quad (4)$$

$$H_2O + h\nu \rightarrow H + OH \quad (5)$$

$$CO + H + M \rightarrow HCO + M \quad (6)$$

$$HCO + NO \rightarrow HNO + CO \quad (7)$$

$$HNO \rightarrow H^+ + NO^- \quad (8)$$

$$NO^- + NO \rightarrow N_2O_2^- \quad (9)$$

$$N_2O_2^- + NO \rightarrow N_3O_3^- \quad (10)$$

$$N_xO_x^- \rightarrow NO_3^- + NO_2^- + N_2O \quad (11)$$

Formation of NH_3:[17]

$$NO_2^- + 6\ Fe^{2+} + 7\ H^+ \rightarrow 6\ Fe^{3+} + 2\ H_2O + NH_3 \quad (12)$$

Formation of NH_2OH (**6**):[1]

$$NO_2^- + 2\ HSO_3^- \rightarrow HON(SO_3^-)_2 \quad (13)$$

$$HON(SO_3^-)_2 + 2\ H_2O \rightarrow NH_2OH + 2\ HSO_4^- \quad (14)$$

Formation of H_2CO (**7**):[18]

$$CO_2 + h\nu \rightarrow CO + O \quad (15)$$

$$H_2O + h\nu \rightarrow H + OH \quad (16)$$

$$H + CO + M \rightarrow HCO + M \quad (17)$$

$$HCO + HCO \rightarrow H_2CO + CO \quad (18)$$

Formation of urea (**11**):[13]

$$H_2CO + NH_2OH \rightarrow CH_2NOH + H_2O \quad (19)$$

$$CH_2NOH \rightarrow HCN + H_2O \quad (20)$$

$$HCN + NH_2OH \rightarrow H_2NCN + H_2O \quad (21)$$

$$H_2NCN + H_2O \rightarrow CO(NH_2)_2 \quad (22)$$

Crystallographic Data

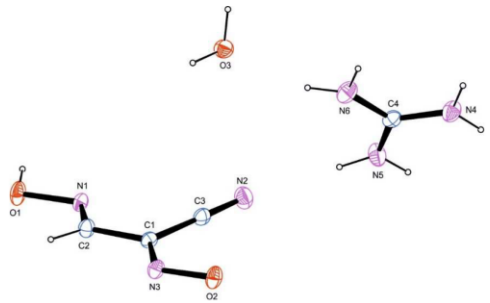

Figure S29: Crystal structure of the monohydrate guanidinium (**12**) salt of *N*-hydroxy-2-(hydroxyimino)acetimidoyl cyanide (**29**). Nitrogen atoms (pink), oxygen atoms (red) and carbon atoms (blue) are represented by large spherical structures. Hydrogen atoms (white) are represented by small spherical structures. CCDC 2189560 contains the supplementary crystallographic data for this paper. These data can be obtained free of charge from The Cambridge Crystallographic Data Centre via www.ccdc.cam.ac.uk/structures.

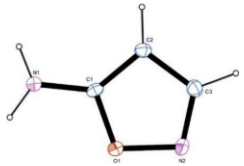

Figure S30: Crystal structure of 5-aminoisoxazole (**20**). Nitrogen atoms (pink), oxygen atoms (red) and carbon atoms (blue) are represented by large spherical structures. Hydrogen atoms (white) are represented by small spherical structures. CCDC 2051594 contains the supplementary crystallographic data for this paper. These data can be obtained free of charge from The Cambridge Crystallographic Data Centre via www.ccdc.cam.ac.uk/structures.

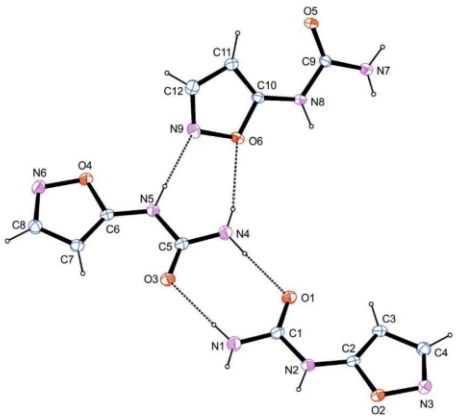

Figure S31: Crystal structure of 5-aminoisoxazolyl-urea **22**. Nitrogen atoms (pink), oxygen atoms (red) and carbon atoms (blue) are represented by large spherical structures. Hydrogen atoms (white) are represented by small spherical structures. CCDC 2189559 contains the supplementary crystallographic data for this paper. These data can be obtained free of charge from The Cambridge Crystallographic Data Centre via www.ccdc.cam.ac.uk/structures.

Uncategorized References

1 Becker, S. *et al.* Unified prebiotically plausible synthesis of pyrimidine and purine RNA ribonucleotides. *Science* **366**, 76-82 (2019).

2 Becker, S. *et al.* Wet-dry cycles enable the parallel origin of canonical and non-canonical nucleosides by continuous synthesis. *Nat. Commun.* **9**, 1-9 (2018).

3 Grabowski, E. & Autrey, R. Oxygenated dienes and the synthesis of methylenedioxybiphenyl derivatives. *Tetrahedron* **25**, 4315-4330 (1969).

4 Betke, T. & Gröger, H. (2018).

5 Malcor, J.-D. *et al.* Synthesis and reactivity of pyrrolo [3, 2-d][1, 3] oxazine-2, 4-dione. Access to new pyrrolo [3, 2-e][1, 4] diazepine-2, 5-diones. *Tetrahedron* **70**, 4631-4639 (2014).

6 Štimac, A. & Kobe, J. An improved preparation of 2, 3, 5-tri-O-acyl-β-D-ribofuranosyl azides by the Lewis acid-catalysed reaction of β-D-ribofuranosyl acetates and trimethylsilyl azide: an example of concomitant formation of the α anomer by trimethylsilyl triflate catalysis. *Carbohydr. Res.* **232**, 359-365 (1992).

7 Davis, M. C. & Groshens, T. J. Orthoamides by selective borohydride reduction of N, N′, N ″-triacyl-and N, N′, N ″-tri (alkoxycarbonyl)-guanidines. *Tetrahedron Lett.* **60**, 427-431 (2019).

8 Zacuto, M. J. & Cai, D. α-Hydroxylation of carbonyls using iodine. *Tetrahedron Lett.* **46**, 447-450 (2005).

9 Bruker, A. Inc: Madison, Wisconsin, 2012.

10 Sheldrick, G. (University of Göttingen, 1996).

11 Sheldrick, G. M. Crystal structure refinement with SHELXL. *Acta Crystallographica Section C: Structural Chemistry* **71**, 3-8 (2015).

12 Farrugia, L. J. WinGX and ORTEP for Windows: an update. *J. Appl. Crystallogr.* **45**, 849-854 (2012).

13 Yanagawa, H. & Egami, F. Formation of molecules of biological interest from formaldehyde and hydroxylamine in a modified sea medium. *J. Biochem.* **85**, 1503-1507 (1979).

14 Patel, B. H., Percivalle, C., Ritson, D. J., Duffy, C. D. & Sutherland, J. D. Common origins of RNA, protein and lipid precursors in a cyanosulfidic protometabolism. *Nat. Chem.* **7**, 301-307 (2015).

15 Mvondo, D. N., Navarro-González, R., McKay, C. P., Coll, P. & Raulin, F. Production of nitrogen oxides by lightning and coronae discharges in simulated early Earth, Venus and Mars environments. *Adv. Space Res.* **27**, 217-223 (2001).

16 Summers, D. P. & Khare, B. Nitrogen fixation on early Mars and other terrestrial planets: experimental demonstration of abiotic fixation reactions to nitrite and nitrate. *Astrobiology* **7**, 333-341 (2007).

17 Summers, D. P. & Chang, S. Prebiotic ammonia from reduction of nitrite by iron (II) on the early Earth. *Nature* **365**, 630-633 (1993).

18 Pinto, J. P., Gladstone, G. R. & Yung, Y. L. Photochemical Production of Formaldehyde in Earth's Primitive Atmosphere. *Science* **210**, 183-185 (1980).